PhD-FSTM-2020-60
The Faculty of Sciences, Technology and Medicine

DISSERTATION

Defence held on 26/10/2020 in Luxembourg

to obtain the degree of

DOCTEUR DE L'UNIVERSITÉ DU LUXEMBOURG

EN INFORMATIQUE

by

Ashok BANDI
Born on 19 June 1988 in Kunkalagunta, (Inde)

JOINT DESIGN OF USER SCHEDULING AND PRECODING IN WIRELESS NETWORKS: A DC PROGRAMMING APPROACH

Dissertation defence committee

Dr Bhavani Shankar, dissertation supervisor
Research Scientiste, Université du Luxembourg

Dr Joel Grotz
Senior manager, SES Satellites

Dr Djamila Aouada, Chairman
Professor, Université du Luxembourg

Dr Mats Bengtsson
Professor, Technische Universität Darmstadt

Dr Bjorn Ottersten, Vice Chairman
Professor, Université du Luxembourg

Abstract

Unprecedented proliferation of mobile devices is leading to ever-increasing densification of the networks. Densification and increase in demand overwhelm the dedicated allocation of spatial and frequency resources, hence, leading to their reuse. Several techniques, e.g., precoding, have been considered for the mitigation of interference from this reuse. Despite this, due to resource limitations, only a few requests can be handled during transmission in a given transmit slot. This naturally leads to the scheduling of the requests (or typically referred to as users) which, in turn, impacts co-channel interference. Thus, the average performance of the multiuser multiple-input single-output (MISO) downlink channel, with a large number of users compared to transmit antennas of the base station, depends on the interference management which necessitates the joint design of scheduling and precoding. Typically, the joint design of scheduling and precoding is addressed by mixed-Boolean non-linear programming (MINLP) where the Boolean variables are associated with scheduling. These MINLP formulations in the literature lead to the coupling of Boolean and precoding variables; this coupled nature thwarts the joint update of scheduling and precoding variables. Unlike the previous works which do not offer a truly joint design, this thesis focuses on a joint design that truly facilitates the joint update of scheduling and precoding variables for the following cases in single-cell multiuser MISO downlink channels: per slot joint design for the unicast scenario, per slot design for multigroup multicast (MGMC) scenario and joint design over multiple slots for unicast and multicast scenarios.

These scenarios are of relevance and are already being considered in current and upcoming standards including 4G and 5G. This thesis begins by presenting the necessity of the joint design of scheduling and precoding for the aforementioned scenario in detail in chapter 1. Further, the coupled nature of scheduling and precoding that prevails in many other designs is discussed. Following this, a detailed survey of the literature dealing with the joint design is presented. In chapter 2, the joint design of scheduling and precoding in the unicast scenario for multiuser MISO downlink channels for network functionality optimization considering sum-rate, Max-min SINR, and power. Thereafter, different challenges in terms of the problem formulation and subsequent reformulations for different metrics are discussed. Different algorithms, each focusing on optimizing the corresponding metric, are proposed and their performance is evaluated through numerical results. In chapter 3, the joint design of user grouping, group scheduling, user scheduling, and precoding is considered for MGMC. Differently to chapter 2, the optimization of a novel metric called multicast energy efficiency (MEE) is considered. This new paradigm for joint design in MGMC poses several additional challenges that can not be dealt with by the design in chapter 2. Therefore, towards addressing these additional challenges, a novel algorithm is proposed for MEE maximization and its efficacy is presented through simulations. In chapters 2 and 3, the joint design is considered within a given transmit slot and temporal design is not considered. In chapter 4, the joint design scheduling and precoding are considered over a block of multiple time slots for a unicast scenario. Differently to single slot design, the multi-slot joint design facilitates to address users' latency directly in terms of time slots. Noticing this, joint design across multiple slots is considered with the objective of minimizing the number of slots to serve all the users subject to users' QoS and latency constraints. Further, this multi-slot joint design problem is modeled as a structured group sparsity problem. Finally, by rendering the problem as a DC, high-quality stationary points are obtained through an efficient CCP based algorithm. In chapter 5, the joint scheduling and precoding schemes proposed in previous chapters are applied to satellite systems.

Finally, The thesis concludes with the main research findings and the identification of new research challenges in chapter 6.

Acknowledgment

First of all, I would like to thank my supervisor, Dr. Bhavani Shankar MYSORE RAMARAO, for his continuous support and technical guidance throughout my doctoral studies. His daily supervision and his positive attitude had a pivotal role in the accomplishment of this thesis. I would also like to thank Prof. Bjorn OTTERSTEN, for giving me the chance to pursue my PhD studies in an excellent research group, and for his valuable advice and constructive comments. Further, I would like to thank Prof. Symeon CHATZINOTAS for pitching the idea for my thesis and his continuous support and constructive comments. Further, I would like to thank Dr. Joel Grotz for shaping the thesis with critical comments and suggestions.

I would like to thank all my (current and past) colleagues of the SIGCOM group of SnT, for many fruitful research collaborations, and for creating an enjoyable working environment. A big gratitude is owed to all the new friends that came into my life in these years while living in Luxembourg, who made me feel at home away from home. I am grateful to my friends from India and Luxembourg. Among all, I owe a special thanks to my hiking friends who helped to make Luxembourg as my second home and took me on many adventures across the Europe. The biggest thanks goes to my family, for giving me the possibility to pursue my studies and for the unquestionable support throughout all the path. A special mention goes to my brother, Anil BANDI, a torch bearer for me all my life. At crucial stages in my life, he showed me the endless possibilities that are at my disposal through his life choices.

I could not have accomplished it without the support and understanding of my parents Ankamma BANDI and Veeramma BANDI. I wish to thank my wife Alekhya KOTHAPALLI for being my constant support. Last, but not the least, thanks to the University of Luxembourg community for giving me an inspiring environment and lots of opportunities to grow.

The generous financial help from the Fonds National de la Recherche (FNR - Luxembourg National Research Fund) via University of Luxembourg is gratefully acknowledged.

Notations

$\log(x)$	Natural logarithm function of x.
e^x	Exponential function of x.
$\mathbb{E}\{\cdot\}$	Expected value.
$\mathbb{R}\mathbf{e}\{\cdot\}$	Real part.
$\mathbb{I}\mathbf{m}\{\cdot\}$	Imaginary part.
a**, a, A**	A scalar, a column vector and a matrix.
$\lvert a\rvert$	Modulus of scalar a.
$\mathbf{A}_{ij}$	The entry of the i-th row and j-th column of matrix **A**.
$\mathbf{a}^T$**,** $\mathbf{A}^T$	Transpose of vector **a**, transpose of matrix **A**.
$\mathbf{a}^H$**,** $\mathbf{A}^H$	Complex conjugate and transpose (hermitian) of vector **a**, complex conjugate and transpose (hermitian) of matrix **A**.
$\mathbf{A} \succeq 0$	Matrix **A** positive semidefinite.
$\mathbf{A} \odot \mathbf{B}$	Hadamard product between matrices **A** and **B**, i.e., the element-wise multiplication of their elements.
$\mathbf{A} \otimes \mathbf{B}$	Kronecker product between matrices **A** and **B**.
$\mathbf{Tr}(\mathbf{A})$	Trace of matrix **A**.
$\mathbf{diag}(\mathbf{a})$	Diagonal matrix whose entries are the elements of vector **a**.
$\mathbf{I}_Q$	Identity matrix of dimension Q.
$\arg$	Argument.
$\max$	Maximum.
$\min$	Minimum.
$\mathcal{N}(\tilde{\mu}, \tilde{\sigma}^2)$	Gaussian or Normal distribution with mean $\tilde{\mu}$ and variance $\tilde{\sigma}^2$.

Acronyms

MISO	multiple input single output.
MINLP	Mixed integer non-liner programming.
DC	Difference-of-convex/ concave.
SINR	Signal-to-noise and interference-ratio
SE	Spectral efficiency.
WSR	Weighted sum rate.
EE	Energy efficiency.
MEE	Multicast energy efficiency.
MGMC	Multigroup multicast.
SUS	Semi orthogonal user scheduling
JSP	Joint design of scheduling and precoding.
JGSP	Joint design of user grouping, group scheduling, user scheduling and precoding.
CCP	Convex-concave procedure

Contents

List of Tables

List of Figures

1

Introduction

1.1 Introduction

The mobile data traffic is exploding unprecedentedly due to the exponential increase in mobile devices and their demand for throughput hungry services and applications [1]; this overwhelms the existing networks in terms of resources. Therefore, resource management/allocation policies play a vital role in wireless communication networks. Resource management policies typically address a wide spectrum of network functionalities such as scheduling, power control, bandwidth reservation, call admission control, transmitter assignment, handover, etc [2, 3]. The aforementioned resource management typically spreads across multiple layers i.e, physical layer, data link layer, etc. This thesis considers the problems related to resource allocation at the physical layer. Physical resource management usually includes managing time, frequency, and spatial resources which are limited in comparison to the number of devices/requests. To cope with the demand of high throughput services and exponentially increasing devices/requests/users, full frequency and time resources reuse among the users along with multi-antenna technologies, that facilitate serving multiple users simultaneously, is considered in the current generation networks. To realize and leverage the benefits of the aforementioned techniques, the resulting interference among the users/devices stemming from the reuse of resources and simultaneously serving multiple users must be addressed [4–7]. Besides the exponential increase in number of devices, multiple requests per device further exhausts the physical layer resources. Even with aforementioned technologies, serving all the users concurrently using same spatial and frequency resources becomes unrealistic. This inevitably leads to the scheduling of users per resources in a transmission slot. Further, multiple slots are necessary to serve all the yet-to-be served users. Therefore, user scheduling is a inevitable design aspect that must be considered for the resource allocation. Moreover, the user scheduling when combined with aforementioned technologies like multi antenna, precoding etc further enhances the gains obtained by these technologies. Therefore, this thesis focuses on the joint design of user scheduling and precoding in multiuser multiple input single out downlink channels for unicast and multicast transmission scenarios within a transmission slot. Further, we investigate the joint design user scheduling and precoding across the multiple transmission slots for unicast scenario.

1.1.1 Joint unicast and multicast scheduling and precoding across multiple slots

We consider a network with large number of users each equipped with a single receive antenna. This is typically the scenario is modern networks like 4G and 5G. Further, a rudimentary processing is assumed at the users hence a user can receive only one data stream at a time. In a typical network, some data is requested by only one user and some data is requested by multiple users. Multiple users requesting the same data is referred to as a group. Data transmission to a user requesting independent data is referred to as unicast transmission and data transmission of same data to a group of users is referred to as multicast transmission. In such networks, the service needed to serve all the users can only be measured by the number of independent data transmissions. The number of users and the number of requests per users easily overwhelms the number of independent data transmissions that can be carried by network in a given transmit slot. Therefore, the scheduling of groups is inevitable. Further, in some scenarios, all the users in a group also may not be served as these users may fail to satisfy the associated QoS requirements like minimum rate. Hence, these users need to be dropped from scheduling; this is referred to as user scheduling in the thesis. Further, some users may be requesting multiple data simultaneously. Therefore, a user may show the interest to be member of multiple groups. Since, a simple decoding is assumed at each user, a user can be member of at most one group. Therefore, despite a user's interest multiple groups, a user can be member of utmost one group; this is referred to as user grouping.

In a single transmission, only a fraction of total requests can be served and, hence, typically multiple time slots required to serve all the requests. For example, a user requesting two services are served in two different slots. Therefore, all the above mentioned scheduling aspects are performed over the multiple slots. Moreover, the precoding design for the users scheduled in all these levels must be feasible. Therefore, the joint design of group scheduling, user grouping, user scheduling and precoding over multiple slots is needed. This problem is gigantic and complex to solve. Therefore, towards reaching this goal we adopt the bottom-up approach of solving the sub-problems where each sub-problem in the subsequent chapters subsume the sub-problems in the previous chapters. The rest of chapter presents the overview of the sub-problems in the ascending order in the bottom-up approach.

1.1.2 Unicast scenario

In a unicast scenario, each user is treated independently and addressed by an independent data transmission. So, the base station equipped with M transmit antenna can serve simultaneously up to M users. However, the users that receive the data simultaneously experience interference. Moreover, this interference decides the maximum rate at which users can be served. Typically, each user is associated with a minimum rate requirement depending on service the user is subscribed to. The severe interference may preclude the design from serving the users with the requested data speed. This leads to the infeasibility of the design. Therefore, interference is a vital factor to be reckoned with and, hence, a great deal of literature has been dedicated towards addressing it.

Typically, the interference is canceled at the transmitter assuming the availability of channel state information (CSI) and employing a signal processing technique called precoding (also referred to as beamforming) [8, 9]. In multiuser downlink precoding, the BS can cancel the interference towards the unintended mobile stations (MS) to minimize the co-channel interference, e.g., by employing multiuser zero-forcing precoding [10, 11]. As a result, multiple MSs can be served jointly at the same time and frequency resources, resulting in the so-called space-division multiple access (SDMA) schemes [12–14]. Through serving multiple MSs with SDMA concurrently, multiuser downlink beamforming achieves high spectrum efficiency. In light of the potential advancement towards energy and spectrum-efficient mobile communications, multiuser downlink beamforming has been adopted into modern third-generation (3G), fourth-generation (4G) and fifth-generation (5G) cellular standards, e.g., in long-term evolution (LTE) and LTE-advanced

(LTE-A) of the third generation partnership project (3GPP) [15–18]. In this framework, different strategies have been considered for the precoder design. The optimal precoding strategy for the minimization of the total transmit power, whilst guaranteeing some Quality-of-Service (QoS) targets at each user was given in [8,19], while the problem of precoding for maximizing the minimum signal-to-interference-plus-noise ratio (SINR) across the users, under sum power constraints, was optimally solved in [20]. The goal of the latter formulation is to increase the fairness of the system, hence the approach is also referred to as the *max-min* fair. This work on precoding was extended in [21] accounting for per-antenna power constraints considering generalized power constraints. The precoding design for energy efficiency maximization in orthogonal frequency division multiple access networks is considered in [22]. Furthermore, the problem of channel level precoding in a multigroup multicast framework has been tackled in [23, 24].

Typically, the number of users in a cell, say N, are greater than the number of antennas, M, at the base station (BS). Assuming independent transmissions on each antenna, BS can support utmost M independent data transmissions simultaneously in a slot. This naturally leads to the scheduling of utmost M users (also referred to as user selection and admission control in the literature). As mentioned previously, the simultaneously served users cause interference among each other. This interference is thus a function of user scheduling. Users with similar channels have the highest interference and users with orthogonal channels can lead to zero interference depending on the beamforming strategy. Further, user scheduling is also a function of the quality-of-service (QoS) requirements of the users. All users with high QoS requirements may not be served in the same slot due to the limitation of resources like power or severe interference. In this case, the precoding design for the independently scheduled users may become infeasible. In other words, the scheduling need to consider the feasibility of precoding as well. Therefore, the scheduling and precoding problem are coupled and requires their joint design.

The data transmission is performed by slot, and, so the joint design of scheduling and precoding. In slot one, joint scheduling and precoding are performed on the total number of users based on the objectives of the design. Further, the joint design for the users that are not scheduled in the current slot is considered in the future slot. This process is repeated until all the users are served. In this regard, many works considered the design of scheduling and precoding in a slot for the following objectives: sum-rate maximization [25], maximize the minimum signal-interference plus noise ratio (max-min SINR) [26], power minimization [27] and energy efficiency maximization [28]. Further, the designs are subject to the subset or all of the following constraints: minimum rate/SINR requirement, total power, or per antenna power consumption, minimum desired number of scheduled users or maximum number of scheduled users.

1.1.3 From unicasting to multicasting

In many scenarios, identical data is requested simultaneously by multiple users in the same cell, for example, live streaming of popular events. Unlike the unicast scenario, which addresses each user differently, the same information can be multicast to the set of users requesting the same data using a single beamforming vector in the same time-frequency slot; this design is referred to as physical layer multicasting (MC) [29, 30]. In the case of a unicast scenario, a data stream serves only one user, hence, the number of received bits per second per Hz across all the users is the same as the transmitted bits per second per Hz. Generally, transmitted bits per second per Hz is commonly referred to as spectral efficiency (SE). However, in the case of MC, a group of users is served by a single data stream. Therefore, the total number of received bits per second per Hz is simply the number of users in a group times the SE; this is simply referred to as multicast spectral efficiency (MSE) in this thesis. Further, the MC technique is extended to multiple antennas scenarios to serve multiple groups simultaneously where each group receives a independent information; this is referred to as multigroup multicasting (MGMC) [29]. However, similar to the unicast scenario, MGMC experiences the following challenges that need to be addressed to fully leverage the gains of MGMC. The similarity among the users in different groups generates

interference across the groups; this is referred to as inter-group interference (IGI). A study of IGI is essential as it fundamentally limits achievable minimum rate of the groups and hence the total throughput of the network [31]. Further, IGI can make the design infeasible [31]. The infeasibility of MGMC is crucial to the design and is, therefore, typically addressed by *user scheduling* (also referred to as admission control in the literature) [32, 33]. Following two examples gives an idea of how the user scheduling is used for addressing infeasibility of MGMC:

- In some cases, by simply omitting a user IGI can be reduced to a level where the groups can be served with intended QoS.
- In some other cases, omitting a user with poor channel gain, the groups can be served with available power budget.

Due to the exponentially growing number of devices, the number of groups, say G, is typically larger than the number of antennas M. Since the utmost M groups can be served simultaneously, this naturally leads to the scheduling of the utmost M out of G groups; this is referred to as group scheduling. Further, some users are interested in multiple information (or groups) but can only be a member of one group since the users' are equipped with a single receive antenna with simple decoding strategy; this is referred to as user grouping. Further, the user in a scheduled group that do not meet the QoS requirement are simply not scheduled; this is referred to as user scheduling. Notice that there are three different scheduling (or selection) schemes at different levels: user grouping (user's assignment to a group), user scheduling (addressing scheduling within a group), group scheduling. User grouping, group scheduling, and user scheduling are inter-related. To see this, user grouping decides the achievable minimum SINR of the groups (or IGI) which influences the group scheduling. The IGI among the scheduled group influence the user scheduling. Further, omitting or adding a user (i.e., user scheduling) to a group changes the IGI, thereby influencing group scheduling. Similarly, user scheduling in a group might necessitate the re-grouping of users (i.e., user grouping); this affects IGI and group scheduling. Furthermore, IGI is a function of precoding [34]. Therefore, optimal performance requires the *joint design of user grouping, group scheduling, user scheduling, and precoding*.

1.1.4 One slot joint design to multi-slot joint design

To provide the service to all the users the multi slot design is inevitable as only a fraction of users can be served in a single slot (ex: 8 out of 1500 users in a 4G advanced LTE network). Therefore, the users that are not scheduled in the current slot are scheduled in the future slot based on some procedure like round-robin scheduling, random scheduling etc; these methods are referred to as sequential designs. However, the scheduled users in the current slot influence the scheduling in the future time slot. In the worst-case scenario, in the sequential approach, the joint design problem may become infeasible (the inability of finding a feasible solution) in the future slots. This could happen due to the following reasons:

- Unmet capacity: In a typical network, user channels are independent due to which some users may have good channel gains over multiple slots and some users may experience decay in channel gains over the slots. Failing to schedule the users with decaying channel gains in the early slots makes it impossible for the design to serve these users in the future slots with their required capacity.
- Unmet latency: Typically, each user's request is associated with an independent timer and the data needs to be delivered within the expiry of the timer. This is referred to as a latency requirement. Scheduling users with relatively lower timer values may not always be a feasible choice. For example, users with similar channels causes strong interference to each other, and, hence these two users can not be served in the same slot irrespective of the urgency in the latency requirement. Failing to consider the current slot scheduling impact

on the future slots may lead scenario that requires the joint design for the users with similar channels, hence, the infeasibility of the joint design.

- Unmet capacity and latency: In a typical network, each user is associated with an independent capacity and latency requirements. This case subsumes both unmet capacity and unmet latency. Hence, ignoring the impact of the joint design in the current slot on the future slots only increases the probability of infeasibility of the joint design in the future slots.

In this case, scheduling exists in two levels: scheduling within a time slot and scheduling across time slots. Without loss of generality, these are simply referred to as scheduling. It is clear from the above discussion that it is vital to consider the joint design of scheduling and precoding over all time slots. In this chapter, we consider the joint design of scheduling and precoding over multiple slots; this is simply referred to as joint temporal design. For the above mentioned reasons, the joint temporal design provides a feasible solution where the sequential approach fails to provide one. This is because, for the cases where joint design becomes infeasible in the future slots, the joint temporal design offers the flexibility of adjusting scheduling in the previous slots that can make the joint design feasible in the future slots. Moreover, for the cases where the user can not be served completely in one slot, the joint temporal design offers the flexibility of serving the user in multiple slots while meeting the user's overall QoS and latency requirement; this model is simply referred to as *rate-splitting*

1.1.5 Motivation

Most of the existing literature on the design of scheduling and precoding can be classified as:

- *Non-iterative decoupled approach*: In this approach, scheduling and precoding are treated as two decoupled problems where usually the users are scheduled according to some criteria followed by precoding [10, 25], [26, 35, 36].

- *Iterative decoupled approach*: In this approach, scheduling and precoding are still treated as two separate problems. However, scheduling and precoding parameters are refined in each iterate to improve the objective based on the feedback from the previous iterate [27, 37–39].

- *Joint formulation with alternate update*: In this approach, the joint design problem is formulated as a function of both scheduling and precoding [40–42]. However, these formulations are not amenable for the joint update as the scheduling variables are coupled to precoding variables which inhibits their joint update. Hence, during the solution stage either scheduling constraints are ignored [40] or the scheduling and precoding variables are updated alternatively [41].

Recalling the above discussions, the aforementioned problems requires the respective scheduling variables and precoding variables are inter-coupled [43]. Hence, the joint update scheduling and precoding has the potential to achieve better performance over the aforementioned approaches [10, 25, 40], [26, 27, 35–39]. The authors in [44] have shown the user scheduling and power allocation problem to be NP-hard. The joint design problems that are considered in this thesis encapsulate the problem considered in [44] as a special case. Hence, considered joint design problems are non-convex and difficult [37]. Hence, the optimal solution entails an exhaustive search over Boolean space (user scheduling) and further involves the solution of a non-convex precoding problem. The exponential complexity of an exhaustive search for practical system dimensions motivates a shift towards low-complexity achievable solutions.

This thesis focuses on the joint design of various scheduling and precoding aspects that occur in unicast and multicast downlink transmission in cellular and satellite systems. The applicability of joint design framework developed in this thesis is not just limited to these problems. Many of the mixed-integer non-linear programming (MINLP) problems that arise in the context of resource

allocation in wireless communications can be addressed within this framework (see e.g., [45,46]). The coupled nature of binary variables with precoding vector appears in many other formulations [47, 48] etc. For example, towards maximizing the weighted sum-rate in a hierarchical network, binary variables associated with users get multiplied to signal power and interference power of SINR [40]. Similarly, in [42], a binary variable is multiplied to the rate of the users in the weighted sum-rate maximization problem. Please note that system models and objectives discussed in [40,42,48] are different from each other, and the emphasis is only on the occurrence of the joint design (coupled discrete and continuous) nature that prevails in different designs. The multiplicative nature in previous formulations precludes the joint update of scheduling and precoding. In this thesis, we focus on developing algorithmic framework that can be adopted to most of the MINLPs that occur in many wireless applications. For this purpose, to provide the emphasis on algorithmic framework, the joint design framework is presented for the abstract system models which provide the basis for the most of the existing models. Moreover, the proposed framework provides solutions with low to moderate complexity with provable theoretical convergence guarantees. To this end, the main objectives, contributions, and outline of the thesis summarized in the sequel.

1.2 Objectives, contributions, and outline of the thesis

The objective of this thesis is to jointly design the various scheduling and precoding aspects that occur in unicast, multicast, and multislot-unicast downlink transmission scenarios for the optimization of various design objectives (such as sum-rate, max-min SINR, etc) in MU-MISO systems.

Chapter 2

In chapter 2, the joint design of scheduling and precoding for unicast scenario is considered in the downlink transmission of MU-MISO systems unlike the quasi-joint approaches of the literature. In this chapter, scheduling simply refers to the user scheduling. In this model, to address the current ultra-dense networks, the number of users is assumed to be larger than the number of transmit antennas. Hence, scheduling of the users in inevitable in such networks. The sum-rate maximization, max-min SINR maximization, and power minimization are considered as the objective of optimization subject to suitable design constraints. Unlike the previous works, user scheduling is handled through the norm of the precoding vectors where the non-zero norm represents the user being scheduled. Further, with the help of binary variables which control the norm of the precoding vectors, the joint design of scheduling and precoding for the aforementioned objectives are formulated as a structured MINLP problems; this special structure allows the decoupling of the scheduling and precoding variables which otherwise hinders their joint update. This decoupling provides the possibility of updating the all of the design variables jointly. Generally, MINLP problems are hard to solve, however, understanding the underlying structure helps in proposing the algorithms which theoretically guarantee their convergence to high-quality solutions like stationary points. Realizing this, through novel reformulations, that reveal the hidden difference-of-convex (DC) structure, followed by binary relaxation and penalization the MINLP problems are transformed as DC problems. Finally, the stationary points of the DC problems are obtained through the convex-concave procedure (CCP) with theoretical guarantees on their convergence. Due to the effectiveness of penalization methods, the stationary point of the DC problems includes binary solutions with high probability. Since the stationary point of DC problems with binary solutions is also the stationary point of the original MBNLP problems, the proposed algorithms typically obtain the stationary point of the original problems. The proposed joint design algorithms provide the gains up to 28% in comparison to decoupled approaches.

Following are the publications that are results as a part of this study:

[J1]: A. Bandi, B. Shankar M. R, S. Chatzinotas and B. Ottersten, "A Joint Solution for Scheduling and Precoding in Multiuser MISO Downlink Channels," in IEEE Transactions on Wireless Communications, vol. 19, no. 1, pp. 475-490, Jan. 2020, doi: 10.1109/TWC.2019.2946161.

[C1]: A. Bandi, B. S. Mysore R, S. Maleki, S. Chatzinotas and B. Ottersten, "A Novel Approach to Joint User Selection and Precoding for Multiuser MISO Downlink Channels," 2018 IEEE Global Conference on Signal and Information Processing (GlobalSIP), Anaheim, CA, USA, 2018, pp. 206-210, doi: 10.1109/GlobalSIP.2018.8646373.

Chapter 3

In chapter 2, we studied the joint design of user scheduling and precoding for unicast scenario. In chapter 3, the joint design framework proposed in chapter 2 is extended to the multigroup multicast scenario. In more detail, the joint design of user grouping, group scheduling, user scheduling, and precoding is considered for a message-based MGMC scenario in the downlink transmission of an MU-MISO system. In the context of user grouping, group scheduling and user scheduling to encapsulate the group sizes a novel metric called multicast energy efficiency (MEE) is proposed. MEE is defined as ratio of multicast spectral efficiency and total consuming power, maximization is considered as the objective of the optimization. Further, the network power model that accounts for the rate-dependent processing power is considered. Unlike the objectives in chapter 1, MEE, beside the combinatorial nature due to different scheduling aspects, brings in additional fractional programming complexities into the design. Hence, the joint design problem becomes a mixed-Boolean fractional programming problem (MBFLP). Through novel reformulation, binary relaxations, and penalization the MBFLP problem is transformed as a DC problem. Finally, through CCP, first-order stationary points of the DC problems with binary solutions are obtained. Therefore, the proposed algorithm obtains the stationary points of the original MBFLP problem.
Following are the submitted and accepted publications as part of the study in this chapter:
[J2]: A. Bandi, B. Shankar M. R, S. Chatzinotas and B. Ottersten, "Joint User Grouping, Scheduling, and Precoding for Multicast Energy Efficiency in Multigroup Multicast Systems," *submitted* to IEEE Transactions on Wireless Communications.

[C2]: A. Bandi, B. S. Mysore R., S. Chatzinotas and B. Ottersten, "Joint User Scheduling, and Precoding for Multicast Spectral Efficiency in Multigroup Multicast Systems," 2020 IEEE International Conference on Signal Processing and Communications (SPCOM), Bangalore, India, 2020

Chapter 4

Chapters 2 and 3 deal with joint designs for unicast and multicast scenarios respectively in a given transmit slot. In chapter 4, the joint design of user scheduling and precoding over multiple slots is considered for a unicast scenario in MU-MISO channels. Unlike per transmit slot joint designs in chapters 2 and 3, the multi-slot joint design brings in the additional flexibility to incorporate two design aspects: user latency and rate-splitting. Assuming the constant traffic arrival process, under the availability of perfect channel state information, the joint temporal design is considered for two scenarios: unicast and multicast. Minimization of the service time (STM) required to serve all the users is considered as the objective of the optimization. Similar to the problems in Chapter 1, these optimization problems are MINLP and NP-hard. Further, STM is modeled as minimization of highest column index of a non-zero column in the matrix where column j contains scheduled users in slot j; this renders the problem as structured group sparsity problem. Further, using similar reformulations, binary relaxations, and penalization as in chapter 1, the joint design problem is formulated as a DC problem. Finally, using CCP the first-stationary points of DC (also original problems as the binary solutions included) are obtained.
Following are the publications to be submitted:

[J3]: A. Bandi, B. Shankar M. R, S. Chatzinotas and B. Ottersten, "Joint Design of User Scheduling and Precoding over Multiple Slots: A Structured Group Sparsity based Approach," *to be submitted* to IEEE Transactions on Wireless Communications.

Chapter 5

In chapter 5, we apply the joint scheduling and precoding techniques mentioned in the previous chapters to satellite systems, assuming digital on-board processing. Unlike the cellular networks, the satellite systems are limited by the onboard available power which in turn limits the processing power. Due to the limited processing realization of the existing precoding schemes in practice is possibly infeasible. The precoder is designed once per coherence time which typically lasts for multiple slots. Therefore, the processing power needed to apply the calculated precoding matrix dominates the overall processing power rather than the computational complexity of precoding design. Therefore, in the first part of this chapter, we design a sparse precoder with as minimum non-zeros as possible subject to QoS and total processing power constraints. Further, the joint design of group scheduling, user scheduling and precoding is considered for the frame-based MGMC. Finally, the joint temporal design is considered.

Following are the accepted publications as part of the study in this chapter:

[C3]: A. Bandi, V. Joroughi, B. S. Mysore R., J. Grotz and B. Ottersten, "Sparsity-Aided Low-Implementation cost based On-Board beamforming Design for High Throughput Satellite Systems," 2018 9th Advanced Satellite Multimedia Systems Conference and the 15th Signal Processing for Space Communications Workshop (ASMS/SPSC), Berlin, 2018, pp. 1-6, doi: 10.1109/ASMS-SPSC.2018.8510731.

[C4]: A. Bandi, B. S. Mysore R., S. Chatzinotas and B. Ottersten, "Joint Scheduling and Precoding for Frame-Based Multigroup Multicasting in Satellite Communications," 2019 IEEE Global Communications Conference (GLOBECOM), Waikoloa, HI, USA, 2019, pp. 1-6, doi: 10.1109/GLOBECOM38437.2019.9014235.

Chapter 6

The gigantic problem of joint temporal scheduling and precoding for the MGMC can be solved using the framework proposed in chapter 2, 3 and 4. However, the complexity of solutions becomes a bottleneck. The quest for more elegant solutions is left for the future work. To this end, discussions, and future research directions are provided in Chapter 6.

1.3 Publications

This dissertation is based on the following publications, which have been published or submitted during the course of my doctoral studies:

Journals

J1: A. Bandi, B. Shankar M. R, S. Chatzinotas and B. Ottersten, "A Joint Solution for Scheduling and Precoding in Multiuser MISO Downlink Channels," in IEEE Transactions on Wireless Communications, vol. 19, no. 1, pp. 475-490, Jan. 2020, doi: 10.1109/TWC.2019.2946161.

J2: A. Bandi, B. Shankar M. R, S. Chatzinotas and B. Ottersten, "Joint User Grouping, Scheduling, and Precoding for Multicast Energy Efficiency in Multigroup Multicast Systems," *submitted* to IEEE Transactions on Wireless Communications.

J3: A. Bandi, B. Shankar M. R, S. Chatzinotas and B. Ottersten, "Joint Design of User Scheduling and Precoding over Multiple Slots: A Structured Group Sparsity based Approach," *to be submitted*

to IEEE Transactions on Wireless Communications.

J4: A. Bandi, B. Shankar M. R, S. Chatzinotas and B. Ottersten, "Joint User Grouping, Scheduling, and Precoding for Multigroup Multicast Scenario in Satellite Systems," *to be submitted.*

Conferences

C1: A. Bandi, B. S. Mysore R, S. Maleki, S. Chatzinotas and B. Ottersten, "A Novel Approach to Joint User Selection and Precoding for Multiuser MISO Downlink Channels," 2018 IEEE Global Conference on Signal and Information Processing (GlobalSIP), Anaheim, CA, USA, 2018, pp. 206-210, doi: 10.1109/GlobalSIP.2018.8646373.

C2: A. Bandi, B. S. Mysore R., S. Chatzinotas and B. Ottersten, "Joint Scheduling and Precoding for Frame-Based Multigroup Multicasting in Satellite Communications," 2019 IEEE Global Communications Conference (GLOBECOM), Waikoloa, HI, USA, 2019, pp. 1-6, doi: 10.1109/GLOBECOM38437.2019.9014235.

C3: A. Bandi, B. S. Mysore R., S. Chatzinotas and B. Ottersten, "Joint User Scheduling, and Precoding for Multicast Spectral Efficiency in Multigroup Multicast Systems," 2020 IEEE International Conference on Signal Processing and Communications (SPCOM), Bangalore, India, 2020

C4: A. Bandi, V. Joroughi, B. S. Mysore R., J. Grotz and B. Ottersten, "Sparsity-Aided Low-Implementation cost based On-Board beamforming Design for High Throughput Satellite Systems," 2018 9th Advanced Satellite Multimedia Systems Conference and the 15th Signal Processing for Space Communications Workshop (ASMS/SPSC), Berlin, 2018, pp. 1-6, doi: 10.1109/ASMS-SPSC.2018.8510731.

The following are the publications that are resulted in the outcome of my collaboration during the Ph.D. period. My contributions in these publications are limited to the discussion on optimization and adaptation of the proposed framework to scenarios considered in these works.

[J5]: S Gautam, E Lagunas, A Bandi,S Chatzinotas ; Shree Krishna Sharma ; Thang X. Vu et al., "Multigroup Multicast Precoding for Energy Optimization in SWIPT Systems With Heterogeneous Users," in IEEE Open Journal of the Communications Society, vol. 1, pp. 92-108, 2020, doi: 10.1109/OJCOMS.2019.2962077.

[J6]: P. Korrai, E. Lagunas, S. K. Sharma, S. Chatzinotas, A. Bandi and B. Ottersten, "A RAN Resource Slicing Mechanism for Multiplexing of eMBB and URLLC Services in OFDMA Based 5G Wireless Networks," in IEEE Access, vol. 8, pp. 45674-45688, 2020, doi: 10.1109/ACCESS.2020.2977773.

[J7]: P. K. Korrai, E. Lagunas, A. Bandi, S. K. Sharma and S. Chatzinotas, "Joint Power and Resource Block Allocation for Mixed-Numerology-Based 5G Downlink Under Imperfect CSI," in IEEE Open Journal of the Communications Society, doi: 10.1109/OJCOMS.2020.3029553.

2

Joint scheduling and precoding for unicast scenario

2.1 Introduction

With the adoption of full frequency reuse in the next-generation cellular networks, interference among the simultaneously served users becomes a limiting factor thwarting the achievement of near-optimal capacity [4–7]. Linear precoding has been largely used to achieve satisfactory interference mitigation at low complexity [8, 9]. Moreover, in a network with a large number of users compared to the number of BS transmit antennas, user scheduling for simultaneous transmission is pivotal for interference management [10, 25]. Optimizing performance in such a network involves the design of precoding variables and user scheduling. Further, different perspectives to network performance motivate the need to investigate multiple figures of merit; these include network throughput, user Quality of Service (QoS) power consumed among others. In this context, we address the joint design of scheduling and precoding problem for multiuser MISO downlink channels in single-cell scenario for the following network optimization design criteria: 1) Maximize the weighted sum rate subject to user's minimum signal-to-interference plus noise ratio (MSINR), scheduling and power constraints referred to in the sequel simply as WSR. 2) Maximize the MSINR of the scheduled users subject to scheduling and total power constraints henceforth referred to as MMSINR. 3) Minimize the power utilized subject to scheduling and MSINR constraints henceforth referred to as PMIN.

The aforementioned criteria are designed to improve the complementary aspects of the networks. In all practical wireless systems, a certain minimum received SINR is required for the successful transmission of information. In light of this, to enhance the practical relevance, SINR constraints are introduced in these design criteria. The WSR problem improves the overall throughput of a network while satisfying the scheduling constraint and QoS requirement on the scheduled users. On the contrary, the MMSINR problem improves the performance of the poorest user (in terms of SINR) among those scheduled. Unlike WSR and MMSINR, PMIN optimizes the consumed power while meeting the scheduling and SINR constraints. An elaborate discussion on each design is provided in the subsequent sections.

The joint design of scheduling and precoding, which we simply refer to as joint design, is well studied during the last decade (see [43] and references therein). Most of the existing literature on the joint design can be classified as:

- *Non-iterative decoupled approach*: In this approach, scheduling and precoding are treated as two decoupled problems where usually the users are scheduled according to some criteria followed by precoding [10, 25], [26, 35, 36].

- *Iterative decoupled approach*: In this approach, scheduling and precoding are still treated as two separate problems. However, scheduling and precoding parameters are refined in each iterate to improve the objective based on the feedback from the previous iterate [27, 37–39, 49].
- *Joint formulation with alternate update*: In this approach, the joint design problem is formulated as a function of both scheduling and precoding [40–42]. However, these formulations are not amenable for the joint update as the scheduling variables are coupled to precoding variables which inhibits their joint update. Hence, during the solution stage either scheduling constraints are ignored [40] or the scheduling and precoding variables are updated alternatively. [41].

The joint design is a coupled problem where the efficiency of the precoder design depends on the interference among the users which, in turn, is a function of the scheduled users [43]. Hence, the joint update of scheduling and precoding has the potential to achieve better performance over the aforementioned approaches [10, 25, 40], [26, 27, 35–39]. The authors in [44] shown the user scheduling and power allocation problem to be NP-hard. The joint design problems that are considered in this work encapsulate the problem considered in [44] as a special case. Hence, the considered joint design problems are NP-hard. It is also non-convex due to the constraints on the SINR or rate of users and scheduling are coupled [37]. Hence, the optimal solution entails an exhaustive search over Boolean space (user scheduling) and further involves the solution of a non-convex precoding problem. The exponential complexity of an exhaustive search for practical system dimensions motivates a shift towards low-complexity achievable solutions. In this context, we quickly review the various relevant works to place ours in perspective.

The joint design problem to maximize the WSR subject to total power constraint, which is referred to as the classical WSR problem, is considered for single cell networks in [10,25,35]. The channel orthogonality based scheduling followed by zero-forcing precoding (SUS-ZF) proposed in [25] is proven to be asymptotically optimal for sum rate maximization. However, it is easy to see that SUS-ZF is not optimal for WSR with non-uniform weights and QoS constraints. Similarly, the classical WSR is addressed for multicell networks in [37–39, 50] and hierarchical networks in [40]. The joint design problem is also considered for MMSINR in [26] and PMIN in [27]. However, scheduling and precoding are not jointly updated in the aforementioned works.

The coupled nature of binary variables with precoding vector appears in many other formulations [47, 48] etc. For example, towards maximizing the weighted sum-rate in a hierarchical network, binary variables associated with users get multiplied to signal power and interference power of SINR [40]. Similarly, in [42], a binary variable is multiplied to the rate of the users in the weighted sum-rate maximization problem. Please note that system models and objectives discussed in [40, 42, 48] are different from each other, and the emphasis is only on the occurrence of the joint design (coupled discrete and continuous) nature that prevails in different designs. The multiplicative nature in previous formulations precludes the joint update of scheduling and precoding. To the best of our knowledge, no prior work exists that update the scheduling and precoding jointly for the aforementioned WSR, MMSINR and PMIN problems. Therefore, we focus on formulating the joint design problem for WSR, MMSINR, and PMIN that facilitates the joint scheduling and precoding solutions.

Revisiting the WSR and MMSINR design problems for fixed scheduled users, it is well-known that the problems are non-convex with difficulty to obtain a global solution. However, efficient suboptimal solutions have been proposed for WSR in [51] and MMSINR in [52, 53] by formulating these as difference-of-convex (DC) programming problems with the help of auxiliary variables and semidefinite programming (SDP) transformations and relaxations. However, the semidefinite relaxations for WSR and MMSINR often lead to non-unity rank solutions from which the approximate rank-1 solutions are extracted [51–53]. The rank-1 approximation results in a loss of performance. Moreover, the transformed problems have higher complexity than the original problems due to auxiliary variables and SDP transformations. In this work, we pose the WSR and

MMSINR joint design as DC programming problems without SDP transformation and employing a minimal number of auxiliary variables.

The aforementioned discussion reflects on the novelties of the paper-based both on problem formulation and its solution. The contributions of the paper include:

- The scheduling is handled through the power of the precoding vector of the corresponding user, where non-zero power indicates the user being scheduled (and not scheduled otherwise). Unlike the previous works [40, 42, 48], a binary variable is used for upper bounding the power of the precoding vector. This renders the formulation amenable to the joint design of scheduling and precoding.

- With the help of the aforementioned scheduling, the joint design problem for WSR, MMSINR, and PMIN design criteria are formulated as mixed-integer non-linear programming (MINLP) in a way that would facilitate the joint updates of scheduling and precoding. Here, the nonconvexity of the problem stems from rate and SINRs in the objective and constraints.

- The binary nature of the problem due to scheduling constraints is addressed by relaxing the binary variables into real values. This is followed by penalizing the objective with a novel entropy-based penalty function to promote a binary solution for the scheduling variables. This step transforms the optimization into a continuous non-convex problem.

- Unlike the classical DC formulation using SDP transformation [51–53], a novel useful reformulation of the objective and/or SINR constraints are proposed to manipulate the joint design as DC programming without SDP transformation.

- Further, a convex-concave procedure (CCP) based iterative algorithm is proposed for WSR, MMSINR and PMIN DC problems. A procedure is proposed to find a feasible initial point, which is sufficient for these algorithms to converge to a stationary point [54, 55].

- Subsequently, the per iteration complexity of the CCP based algorithms, is discussed. Further, a fast convergence behavior of the proposed algorithms is observed through extensive simulations. Finally, the efficiency of the proposed DC reformulations is compared to the decoupled solutions using the Monte-Carlo simulations.

The rest of the paper is organized as follows. Section 2.2 presents the system model and problem formulation of WSR, MMSINR, and PMIN problem. The reformulations and algorithm are proposed for WSR in Section 2.3, MMSINR in Section 2.4 and PMIN in Section 2.5 respectively. Section 2.5.4 presents simulation results, followed by Conclusions in Section 2.6.

2.2 System Model

Consider the downlink transmission of a single cell MISO system with N users in a cell and a BS with $M(\leq N)$ antennas. Let $\mathbf{h}_i \in \mathbb{C}^{M\times 1}$, $\mathbf{w}_i \in \mathbb{C}^{M\times 1}$ and x_i denote the downlink channel, precoding vector and data of user i respectively. The BS is assumed to transmit independent data to utmost M among N users and $\mathbb{E}\{|x_i|^2\} = 1, \forall i$. Further, let n_i be the noise at user i; the noise realizations at all users are assumed to be independent and characterized as additive white complex Gaussian with zero mean and variance σ^2. Further, it is assumed that perfect channel state information of all the users is available at BS and that the user channels are constant during the transmission. Let y_i be the noisy received signal of the user i and $\mathbf{y} \triangleq [y_1, \dots y_N]^T$, $\mathbf{H} \triangleq [\mathbf{h}_1, \dots, \mathbf{h}_N]^H$, $\mathbf{W} \triangleq [\mathbf{w}_1, \dots, \mathbf{w}_N]$, $\mathbf{x} \triangleq [x_1, \dots x_N]^T$, $\mathbf{n} \triangleq [n_1, \dots n_N]^T$. The received signal vector $\mathbf{y}$ of all users is given by,

$$\mathbf{y} = \mathbf{HWx} + \mathbf{n}, \tag{2.1}$$

Towards defining the WSR problem mathematically, let $\mathcal{T} = \{1, \dots N\}$ be the set containing indices of all users and $\bar{\mathcal{K}}$ be a subset of $\mathcal{T}$ with cardinality less than or equal to M. Further, let $\mathcal{K}$ be the collection of all the possible subsets of type $\bar{\mathcal{K}}$; clearly, the cardinality of $\mathcal{K}$ is $C \triangleq \sum_{i=0}^{M} \binom{N}{i}$. With the notations defined, the WSR problem is defined as,

$$\mathcal{P}_{\text{WSR}}: \max_{\forall \bar{\mathcal{K}} \in \mathcal{K}} \underbrace{\max_{\mathbf{W}_{\bar{\mathcal{K}}}} \sum_{\forall i \in \bar{\mathcal{K}}} \alpha_i R_i}_{\text{Joint scheduling and Precoding problem}} \quad \underbrace{\begin{aligned} \text{s.t } & R_i \geq \epsilon_i, \forall i \in \bar{\mathcal{K}}, \\ & \sum_{\forall i \in \bar{\mathcal{K}}} \|\mathbf{w}_i\|_2^2 \leq P_T, \end{aligned}}_{\text{precoding problem for selected users}} \tag{2.2}$$

where $\gamma_i \triangleq \dfrac{|\mathbf{h}_i^H \mathbf{w}_i|^2}{\sigma^2 + \sum_{j \neq i \in \bar{\mathcal{K}}} |\mathbf{h}_i^H \mathbf{w}_j|^2}$, $R_i \triangleq \log_2(1 + \gamma_i)$ and $\epsilon_i \geq 0$ are the SINR, rate and minimum rate requirement of the user i respectively and $\bar{\mathcal{K}}$ is the set of scheduled users. Further $\alpha_i \in \mathcal{R}^+$ denotes the weight for ith user offering design flexibility, P_T is the total available power, and $\mathbf{W}_{\bar{\mathcal{K}}} = \{\mathbf{w}_i\}_{i=1}^{|\bar{\mathcal{K}}|}$ is the matrix containing the precoding vectors of users of set $\bar{\mathcal{K}}$.

Unlike the WSR design, scheduling of exactly $K (\leq M)$ users is considered in MMSINR formulation. This is because constraining the scheduling to utmost K users always leads to the trivial solution of scheduling only one user and an elaborate discussion is provided at the beginning of Section 2.4. Let $\bar{\mathcal{S}}$ be a subset of $\mathcal{T}$ with cardinality equal to K. Let $\mathcal{S}$ be the collection of all the possible subsets of type $\bar{\mathcal{S}}$; clearly, the cardinality of $\mathcal{S}$ is $\binom{N}{K}$. Letting $\tilde{\epsilon}_i$ to the MSINR requirement of user i, $\forall i$, the design problem for MMSINR can then be defined as,

$$\mathcal{P}_{\text{MMSINR}}: \max_{\bar{\mathcal{S}} \subseteq \mathcal{S}} \underbrace{\max_{\mathbf{W}_{\bar{\mathcal{S}}}} \min_{i \subseteq \bar{\mathcal{S}}} \{\beta_i \gamma_i\}}_{\text{Joint schedueling and Precoding problem}} \quad \underbrace{\begin{aligned} \text{s.t} & \sum_{i \in \bar{\mathcal{S}}} \|\mathbf{w}_i\|_2^2 \leq P_T, \\ & \gamma_i \geq \tilde{\epsilon}_i, i \in \bar{\mathcal{S}}, \end{aligned}}_{\text{precoding problem for selected users}} \tag{2.3}$$

where $\beta_i \in \mathcal{R}^+$, is weight and $\mathbf{W}_{\bar{\mathcal{S}}} = \{\mathbf{w}_i\}_{i=1}^{|\bar{\mathcal{S}}|}$ is the matrix containing the precoding vectors of users in the set $\bar{\mathcal{S}}$. Notice that to accommodate the fairness in the designs, weights or priority factors are introduced through α and β in WSR and MMSINR problems respectively. Various fairness metrics are proposed in the literature, e.g. fairness in terms of rates and allocated power are considered at the physical layer. We refer to [56] and references therein for details on fairness.

Finally, towards defining the PMIN problem, scheduling exactly $K (\leq M)$ users is considered for the same reason mentioned in MMSINR. With notations defined for MMSINR criteria, the PMIN problem is defined as:

$$\mathcal{P}_{\text{PMIN}}: \underbrace{\min_{\bar{\mathcal{S}} \subseteq \mathcal{S}} \underbrace{\min_{\mathbf{W}_{\bar{\mathcal{S}}}} \sum_{i \in \bar{\mathcal{S}}} \|\mathbf{w}_i\|_2^2 \text{ s.t. } \gamma_i \geq \tilde{\epsilon}_i, \; i \subseteq \bar{\mathcal{S}}.}_{\text{PMIN problem for selected users}}}_{\text{Joint user scheduling and PMIN problem}} \tag{2.4}$$

The inner optimization in (2.2), (2.3), and (2.4) solves the precoding problem for the scheduled users. The outer optimization, on the other hand, ensures scheduling users with a maximum

objective value among all scheduling possibilities. Notice that the inner and outer optimization are coupled - the design of precoder depends on the selected set of users, while the user scheduling depends on the objectives in (2.2), (2.3) and (2.4) which, in turn, are functions of the precoder [57].

Towards proposing low-complexity algorithms, we begin by addressing the user scheduling through the norm of precoding vectors as given below,

$$\|\mathbf{w}_i\|_2 = \begin{cases} = 0; \text{user not selected,} \\ \neq 0; \text{user selected.} \end{cases} \tag{2.5}$$

The zero norm of $\mathbf{w}_i$ ensures that all elements of $\mathbf{w}_i$ are zero. Hence, the user i is not scheduled. Similarly, the non-zero norm of the precoder vector $\mathbf{w}_i$ indicates user i being scheduled with an assigned power of $\|\mathbf{w}_i\|_2^2$. In the sequel, we focus on the design of low-complexity solutions to the joint design using (2.5) to achieve better performance than the decoupled designs.

2.3 Weighted Sum Rate maximization

In (2.2), the weighted sum rate objective is considered to improve the overall weighted throughput of the network. Thus, WSR problem schedules only the users who contribute to maximizing the objective. Given sufficient resources, the WSR design schedules close to M users as the objective increases linearly with the number of scheduled users; on the other hand, scheduling of few users with high SINRs only contributes logarithmically to the objective. Hence, the constraint of scheduling utmost of M users is considered as opposed to the harder constraint of scheduling to exactly M users. Besides, the design is flexible to favor users by increasing the corresponding weights i.e., α_i to relatively larger values over the users. The minimum rate constraints preclude scheduling of the users whose rates are not in the range of interest. Since the scheduling of zero users is also included in the feasible set, the problem (2.2) is always feasible. In the sequel, the WSR problem (i.e., (2.2)) is transformed as a DC programming problem through a sequence of novel reformulations and low-complexity sub-optimal algorithms within the framework of CCP.

2.3.1 Joint Design Problem Formulation: WSR

Letting $\bar{\mathcal{K}}$ to be the set of scheduled users, a tractable formulation of (2.2) using (2.5) is,

$$\begin{aligned} \mathcal{P}_1^{\text{WSR}}: \max_{\mathbf{W}, \forall \bar{\mathcal{K}} \in \mathcal{K}} \; & \sum_{i=1}^{N} \alpha_i R_i \\ \text{s.t. } C_1: \; & \|[\|\mathbf{w}_1\|_2, \ldots, \|\mathbf{w}_N\|_2]\|_0 \leq M, \\ C_2: \; & \sum_{i=1}^{N} \|\mathbf{w}_i\|_2^2 \leq P_T, \\ C_3: \; & R_i \geq \epsilon_i, \; i \in \bar{\mathcal{K}}. \end{aligned} \tag{2.6}$$

Remarks:

- It is clear from (2.5) and the definition of ℓ_0 norm, that the constraint C_1 imposes restrictions on the total number of selected users to utmost M. We refer to this constraint as the user scheduling constraint throughout this section.
- The constraint C_2 precludes the design from using a transmission power greater than P_T.
- The constraint C_3 imposes a minimum rate required for the scheduled users.

A Novel MINLP formulation: The problem $\mathcal{P}_1^{\text{WSR}}$ is combinatorial due to the constraint C_1 and C_3, and non-convex due to the objective and constraints C_1 and C_3. Towards addressing

the combinatorial nature, we let η_i and ζ_i to be the binary scheduling variable and slack variable associated with user i respectively, and $\boldsymbol{\eta} = [\eta_1, \ldots, \eta_N]^T$, $\boldsymbol{\zeta} = [\zeta_1, \ldots, \zeta_N]^T$ and $\tilde{\epsilon}_i \triangleq 2^{\epsilon_i} - 1, \forall i$. With the defined notations, a tractable formulation of C_1 and C_3 of $\mathcal{P}_1^{\text{WSR}}$ then takes the form,

$$\begin{aligned}
\mathcal{P}_2^{\text{WSR}} : \max_{\mathbf{W},\boldsymbol{\zeta},\boldsymbol{\eta}} \; & f(\boldsymbol{\zeta}, \boldsymbol{\eta}) \triangleq \sum_{i=1}^{N} \alpha_i \log(\zeta_i) \\
\text{s.t. } & C_1 : \; \eta_i \in \{0, 1\}, \; \forall i, \\
& C_2 : \; \|\mathbf{w}_i\|_2^2 \; \leq \; P_T \eta_i, \; \forall i, \\
& C_3 : \; \sum_{i=1}^{N} \eta_i \leq M, \\
& C_4 : \; \sum_{i=1}^{N} \|\mathbf{w}_i\|_2^2 \leq P_T, \\
& C_5 : \; 1 + \gamma_i \geq \zeta_i, \forall i, \\
& C_6 : \; \zeta_i \geq 1 + \eta_i \tilde{\epsilon}_i, \; \forall i,
\end{aligned} \tag{2.7}$$

Remarks:

- The binary nature of η_i (i.e., C_1) together with C_2 determines the scheduling of users. In other words, $\eta_i = 0$ leads to a precoding vector containing all zero entries. Similarly $\eta_i = 1$ leads to $\|\mathbf{w}_i\|_2^2 \leq P_T$ which is a trivial upper bound compared to C_4. Hence the constraint C_2 along with C_1 contributes only to the scheduling aspects of the problem.
- From the objective and constraint C_5, the variable ζ_i provides a lower bound for $1 + \gamma_i$.
- The constraint C_6 ensures MSINR or rate constraint of the scheduled users. If user i is scheduled i.e., $\eta_i = 1$, from C_6, $\zeta_i \geq 1 + \tilde{\epsilon}_i$. Similarly, for an unscheduled user i, C_6 becomes $\zeta_i \geq 1$. In fact for $\eta_i = 0$, constraint is met with equality i.e., $\zeta_i = 1$ due to C_2.
- It is easy to see that, at the optimal solution, the constraints C_5 and C_6 are met with equality.

Novelty of $\mathcal{P}_2^{WSR}$: Novelty of $\mathcal{P}_2^{\text{WSR}}$ lies in the formulation of scheduling constraint, C_2. This reformulation is vital to the facilitation of the joint update of $\boldsymbol{\eta}$ and $\mathbf{W}$ as discussed in the sequel. Notice that this formulation differs from those in the literature ([40, 42, 48, 58, 59], etc) where the scheduling constraint is handled by a binary slack variable which multiplies either the precoding vector or the rate of the user, to control the user scheduling. This multiplication not only makes the constraints non-convex but also makes it difficult to obtain the joint update of Boolean and continuous variables due to the coupling of variables. Moreover, the constraints C_5 and C_6 help to reformulate the objective as a concave function and connects the minimum rate constraints to the objective. This reformulation is crucial as it facilitates the reformulation of $\mathcal{P}_2^{\text{WSR}}$ as DC programming problem without resorting to SDP transformations [51, 60–62].

2.3.2 A Novel DC reformulation: WSR

A novel rearrangement of SINR constraint C_5 in $\mathcal{P}_2^{\text{WSR}}$ that transforms $\mathcal{P}_2^{\text{WSR}}$ as a DC programming problem without SDP transformation is,

$$\begin{aligned}
\mathcal{P}_3^{\text{WSR}} : \max_{\mathbf{W},\boldsymbol{\zeta},\boldsymbol{\eta}} \; & f(\boldsymbol{\zeta}, \boldsymbol{\eta}) \triangleq \sum_{i=1}^{N} \alpha_i \log(\zeta_i) \\
\text{s.t. } & C_1, C_2, C_3, C_4 \text{ and } C_6 \text{ in (2.7)} \\
& C_5 : \mathcal{I}_i(\mathbf{W}) - \mathcal{G}_i(\mathbf{W}, \zeta_i) \leq 0, \forall i,
\end{aligned} \tag{2.8}$$

where $\mathcal{I}_i(\mathbf{W}) = \sigma^2 + \sum_{j \neq i} |\mathbf{h}_i^H \mathbf{w}_j|^2$ and $\mathcal{G}_i(\mathbf{W}, \zeta_i) = \dfrac{\sigma^2 + \sum_{j=1}^{N} |\mathbf{h}_i^H \mathbf{w}_j|^2}{\zeta_i}$. Notice that $\mathcal{I}_i(\mathbf{W})$ is convex in $\mathbf{W}$, and for $\zeta_i > 0$, $\mathcal{G}_i(\mathbf{W}, \zeta_i)$ is also jointly convex in $\mathbf{W}$ and ζ_i. Hence, (2.8) is a DC programming problem with combinatorial constraint C_1. This is the first attempt at reformulating the WSR towards a tractable form without resorting to SDP methods or use of additional slack variables thereby rendering a low-complexity solution to the problem.

Beyond SDP based DC formulation: Notice that for fixed $\boldsymbol{\eta}$, the problem $\mathcal{P}_3^{\text{WSR}}$ becomes a classical WSR maximization problem subject to SINR and total power constraints [51, 60–62]. The problem $\mathcal{P}_3^{\text{WSR}}$ is non-convex due to the constraint C_5. Although, for fixed $\boldsymbol{\zeta}$ (i.e. fixed $\boldsymbol{\eta}$), the constraint C_5 in $\mathcal{P}_3^{\text{WSR}}$ is formulated as a second-order cone programming (SOCP) constraint [8,9], a similar SOCP transformation of C_5 is not known when $\boldsymbol{\zeta}$ is variable. On the other hand, many previous works have exploited the DC structure in WSR maximization problem without SINR constraint in [60–62] and with SINR constraint in [51] by transforming it into an SDP problem. However, the SDP transformations in [51, 60–62], essentially increase the number of variables, thereby increasing the complexity. Moreover, SDP transformations also introduce the non-convex rank-1 constraint on the solutions which is difficult to handle in general; this has led to semidefinite relaxations [8] followed by extraction of feasible rank-1 solutions.

The problem $\mathcal{P}_3^{\text{WSR}}$ is still an MINLP with a DC structure in the non-convexity. This structure can be leveraged with the optimization tools like CCP. Now, to circumvent the combinatorial nature of $\mathcal{P}_3^{\text{WSR}}$, η_i is relaxed to a box constraint between 0 and 1, and penalized with $\mathbb{P}(\eta_i)$ so that the relaxed problem favours 0 or 1. The penalized reformulation of $\mathcal{P}_3^{\text{WSR}}$ with penalty parameter $\lambda_1 \in \mathcal{R}^+$ is,

$$\begin{aligned} \mathcal{P}_4^{\text{WSR}} : \max_{\mathbf{W}, \boldsymbol{\eta}, \boldsymbol{\zeta}} \; & \sum_{i=1}^{N} \left(\alpha_i \log(\zeta_i) + \lambda_1 \mathbb{P}(\eta_i) \right) \\ \text{s.t. } & C_1 : 0 \leq \eta_i \leq 1, \; \forall i, \\ & C_2, C_3, \ldots, C_6 \text{ in (2.8).} \end{aligned} \tag{2.9}$$

We propose a new penalty function $\mathbb{P}(\eta_i) \triangleq \eta_i \log \eta_i + (1 - \eta_i) \log(1 - \eta_i)$ which is a convex function in $\eta_i \geq 0$. $\mathbb{P}(\eta_i)$ incurs no penalty at $\eta_i = 0$ or 1 and the penalty increases logarithmically as η_i drifts away from $\eta_i = 0$ or 1 with the highest penalty at $\eta_i = 0.5$. Hence, by choosing λ_1 appropriately, binary nature of $\boldsymbol{\eta}$ is ensured.

Now, notice that the objective in $\mathcal{P}_4^{\text{WSR}}$ a difference of concave functions i.e. $f(\boldsymbol{\zeta}, \boldsymbol{\eta}) = \sum_{i=1}^{N} (\alpha_i \log(\zeta_i)) - \left(- \sum_{i=1}^{N} \lambda_1 \mathbb{P}(\eta_i) \right)$ and constraints are convex and DC. Hence, the problem $\mathcal{P}_4^{\text{WSR}}$ is a DC programming problem. In the sequel, a CCP based algorithm is proposed [63].

2.3.3 JSP-WSR: A Joint Design Algorithm

In this section, we propose a CCP based iterative algorithm to the DC problem in (2.9) which we refer to as *JSP-WSR*. CCP is a powerful tool to find a stationary point of DC programming problems. Within this framework, an iterative procedure is performed, wherein the two steps of Convexification and Optimization are executed in each iteration. In the convexification step, a convex optimization problem is obtained from $\mathcal{P}_4^{\text{WSR}}$ by linearizing the objective and constraints. Hence, by definition, the modified objective and constraints lower bound the actual objective and constraints of $\mathcal{P}_4^{\text{WSR}}$ where the lower bound is tight at the previous iteration [55,63]. The optimization step then solves the convex sub-problem globally. Thus, the proposed JSP-WSR algorithm iteratively executes the following two steps until convergence:

- Convexification: Let $(\mathbf{W}, \boldsymbol{\eta}, \boldsymbol{\zeta})^{k-1}$ be the estimates of $\mathbf{W}, \boldsymbol{\eta}, \boldsymbol{\zeta}$ in iteration $k-1$ and $\mathcal{G}_i(\mathbf{W}, \zeta_i)$. In iteration k, the convex part of the objective in $\mathcal{P}_4^{\text{WSR}}$ i.e., $\sum_{i=1}^{N} \lambda_1 \mathbb{P}(\eta_i)$,

and the concave part of constraint C_5 in $\mathcal{P}_4^{\text{WSR}}$ for user i are replaced by their first order Taylor approximations around the estimate of $(\mathbf{W}, \boldsymbol{\eta}, \boldsymbol{\zeta})^{k-1}$

$$\begin{aligned}
&\tilde{\mathbb{P}}\left(\eta_i\right) \triangleq \lambda_1 \left(\mathbb{P}\left(\eta_i^{k-1}\right) + \left(\eta_i - \eta_i^{k-1}\right) \nabla \mathbb{P}\left(\eta_i^{k-1}\right)\right), \\
&\tilde{\mathcal{G}}_i(\mathbf{W}, \zeta_i)^{k-1} \triangleq -\mathcal{G}_i(\mathbf{W}, \zeta_i) - \\
&\quad \mathbb{R}\left\{\nabla^H \mathcal{G}_i(\mathbf{W}, \zeta_i)^{k-1} \begin{bmatrix} \{\mathbf{w}_l - \mathbf{w}_l^{k-1}\}_{l=1}^N \\ \zeta i - \zeta_i^{k-1} \end{bmatrix}\right\},
\end{aligned} \tag{2.10}$$

where

$$\nabla \mathcal{G}_i(\mathbf{W}, \zeta_i)^{k-1} = \begin{bmatrix} \dfrac{2\mathbf{h}_i \mathbf{h}_i^H \mathbf{w}_1^{k-1}}{\zeta_i^{k-1}} \\ \vdots \\ \dfrac{2\mathbf{h}_i \mathbf{h}_i^H \mathbf{w}_N^{k-1}}{\zeta_i^{k-1}} \\ -\dfrac{\sigma^2 + \sum_{j=1}^N |\mathbf{h}_i^H \mathbf{w}_j^{k-1}|^2}{{\zeta_i^{k-1}}^2} \end{bmatrix}. \tag{2.11}$$

- Optimization: The next update $(\mathbf{W}, \boldsymbol{\eta}, \boldsymbol{\zeta})^{k+1}$ is obtained by solving the following convex problem (which is obtained by replacing convex part of the objective and constraints in $\mathcal{P}_4^{\text{WSR}}$ with (2.10) and ignoring the constant terms in the objective) :

$$\begin{aligned}
\mathcal{P}_5^{\text{WSR}} : &\max_{\mathbf{W}, \boldsymbol{\zeta}, \boldsymbol{\eta}} \sum_{i=1}^N \left(\alpha_i \log\left(\zeta_i\right) + \lambda_1 \eta_i \nabla \mathbb{P}\left(\eta_i^{k-1}\right)\right) \\
&\text{s.t } C_1, C_2, C_3, C_4 \text{ and } C_6 \text{ in (2.9)} \\
&\quad C_5 : \mathcal{I}_i\left(\mathbf{W}\right) - \tilde{\mathcal{G}}_i(\mathbf{W}, \zeta_i) \leq 0, \forall i.
\end{aligned} \tag{2.12}$$

Remarks:

- Note that the proposed JSP-WSR algorithm is based on CCP framework hence a feasible initial point (FIP) is sufficient for the CCP procedure to converge to a stationary point [54, 55].
- Given the binary nature of $\boldsymbol{\eta}$, at convergence, the resulting stationary point is a valid feasible solution to the original problem $\mathcal{P}_1^{\text{WSR}}$. As mentioned previously, with appropriate λ_1 a stationary point with binary $\boldsymbol{\eta}$ can be obtained easily from the above iterative procedure.

In many cases, obtaining a FIP is difficult. However, in the next section, we propose a method which promises to obtain at least one FIP.

2.3.4 Feasible Initial Point: WSR

CCP is an iterative algorithm and an initial feasible point guarantees the solutions of all iterations remain feasible. A trivial initial FIP is obtained by the initializing $\{\mathbf{w}_i = \mathbf{0}\}_{i=1}^N$, $\boldsymbol{\eta} = \mathbf{0}$ and $\boldsymbol{\zeta} = \mathbf{1}$ where, $\mathbf{1}$ and $\mathbf{0}$ are the column vectors of length N with all ones and zeros respectively. Since the quality of the solution depends on the FIP, the harder task of finding a better FIP is considered through the following iterative procedure.

- Step 1: Initialize $\boldsymbol{\eta} = \hat{\boldsymbol{\eta}}$ that satisfies constraints C_1 and C_3 in $\mathcal{P}_4^{\text{WSR}}$, and $0 < \delta < 1$.

- Step 2: Solve the following optimization:

$$\begin{aligned}
\mathcal{P}_{\text{FESWSR}} : \{\hat{\mathbf{W}}\} : \ & \text{find } \mathbf{W} \\
\text{s.t. } \tilde{C}_1 : & \|\mathbf{w}_i\|_2^2 \ \leq \ \hat{\eta}_i P_T, \ \forall i, \\
\tilde{C}_2 : & \left\| \left[\sigma \ldots \{\mathbf{h}_i^H \mathbf{w}_j\}_{j \neq i} \ldots \right] \right\|_2 \leq \frac{\mathbf{h}_i^H \mathbf{w}_i}{\sqrt{\hat{\eta}_i \tilde{\epsilon}_i}}, \ \forall i, \\
\tilde{C}_3 : & \mathbb{R}\{\mathbf{h}_i^H \mathbf{w}_i\} \geq 0, \forall i, \\
\tilde{C}_4 : & \Im\{\mathbf{h}_i^H \mathbf{w}_i\} == 0, \forall i, \\
\tilde{C}_5 : & \|\mathbf{W}\|_2^2 \leq P_T.
\end{aligned} \tag{2.13}$$

- Step 3: If $\mathcal{P}_{\text{FESWSR}}$ is feasible go to step 4 else update $\boldsymbol{\eta} = \delta \hat{\boldsymbol{\eta}}$ and go to step 2.
- Step 4: Let $\hat{\mathbf{W}}$ be the solution of $\mathcal{P}_{\text{FESWSR}}$. Choose $\hat{\zeta}_i$ such that $1 + \hat{\eta}_i \tilde{\epsilon}_i \leq \hat{\zeta}_i \leq 1 + \hat{\gamma}_i$ where $\hat{\gamma}_i$ is the SINR of the user i calculated using $\hat{\mathbf{W}}$.

Remarks:

- Notice that the updates of $\hat{\boldsymbol{\eta}}$ are always feasible. Different $\hat{\boldsymbol{\eta}}$ in step 1 which satisfy the constraint C_1 and C_3 in $\mathcal{P}_4^{\text{WSR}}$ may lead to different FIPs. Similarly, different choices of $\delta \in (0, 1)$ in step 1 may also lead to different FIPs.
- The optimization problem in Step 2 is only a function of $\mathbf{W}$ since $\boldsymbol{\eta}$ is fixed apriori and $\boldsymbol{\zeta}$ can be calculated easily from the solution of $\mathcal{P}_{\text{FESWSR}}$ as given in step 4.
- Following [9], the MSINR constraint, i.e. $\gamma_i \geq \hat{\eta}_i \tilde{\epsilon}_i$ is reformulated as a second-order cone (SOC) constraint as given in $\tilde{C}_2$ with the help of $\tilde{C}_3$ and $\tilde{C}_4$.
- If $\mathcal{P}_{\text{FESWSR}}$ in step 2 is in-feasible for $\boldsymbol{\eta}$ in step 1, update $\boldsymbol{\eta}$ as given in step 3 and repeat step 2. This is repeated until $\mathcal{P}_{\text{FESWSR}}$ in step 2 becomes feasible.
- If the initial iterates fail to result an non-zero based initial feasible point, the proposed method eventually lead to $\hat{\boldsymbol{\eta}} = \mathbf{0}$ and thus $\mathcal{P}_{\text{FESWSR}}$ in step 2 becomes feasible with $\hat{\mathbf{W}} = 0$. Hence, the proposed methods always results an FIP. By initializing $\hat{\boldsymbol{\eta}}$ close to $\mathbf{0}$, FIP can be obtained in fewer iterations.
- The FIP obtained by this procedure may not be feasible for the original WSR problem $\mathcal{P}_{\text{WSR}}$ in (2.2) unless $\mathcal{P}_{\text{FESWSR}}$ becomes feasible for $\{\hat{\eta}_i \in \{0, 1\}\}_{i=1}^N$ satisfying $\sum_{i=1}^N \hat{\eta}_i \leq M$.
- Although the FIP obtained by this method is not feasible for $\mathcal{P}_{\text{WSR}}$, the final solution obtained by JSP-WSR with this FIP becomes a feasible for $\mathcal{P}_{\text{WSR}}$ since the solution satisfies the scheduling and SINR constraints of $\mathcal{P}_{\text{WSR}}$.

Letting $\mathcal{P}_5^{\text{WSR}}(k)$ be the objective value of the problem $\mathcal{P}_5^{\text{WSR}}$ at iteration k, the pseudo code of JSP-WSR for the joint design problem is given in algorithm 1.

Algorithm 1 JSP-WSR

Input: $\mathbf{H}, [\epsilon_1, \ldots, \epsilon_N], P_T, \Delta, \boldsymbol{\eta}^0, \mathbf{W}^0, \lambda_1 = 0, k = 1$; **Output**: $\mathbf{W}, \boldsymbol{\eta}$
while $|\mathcal{P}_5^{\text{WSR}}(k) - \mathcal{P}_5^{\text{WSR}}(k-1)| \geq \Delta$ **do**
  Convexification: Convexify the problem (2.10)
  Optimization: Update $(\mathbf{W}, \boldsymbol{\eta}, \boldsymbol{\zeta})^k$ by solving $\mathcal{P}_5^{\text{WSR}}$
  Update : $\mathcal{P}_5^{\text{WSR}}(k), \lambda_1, k$
end while

2.3.5 Complexity: WSR

The computational complexity of JSP-WSR depends on the complexities of iterative procedures proposed in Section 2.3.3 and Section 2.3.4. The proposed JSP-WSR in Section 2.3.3 is a CCP based iterative algorithm; hence, the complexity of the algorithm depends on complexity of the sub-problems $\mathcal{P}_5^{\text{WSR}}$. The convex problem $\mathcal{P}_5^{\text{WSR}}$ has $(NM + 2N)$ decision variables and $(2N + 1)$ convex constraints and $2N + 1$ linear constraints. Hence, the computational complexity of $\mathcal{P}_5^{\text{WSR}}$ is $\mathcal{O}\left((NM + 2N)^3 (4N + 2)\right)$ [64]. Similarly, the computational complexity of the proposed procedure in Section 2.3.4 to obtain a FIP depends on the per iteration complexity of $\mathcal{P}_{\text{FESWSR}}$. $\mathcal{P}_{\text{FESWSR}}$ is a convex problem with MN decision variables, $2N+1$ convex constraints and $2N$ linear constraints. Hence, the computational complexity of $\mathcal{P}_{\text{FESWSR}}$ is $\mathcal{O}\left((MN)^3 (4N + 1)\right)$ [64].

2.4 Max Min SINR

In this section, we focus on the development of a low-complexity algorithm for the MMSINR problem defined in (2.3). Dropping a user with low SINR clearly improves MSINR. It also reduces the interference to the other users and the power of the dropped user can be used to further improve the MSINR of other users. Hence, the constraint of scheduling utmost K users leads to the global solution which has highest MSINR which is achieved by scheduling only one user. To avoid this, scheduling exactly K users is considered for MMSINR design. Besides the scheduling constraint, the MSINR requirements of the scheduled users are also considered. Without the MSINR requirement, the design becomes superficial as the solution might include zero SINR or SINR values which are not usable in practice.

Infeasibility of MMSINR The infeasibility of the problem due to the MSINR requirement is explained in [9] for fixed set of users. Similarly, it may not be possible to find exactly K users while satisfying an arbitrarily chosen MSINR, power and system dimension constraints [9]; this renders the problem (3) infeasible. In this work, it is assumed that problem $\mathcal{P}_{\text{MMSINR}}$ has at least one feasible solution for the given scheduling and MSINR constraints. Considering this, a low-complexity sub-optimal algorithm using the framework of CCP is developed for the MMSINR problem in the sequel.

2.4.1 Joint Design Problem Formulation: MMSINR

A tractable mathematical formulation of (2.3) is,

$$\begin{aligned} \mathcal{P}_1^{\text{MM}} : & \max_{\mathbf{W}} \min_{i=\{1,\ldots,N\}} \{\beta_i \gamma_i\} \\ \text{s.t. } C_1 : & \left\| [\|\mathbf{w}_1\|_2, \ldots, \|\mathbf{w}_N\|_2] \right\|_0 == K, \\ C_2 : & \sum_{i=1}^{N} \|\mathbf{w}_i\|_2^2 \leq P_T, \\ C_3 : & \gamma_i \geq \mathbf{1}\left(\|\mathbf{w}_i\|_2\right) \tilde{\epsilon}_i, \forall i \end{aligned} \tag{2.14}$$

where $\mathbf{1}$ is an indicator function with $\mathbf{1}\left(\|\mathbf{w}_i\|_2\right) = 0$ if $\|\mathbf{w}_i\|_2 = 0$ otherwise $\mathbf{1}\left(\|\mathbf{w}_i\|_2\right) = 1$.

The SINR γ_i is non-convex and piece-wise minimum of $\{\gamma_i\}_{i=1}^N$ is also non-convex. So, $\mathcal{P}_1^{\text{MM}}$ maximizes a non-convex objective subject to a combinatorial constraint C_1; this is generally a NP-hard problem. Moreover obtaining a global solution to $\mathcal{P}_1^{\text{MM}}$ requires an exhaustive search over all the possible sets and solving the classical MMSINR problem for each set.

A Novel Reformulation: In the classical MMSINR problem, for the predefined selected users, SINRs of all users is addressed with a slack variable, say s, that lower bounds $\beta_i \gamma_i$, $\forall i$ i.e.,

$\{\beta_i\gamma_i\}_{i=1}^N \geq s$ [65,66]. However, this approach cannot be applied to the present joint design problem since there always exist $N-K$ unscheduled users whose SINR is identically zero. Therefore, lower bounding all $\{\beta_i\gamma_i\}_{i=1}^N$ with s, makes the problem trivial and the solution, say s^*, is always zero. Letting η_i to be a binary variable associated to user i and $\mathcal{S}$ to be the set of scheduled users and adopting the epigraph formulation, an equivalent formulation of $\mathcal{P}_1^{\text{MM}}$ is,

$$\begin{aligned}
\mathcal{P}_2^{\text{MM}}: \max_{\mathbf{W},\boldsymbol{\eta},s} \quad & s \\
\text{s.t. } C_1: & \eta_i \in \{0,1\}, \ \forall i, \\
C_2: & \ \|\mathbf{w}_i\|_2^2 \leq \eta_i P_T, \\
C_3: & \sum_{i=1}^N \eta_i == K, \\
C_4: & \sum_{i=1}^N \|\mathbf{w}_i\|_2^2 \leq P_T, \\
C_5: & \beta_i\gamma_i \geq \eta_i\tilde{\epsilon}_i, \forall i, \\
C_6: & \beta_i\gamma_i \geq \eta_i s, \forall i.
\end{aligned} \tag{2.15}$$

Remarks:

- Constraint C_5 is the MSINR constraint equivalently written with the help of $\eta_i s$.
- The variable s in C_6 is active only when $\eta_i = 1$. For example, when user i not scheduled i.e., $\eta_i = 0$, its SINR is lower bounded by 0 which is always satisfied by the SINR definition. Similarly, when user i scheduled i.e., $\eta_i = 1$, its SINR is lower bounded by s. Thus the maximization of s optimizes the MSINR of only the scheduled users.

2.4.2 A Novel DC reformulation: MMSINR

The problem $\mathcal{P}_2^{\text{MM}}$ is a MINLP where the non-convexity is due to constraints C_5 and C_6, while the combinatorial nature is due to constraint C_1. Similar to constraint C_5 of $\mathcal{P}_4^{\text{WSR}}$, constraint C_5 of the problem $\mathcal{P}_2^{\text{MM}}$ can be formulated as a DC constraint. However, the same approach cannot be applicable to constraint C_6 in $\mathcal{P}_2^{\text{MM}}$ as η_i and s are both variables. Moreover, to the best of our knowledge DC reformulation of constraints of type C_6 in $\mathcal{P}_2^{\text{MM}}$ is not known. In this section, a novel procedure is proposed to transform constraints of type C_6 in $\mathcal{P}_2^{\text{MM}}$ as DC constraints which involves the change of variable s by $\frac{1}{t}$ followed by rearrangement as described below,

$$1 + \beta_i\gamma_i \geq 1 + \frac{\eta_i}{t} \Rightarrow \mathcal{L}_i(\mathbf{W}, t) - \mathcal{H}_i(\mathbf{W}, \eta_i, t) \leq 0, \tag{2.16}$$

where $\mathcal{I}_i(\mathbf{W}) = \sigma^2 + \sum_{j\neq i}|\mathbf{h}_i^H\mathbf{w}_j|^2$, $\mathcal{H}_i(\mathbf{W}, \eta_i, t) = \dfrac{\mathcal{I}_i(\mathbf{W}) + \beta_i|\mathbf{h}_i^H\mathbf{w}_i|^2}{t + \eta_i}$ and $\mathcal{L}_i(\mathbf{W}, t) = \dfrac{\mathcal{I}_i(\mathbf{W})}{t}$. Notice that, for $t > 0$, $\mathcal{L}_i(\mathbf{W}, t)$ is jointly convex in $\mathbf{W}$ and t and $\mathcal{H}_i(\mathbf{W}, \eta_i, t)$ is also jointly convex in $\mathbf{W}, \eta_i$ and t. Hence, (2.16) is a DC constraint.

Towards addressing combinatorial constraint C_1, following the approach in Section 2.3, the binary constraint η_i is relaxed to a box constraint between 0 and 1 and η_i is penalized with $\mathbb{P}(\eta_i)$. Letting $\mathcal{J}_i(\mathbf{W}, \eta_i, t) = \dfrac{\mathcal{I}_i(\mathbf{W}) + \beta_i|\mathbf{h}_i^H\mathbf{w}_i|^2}{1 + \eta_i\tilde{\epsilon}_i}$, for the sake of completion, with the help of variable t, (2.16) and penalization approach proposed in Section 2.3, the problem $\mathcal{P}_2^{\text{MM}}$ is reformulated as,

$$\mathcal{P}_3^{\text{MM}}: \min_{\mathbf{W},\boldsymbol{\eta},t} \quad t - \lambda_2\mathbb{P}(\eta_i) \tag{2.17}$$

$$
\begin{aligned}
\text{s.t. } & C_1 : 0 \leq \eta_i \leq 1, \forall i, \\
& C_2, C_3, C_4 \text{ in (2.15)}, \\
& C_5 : \mathcal{I}_i(\mathbf{W}) - \mathcal{J}_i(\mathbf{W}, \eta_i, t) \leq 0, \forall i, \\
& C_6 : \mathcal{L}_i(\mathbf{W}, t) - \mathcal{H}_i(\mathbf{W}, \eta_i, t) \leq 0, \ \forall i, \\
& C_7 : t > 0,
\end{aligned}
$$

where $\lambda_2 \in \mathcal{R}^+$ is a penalty parameter of the design.

The problem $\mathcal{P}_3^{\text{MM}}$ maximizes a convex objective subject to convex and DC constraints. Hence $\mathcal{P}_3^{\text{MM}}$ is a DC problem and a CCP based algorithm could be solved with an FIP obtained from Section 2.4.4 . However, the strict equality constraint C_3 in $\mathcal{P}_3^{\text{MM}}$, limits the update of the $\boldsymbol{\eta}$. In order to allow the flexibility in choosing $\boldsymbol{\eta}$, the following problem is considered instead,

$$
\begin{aligned}
\mathcal{P}_4^{\text{MM}} : \min_{\mathbf{W}, \boldsymbol{\eta}, t} \ & t - \lambda_2 \mathbb{P}(\eta_i) + \Omega \left(\sum_{i=1}^{N} \eta_i - K \right)^2 \\
\text{s.t. } & C_1, C_2, C_4, C_5, C_6, C_7 \text{ in (2.17)},
\end{aligned} \tag{2.18}
$$

where $\Omega \in \mathcal{R}^+$ is a penalty parameter. It is easy to see that choosing the appropriate Ω (usually higher value) ensures the equality constraint. The problem $\mathcal{P}_4{}^{\text{MM}}$ is also a DC problem and a CCP based algorithm, JSP-MMSINR, is proposed in the sequel to solve it efficiently.

2.4.3 JSP-MMSINR: A Joint Design Algorithm

In this section, we propose a CCP framework based iterative algorithm to the problem $\mathcal{P}_4^{\text{MM}}$, which is referred to as JSP-MMSINR, wherein the JSP-MMSINR executes the following Convexification and Optimization steps in each iteration:

- Convexification: Let $(\mathbf{W}, \boldsymbol{\eta}, t)^{k-1}$ be the estimates of $\mathbf{W}_i, \eta_i, t$ in iteration $k-1$. In iteration k, the concave part of C_5 and C_6 for user i in $\mathcal{P}_4^{\text{MM}}$ i.e., $-\mathcal{H}_i(\mathbf{W}, \eta_i, t)$ and $-\mathcal{J}_i(\mathbf{W}, \eta_i, t)$ are replaced by its affine approximation around $(\mathbf{W}, \boldsymbol{\eta}, t)^{k-1}$ which is given by,

$$
\begin{aligned}
&\tilde{\mathcal{H}}_i(\mathbf{W}, \boldsymbol{\eta}, t)^{k-1} \triangleq -\mathcal{H}_i(\mathbf{W}, \boldsymbol{\eta}, t)^{k-1} \\
&- \mathbb{R}\left\{ \nabla^H \mathcal{H}_i(\mathbf{W}, \boldsymbol{\eta}, t)^{k-1} \begin{bmatrix} \{\mathbf{w}_l - \mathbf{w}_l^{k-1}\}_{l=1}^N \\ \eta_i - \eta_i^{k-1} \\ t - t^{k-1} \end{bmatrix} \right\}, \\
&\tilde{\mathcal{J}}_i(\mathbf{W}, \boldsymbol{\eta}, t)^{k-1} \triangleq -\mathcal{J}_i(\mathbf{W}, \boldsymbol{\eta}, t)^{k-1} \\
&- \mathbb{R}\left\{ \nabla^H \mathcal{J}_i(\mathbf{W}, \boldsymbol{\eta}, t)^{k-1} \begin{bmatrix} \{\mathbf{w}_l - \mathbf{w}_l^{k-1}\}_{l=1}^N \\ \eta_i - \eta_i^{k-1} \\ t - t^{k-1} \end{bmatrix} \right\},
\end{aligned} \tag{2.19}
$$

  where $\nabla \mathcal{H}_i(\mathbf{W}, \boldsymbol{\eta}, t)^{k-1}$ and $\nabla \mathcal{J}_i(\mathbf{W}, \boldsymbol{\eta}, t)^{k-1}$ are the evaluated gradients of $\mathcal{H}_i(\mathbf{W}, \boldsymbol{\eta}, t)$ and $\mathcal{J}_i(\mathbf{W}, \boldsymbol{\eta}, t)$ at $(\mathbf{W}, \boldsymbol{\eta}, t)^{k-1}$ respectively. The expressions for $\nabla \mathcal{H}_i(\mathbf{W}, \boldsymbol{\eta}, t)^{k-1}$ and $\nabla \mathcal{J}_i(\mathbf{W}, \boldsymbol{\eta}, t)^{k-1}$ can be obtained by following (2.11). Similarly, the first order Taylor series approximation of the objective in $\mathcal{P}_4^{\text{MM}}$ after ignoring the constant terms,

$$
\mathcal{F}(t, \boldsymbol{\eta}) = t - \lambda_2 \sum_{i=1}^{N} \eta_i \nabla \mathbb{P}\left(\eta_i^{k-1}\right) + \Omega \left(\sum_{i=1}^{N} \eta_i - K \right)^2
$$

- Optimization: The update $(\mathbf{W}, \boldsymbol{\eta}, t)^k$ is obtained by solving the following convex problem:

$$
\mathcal{P}_5^{\text{MM}} : \max_{\mathbf{W}, \boldsymbol{\eta}, t} \ \mathcal{F}(t, \boldsymbol{\eta}) \tag{2.20}
$$

$$
\begin{aligned}
&\text{s.t. } C_1, C_2, C_3, C_4 \text{ in (2.18)} \\
&C_5 : \mathcal{I}_i(\mathbf{W}, t) + \tilde{\mathcal{J}}(\mathbf{W}, \boldsymbol{\eta}, t)^{k-1} \leq 0, \ \forall i, \\
&C_6 : \mathcal{L}_i(\mathbf{W}, t) + \tilde{\mathcal{H}}(\mathbf{W}, \boldsymbol{\eta}, t)^{k-1} \leq 0, \ \forall i.
\end{aligned}
$$

2.4.4 Feasible Initial Point: MM-SINR

Notice that JSP-MMSINR is a CCP framework based algorithm and hence a FIP is sufficient for the algorithm to converge to a stationary point [54, 55]. Unlike WSR problem, obtaining a trivial FIP to the problem $\mathcal{P}_4^{\text{MM}}$ is difficult as initializing $\mathbf{W}$ to all zeros results in zero SINR for all the users and thus $t = 0$ where later is the violation of the constraint C_5. However, one may find a FIP by the following iterative procedure.

- Step 1: Initialize $\boldsymbol{\eta} = \hat{\boldsymbol{\eta}}$ that satisfies constraints C_1 and C_3 in $\mathcal{P}_4^{\text{MM}}$.
- Step 2: For a fixed $\boldsymbol{\eta}$, ignoring the constraints dependent on t, $\mathcal{P}_4^{\text{MM}}$ can be reformulated as a convex problem by [9] or [8]. This would result similar formulation as shown in $\mathcal{P}_{\text{FESWSR}}$; hence omitted due to space limitation. Let $\hat{\mathbf{W}}$ be the solution from this step.
- Step 3: Exit the loop if $\hat{\mathbf{W}}$ from step 2 is feasible and $t^0 = \dfrac{1}{\min_i\{\eta_i \tilde{\epsilon}_i\}}$ else set $\boldsymbol{\eta} = \delta\hat{\boldsymbol{\eta}}$ and continue to step 2.

Remarks:

- By construction, the initial $\hat{\boldsymbol{\eta}}$ from step 1 is always feasible to $\mathcal{P}_4^{\text{MM}}$.
- Efficient algorithms to solve the convex precoding problem in step 2 is proposed in [9] and [8], and is solvable globally using tools like CVX [67].
- The number of iterations that are needed to obtain a FIP from above procedure depends on $\hat{\boldsymbol{\eta}}$, δ and K. Suppose, if the initial $\hat{\boldsymbol{\eta}} \approx 0$, a FIP is obtained in one iteration with high probability. Similarly, if the initial $\hat{\boldsymbol{\eta}} \approx 1$ the solution from above can be infeasible in the initial iterations. For the latter case, smaller δ leads to a FIP in few iterations and larger δ takes longer iterations to find a FIP.

Notice that a FIP obtained from this process is only feasible to problem $\mathcal{P}_4^{\text{MM}}$ but not to the problem $\mathcal{P}_{\text{MMSINR}}$ since it violates scheduling constraint and binary constraint of $\boldsymbol{\eta}$. However, appropriate adaptation of the penalty parameters λ_2 and Ω (e.g. monotonic increment) ensures that the obtained final solution from algorithm 2 is always feasible to $\mathcal{P}_{\text{MMSINR}}$.

Letting $\mathcal{P}_5^{\text{MM}}(k)$ be the objective value of the problem $\mathcal{P}_5^{\text{MM}}$ at iteration k, the pseudocode of JSP-MMSINR for the joint design problem is given in algorithm 2.

Algorithm 2 JSP-MMSINR

Input: $\mathbf{H}, [\tilde{\epsilon}_1, \ldots, \tilde{\epsilon}_N], P_T, \Delta, \boldsymbol{\eta}^0, \mathbf{W}^0, \lambda_1 = 0, k = 1$; **Output**: $\mathbf{W}, \boldsymbol{\eta}, t$
while $|\mathcal{P}_7^{\text{MM}}(k) - \mathcal{P}_7^{\text{MM}}(k-1)| \geq \Delta$ **do**
  Convexification: Convexify the problem (2.19)
  Optimization: Update $(\mathbf{W}, \boldsymbol{\eta}, t)^k$ by solving $\mathcal{P}_5^{\text{MM}}$
  Update : $\mathcal{P}_7^{\text{MM}}(k), \lambda_2, k$;
end while

2.4.5 Complexity: MM-SINR

Similar to JSP-WSR, the computational complexity of JSP-MMSINR depends on the complexities of iterative procedures proposed in Section 2.4.3 and Section 2.4.4. The proposed JSP-MMSINR in Section 2.3.3 is a CCP based iterative algorithm; hence, the complexity of the algorithm depends on complexity of the sub-problems $\mathcal{P}_5^{\text{MM}}$. The problem $\mathcal{P}_5^{\text{MM}}$ has $(NM+N+1)$ decision variables, $2N+1$ convex and $2N+1$ linear constraints, hence the computational complexity of $\mathcal{P}_5^{\text{MM}}$ is $\mathcal{O}\left((NM+N+1)^3(4N+2)\right)$. Similarly, the computational complexity of the procedure in Section 2.4.4 depends on the per iteration complexity of problem in step 2 which is a convex problem with MN decision variables, $2N+1$ convex constraints and $2N$ linear constraints. Hence, the computational complexity of problem in step2 in Section 2.4.4 is $\mathcal{O}\left((MN)^3(4N+1)\right)$ [64].

2.5 Power Minimization

In this section, we consider the joint design problem with the objective of minimizing the sum power consumed at the BS subject to scheduling of K users whose MSINR requirement is met. As mentioned previously, scheduling utmost K users leads to the trivial solution of no users being scheduled which results in zero consumed power.

2.5.1 Joint Design Problem Formulation: PMIN

Similar to Section 2.4, the user scheduling is handled through the norm of the precoder as shown in (2.5). With the help of (2.5) and notations defined, and letting $\bar{\mathcal{S}}$ to be the set of scheduled users, a tractable formulation of $\mathcal{P}_{\text{PMIN}}$ solely as a function of precoding vectors as follows:

$$\begin{aligned}\mathcal{P}_1^{\text{PMIN}}: &\min_{\mathbf{W},\bar{\mathcal{S}}} \sum_{i\in\bar{\mathcal{S}}} \|\mathbf{W}_i\|_2^2 \\ \text{s.t. } C_1: &\left\|\left[\|\mathbf{w}_1\|_2,\ldots,\|\mathbf{w}_N\|_2\right]\right\|_0 == K, \\ C_2: &\gamma_i \geq \tilde{\epsilon}_i,\ i\in\bar{\mathcal{S}}.\end{aligned} \tag{2.21}$$

The problem $\mathcal{P}_1^{\text{PMIN}}$ is combinatorial due to the constraints C_1 and C_2 and also non-convex due to $\{\gamma_i\}_{i=1}^N$ in constraint C_2. Letting $\Upsilon \in \mathcal{R}^+$ to be a constant, a mathematically tractable formulation that allows us to design a low-complexity algorithm is

$$\begin{aligned}\mathcal{P}_2^{\text{PMIN}}: &\min_{\mathbf{W},\boldsymbol{\eta}} \ \|\mathbf{W}\|_2^2 \\ \text{s.t. } C_1: &\eta_i \in \{0,1\},\ \forall i, \\ C_2: &\ \|\mathbf{w}_i\|_2^2 \leq \eta_i\Upsilon,\ \forall i, \\ C_3: &\sum_{i=1}^N \eta_i == K, \\ C_4: &\gamma_i \geq \tilde{\epsilon}_i\eta_i,\ \forall i.\end{aligned} \tag{2.22}$$

Remarks:

- For $\eta_i = 1$, Υ in C_2 provides upper bound on the power of user i. Moreover, a lower bound on Υ would be the total system power.

A DC reformulation: The problem $\mathcal{P}_2^{\text{PMIN}}$ is an MINLP due to combinatorial constraint C_1 and non-convex constraint C_4. Similar to WSR and MMSINR problems, using the DC formulation of constraint C_4 and penalization method for C_1, the DC formulation of the problem $\mathcal{P}_2^{\text{PMIN}}$ is,

$$\mathcal{P}_3^{\text{PMIN}}: \min_{\mathbf{W},\boldsymbol{\eta}} \ \|\mathbf{W}\|_2^2 - \lambda_3 \sum_{i=1}^N \mathbb{P}(\eta_i) \tag{2.23}$$

$$\begin{aligned}
&\text{s.t. } C_1 : 0 \leq \eta_i \leq 1,\ \forall i,\\
&\quad C_2,\ C_3 \text{ in (2.22)},\\
&\quad C_4 : \mathcal{I}_i\left(\mathbf{W}\right) - f_i\left(\mathbf{W}, \eta_i\right),\ \forall i,
\end{aligned}$$

where $\lambda_3 \in \mathcal{R}^+$ is the penalty parameter and $f_i\left(\mathbf{W}, \eta_i\right) = \dfrac{\mathcal{I}_i\left(\mathbf{W}\right) + |\mathbf{h}_i^H \mathbf{w}_i|^2}{1 + \tilde{\epsilon}_i \eta_i}$.

The problem $\mathcal{P}_3^{\text{PMIN}}$ is a DC problem which can be solved using CCP. However, finding a FIP becomes difficult as for chosen $\boldsymbol{\eta}$, $\mathcal{P}_3^{\text{PMIN}}$ may become infeasible [9]. For the ease of finding an FIP, the constraint C_2 in $\mathcal{P}_4^{\text{PMIN}}$ is relaxed and penalized as follows:

$$\begin{aligned}
\mathcal{P}_4^{\text{PMIN}} :\ &\min_{\mathbf{W},\boldsymbol{\eta}}\ \|\mathbf{W}\|_2^2 - \Omega \sum_{i=1}^{N} \mathbb{P}\left(\eta_i\right) + \mu \left(\sum_{i=1}^{N} \eta_i - K\right)^2 \\
&\text{s.t. } C_1, C_2, C_4 \text{ in (2.23)}
\end{aligned} \tag{2.24}$$

where $\mu > 0$ is penalty parameter. Notice that for the appropriate μ, equality constraint is ensured. Moreover, The problem $\mathcal{P}_4^{\text{PMIN}}$ is a DC problem which solvable using CCP.

2.5.2 Joint Design Algorithm: PMIN

In this section, following the CCP framework proposed in Section 2.4.3, the CCP based algorithm for PMIN is proposed. The proposed joint scheduling and precoding (JSP) for PMIN (JSP-PMIN) algorithm executes the following two steps iteratively until the convergence:

- Convexification: Let $(\mathbf{W}, \boldsymbol{\eta})^{k-1}$ be the estimates of $(\mathbf{W}, \boldsymbol{\eta})$ in iteration $k-1$. In iteration k, the concave part of C_3 in $\mathcal{P}_4^{\text{PMIN}}$ for user i i.e., $-f_i(\mathbf{W}, \eta_i)$ is replaced by its affine approximation around the estimate of $(\mathbf{W}, \boldsymbol{\eta})^{k-1}$ which is given by,

$$\begin{aligned}
&\tilde{f}(\mathbf{W}, \eta_i) \triangleq -f\left(\mathbf{W}, \eta_i\right)^{k-1} - \\
&\mathbb{R}\left\{\nabla^H f\left(\mathbf{W}, \eta_i\right)^{k-1} \begin{bmatrix} \{\mathbf{w}_l - \mathbf{w}_l^{k-1}\}_{l=1}^{N} \\ \eta_i - \eta_i^{k-1} \end{bmatrix}\right\}.
\end{aligned} \tag{2.25}$$

- Optimization: Update $(\mathbf{W}, \boldsymbol{\eta})^k$ is obtained by solving the following convex problem:

$$\begin{aligned}
\mathcal{P}_5^{\text{PMIN}} :&\min_{\mathbf{W},\boldsymbol{\eta}}\ \|\mathbf{W}\|_2^2 + \mu \left(\sum_{i=1}^{N} \eta_i - K\right)^2 \\
&\qquad - \lambda_3 \sum_{i=1}^{N} \eta_i \nabla \mathbb{P}\left(\eta_i^{k-1}\right) \\
&\text{s.t. } C_1 : 0 \leq \eta_i \leq 1,\ \forall i,\\
&\quad C_2 : \|\mathbf{w}_i\|_2^2 \leq \eta_i \Upsilon, \forall i,\\
&\quad C_3 : \mathcal{I}_i\left(\mathbf{W}\right) + \tilde{f}(\mathbf{W}_i, \eta_i)^{k-1} \leq 0,\ \forall i.
\end{aligned} \tag{2.26}$$

The convex problem $\mathcal{P}_5^{\text{PMIN}}$ has $(NM + N)$ decision variables, $2N$ convex and $2N$ linear constraints, hence the computational complexity of $\mathcal{P}_5^{\text{MM}}$ is $\mathcal{O}\left(\left(NM + N\right)^3 \left(4N\right)\right)$.

2.5.3 Feasible Initial Point: PMIN

An initial feasible point, which suffices the convergence of JSP-PMIN to a stationary point [54,55], for the problem $\mathcal{P}_5^{\text{PMIN}}$ is obtained by the following iterative procedure.

- Step 1: Initialize $\boldsymbol{\eta} = \hat{\boldsymbol{\eta}}$ that satisfies C_1 and C_3 in $\mathcal{P}_4^{\text{PMIN}}$.
- Step 2: The precoding problem of $\mathcal{P}_4^{\text{PMIN}}$ for fixed $\boldsymbol{\eta}$ can be reformulated as a convex problem by [9] or [8]. Let $\hat{\mathbf{W}}$ be the solution from this step.
- Step 3: Exit the loop if $\hat{\mathbf{W}}$ is feasible (see [9]) else set $\boldsymbol{\eta} = \delta\hat{\boldsymbol{\eta}}$ and continue to step 2.

Notice that a FIP obtained above may not be feasible to $\mathcal{P}_2^{\text{PMIN}}$ since it may violate binary and scheduling constraints. However, the adopted penalty methods ensure the scheduling and binary constraints. Hence, the final solution obtained from 3 is always a feasible solution to $\mathcal{P}_2^{\text{PMIN}}$.

Letting $\mathcal{P}_5^{\text{PMIN}}(k)$ be the objective value of the problem $\mathcal{P}_5^{\text{PMIN}}$ at iteration k, The pseudo code of the algorithm is illustrated in the algorithm 3.

Algorithm 3 JSP-PMIN

Input: $\mathbf{H}, [\bar{\tilde{\epsilon}}_1, \ldots, \bar{\tilde{\epsilon}}_N], \Delta, \boldsymbol{\eta}^0, \mathbf{W}^0, \lambda_3 = 0, k = 1$; **Output**:$\mathbf{W}, \boldsymbol{\eta}$
while $|\mathcal{P}_5^{\text{PMIN}}(k) - \mathcal{P}_5^{\text{PMIN}}(k-1)| \geq \Delta$ **do**
  Convexification: Convexify the problem (2.19)
  Optimization: Update $\left(\mathbf{W}^k, \boldsymbol{\eta}^k\right)$ by solving $\mathcal{P}_5^{\text{PMIN}}$
  Update : $\mathcal{P}_5^{\text{PMIN}}(k), \Omega, k$
end while

2.5.4 Simulation Setup

In this section, we evaluate the performance of the proposed algorithms for the MMSINR, WSR and PMIN problems. The system parameters and benchmark scheduling method discussed in this paragraph are common for all the figures. Entries of the channel matrix, i.e., $\{h_{ij}\}$s are drawn from the complex normal distribution with zero mean and unit variance and noise variances are considered to be unity i.e., $\sigma^2 = 1$. Simulation results in all the figures are averaged over 500 different channel realizations (CRs). The penalty parameter λ_1 is initialized to 0.5 and incremented as $\lambda_1 = 1.1\lambda_1$ until $\lambda_1 \leq 10$. For all the simulations of MMSINR and PMIN, K is chosen as M. By the nature of MMSINR (PMIN) design, dropping the user with the lowest SINR (higher power) leads to a better objective. This phenomenon continues until it drops $N - M$ users and can not drop any further due to the scheduling constraint. Since, this naturally enforces the binary nature of $\boldsymbol{\eta}$, $\lambda_2 = 0$ ($\lambda_3 = 0$) in MMSINR (PMIN) still yields the binary $\boldsymbol{\eta}$ which is shown Section 2.5.7 and 2.5.8. Hence, λ_2 and λ_3 are fixed zero in all iterations. The penalty parameters Ω and μ are initialized to 0.01 and incremented as $\Omega = 1.2\Omega$ and $\mu = 1.2\mu$ in each iteration until $\Omega \leq 20$ and $\mu \leq 20$.

2.5.5 Benchmark algorithms

To evaluate the performance of the proposed JSP algorithms - due to the lack of a comparable joint solution - the following benchmarks (iterative decoupled solutions that execute the following steps in sequence) are devised:

- In step 1, users are scheduled according to proposed weighted semi-orthogonal user scheduling (WSUS) or exhaustive search-based user scheduling (ES) or random user scheduling (RUS). The considered WSUS is an extension of the SUS algorithm proposed in [25]. In SUS, the users are selected sequentially based on the orthogonality of their channels with those of already scheduled ones. In WSUS, orthogonality indices calculated according to SUS are multiplied with their associated weights and the user with the highest weighted orthogonality index is scheduled. This process is repeated until M users are scheduled.
- In step 2, the precoding problem for the scheduled users is solved by the following methods:

Design criteria	Scheduling schemes	Precoding schemes
WSR: weighted sum rate	SUS: Semi orthogonal user scheduling	WSR: proposed precoding; WSR-Z: proposed precoding with a trivial FIP; RWSR: reference precoding [51]
MMSINR: Max-Min SINR	WSUS: Weighted SUS	MMSINR: proposed precoding scheme
PMIN: Power Minimization	RUS: Random user scheduling	PMIN: reference precoding in [8]

TABLE 2.1: Summary of the acronyms of different benchmark algorithms based on design criteria.

  - It is easy to see that, retaining only the terms corresponding to scheduled users by substituting corresponding η_is to 1 (rest are made zero) and ignoring the constraint solely dependent on η_is in (2.9), (2.18) yields the DC formulation of the precoding problem for the scheduled users for WSR and MMSINR respectively. These problems can be solved using CCP with a FIP obtained from $\mathcal{P}_{\text{FESWSR}}$ and $\mathcal{P}_{\text{FESPMIN}}$ by substituting corresponding η_is with 1. RUS, ES, SUS and WSUS combined with this proposed WSR is simply referred to as RUS-WSR, ES-WSR, SUS-WSR, and WSUS-WSR respectively and for MMSINR as RUS-MMSINR, ES-MMSINR, SUS-MMSINR, and WSUS-MMSINR respectively. Similarly, RUS, ES, SUS and WSUS based scheduling followed by the SDP based power minimization proposed in [8] is used for PMIN precoding problem and is referred to simply as RUS-PMIN, ES-PMIN, SUS-PMIN, and WSUS-PMIN respectively. For the ease of reference, acronyms used for benchmark (BM) algorithms are tabulated in Table 2.5.5.
  - An SDR version of DC formulation proposed in [51] also used for solving the precoding for the scheduled users in WSR case as a reference hence is referred to as RWSR. WSUS combined with RWSR is referred to as WSUS-RWSR.

- In step 3: If the precoding problem in step 2 is infeasible exit the loop else drop the user with least orthogonality and repeat step 2 for an updated set of scheduled users. However, the precoding problems for MMSINR and PMIN are assumed to be feasible.

2.5.6 WSR Performance Evaluation

In figure 2.1(a), we compare the performance of JSP-WSR as a function of N varying from 15 to 30 in steps of 5 for $M = 10$, $P_T = 10$dB and $\tilde{\epsilon}_i = 4$dB, $\forall i$. Weights $\{\alpha_i\}_{i=1}^N$ are randomly drawn from the set $\{\frac{k}{N}\}, k = 1, \ldots, N$. In figure 2.1(a), RUS-WSR, SUS-WSR, WSUS-WSR and WSUS-RWSR are the decoupled benchmark algorithms. The JSP-WSR initialized with a trivial solution ($\mathbf{W}^0 = \mathbf{0}$, $\boldsymbol{\eta}^0 = \mathbf{0}$) is referred to as JSP-WSR-Z and JSP-WSR initialized with an FIP obtained from Section 2.3.4 continues to be referred to as JSP-WSR. From figure 2.1(a), it is clear that the joint solution JSP-WSR outperforms all the other decoupled benchmarks. Although JSP-WSR, RUS-WSR, SUS-WSR, and WSUS-WSR have the same underlying precoding algorithm, JSP-WSR achieves better performance as it jointly updates scheduling and precoding. Considering weights into scheduling in WSUS-WSR improves over SUS-WSR, as shown in figure 2.1(a), but it still outperformed by JSP-WSR. However, the gains diminish as N increases as the probability of finding nearly orthogonal user channels (for the considered Gaussian model) increases; this implies that the user scheduling has minimum impact on performance. Hence, WSUS-WSR performs close to JSP-WSR for N relatively larger than M. However, the gains obtained by JSP-WSR even in comparison with WSUS-WSR still amounts up to 28% ($N = 15$). Notice that despite the difference in the rate of growth, all methods benefit from multiuser diversity to improve SR as N increases.

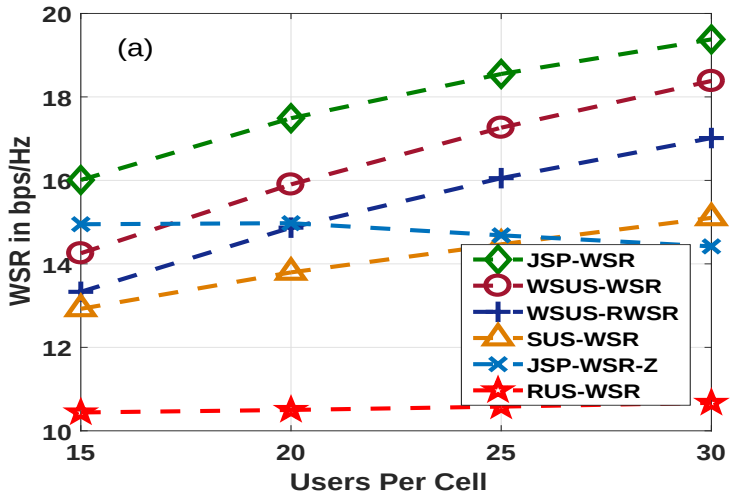

(a)

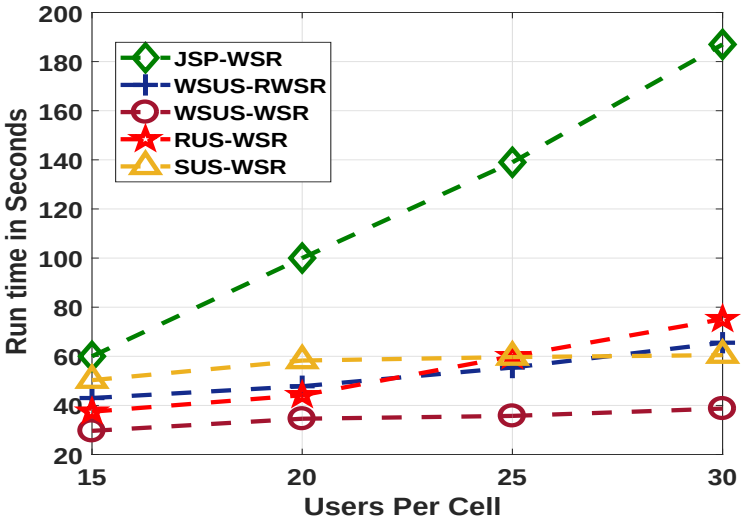

(b)

FIGURE 2.1: Comparison of different WSR optimization approaches for M =10, $\{\tilde{\epsilon}_i = 4\text{dB}\}_{i=1}^{N}$, $P_T = 10$ dB, and N is varied from 15 to 30 (a) Achieved WSR and (b) algorithm run time

Notice that JSP-WSR and JSP-WSR-Z are identical except the FIPs. JSP-WSR and JSP-WSR-Z are CCP based algorithms hence the performance differentiation depends on FIP. Figure 2.1(a) shows that while a poor FIP like $\mathbf{W}^0 = \mathbf{0}$, $\boldsymbol{\eta}^0 = \mathbf{0}$ results in worse performance than decoupled solutions, the FIPs from Section 2.3.4 achieves better performance. This shows the efficiency of the FIP mechanism detailed in Section 2.3.4. In particular, $\mathbf{W}^0 = \mathbf{0}$, $\boldsymbol{\eta}^0 = \mathbf{0}$ is a bad choice since it is the solution that achieves lowest WSR i.e., zero and hence the solutions of JSP-WSR-Z are generally the stationary points around the lowest objective.

Despite having the same WSUS scheduling algorithm and the same FIP for precoding, WSUS-WSR outperforms WSUS-RWSR due to the difference in precoding algorithms as shown in figure 2.1(a). Although classical WSR can be formulated as a DC problem using proposed reformulations and also by the approach in [51], due to the efficiency of proposed reformulations, WSUS-WSR achieves the better objective which is confirmed by figure 2.1(a).

Figure 2.1(b) illustrates the complexity of algorithms as a function of running time in seconds. Notice that the running time includes the time to calculate the FIPs and the final solutions. In the decoupled algorithms i.e., WSUS-WSR and WSUS-RWSR the complexity of scheduling algorithms is negligible compared to the latter precoding problem. Since the precoding is always

performed on M users, the precoding complexity of RUS-WSR, WSUS-WSR, and WSUS-RWSR is only a function of M. On the contrary, joint design algorithms, JSP-WSR, JSP-WSR-Z operate on N users hence the complexity increases with N. However, due to the efficiency in the design of JSP-WSR, its complexity can be comparable to that of WSUS-WSR for relatively low values of N, e.g. $N = 15$.

In table 2.3, the number of iterations needed for JSP-WSR to converge to a stationary point is illustrated as a function of $M = 10$, $\{\tilde{\epsilon}_i = 4\text{dB}\}_{i=1}^{N}$, $P_T = 10$ dB, and N is varied from 15 to 30 (in steps of 5). The per-iteration complexity of JSP-WSR is known to be polynomial and Table 2.3 confirms the number of iterations that are need for JSP-WSR to converge is also in $\mathcal{O}(N)$. Figure 1-b shows an approximately linear increase in run-time for JSP-WSR to converge, despite the sub-linear increase in number of iterations. This confirms the predominant contribution of the per-iteration complexity in $\mathcal{P}_5^{\text{WSR}}$ to the total run-time. Moreover, table 2.3 confirms that JSP-WSR, in general, has a fast convergence rate (i.e., low-complexity). However, in some scenarios, JSP-WSR may not exhibit fast convergence (i.e., high complexity).

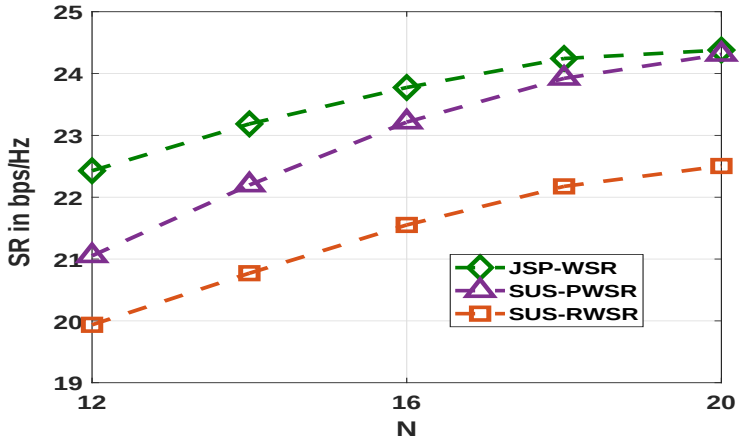

(a)

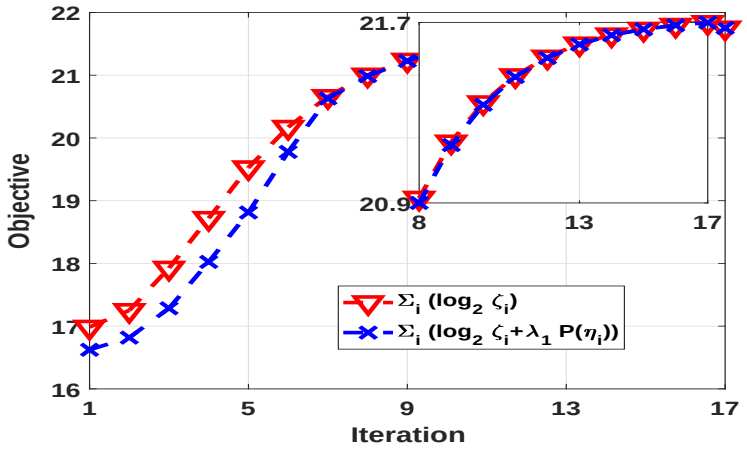

(b)

FIGURE 2.2: Comparison of various WSR optimization methods for uniform weighted case with $M = 10$, $\{\tilde{\epsilon}_i = 4\text{dB}\}_{i=1}^{N}$, $P_T = 10\text{dB}$ (a) N varying from 12 to 20. (b) convergence of the JSP-WSR (with penalty) and convergence of $\boldsymbol{\eta}$ to binary for $N = 20$.

In table 2.2, the performance of JSP-WSR is compared with ES-WSR and WSUS-WSR for $M = 3$, $\{\tilde{\epsilon}_i = 4\text{dB}\}_{i=1}^{N}$, $P_T = 10$ dB, and N is varied from 5 to 7 in steps of 1. Although the JSP-WSR is guaranteed to converge only to a stationary point theoretically, the results in table 2.2 confirms that these stationary points are indeed high-quality solutions. On the other hand, the

TABLE 2.2: Comparison of various WSR solutions for M =3, $\{\tilde{\epsilon}_i = 4\text{dB}\}_{i=1}^{N}$, $P_T = 10$ dB, and N varying from 5 to 7 .

Users in cell (N)	weighted sum rate in bps/Hz		
	ES-WSR	JSP-WSR	WSUS-WSR
$N = 5$	5.83	5.67	5.32
$N = 6$	6.51	5.97	5.59
$N = 7$	6.64	6.33	6.02

TABLE 2.3: Convergence rate of JSP-WSR for $M = 10$, $\{\tilde{\epsilon}_i = 4\text{dB}\}_{i=1}^{N}$, $P_T = 10$ dB as a function of N.

Number of users in a cell	Average number of iterations to converge
$N = 15$	16
$N = 20$	20.3
$N = 25$	22.5
$N = 30$	24.8

shortcomings of the decoupled solution i.e., WSUS-WSR, leads to a large performance gap from both ES-WSR and JSP-WSR.

The performance of the JSP-WSR is illustrated for uniform weighted case i.e. $\{\alpha_i = 1\}_{i=1}^{N}$ in figure 2.2(a) as a function of N. The performance gain by jointly updating scheduling and precoding in JSP-WSR over the decoupled SUS-WSR and SUS-RWSR is clear from figure 2.2(a). However, as N increases ($N \approx 20$), SUS schedules the users with strong channel gains and least interference; hence SUS-WSR performs close to JSP-WSR. Despite the efficiency of SUS in the region around $N = 20$, SUS-RWSR performs poor due to the inefficiency of the RWSR precoding scheme.

Figure 2.2(b) illustrates the convergence behavior of the JSP-WSR and the convergence of $\boldsymbol{\eta}$ to binary values as a function of iterations. The SR obtained in each iteration is shown by the red curve while the penalized SR is shown by the blue curve. As the FIP of JSP-WSR contains a non-binary $\boldsymbol{\eta}$, the solutions obtained in the initial iterations include the non-binary $\boldsymbol{\eta}$; hence, the difference between SR (red curve) and SR plus penalty (blue curve). However, as the penalty factor (λ_1) increases over the iterations, JSP-WSR favors the solutions with binary η_is. As a result, the penalty approaches zero over the iterations i.e., $\mathbb{P}(\eta_i) \approx 0, \forall i$. This behavior is clear from iteration 8 onwards. Moreover, the convergence behavior of the JSP-WSR to a stationary point of $\mathcal{P}_5^{\text{WSR}}$ is shown by the convergence of the blue curve which depicts its objective value.

2.5.7 MMSINR Performance Evaluation

Figure 2.3 illustrates the weighted MSINR of the scheduled users (averaged over 500 different CRs and referred to as average weighted MSINR) as a function of SINR levels. For SINR level 1, 2, 3 and 4, the weight β_i associated with user i is randomly drawn from the sets $\{1\}$, $\{0.5, 1\}$, $\{0.333, 0.6666, 0.9999\}$ and $\{0.25, 0.5, 0.75, 1\}$ respectively. For example, for SINR levels 2, β_i is randomly selected from $\{0.5, 1\}$. Hence the MMSINR requirement of each user is $\tilde{\epsilon}_i/0.5$ or $\tilde{\epsilon}_i$ (also $\tilde{\epsilon}_i = 1$). Notice that a higher value of β_i increases the likeliness of user i being scheduled.

The performance of JSP-MMSINR is compared with SUS-MMSINR and WSUS-MMSINR for $M = 10$, $\{\tilde{\epsilon}_i = 1\ (0\text{ dB})\}_{i=1}^{N}$, $P_T = 10$dB and $N = 15$ in figure 2.3(a) and $N = 20$ in figure 2.3(b). It is clear from figure 2.3(a) and 2.3(b) , that the joint solution JSP-MMSINR improves the performance over the decoupled design RUS-MMSINR, SUS-MMSINR, and WSUS-MMSINR. Despite identical underlying precoding scheme in JSP-MMSINR, RUS-MMSINR, SUS-MMSINR, and WSUS-MMSINR, the systematic approach of joint scheduling and precoder update considering the weights helps JSP-MMSINR to achieve better performance. The naive user

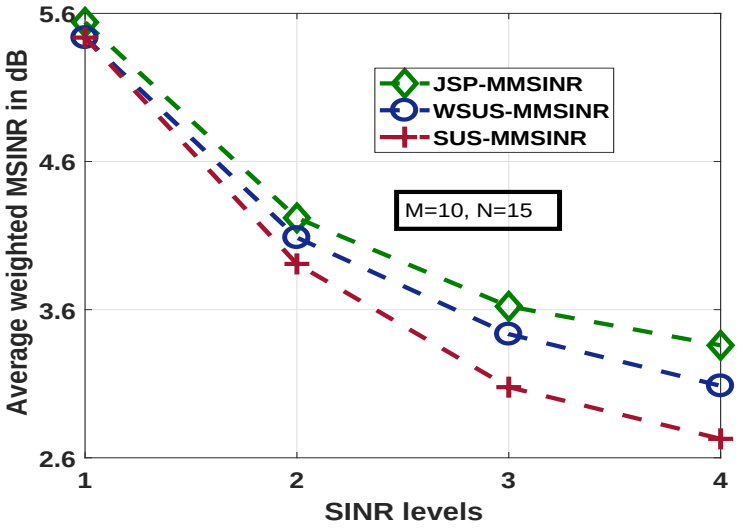

(a)

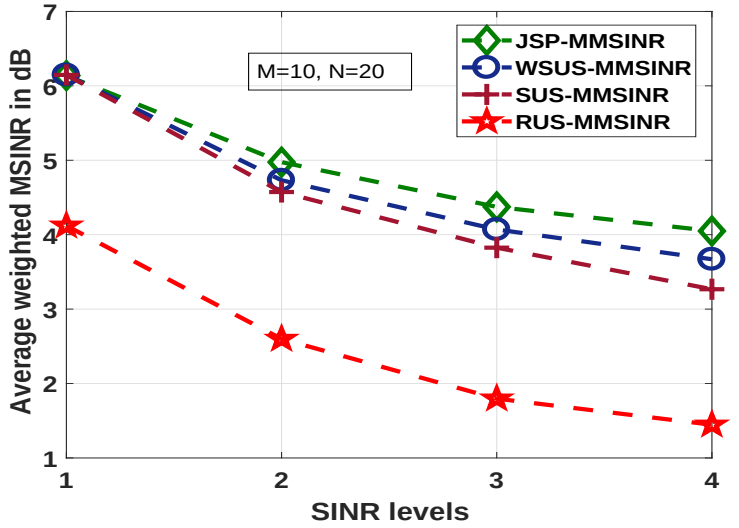

(b)

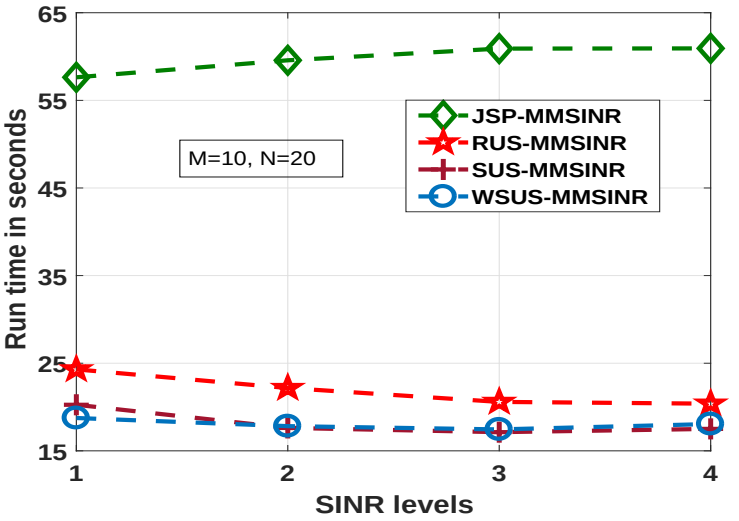

(c)

FIGURE 2.3: Comparison of different MMSINR optimization approaches for $P_T = 10$dB, $\{\bar{\epsilon}_i = 0\text{dB}\}_{i=1}^{N}$ and SINR levels are varied from 1 to 4 (a) $N = 15$ (b) $N = 20$ (C) algorithm run time.

TABLE 2.4: Performance of various MMSINR solutions for M =3, SINR level 4, P_T = 10dB and N varying from 5 to 7

Users in cell (N)	Average MSINR in dB with		
	ES-MMSINR	JSP-MMSINR	WSUS-MMSINR
$N = 5$	5.23	5.15	4.63
$N = 6$	5.95	5.79	5.03
$N = 7$	6.71	6.56	5.99

Users in cell (N)	Average power consumed in dB with		
	ES-PMIN	JSP-PMIN	WSUS-PMIN
$N = 5$	5.4477	5.99	6.2448
$N = 6$	5.116	5.6164	5.8771
$N = 7$	3.95	4.5365	5.1270

TABLE 2.5: Performance comparison of various PMIN solutions for M =3, SINR level 4 and N is varied from 5 to 7.

scheduling based method i.e., RUS-MMSINR clearly performs poorer than other benchmark methods. Although WSUS-MMSINR achieves better performance over SUS-MMSINR by considering the weights into scheduling, it still performs worse than JSP-MMSINR showing the inefficiency of decoupled design. The gains obtained by JSP-MMSINR compared to best performing decoupled method i.e., WSUS-MMSINR amounts up to 10% (figure 2.3(b), SINR level 4).

In figure 2.3(c), the run time of the algorithms is illustrated as a function of SINR levels for $M = 10$, $N = 20$ and $P_T = 10$dB. Figure 2.3(c) shows that the gains of JSP-MMSINR are achieved at the expense of high computational complexity as illustrated in figure 2.3(c). Moreover, the complexity of JSP-MMSINR increases as SINR levels increase. The increase in SINR levels enforces the inclusion of users with higher SINR requirement since the users with lower SINR requirement may not be sufficient to schedule exactly M users. Hence, JSP-MMSINR takes relatively longer time to converge compared lower SINR levels.

The performance of JSP-MMSINR is illustrated for uniform weighted case i.e., $\{\beta_i = 1\}_{i=1}^{N}$ in figure 2.4 for $M = 10$ and $P_T = 10$dB. In figure 2.4(a), the average MSINR is illustrated as a function of N varying from 12 to 18 in steps of 2. The superior performance of JSP-MMSINR over SUS-MMSINR is clear from 2.4(a). However, the gains diminish as N increases as the SUS based solution becomes efficient as mentioned previously.

In figure 2.4(b), the convergence behavior of the algorithm and progression towards achieving exact scheduling constraint i.e., $\sum_{i=1}^{N} \eta_i == M$ are illustrated as a function of the iteration number. While the blue curve depicts the inverse of MSINR (i.e., t in $\mathcal{P}_4^{\text{MM}}$) achieved over the iteration, the red curve depicts the penalized objective where the penalty aims to satisfy the constraint of scheduling exactly M users. As FIPs violate the exact scheduling constraint, the penalized objective (red curve) is far from the objective (blue curve). However, increasing the penalty parameter Ω over the iterations until $\Omega \leq 20$ ensures the scheduling constraint. This behavior is observed from iteration 8 in figure 2.4(b) as the difference between penalized objective and objective is approximately zero. Moreover, the binary nature of $\boldsymbol{\eta}$ is also achieved over the iterations due to nature of MMSINR for fixed $\lambda_2 = 0$ in figure 2.3 and 2.4.

Table 2.4 compares the performance of JSP-MMSINR, WSUS-MMSINR and ES-WSR for $M = 3$, SINR level 4, $P_T = 10$ dB. The relatively similar performance of JSP-MMSINR and ES-MMSINR confirms the efficiency of JSP-MMSINR and high-quality nature of stationary points that the JSP-MMSINR converges to.

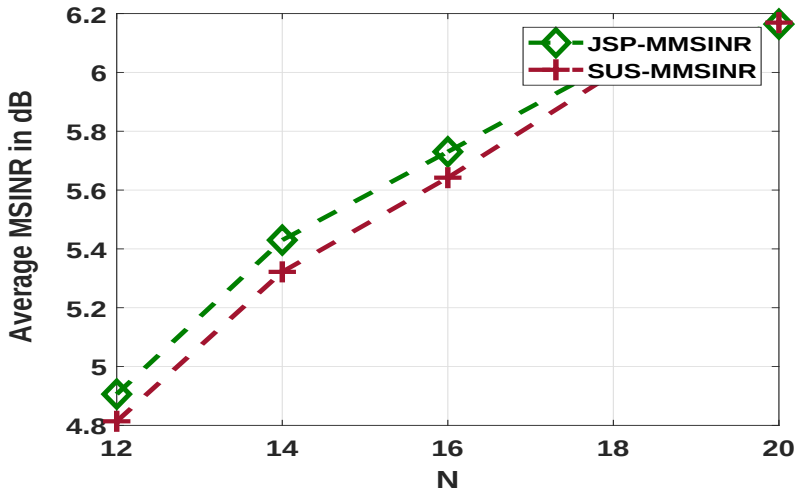

(a)

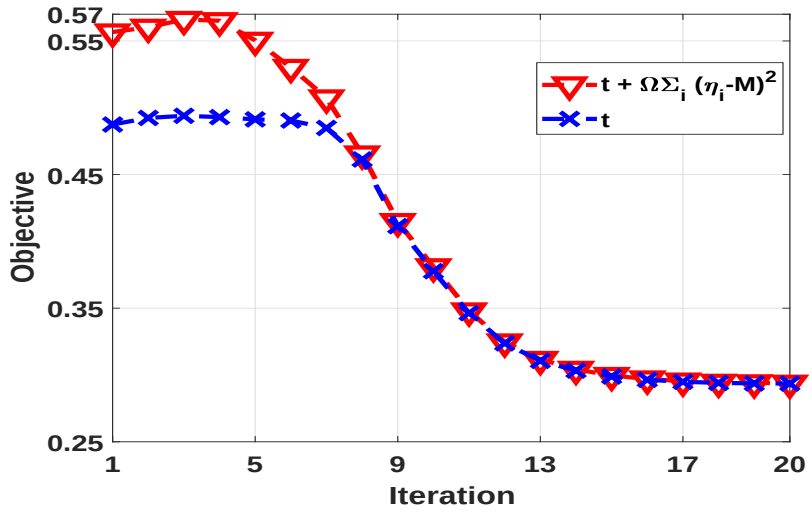

(b)

FIGURE 2.4: Comparison of MMSINR for uniform weighted case, $M = 10$, $\beta_i = 1, \tilde{\epsilon}_i = 0$ dB, $\forall i$, $P_T = 10$ dB (a) N varies from 12 to 20. (b) Convergence of the JSP-MMSINR (with penalty) and convergence of $\boldsymbol{\eta}$ to binary for $N = 20$.

2.5.8 PMIN Performance Evaluation

The total power consumed by the scheduled users (for each channel realization) is averaged over 500 channel realizations (CRs) which is referred to as average total power per CR. In figure 2.5, the average total power per CR is depicted as a function of SINR levels for $M = 10$, $N = 15$ in figure 2.5(a) and $N = 20$ in figure 2.5(b). The SINR level 1, 2, 3 and 4 (chosen differently than MMSINR design) on the x-axis indicate that $\tilde{\epsilon}_i$ is randomly chosen from the sets $\{1\}$, $\{1, 2\}$, $\{1, 2, 3\}$ and $\{1, 2, 3, 4\}$ for user i respectively. For example, for the SINR level 2, $\tilde{\epsilon}_i$ for user i is randomly chosen from the set $\{1, 2\}$.

Figure 2.5(a) and 2.5(b) clear shows that the joint solution JSP-PMIN outperforms RUS-PMIN, SUS-PMIN and WSUS-PMIN. Although the precoding problem for the scheduled users by RUS, SUS, and WSUS is solved globally using [8], the inefficient scheduling leads to poorer performance compared to JSP-PMIN. On the contrary, the system design in JSP-PMIN helps to gain up to 25% (SINR level 4, figure 2.5(b)) in comparison with WSUS-PMIN. In figure 2.5(c), the run time of algorithms is illustrated in seconds as a function of SINR levels. As shown in

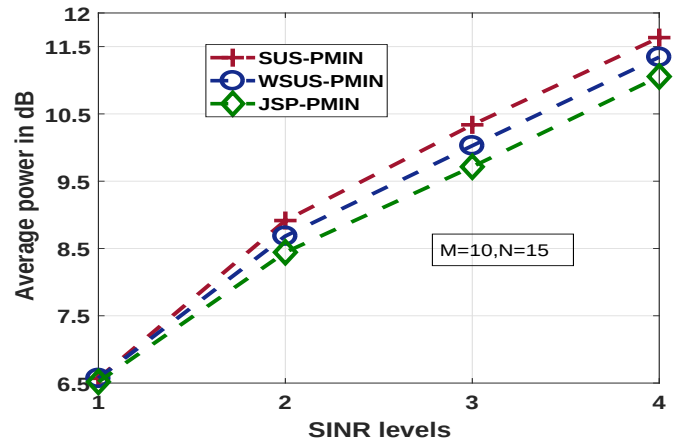

(a)

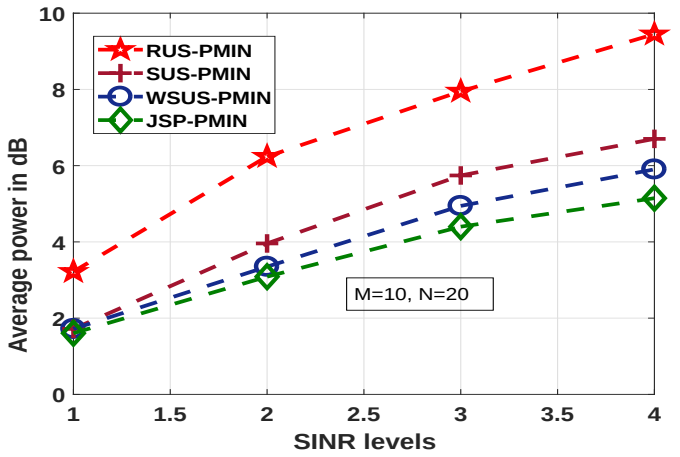

(b)

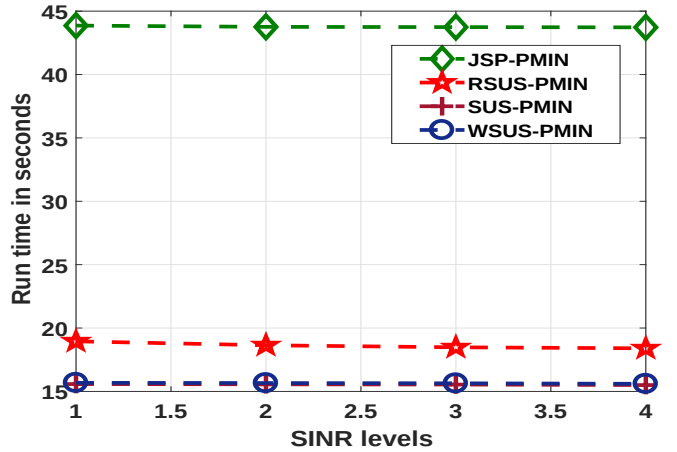

(c)

FIGURE 2.5: Comparison of different PMIN optimization approaches for $M = 10$, $P_T = 10$ dB and SINR levels varying from 1 to 4 (a) $N = 15$ (b) $N = 20$ (c) algorithm run time.

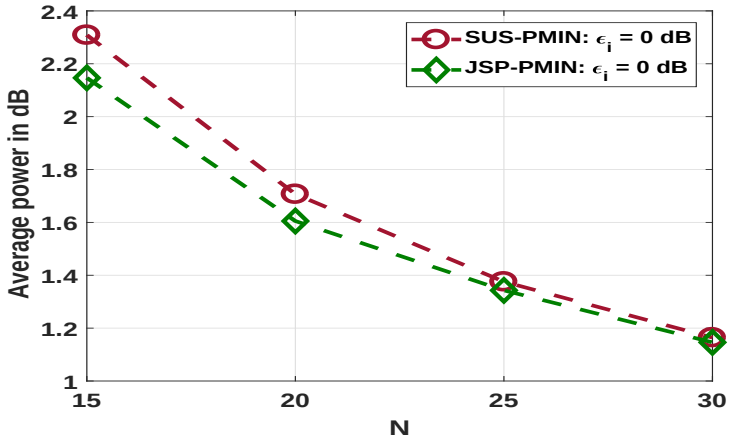

(a)

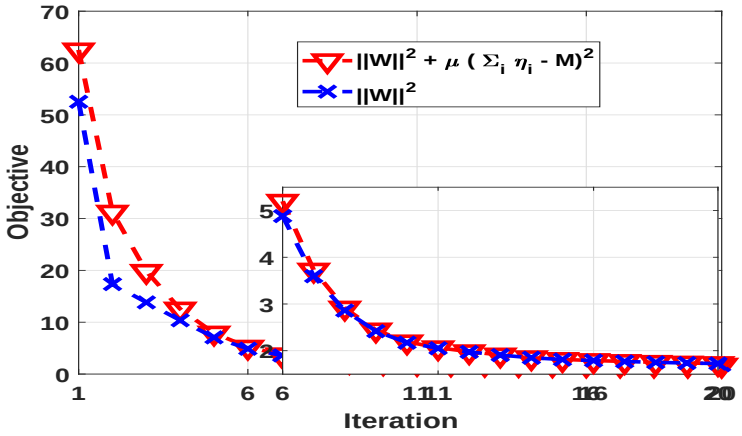

(b)

FIGURE 2.6: Comparison of different PMIN optimization approaches for $M = 10$, $P_T = 10$dB and $\{\epsilon_i = 0\text{dB}\}_{i=1}^{N}$ (a) N varying from 10 to 30 in steps of 5 (b) convergence of the JSP-PMIN (with penalty) and convergence of $\boldsymbol{\eta}$ to binary for $N = 15$.

figure 2.5(c), the performance gains of JSP-MMSINR incur higher computational complexity.

In table 2.5, the performance of JSP-PMIN and WSUS-PMIN is compared with ES-PMIN for $M = 5$, $\tilde{\epsilon}_i \in \{0, 1, 2, 3\}, \forall i$ for different N. Despite the theoretical guarantees of convergence JSP-PMIN only to a stationary point, JSP-PMIN performs close to ES-PMIN as can be observed in table 2.5. This justifies the efficiency of JSP-PMIN approach.

The performance JSP-PMIN for uniform weighted case (i.e., all users with same MSINR requirement) is illustrated in figure 2.6 for $M = 10$ and $\{\tilde{\epsilon}_i = 1\}_{i=1}^{N}$. In figure 2.6(a), the average total power per CR in dB is depicted as a function of N varying from 15 to 30 in steps of 5. The superior performance of JSP-PMIN over SUS-PMIN is clear from figure 2.6(a). However, the gains diminish as N increases as the SUS based scheduling becomes efficient (kindly refer to similar discussion on WSR results).

In figure 2.6(b), the convergence behavior of the JSP-PMIN algorithm (red curve) and the progression towards ensuring the exact scheduling constraint is depicted as a function of iterations for $N = 15$. The FIP may include the solutions that violate exact scheduling constraint due to which the penalized objective and objective differs by a large factor in the initial iterations. However, the increment in the penalty parameter μ ensures the exact scheduling constraint over the iterations. This is confirmed by figure 2.6(b), as the difference between penalized objective and objective, becomes approximately zero. For the reasons at the beginning of this section, $\lambda_3 = 0$ still achieves the binary nature of $\boldsymbol{\eta}$ over iterations.

2.6 Conclusions

In this paper, the joint scheduling and precoding problem was considered for multiuser MISO downlink channels for three performance optimization criteria: weighted sum rate maximization, maximization of minimum SINR and power minimization. Unlike the existing works, the design is formulated in a way that is amenable to the joint update of scheduling and precoding. Observing that the original optimization to be an instance of the MINLP problem for the three considered criteria, the paper proposed efficient reformulations and relaxations to transform these into structured DC programming problems. Subsequently, the paper proposed joint scheduling and precoding CCP based algorithms (JSP-WSR, JSP-MMSINR, and JSP-PMIN) which are guaranteed to converge to a stationary point for the aforementioned DC problems. Finally, the paper proposed a low-complexity procedure to obtain a good feasible initial point, critical to the implementation of CCP based algorithms. Through simulations, the paper established the efficacy of the proposed joint techniques with respect to the decoupled benchmark solutions.

3

Joint user grouping, scheduling and precoding for multigroup multicast scenario

3.1 Introduction

The adaptation of full-spectrum reuse and multi-antenna technologies result in significantly improved spectral efficiency (SE). On the other hand, the demand for green communications necessitates achieving these high SEs with limited energy [68]. In this regard, energy efficiency (EE), which measures the performance in throughput/Watts, becomes a key factor to be considered in the next-generation wireless networks [69]. Notice that the power minimization or energy minimization is also referred to as energy efficiency in the literature. The aforementioned EE which measure the performance in throughput/Watts is the focus of this paper.

On the other hand, in some scenarios like live-streaming of popular events, multiple users are interested in the same data. Realizing that multicasting such information to groups of users leads to better utilization of the resources, physical layer multigroup multicasting (MGMC) has been proposed in [29, 30]. Noticing the significant improvement in EE, multicasting has been adopted into 3GPP standards [70]. However, the following challenges need to be addressed to fully leverage the gains of MGMC:

- Inter-group interference: The co-channel users in different groups generate interference across the groups which is referred to as inter-group interference (IGI). A study of IGI is essential as it fundamentally limits the minimum rate of the groups that can be achieved [31] and, hence, the total throughput of the network. In this context, *user grouping* is a pivotal factor to be considered since it dominantly influences IGI [33, 34].

- Infeasibility: In a real scenario, each user needs to be served with a certain quality-of-service (QoS); failing to meet the QoS leads to retransmissions which significantly decrease the EE of the network. The severe IGI and/ or poor channel gains may thwart some users from meeting their QoS [31]. On the contrary, even in the cases with lower IGI, limited power may restrain the users from meeting their QoS [29]. Due to a combination of these three factors, the system may fail to satisfy the QoS requirements of all the users in all groups. This scenario is referred to as the infeasibility of the MGMC design in the literature [29,31]. The infeasibility of MGMC is crucial to the design and is, therefore, typically addressed by *user scheduling* (also referred to as admission control in the literature) [32, 33].

3.1.1 Joint user grouping, group scheduling and user scheduling for message-based MGMC systems

In this chapter, similar to [33, 71], a message based user grouping and scheduling are considered. In the message based MGMC model, each group is associated with a different message, and a user may be interested in multiple messages, thus requiring user grouping. Unlike [71] and similar to [33], a limited antenna BS system is considered with the number of groups being larger than the number of antennas at BS. Therefore, in a given transmit slot, only a few groups (equal to the number of antennas of BS) are scheduled; this is referred to as group scheduling. Further, a user that fail to satisfy the QoS requirements of subscribed group is simply excluded from the grouping; this is referred to as user scheduling. So, the considered model requires the design of user grouping, group scheduling, and user scheduling. User grouping, group scheduling, and user scheduling are inter-related. To see this, user grouping decides the achievable minimum signal-to-interference and noise ratio (SINR) of the groups (or IGI) which influences the group scheduling and user scheduling. Further, omitting or adding a user (i.e., user scheduling) in a group changes the IGI, thereby impacting group scheduling. Similarly, user scheduling in a group might necessitate the re-grouping of users (i.e., user grouping); this affects IGI and group scheduling. Furthermore, IGI is a function of precoding [34]. Therefore, the optimal performance requires the *joint design of user grouping, group scheduling, user scheduling, and precoding; this is compactly referred to as joint design in this paper*.

3.1.2 EE in the context of the joint design of user grouping, scheduling, and precoding

this chapter, for the reasons mentioned earlier, EE is considered as the measure of the system performance. All the existing works on EE maximization in MGMC systems [30,69,72–74], presume a particular user grouping and scheduling, therefore, the EE for MGMC systems is defined as the ratio of the sum of minimum throughput within each group and the total consumed energy. Notice that the existing EE definition accounts for only the minimum rate of a group ignoring the number of users in the groups (group sizes). However, in the context of user grouping and scheduling, group sizes need to be accounted for, in addition to their minimum rates. To comprehend the necessity, consider two groups with an equal minimum rate and a large difference in group sizes. According to the existing EE definition, the group with few users could be scheduled as the EE maximization is not biased to schedule a group with the larger size. However, from the network operator perspective, scheduling the group with more users results in efficient utilization of the resources. Moreover, the event of scheduling the group with few users is likely for EE maximization since it usually consumes less energy. However, if a large number of users can be served with a slight increase in energy, scheduling such a larger group improves the efficiency in the utilization of resources. The existing frameworks can not handle these scenarios as the number of users is not included in the EE definition. Noticing the drawbacks of existing EE definition, this chapter, a new metric called multicast energy efficiency (MEE) is proposed to account for the group sizes along with the minimum rates. In contrast to EE, in the numerator of MEE minimum throughput within a group times number of users in that group, is considered. Realizing the importance of MEE, this chapter, we consider the joint design of user grouping, scheduling, and precoding for MGMC systems subject to grouping, scheduling, quality-of-service (QoS) and total power constraints for the maximization of three design criteria: MEE, EE and scheduled users. In this context, related works in the literature and contributions/novelty of the paper are summarized in the sequel of this section.

3.1.3 Related works

Energy efficiency for MGMC systems

The EE maximization problem for MGMC systems was first addressed in the context of coordinated beamforming for multicell networks [72]. By definition, EE belongs to fractional programming. The authors in [72] used Dinkelbach's method to transform this fractional program to subtractive non-linear form and further solved the problem with an iterative algorithm wherein each iterate precoding and power vectors are updated alternatively. Later, this work is extended to the case of imperfect channel state information in [73]. Dinkelbach's method based transformation works efficiently if the denominator is a simple linear objective and numerator is convex otherwise it leads in a multi-level parametric iterative algorithm that is not efficient [75]. In [75], the authors optimized the EE for MGMC in multicell networks considering the rate-dependent processing power. The authors in [75] use successive convex approximation to transform fractional EE maximization problem as convex-concave programming in iteration k and further solved the subproblem using Charnes-Cooper transformation (CCT). In [69], EE maximization in a large antenna system with antenna selection is solved using SCA based CCT. Further, the authors in [69] addressed the boolean nature stemming from antenna selection by continuous relaxation and followed by thresholding. In [74], EE maximization for non-orthogonal layered-division multiplexing based joint multicast and the unicast system is considered. A pseudoconvex approach based parallel solution is developed for EE maximization in MIMO interference channels in [76]. EE user scheduling and power control is considered for multi-cell OFDMA networks for a unicast scenario in [77]. Moreover, precoding is not considered in [77]. The methodologies used in all these works are either SCA based CCT [69,72,75] or SCA based Dinkelbach's method [74,76,78]. Unlike the aforementioned works which assume the rate-dependent processing power to be a convex function of rate, a non-convex power consumption model is considered this chapter. Therefore, unlike EE maximization considered in the literature, MEE maximization considered this chapter belongs to mixed-integer fractional programming where the numerator is mixed-integer non-convex and denominator is also non-convex. Hence, the SCA based CCT can not be applied and Dinkelbach's method yields parametric multilevel iterative algorithms [76]. Moreover, the integer nature stemming from the user grouping and scheduling is different to the antenna selection problems (see [69] and references therein) and, hence, problem formulation and solution methodologies used in the antenna selection literature can not be employed.

User grouping, scheduling, and precoding for EE maximization in MGMC systems

this chapter, we consider the joint design of user grouping, group scheduling, user scheduling, and precoding for MEE maximization in message-based MGMC systems. Joint design of admission control and beamforming for MGMC systems was initially addressed in [32] for the power minimization problem. The authors in [32] addressed the admission control using binary variables and transformed the resulting mixed-integer non-linear problem (MINLP) into a convex problem using semidefinite programming (SDP) transformations; SDR based precoding is likely to include high-rank matrices for MGMC systems [79]; hence, the solutions may become infeasible to the original problems. Later, the design of user grouping and precoding without admission control is considered in [34] for satellite systems. However, the authors in [34] adopted the decoupled approach of heuristic user grouping followed by a semidefinite relaxation (SDR) based precoding. In [71], the authors considered the joint user grouping and beamforming without user scheduling for massive multiple-input multiple-output (MIMO) systems and proved that arbitrary user grouping is asymptotically optimal for max-min fairness criteria. However, the arbitrary grouping is not optimal for other design criteria and also not optimal for max-min criteria in the finite BS antenna system. Moreover, the underlying precoding problem in [32–34] is solved by SDR transformation, hence, as mentioned earlier the solutions may become infeasible to the original problems [79]. In [80], joint adaptive user grouping and beamforming is considered for MGMC

scenario in massive MIMO system. The authors in [80] adapted iterative approach wherein each iterate user grouping and beamforming are solved separately by decoupling the two problems. However, the EE or MEE maximization problem in the context of user grouping, scheduling, and precoding is not considered in the literature.

The system model considered in this chapter is similar to [33]. The authors in [33] considered the joint design for power minimization and its extension to EE maximization is not clear. Moreover, at the solution level, the problem is decoupled into user grouping and scheduling followed by SDR based precoding which is likely to include high-rank matrices for MGMC systems [79]; hence, the solutions may become infeasible to the original problems. In our previous work [81], we considered the joint design of scheduling and precoding for the unicast scenario to optimize sum rate, Max-min SINR, and network power. In [81], scheduling is addressed by bounding the power of the precoder with the help of a binary variable. However, in the MGMC system, each precoder is associated with a group of users, hence, the same method can not be employed. Moreover, the MEE or EE maximization in the context of user grouping, scheduling, and precoding belongs to mixed-integer fractional programming which is not dealt in [81], and its extension to proposed system model is not clear. Furthermore, the proposed MEE belongs to Mixed-integer fractional programming problems with a mixed-integer non-convex objective in the numerator and a non-convex objective in the denominator. Therefore, the MEE maximization problem considered this chapter is significantly different from [81] in terms of the system model, performance metric of optimization, problem formulation, and the nature of the optimization problem. Hence, the solution in [81] can not be applied directly here. The MEE maximization problem considered for the joint design this chapter is highly complex as it inherits the complications of user grouping, group scheduling and user scheduling, and EE problems, and poses additional challenges.

3.1.4 Contributions

Below we summarize the contribution on the joint design of user grouping, scheduling, and precoding for the MGMC system to maximize the MEE and EE as follows:

- Noticing that the existing EE definition accounts only for the minimum rate of groups ignoring group size, in the context of user grouping and scheduling a new metric called MEE is proposed to account for the group sizes along with the minimum rate of the groups in the messaged-based MGMC systems [33]. Unlike the existing works e.g., [33, 75, 81], this results in a new mixed-Boolean fractional objective function posing additional challenges to the existing challenges in user grouping, scheduling, and EE designs.

- Further, unlike existing models which assumes rate-dependent processing power to be a convex function of rate [69, 72, 74, 75, 77], rate-dependent processing power is assumed to be a non-convex function of rate with admissible DC decomposition. Therefore, the considered power consumption model applies to a broader class of models.

- Inspired by the work in [81], user grouping, group scheduling, and user scheduling are addressed with the help of binary variables. Unlike [81], MEE maximization problems along with binary constraints result in a new mixed-Boolean fractional programming to which the existing SCA based CCT [75] can not be applied and Dinkelbach's [72] method results in the parametric multilevel iterative algorithm which is not efficient.

- The resulting mixed-Boolean fractional formulations are non-convex and NP-hard. Towards obtaining a low-complexity stationary solution, with the help of novel reformulations, the fractional and non-convex nature of the problems is transformed as DC functions. Further, Boolean nature is handled with appropriate relaxation and penalization. These reformulations render the joint design as a DC problem, a fact hitherto not considered.

- Finally, within the framework of the convex-concave procedure (CCP) [63] (which is a special case of SCA [82]), an iterative algorithm is proposed to solve the resulting DC problem wherein each iterate a convex problem is solved. A simple low-complexity non-iterative procedure to obtain a feasible initial point, which inherently establishes convergence of the proposed algorithms to a stationary point [54, 55], is proposed.

- The performance of the proposed algorithms affecting the three design aspects, namely MEE, EE, and number of scheduled users, and their typical quick convergence behavior (which confirms the low-complexity nature) are numerically evaluated through Monte-Carlo simulations.

3.2 System model

3.2.1 Message based user grouping and scheduling

We consider the downlink scenario of a single cell multiuser MISO system with M transmit base station (BS) antennas and $N\,(\geq M)$ users each equipped with a single receive antenna. In this chapter, similar to [33, 71], message-based user grouping, and scheduling is considered. In this context, it is assumed that each group is associated with a unique message. Therefore, the number of groups, say G, is equal to the number of messages. Further, each user is assumed to be interested in at least one message and a user may be interested in multiple messages. Despite the user's interest in multiple messages, a user is allowed to be a member of utmost one group in a given slot. This constraint is simply referred to as user grouping constraint (UGC). Letting $\mathcal{S}_\rangle$ to be the set of users belonging to message (group) i and ϕ to be the empty set, the UGC is formulated as $\mathcal{S}_\rangle \cap \mathcal{S}_| = \phi$, for $\rangle \neq |$. Further, to establish the relevance of the design to the real scenarios, a certain QoS requirement (typically depending on the type of service/application) on the messages is assumed. UGC also captures the worst-case scenario of a user failing to meet any QoS requirement associated with any of the interesting messages: hence, the user is simply not scheduled in the current slot. Therefore, UGC naturally leads to $\sum_{i=1}^{G} |\mathcal{S}_\rangle| \leq \mathcal{N}$. Further, it is assumed that $G \geq M$, hence, scheduling of exactly M groups out of G is considered. This constraint is simply referred to as group scheduling constraint (GSC).

User channels are assumed to constant and perfectly known. The noise at all users is assumed to be independent and characterized as additive white complex Gaussian with zero mean and variance σ^2. Furthermore, total transmit power at the BS is limited to P_T for each transmission. Finally, the BS is assumed to transmit independent data to different groups with $\mathbb{E}\{|x_i|^2\} = 1, \forall i$, where x_i is the message associated with group i. Let $\mathbf{w}_i \in \mathbb{C}^{M\times 1}$ be the precoding vector with group i and $\mathbf{W} = [\mathbf{w}_1, \ldots, \mathbf{w}_G]$, $\mathbf{h}_i \in \mathbb{C}^{M\times 1}$ be the downlink channel of user i, and $\gamma_{ij} = \dfrac{|\mathbf{h}_i^H \mathbf{w}_j|^2}{\sum_{l\neq j} |\mathbf{h}_i^H \mathbf{w}_l|^2 + \sigma^2}$ be the SINR of user i belonging to group j.

3.2.2 Power consumption model, Energy efficiency, and Multicast energy efficiency

Power consumption model

this chapter, we adopt the ideal power consumption model proposed in [75]. Let B be the bandwidth of the channel and $r_j = B\log_2\left(1 + \min_{i\in\mathcal{S}_j} \gamma_{ij}\right)$ be the minimum rate of group j. Notice that all the users in a group receive exactly the same message associated with the group. Therefore, the transmission rate of the message j to group j at the BS is simply the minimum rate of the group i.e., r_j. With defined notations, the power consumption at the BS is defined as

$$g(\mathbf{W}, \boldsymbol{r}) \triangleq P_0 + \sum_{j=1}^{G} \left(\frac{1}{\rho} \|\mathbf{w}_i\|^2 + \Pi p\left(r_j\right) \right), \tag{3.1}$$

where $\boldsymbol{r} = [r_1, \ldots, r_G]$, P_0 is the static power spent by the cooling systems, power supplies etc., $\rho < 1$ is the power amplifier efficiency, and $\Pi \geq 0$ is a constant accounting for coding and decoding power loss, and $p(r_j) = p_1(r_j) - p_2(r_j)$ is a differentiable non-negative difference-of-convex function of r_j reflecting the rate-dependent processing power of group j with $p(0) = 0$, and p_1 and p_2 are convex functions. Notice that unlike previous works e.g. [69,75,77] where $p(r_j)$ is assumed to be a convex functions, the considered model $g(\mathbf{W}, \boldsymbol{r})$ represents relatively broader class of rate-dependant power consumption models.

Energy efficiency

EE for MGMC systems is typically defined as a ratio of the throughput of the network to the energy consumed at the BS in the literature. Letting $\mathcal{T}$ to be the set of scheduled groups and B be the bandwidth of the channel, the EE is defined as (3.2).

$$\text{EE} \triangleq \frac{\sum_{j\in\mathcal{T}} B \log\left(1 + \min_{i\in\mathcal{S}_j} \gamma_{ij}\right)}{g(\mathbf{W}, \boldsymbol{r})}. \tag{3.2}$$

The numerator of the EE in (3.2) models the network's multicast throughput as the sum of the minimum throughput of all groups. So, this definition only accounts for the minimum throughput of a group ignoring its size.

Multicast energy efficiency

In the context of user grouping and scheduling for MGMC systems, the standard EE metric needs to be redefined to account for the size of the group. To understand this, consider a scenario of scheduling a group between two groups having the same minimum throughput, consuming the same energy and large difference in group sizes. The EE criterion does not discriminate between two groups. However, scheduling a group with a large number of users leads to better utilization of resources. So, to account for the number of users being served in each group along with its minimum rate, we propose a new metric called MEE for the MGMC systems. With the help of defined notations, MEE is formally defined as,

$$\text{MEE} \triangleq \frac{\sum_{j\in\mathcal{T}} \left(\Psi_j |\mathcal{S}_j| B \log\left(1 + \min_{i\in\mathcal{S}_j} \gamma_{ij}\right)\right)}{g(\mathbf{W}, \boldsymbol{r})}. \tag{3.3}$$

where Ψ_j is the weight associated with group j. The weights i.e., Ψ_js are introduced in MEE to address the fairness among the groups. For example, by choosing Ψ_1 to be relatively much larger than $\{\Psi_i\}_{j=2}^{G}$ scheduling of group 1 can be prioritized.

Interpretation of MEE as total received bits/Joule

From the physical layer transmission perspective, the network throughput (number of transmitted bits per second) in MGMC systems is same as unicast systems. In unicast scenario, the transmitted information is received by only one user. However, in MGMC scenario, the information transmitted to group j is received by $|\mathcal{S}_j|$ users. Hence, from the network operator perspective, throughput of group j in this multicast scenario is $|\mathcal{S}_j| B \log\left(1 + \min_{i\in\mathcal{S}_j} \gamma_{ij}\right)$ received bits per second. Motivated by this, the numerator of equation (3.3) i.e., $\sum_{j\in\mathcal{T}} \left(|\mathcal{S}_j| B \log\left(1 + \min_{i\in\mathcal{S}_j} \gamma_{ij}\right)\right)$ reflects the combined multicast throughput of all the groups i.e., network throughput, henceforth, simply referred to this chapter as multicast throughput. Similarly, MEE defined in (3.3) reflects MEE for MGMC systems. Thus, MEE can be seen as number of received bits for one joule of transmitted energy.

3.3 Multicast Energy Efficiency

In this section, at first, the joint design of user grouping, scheduling, and precoding is mathematically formulated to maximize the MEE subject to appropriate constraints on the number of groups, users per group, number of scheduled groups, power, and QoS constraints. This problem is simply referred to as the MEE problem. Further, with the help of useful relaxations and reformulations, the MINLP NP-hard MEE problem is transformed as a DC programming problem. Finally, within the framework of CCP, an iterative algorithm is proposed which guarantees to attain a stationary point of the original problem.

3.3.1 Problem formulation: MEE

The EE maximization problem, with the notations defined, in the context of user grouping, scheduling and precoding for the MGMC scenario in Section 3.2 is formulated as,

$$
\begin{aligned}
\mathcal{P}_1^{\text{MEE}}: & \max_{\{\mathbf{w}_j, \mathcal{S}_j\}_{j=1}^{G}} \frac{\sum_{j=1}^{G} \left(\Psi_j |\mathcal{S}_j| B \log\left(1 + \min_{i \in \mathcal{S}_j} \gamma_{ij}\right)\right)}{g(\mathbf{W}, \boldsymbol{r})} \\
\text{s.t. } C_1: & \ \mathcal{S}_i \cap \mathcal{S}_j = \phi, i \neq j, \forall i, \ \forall j, \\
C_2: & \ \|[|\mathcal{S}_1|, \ldots, |\mathcal{S}_G|]\|_0 = M, \\
C_3: & \ \log\left(1 + \gamma_{ij}\right) \geq \epsilon_j, \ i \in \mathcal{S}_j, \ \forall j, \\
C_4: & \ \sum_{j=1}^{G} \|\mathbf{w}_j\|^2 \leq P_T, \\
C_5: & \ \mathcal{S}_i \subset \{1, \ldots, N\}, \forall i,
\end{aligned}
\tag{3.4}
$$

where ϵ_j is the QoS requirement of group j, $\forall i$ refers to $i \in \{1, \ldots, N\}$ and $\forall j$ refers to $j \in \{1, \ldots, G\}$
Remarks:

- Constraint C_1 is the UGC; constrains a user to be a member of at most one group.
- Constraint C_2 is the GSC; it ensures the design to schedule exactly M groups.
- Constraint C_3 is the QoS constraint; it enforces the scheduled users in each group to satisfy the corresponding minimum rate requirement associated with the group. This enables the flexibility to support different rates on different groups. Hereafter, the constraint C_3 is simply referred to as QoS constraint. Moreover, the constraint C_3 together with C_1 ensure the USC.
- Constraint C_4 is the total power constraint (TPC); precludes the design from consuming the power in excess of available power i.e., P_T.

Necessity of low-complexity algorithms for joint design The problem $\mathcal{P}_1^{\text{MEE}}$ is combinatorial due to constraints C_1 and C_2. Hence, obtaining the optimal solution to $\mathcal{P}_1^{\text{MEE}}$ requires an exhaustive search-based user grouping and scheduling. To understand the complexity of the exhaustive search methods, assume that each user is interested in only one message. Further, let N_i be the number of users in the group i. Let $\mathcal{T}_i$ be the all possible scheduling subsets of $\mathcal{S}_i$, so the number of sets in $\mathcal{T}_i$ is $\sum_{j=0}^{N_i} \binom{N_i}{j}$ for $i \in \{1, \ldots, G\}$. So, the exhaustive search needs to be performed over the Cartesian product of sets $\mathcal{T}_i$s i.e., $\times_{i=1}^{G} (\mathcal{T}_i)$. It is easy to see that the exhaustive search algorithms quickly become impractical due to exponential complexity. This case merely a simple case of the problem considered in $\mathcal{P}_1^{\text{MEE}}$. Additionally, for each scheduled combination, the corresponding precoding problems in $\mathcal{P}_1^{\text{MEE}}$ need to be solved. Moreover, these precoding problems

are generally not only NP-hard but also non-convex [29]. Thus, in the sequel, we focus on developing low-complexity algorithms that are guaranteed to obtain a stationary point of the NP-hard and non-convex problem $\mathcal{P}_1^{\text{MEE}}$.

3.3.2 A mixed integer difference of concave formulation: MEE

In this section, firstly, avoiding the set notation by using binary variables the problem $\mathcal{P}_1^{\text{MEE}}$ is equivalently reformulated as an MINLP problem without the set notations. Further, with the help of a minimal number of slack variables and novel reformulations, the resulting MINLP problem is transformed as a difference-of-concave (DC) problem subject to binary constraints.

Towards transforming the MEE problem in $\mathcal{P}_1^{\text{MEE}}$ as DC a problem, let η_{ij} be the binary variable indicating the membership of user $i \in \{1,\ldots,N\}$ in group $j \in \{1,\ldots,G\}$. In other words, $\eta_{ij} = 1$ indicates that user i is a member of the group j and not a member otherwise. Since a user may not be interested in some groups, the η_{ij}s corresponding to these groups is fixed beforehand to zero. Hence, only a subset of the entries in $\boldsymbol{\eta}_i$ are the variables of the optimization. However, for the ease of notation, without the loss of generality, henceforth, we assume that each user is interested in all the groups. In other words, all the entries in $\boldsymbol{\eta}_i$ become variables of optimization. It is easy to see that this is only a generalization to the aforementioned case. Hence, a solution to this generalized problem is a solution to the aforementioned problem.

Letting Θ_j and ζ_j be the slack variables associated with minimum rate of group j respectively, and α_{ij} be the slack variable associated with SINR of user i of group j, the problem $\mathcal{P}_1^{\text{MEE}}$ is equivalently reformulated as,

$$\mathcal{P}_2^{\text{MEE}}: \max_{\mathbf{W},\boldsymbol{\Theta},\boldsymbol{\eta},\boldsymbol{\alpha},\boldsymbol{\zeta}} \frac{\sum_{j=1}^{M}\left(\sum_{i=1}^{N_i}\eta_{ij}\right)B\Psi_j\Theta_j}{g(\mathbf{W},\boldsymbol{\zeta})} \tag{3.5}$$

$$\text{s.t. } C_1: \eta_{ij}\in\{0,1\},\ \forall i,\ \forall j, \qquad C_2: \sum_{j=1}^{G}\eta_{ij}\le 1, \forall i,$$

$$C_3: \left\|\left[\sum_{i=1}^{N}\eta_{i1},\ldots,\sum_{i=1}^{N}\eta_{iG}\right]\right\|_0 = M, \qquad C_4: 1+\gamma_{ij}\ge\alpha_{ij},\ \forall i,\ \forall j,$$

$$C_5: \log\alpha_{ij}\ge\eta_{ij}\Theta_j,\ \forall i,\ \forall j, \qquad C_6: \Theta_j\ge\epsilon_j,\ \forall j,$$

$$C_7: \sum_{i=1}^{M}\|\mathbf{w}_i\|_2^2\le P_T, \qquad C_8:\ 0\le\zeta_j\le\left\|\sum_{i=1}^{N}\eta_{ij}\right\|_0 B\Theta_j, \forall j,$$

where $\boldsymbol{\Theta} = [\Theta_1,\ldots,\Theta_M]$, $\boldsymbol{\zeta} = [\zeta_1,\ldots,\zeta_M]$, $\boldsymbol{\eta} = [\boldsymbol{\eta}_1,\ldots,\boldsymbol{\eta}_G]$, $\boldsymbol{\eta}_i = [\eta_{i1},\ldots,\eta_{iG}]$, $\boldsymbol{\alpha} = [\boldsymbol{\alpha}_1,\ldots,\boldsymbol{\alpha}_G]$, and $\boldsymbol{\alpha}_i = [\alpha_{i1},\ldots,\alpha_{iG}]$

Remarks:

- Constraints C_1 and C_2 in $\mathcal{P}_2^{\text{MEE}}$ ensures the UGC. The constraint C_3 is the equivalent reformulation of GSC constraint C_2 in $\mathcal{P}_1^{\text{MEE}}$.
- For all the users that are not subscribed to group j (i.e., users with $\eta_{ij} = 0$), the constraint C_5 implies $\log\alpha_{ij}\ge 0$ which is satisfied by the definition of rate. On the contrary, for all the users subscribed to group j (i.e., users with $\eta_{ij} = 1$) constraint C_4 implies $\log\alpha_{ij}\ge\Theta_j$. Hence, Θ_j provides the lower bound for the minimum rate of the group. Moreover, at the optimal solution of $\mathcal{P}_2^{\text{MEE}}$, Θ_j is equal to the minimum rate of group j i.e., $\Theta_j = \min_{j\in\mathcal{S}_i}\log\alpha_{ij}$.
- In the objective of $\mathcal{P}_2^{\text{MEE}}$, the term $\sum_{i=1}^{N_i}\eta_{ij}$ is equivalent to $|\mathcal{S}_i|$. Since at the optimal solution $\Theta_j = \min_{j\in\mathcal{S}_i}\log\alpha_{ij}$, the objective in $\mathcal{P}_2^{\text{MEE}}$ is equivalent to the EE objective in $\mathcal{P}_1^{\text{MEE}}$.

- Constraint C_8 is introduced to address the rate-dependent processing power in $g(\mathbf{W}, \boldsymbol{r})$ in problem $\mathcal{P}_1^{\text{MEE}}$. For a unscheduled group j (i.e., $\left\|\sum_{i=1}^{N} \eta_{ij}\right\|_0 = 0$), from constraint C_8 $\zeta_j = 0$ and for a scheduled group i.e., ($\left\|\sum_{i=1}^{N} \eta_{ij}\right\|_0 = 1$) $\zeta_j = \Theta_j$ which is the minimum rate of the group.

Notice that the problem $\mathcal{P}_2^{\text{MEE}}$ is significantly different and much more complex than problems dealt in [33, 69, 71, 72, 75, 76, 81]. The MEE objective in $\mathcal{P}_2$ is unlike any EE objective in the literature (see [69, 72, 75, 76] and reference therein). The power consumption model $g(\mathbf{W}, \boldsymbol{r})$ and multicast throughput i.e., $\sum_{j=1}^{M} \left(\sum_{i=1}^{N_i} \eta_{ij}\right) B\Theta_j$ considered this chapter are non-convex and multicast throughput is a function of binary variables. Hence, SCA based CCT [69] can not be applied to $\mathcal{P}_2$ and Dinkelbach's methods [72] results in a parametric multi level iterative algorithm. Further, problem $\mathcal{P}_2$ differs from [81] where the binary variables are only associated with precoding and SINR terms. The transformation to deal with the MEE objective, constraint C_3 and C_8 are not dealt in [81]. The problem $\mathcal{P}_2^{\text{MEE}}$ inhibits the complexities associated with EE problems and user grouping and scheduling problems, hence, much more challenging than standalone EE and user grouping and scheduling problems.

The reformulation given in $\mathcal{P}_2^{\text{MEE}}$ is equivalent to $\mathcal{P}_1^{\text{MEE}}$ that the optimal solution of $\mathcal{P}_2$ is also the optimal solution of $\mathcal{P}_1$. Hence, the problem $\mathcal{P}_2$ is an equivalent reformulation of $\mathcal{P}_1$. The problem $\mathcal{P}_2$ is combinatorial due to constraint C_1 and C_3, and non-convex due to constraint C_3, C_4 and the objective. Letting δ_i to be the slack variable associated with group i and t to be the slack variable associated with power consumption, $\mathcal{P}_2$ is transformed into a DC problem subject to binary constraints as,

$$\mathcal{P}_3^{\text{MEE}}: \max_{\mathbf{W},\boldsymbol{\Theta},\boldsymbol{\eta},\boldsymbol{\delta},\boldsymbol{\alpha},\boldsymbol{\zeta}} \sum_{i=1}^{N}\sum_{j=1}^{G} f(\eta_{ij}, \Theta_j, t) \triangleq B\Psi_j \frac{(\eta_{ij}+\Theta_j)^2 - \eta_{ij}^2 - \Theta_j^2}{2t} \tag{3.6}$$

$$\text{s.t. } C_1: \eta_{ij} \in \{0,1\},\ \forall i,\ \forall j; \qquad C_2: \sum_{j=1}^{G} \eta_{ij} \leq 1, \forall i;$$

$$C_3: \sum_{i=1}^{N} \eta_{ij} \leq \delta_j N, \forall j, \qquad C_4: \delta_j \in \{0,1\}, \forall j;$$

$$C_5: \sum_{l\neq i} |\mathbf{h}_i^H \mathbf{w}_l|^2 + \sigma^2 \leq \mathcal{J}_{ij}(\mathbf{W}, \alpha_{ij}),\ \forall i,\ \forall j, \qquad C_6: \sum_{j=1}^{M} \|\mathbf{w}_j\|_2^2 \leq P_T,$$

$$C_7: (\eta_{ij}+\Theta_j)^2 - 2\log\alpha_{ij} \leq \eta_{ij}^2 + \Theta_j^2,\ \forall i,\ \forall j, \qquad C_8: \Theta_j \geq \delta_j \epsilon_j,\ \forall j,$$

$$C_9: \frac{\zeta_j}{B} + \delta_j^2 + \Theta_j^2 \leq (\delta_j + \Theta_j)^2,\ \forall j,$$

$$C_{10}: P_0 + \sum_{j=1}^{G}\left(\frac{1}{\rho}\|\mathbf{w}_j\|^2 + \Pi\ (p_1(\zeta_j) - p_2(\zeta_j))\right) \leq t,$$

$$C_{11}: \sum_{j=1}^{G} \delta_j = M,\ \forall j,$$

where $\mathcal{J}_{ij}(\mathbf{W}, \alpha_{ij}) \triangleq \dfrac{\sum_{l=1}^{G} |\mathbf{h}_i^H \mathbf{w}_l|^2 + \sigma^2}{\alpha_{ij}}$, $\boldsymbol{\delta} = [\delta_1, \ldots, \delta_G]^T$. In constraint C_3 in $\mathcal{P}_3^{\text{MEE}}$, the binary slack variable δ_j is used for controlling the scheduling of group j. In other words, $\delta_j = 0$ indicates that group j is not scheduled else scheduled. However, for scheduled group j (i.e., $\delta_j = 1$) constraint C_3 becomes superfluous as it is always satisfied. With the help C_3 and C_4, constraint C_{10} ensures that number of scheduled groups is exactly M. The constraint C_9 in $\mathcal{P}_3^{\text{MEE}}$ is the DC reformulation of $\zeta_j \leq B\delta_j\Theta_j, \forall j$.

3.3.3 Continuous DC using relaxation and penalization: MEE

Ignoring the combinatorial constraints C_1 and C_4, the constraint set of $\mathcal{P}_3^{\text{MEE}}$ can be seen as a DC problem. So, the stationary points of such DC problems can be efficiently obtained by convex-concave procedure (CCP). With the aim of adopting the CCP framework, the binary constraints C_1 and C_4 in $\mathcal{P}_4^{\text{MEE}}$ are relaxed to box constraint between 0 and 1 i.e., $[0, 1]$. The CCP framework can be readily applied to this relaxed continuous problem; however, the obtained stationary points might yield non-binary δ_js and η_{ij}s. Although, a quantization procedure can be used to obtain binary δ_js and η_{ij}s, the resulting solutions may not be even feasible to $\mathcal{P}_1^{\text{MEE}}$. Therefore, obtaining binary δ_js and η_{ij} in the relaxed problem is crucial to ensure that the obtained solution are feasible to the original problem $\mathcal{P}_2^{\text{MEE}}$. Therefore, the relaxed variables δ_js and η_{ij}s are further penalized to encourage the relaxed problem to include binary δ_js and η_{ij}s in the final solutions. Letting $\lambda_1 > 0$ and $\lambda_2 > 0$ be the penalty parameters respectively and $\mathbb{P}(.)$ be the penalty function, the penalized continuous formulation of $\mathcal{P}_4^{\text{MEE}}$ is,

$$\mathcal{P}_4^{\text{MEE}}: \max_{\mathbf{W},\boldsymbol{\Theta},\boldsymbol{\eta},\boldsymbol{\delta},\boldsymbol{\alpha},\boldsymbol{\zeta},t} \sum_{i=1}^{N}\sum_{j=1}^{G} f(\eta_{ij},\Theta_j,t) + \sum_{j=1}^{G}\sum_{i=1}^{N}\lambda_1\mathbb{P}(\eta_{ij}) + \lambda_2\sum_{j=1}^{G}\mathbb{P}(\delta_j) \tag{3.7}$$
$$\text{s.t. } C_1: 0 \le \eta_{ij} \le 1,\ \forall i,\ \forall j, \quad C_4:\ 0 \le \delta_j \le 1, \forall j, \quad C_2, C_3, C_5 \text{ to } C_{11} \text{ in (3.6)}$$

It is easy to see that any choice of convex function $\mathbb{P}(\eta_{ij})$ that promotes the binary solutions suffice to transform $\mathcal{P}_4^{\text{MEE}}$ as a DC problem of our interest. The entropy based penalty function proposed in Chapter 2 i.e., $\mathbb{P}(\eta_{ij}) \triangleq \eta_i \log \eta_{ij} + (1-\eta_{ij})\log(1-\eta_{ij})$ is considered for this work. With this choice of $\mathbb{P}(\eta_{ij})$, the problem $\mathcal{P}_4^{\text{MEE}}$ becomes a DC problem. In order to apply the CCP framework to the problem $\mathcal{P}_4^{\text{MEE}}$, a feasible initial point (FIP) needs to supplied. However, the constraint C_5 in $\mathcal{P}_4^{\text{MEE}}$ limits the choices of FIPs. For ease of finding the FIPs, the constraint C_{10} is brought into the objective with another penalty parameter $\Omega_1 > 0$ as,

$$\begin{aligned}\mathcal{P}_5^{\text{MEE}}: \max_{\mathbf{W},\boldsymbol{\Theta},\boldsymbol{\eta},\boldsymbol{\delta},\boldsymbol{\alpha},\boldsymbol{\zeta},t} & \sum_{i=1}^{N}\sum_{j=1}^{G} f(\eta_{ij},\Theta_j,t) + \lambda_2\sum_{j=1}^{G}\mathbb{P}(\delta_j) \\ & + \sum_{j=1}^{G}\sum_{i=1}^{N}\lambda_1\mathbb{P}(\eta_{ij}) - \Omega_1\left\|\sum_{j=1}^{G}\delta_j - M\right\|^2 \\ \text{s.t. } & C_1 \text{ to } C_{10} \text{ in (3.7)}\end{aligned} \tag{3.8}$$

3.3.4 A CCP based Joint Design Algorithm: MEE

In this section, a CCP based algorithm is proposed for joint user grouping, scheduling and precoding for MEE (JGSP-MEE) problem given in problem (3.8). CCP proposed in [63] is a special case of successive convex approximation framework [82] designed for DC programming problem. So, CCP is an iterative framework where in each iteration convexification and optimization steps are applied to the DC problem until the convergence. The convexification and optimization steps of $\mathcal{P}_5^{\text{MEE}}$ of JGSP-MEE at the iteration k is given as,

- Convexification: Let $(\mathbf{W}, \boldsymbol{\eta},\ \boldsymbol{\delta}, \boldsymbol{\Theta}, \boldsymbol{\alpha}, , t)^{k-1}$ be the estimates of $(\mathbf{W}, \boldsymbol{\eta},\ \boldsymbol{\delta}, \boldsymbol{\Theta}, \boldsymbol{\alpha}, t)$ in iteration $k-1$ respectively. In iteration k, the functions $\mathbb{P}(\delta_j), \mathbb{P}(\eta_{ij}), p_2(\zeta_j)$ and $f(\eta_{ij},\Theta_j,t)$ are replaced their first Taylor approximations $\tilde{\mathbb{P}}^k(\eta_{ij}), \tilde{\mathbb{P}}^k(\delta_j), \tilde{p}_2(\zeta_j)$, and $f^k(\eta_{ij},\Theta_j,t)$ respectively which are given in Appendix I. Similarly, the concave parts in of C_5, C_7 and C_9 in $\mathcal{P}_5^{\text{MEE}}$ are replayed their first Taylor approximations $\tilde{\mathcal{G}}_{ij}^k(\eta_{ij},\Theta_j), \tilde{\mathcal{K}}_{ij}^k(\delta_j,\Theta_j), \tilde{\mathcal{J}}_{ij}^k(\mathbf{W},\alpha_{ij})$ respectively given in Appendix I.

- Optimization: Updated $(\mathbf{W}, \boldsymbol{\alpha}, \boldsymbol{\Theta}, \boldsymbol{\eta}, \boldsymbol{\delta}, t)^{k+1}$ is obtained by solving the following convex problem,

$$\mathcal{P}_6^{\text{MEE}}: \max_{\mathbf{W},\boldsymbol{\Theta},\boldsymbol{\zeta},\boldsymbol{\eta},\boldsymbol{\delta},\boldsymbol{\alpha},t} \sum_{i=1}^{N}\sum_{j=1}^{G}\left(f^k\left(\eta_{ij},\Theta_j,t\right)+\lambda_1\tilde{\mathbb{P}}^k\left(\eta_{ij}\right)\right) - \Omega_1\left\|\sum_{j=1}^{G}\delta_j - M\right\|^2 + \sum_{j=1}^{G}\lambda_2\tilde{\mathbb{P}}^k\left(\delta_j\right) \tag{3.9}$$

$$\text{s.t. } C_1 \text{ to } C_4 \text{ and } C_6, C_8 \text{ in (3.8)},$$

$$C_5: \sum_{l\neq i}|\mathbf{h}_j^H\mathbf{w}_l|^2+\sigma^2 \leq \tilde{\mathcal{J}}_{ij}^k(\mathbf{W},\alpha_{ij}),\ \forall i,\ \forall j,$$

$$C_7: \left(\eta_{ij}+\Theta_j\right)^2 \leq 2\log\alpha_{ij}+\tilde{\mathcal{G}}_{ij}^k(\eta_{ij},\Theta_j),\ \forall i,\ \forall j.$$

$$C_9: \frac{\zeta_j}{B}+\delta_j^2+\Theta_j^2 \leq \tilde{\mathcal{K}}_{ij}^k(\delta_j,\Theta_j),\ \forall j,$$

$$C_{10}: P_0+\sum_{j=1}^{G}\left(\frac{1}{\rho}\|\mathbf{w}_j\|^2+\Pi\ \left(p_1\left(\zeta_j\right)-\tilde{p}_2\left(\zeta_j\right)\right)\right) \leq t,$$

The proposed CCP based JGSP-MEE algorithm iteratively solves the problem in $\mathcal{P}_6^{\text{MEE}}$. However, to guarantee its convergence to a stationary point JGSP-MEE needs to be initialized with a FIP (kindly refer [54, 55]). In this case, $\boldsymbol{\delta} = \boldsymbol{\eta} = \mathbf{0}$ results a trivial FIP. Although the trivial solution is a valid FIP to the problem $\mathcal{P}_5^{\text{MEE}}$, it is observed through simulations that it usually converges to a poorly performing stationary point with the poor objective function value. This behavior might be due to the fact the trivial FIP has the lowest objective (i.e., zero), therefore, the JGSP-MEE initialized with the trivial FIP may converge to a stationary point around this lowest objective value. Since, FIP is crucial for JGSP-MEE's performance, in the sequel, a simple procedure is proposed to obtain a FIP that promises the convergence to stationary points which yield better performance.

3.3.5 Feasible Initial Point: MEE

Since, the quality of the solution depends on the FIP, the harder task of finding a better FIP is considered through the following procedure.

- Step 1: Initialize $\mathbf{W}^0$ with complex random values subject to $\left\|\mathbf{W}^0\right\|_2^2 \leq P_T$ and calculate initial SINRs $\boldsymbol{\gamma}^0$.

- Step 2: Solve the following optimization:

$$\mathcal{P}_{\text{FES}}: \{\boldsymbol{\delta}_0, \boldsymbol{\eta}_0\}: \max \sum_{j=1}^{G}\delta_j + \sum_{j=1}^{G}\sum_{i=1}^{N}\eta_{ij} \tag{3.10}$$

$$\text{s.t. } C_1: 0 \leq \eta_{ij} \leq 1,\ \forall i,\ \forall j, \qquad C_2: \sum_{j=1}^{G}\eta_{ij} \leq 1, \forall i,$$

$$C_3: \sum_{i=1}^{N}\eta_{ij} \leq \delta_j N, \forall j, \qquad C_4: 0 \leq \delta_j \leq 1, \forall j,$$

$$C_5: \log\left(1+\gamma_{ij}^0\right) \geq \eta_{ij}\epsilon_j,\ \forall i,\ \forall j,$$

- Step 3: The parameters $\boldsymbol{\Theta}^0, \boldsymbol{\zeta}^0, \boldsymbol{\alpha}^0, t^0$ can easily be derived from $\mathbf{W}^0, \boldsymbol{\delta}^0$ and $\boldsymbol{\eta}^0$.

Remarks:

- The problem $\mathcal{P}_{\text{FES}}$ is a linear programming problem and always feasible since trivial solution $\boldsymbol{\delta}^0 = \boldsymbol{\eta}^0 = \mathbf{0}$ is also a feasible solution. However, the optimization problem $\mathcal{P}_{\text{FES}}$ usually results a better solution than trivial one. Therefore, initial parameters $\mathbf{W}^0, \boldsymbol{\delta}^0, \boldsymbol{\Theta}^0, \boldsymbol{\eta}^0, \boldsymbol{\alpha}^0, t^0$ are always feasible. Different $\mathbf{W}^0$ in step 1 may lead to different FIPs.

- The optimization problem in Step 2 is a linear programming problem which can be solved efficiently to large dimensions with many of the existing tools like CVX.

- The FIP obtained by this procedure may not be feasible for the original MEE problem $\mathcal{P}_1^{\text{MEE}}$ unless $\mathbf{W}^0, \boldsymbol{\eta}^0, \boldsymbol{\delta}^0$ becomes feasible to $\mathcal{P}_2^{\text{MEE}}$.

- Although the FIP obtained by this method is not feasible for $\mathcal{P}_1^{\text{MEE}}$, the final solution obtained by JGSP-MEE with this FIP becomes a feasible for $\mathcal{P}_1^{\text{MEE}}$ since the final solution satisfies the group scheduling constraint C_2 in $\mathcal{P}_1^{\text{MEE}}$.

Letting $\mathcal{P}_6^{\text{MEE}}(k)$ be the objective value of the problem $\mathcal{P}_6^{\text{MEE}}$ at iteration k, the pseudo code of JGSP-MEE for the joint design problem is given in algorithm 4.

Algorithm 4 JGSP-MEE

Input: $\mathbf{H}, [\epsilon_1, \ldots, \epsilon_N], P_T, \Delta, \mathbf{W}^0, \boldsymbol{\delta}^0, \boldsymbol{\Theta}^0, \boldsymbol{\zeta}^0, \boldsymbol{\eta}^0, \boldsymbol{\alpha}^0, t^0, \lambda_1 = 0, k = 1$;
Output: $\mathbf{W}, \boldsymbol{\eta}$
while $|\mathcal{P}_6^{\text{MEE}}(k) - \mathcal{P}_6^{\text{MEE}}(k-1)| \geq \Delta$ **do**
  Convexification: Convexify the problem (3.8)
  Optimization: Update $(\mathbf{W}, \boldsymbol{\eta}, \boldsymbol{\delta}, \boldsymbol{\alpha}, \boldsymbol{\zeta}, \boldsymbol{\Theta}, t)^k$ by solving $\mathcal{P}_6^{\text{MEE}}$
  Update : $\mathcal{P}_6^{\text{MEE}}(k), \lambda_1, \lambda_2, \Omega_1, k$
end while

3.3.6 Complexity of JGSP-MEE

Since JGSP-MEE is a CCP based iterative algorithm, its complexity depends on complexity of the convex sub-problem $\mathcal{P}_6^{\text{MEE}}$. The convex problem $\mathcal{P}_6^{\text{MEE}}$ has $(MG + 2NG + 3G + 1)$ decision variables and $(2NG + 2 + G)$ convex constraints and $(2NG + 4G + N)$ linear constraints. Hence, the complexity of $\mathcal{P}_6^{\text{MEE}}$ is $\mathcal{O}\left((MG + 2NG + 2G + 1)^3 (4NG + 4G + N + 2)\right)$ [64]. Commercial software such as CVX can solve the convex problem of type $\mathcal{P}_6^{\text{MEE}}$ efficiently to a large dimension. Besides the complexity per iteration, the overall complexity also depends on the convergence speed of the algorithm. Through simulations, we observe that the JGSP-MEE converges typically in 15-20 iterations.

3.4 Variants of Multicast Energy Efficiency

In this section, two special cases of the MEE problem namely the maximization of EE and the number of scheduled users are considered.

3.4.1 Energy efficiency

In this section, we focus on developing a CCP based low-complexity algorithm for the joint design of user grouping, scheduling, and precoding for maximization of weighted EE (defined in (3.2)) subject to grouping, scheduling, precoding, power, and QoS constraints. This problem is simply referred to as the EE problem.

Problem formulation: EE

With the defined slack variables in Section 3.3, the EE problem is mathematically formulated as,

$$\mathcal{P}_1^{\text{EE}}: \max_{\mathbf{W},\boldsymbol{\Theta},\boldsymbol{\eta},\boldsymbol{\delta},\boldsymbol{\alpha}} \frac{\sum_{j=1}^{M} B\Psi_j\Theta_j}{t} \tag{3.11}$$

$$\text{s.t. } C_1 \text{ to } C_8 \text{ and } C_{11} \text{ in (3.6)},$$

$$C_9: P_0 + \sum_{j=1}^{G}\left(\frac{1}{\rho}\left\|\mathbf{w}_j\right\|^2 + \Pi\, p\left(\Theta_j\right)\right) \leq t, \quad C_{10}: \Theta_j \leq \delta_j\Theta^*, \forall j,$$

where $\Theta^* \geq \max_{j=1}^{G}\Theta_j$ is a constant. The constant Θ^* in constraint C_{12} in $\mathcal{P}_1^{\text{EE}}$ is used for forcing Θ_j to zero when the group is not scheduled i.e., $\delta_j = 0$. For the scheduled group i.e., $\delta_j = 1$ constraint C_{12} becomes superficial as $\Theta_j \leq \Theta*$ is always true. Without the constraint C_{12} the problem $\mathcal{P}_1^{\text{EE}}$ becomes unbounded as the Θ_j can be infinity for the unscheduled group j thus yielding the highest EE which is infinity. The constraint C_{12} helps in containing Θ_j to zero for the unscheduled group j. Therefore the problem $\mathcal{P}_1^{\text{EE}}$ becomes bounded due to C_{12}. Notice the difference between the constraint C_9 in $\mathcal{P}_1^{\text{EE}}$ and C_{10} in $\mathcal{P}_3^{\text{MEE}}$. Due to C_{10} in $\mathcal{P}_1^{\text{EE}}$ for an unscheduled group j the minimum rate of the group i.e., Θ_j is zero. Therefore, the power consumption can be modelled simply using Θ_j unlike ζ_j in MEE case.

Nature of EE in the context of grouping and scheduling EE problem is not biased to favor the solutions with more number of users since it only considers the minimum rate of the group ignoring its size. Typically, adding more users to groups either leads to increased inter-group interference and/or lower minimum rate of the group due to lower channel gains. Hence, to obtain the same rate as with few users extra power needs to be used. Since the linear increase in rate is achieved at the cost of exponential increase power, newly added users result in lower EE.

DC formulation and CCP based algorithm: EE

The problem $\mathcal{P}_1^{\text{EE}}$ is combinatorial and non-convex similar to the problem $\mathcal{P}_3^{\text{MEE}}$. With the help of a slack variable Γ, and applying reformulations and relaxations proposed in Section 3.3, the problem $\mathcal{P}_1^{\text{EE}}$ is reformulated into a DC problem as,

$$\mathcal{P}_2^{\text{EE}}: \max_{\mathbf{W},\boldsymbol{\Theta},\boldsymbol{\eta},\boldsymbol{\delta},\boldsymbol{\alpha},\Gamma,t} \frac{\Gamma^2}{t} - \Omega_2\left\|\sum_{j=1}^{G}\delta_j - M\right\|^2 + \sum_{j=1}^{G}\sum_{i=1}^{N}\lambda_3\mathbb{P}\left(\eta_{ij}\right) + \lambda_4\sum_{j=1}^{G}\mathbb{P}\left(\delta_j\right) \tag{3.12}$$

$$\text{s.t. } C_1 \text{ to } C_{10} \text{ in (3.11)}, \qquad C_{11}: \sum_{j=1}^{G} B\Psi_j\Theta_j \geq \Gamma^2.$$

where $\lambda_3 > 0, \lambda_4 > 0$ and $\Omega_2 > 0$ are the penalty parameters.

Notice that the DC problem $\mathcal{P}_2^{\text{EE}}$ resembles the DC problem $\mathcal{P}_5^{\text{MEE}}$, hence, the CCP framework proposed in Section 3.3.4 can be simply be adapted. The proposed CCP framework based algorithm for the EE problem is simply referred to as JGSP-EE. Since JGSP-EE is a CCP based iterative algorithm at iteration k it executes the following convex problem:

$$\mathcal{P}_3^{\text{EE}}: \max_{\mathbf{W},\boldsymbol{\Theta},\boldsymbol{\eta},\boldsymbol{\delta},\boldsymbol{\alpha},\Gamma,t} \frac{2\Gamma^{k-1}\Gamma}{t} - \Omega_2\left\|\sum_{j=1}^{G}\delta_j - M\right\|^2 + \lambda_3\sum_{j=1}^{G}\sum_{i=1}^{N}\tilde{\mathbb{P}}^k\left(\eta_{ij}\right) + \sum_{j=1}^{G}\lambda_4\tilde{\mathbb{P}}^k\left(\delta_j\right) \tag{3.13}$$

$$\text{s.t. } C_1 \text{ to } C_8 \text{ in (3.8)}, \qquad C_9: P_0 + \sum_{j=1}^{G}\left(\frac{1}{\rho}\left\|\mathbf{w}_j\right\|^2 + \Pi\ \left(p_1\left(\Theta_j\right) - \tilde{p}_2\left(\Theta_j\right)\right)\right) \leq t,$$

$$C_{10}: \Theta_j \leq \delta_j \Theta^*, \forall j, \qquad C_{11}: \sum_{j=1}^{G} B\Psi_j \Theta_j \geq \Gamma^2.$$

Letting $\mathcal{P}_2^{\text{EE}}(k)$ be the objective value of the problem $\mathcal{P}_2^{\text{EE}}$ at iteration k, the pseudo code of JGSP-EE for the joint design problem is given in algorithm 5.

Algorithm 5 JGSP-EE-SR

Input: $\mathbf{H}, [\epsilon_1, \ldots, \epsilon_N], P_T, \Delta, \mathbf{W}^0, \boldsymbol{\delta}^0, \boldsymbol{\Theta}^0, \boldsymbol{\eta}^0, \boldsymbol{\alpha}^0, t^0, \lambda_3, \lambda_4, \Omega_2, k = 1;$
Output: $\mathbf{W}, \boldsymbol{\eta}$
while $|\mathcal{P}_2^{\text{EE}}(k)\, \mathcal{P}_2^{\text{EE}}(k-1)\,(k-1)| \geq \Delta$ **do**
  Convexification: Convexify the problem (3.8)
  Optimization: Update $(\mathbf{W}, \boldsymbol{\eta}, \boldsymbol{\delta}, \boldsymbol{\alpha}, \boldsymbol{\Theta}, \Gamma, t)^k$ by solving $\mathcal{P}_2^{\text{EE}}(k)$
  Update : $\mathcal{P}_2^{\text{EE}}(k), \lambda_3, \lambda_4, \Omega_2, k$
end while

3.4.2 Maximization of scheduled users

In this section, the problem of maximizing the scheduled users (SUM) is considered subject to grouping, scheduling, precoding, total power, and QoS constraints. This problem is simply referred to as SUM problem in this paper and is formulated as,

$$\mathcal{P}_1^{\text{SUM}}: \max_{\mathbf{W}, \boldsymbol{\Theta}, \boldsymbol{\eta}, \boldsymbol{\delta}} \sum_{i=1}^{N} \sum_{j=1}^{G} \eta_{ij} \tag{3.14}$$

$$\text{s.t. } C_1: \eta_{ij} \in \{0,1\},\ \forall i,\ \forall j, \qquad C_2: \sum_{j=1}^{G} \eta_{ij} \leq 1, \forall i, \qquad C_3: \sum_{i=1}^{N} \eta_{ij} \leq \delta_j N, \forall j,$$

$$C_4: \delta_j \in \{0,1\}, \forall j, \qquad C_5: \sum_{j=1}^{G} \delta_j = M,\ \forall j, \qquad C_6: \sum_{i=1}^{M} \|\mathbf{w}_i\|_2^2 \leq P_T,$$

$$C_7: 1 + \gamma_{ij} \geq 1 + \eta_{ij}\epsilon_j,\ \forall i,\ \forall j.$$

Notice that except for constraint C_6 all the constraints and the objective in $\mathcal{P}_1^{\text{SUM}}$ are linear and convex. Further, similar to the constraint C_4 in $\mathcal{P}_2^{\text{EE}}$, the constraint C_6 can be easily equivalently transformed as a DC. Therefore, with the help of the relaxations and penalization approach provided in Section 3.3 and 3.4, the problem can be transformed as a DC programming problem. Hence, the CCP framework can be adapted to solve the resulting DC problem. The transformed DC problem and the convexified problem to be solved in the CCP framework for the SUM problem are given appendix A. The CCP framework based algorithm proposed for the SUM problem is simply referred to as JGSP-SUM.

3.5 Simulation results

3.5.1 Simulation setup and parameter initialization

Simulation setup

In this section, the performance of the proposed algorithms JGSP-MEE, JGSP-EE and JGSP-SUM is evaluated. The system parameters discussed in this paragraph are common for all the figures. Bandwidth for all the groups is assumed to be 1 Hz i.e., $B = 1$ Hz. The coefficients of the channel matrix, i.e., h_{ij} are drawn from the complex normal distribution with zero mean and unit variance and noise variances at the receivers are considered to be unity i.e., $\sigma^2 = 1$. All the simulation

results are averaged over 100 different channel realizations (CRs). Weights are assumed to be unity i.e., $\{\Psi_j = 1\}_{j=1}^{G}$. Following are the acronyms/definitions commonly used for all simulation results: 1) *Number of scheduled users*: the sum of all the scheduled users in all scheduled groups. 2) *Orthogonal user*: An user with zero channel correlations with all the users in all the other groups. 3) *Non-orthogonal user*: A user with at least one non-zero channel correlation with any user in other groups. 4) *Consumed power* $\triangleq P_0 + \sum_{j=1}^{G} \left(\frac{1}{\rho} \|\mathbf{w}_i\|^2 + \Pi p\left(r_j\right) \right)$. 5) *Throughput* $\triangleq \sum_{j=1}^{M} B\Theta_j$.

Parameter initialization

power amplifier efficiency i.e., ρ is assumed to 0.2 and fixed static power i.e., P_0 is assumed to be 16 Watts, $B = 1$MHz, $\Pi = 2.4\text{Watts}/(\text{bits}/\text{sec})^2$ [69], and $p\left(x\right) = x^2$ [76]. The penalty parameters responsible for binary nature of $\boldsymbol{\eta}$, $\boldsymbol{\delta}$ are initialized as follows $\lambda_1 = \lambda_2 = 0.01$ and , $\lambda_3 = \lambda_4 = 0.5$ and $\lambda_5 = \lambda_6 = 0.05$ and . Further $\{\lambda_i\}_{i=1}^{6}$ are incremented by factor 1.2. Further, penalty parameters corresponding to group scheduling constraint are initialized to relatively larger values such as $\Omega_1 = 2.5$, $\Omega_2 = 5$, and $\Omega_3 = 1$ and are incremented by 1.5 in each iteration. MEE and SUM maximization criteria naturally encourage the solutions towards to non-zero $\boldsymbol{\eta}$ and $\boldsymbol{\delta}$. Therefore, small initial values and slow update of penalty parameters corresponding to MEE and SUM problems eventually result in a binary solution of $\boldsymbol{\eta}$, $\boldsymbol{\delta}$. Further, relatively large initial value and larger increments for Ω_1 and Ω_2 in each iteration, along with binary nature of $\boldsymbol{\delta}$, eventually ensure the group scheduling constraint i.e., $\sum_{j=1}^{G} \delta_j = M$. On the contrary, as discussed in Section 3.4, the EE problem is not biased to favor the solutions with a higher number of users since it only considers the minimum rate of the group ignoring its size. Moreover, the solutions with $\eta_{ij} < 1$ might be encouraged as it would facilitate larger Θ_j hence better objective in $\mathcal{P}_1^{\text{EE}}$ (from constraint C_5 in the problem $\mathcal{P}_1^{\text{EE}}$). Hence, to ensure the group scheduling constraint and the binary nature of $\boldsymbol{\eta}, \boldsymbol{\delta}$, the penalty parameters are initialized to relatively larger values in EE than in MEE and SUM problems and incremented in large steps.

3.5.2 Performance as a function of total users (N)

In figure 3.1, the performance of the proposed algorithm i.e., JGSP-MEE, JGSP-EE, and JGSP-SUM is illustrated as a function of N varying from 20 to 32 in steps of 4 for $M = 5$, $G = 8$, $P_T = 10$dBW and $\epsilon_j = 1$ bps/Hz, $\forall j$.

Number of scheduled users versus N

In figure 3.1(a), the number of scheduled users is illustrated as function of N. Since JGSP-SUM directly maximizes the number of scheduled users, it schedules the maximum number of users compared to JGSP-MEE and JGSP-EE. Moreover, due to low QoS requirement and availability of resources to satisfy the QoS requirement, JGSP-SUM schedules almost all the users despite the increase in N. Since the number of scheduled users contribute linearly to MEE objective a similar increase in the number of scheduled users versus N in JSP-MEE can be observed in figure 3.1(a). However, JSP-MEE also considers the power consumed by the scheduled users, hence, JSP-MEE schedules fewer users than JSP-SUM as scheduling these excess users requires huge power which can be observed in figure 3.1(c). On the contrary, the EE objective is not accounting for the number of scheduled users, hence, JGSP-EE schedules the lowest number of users i.e. $M = 5$. In other words, it is serving one user per group which is nothing but a unicast scenario. Furthermore, despite the increase in N, the number of users scheduled by JGSP-EE remains the same. This can be attributed to three reasons: 1) non-orthogonal users: scheduling any non-orthogonal user increases interference to users in other groups which decreases the minimum rate of the influenced groups hence decreases EE. 2) Orthogonal users with un-equal channel

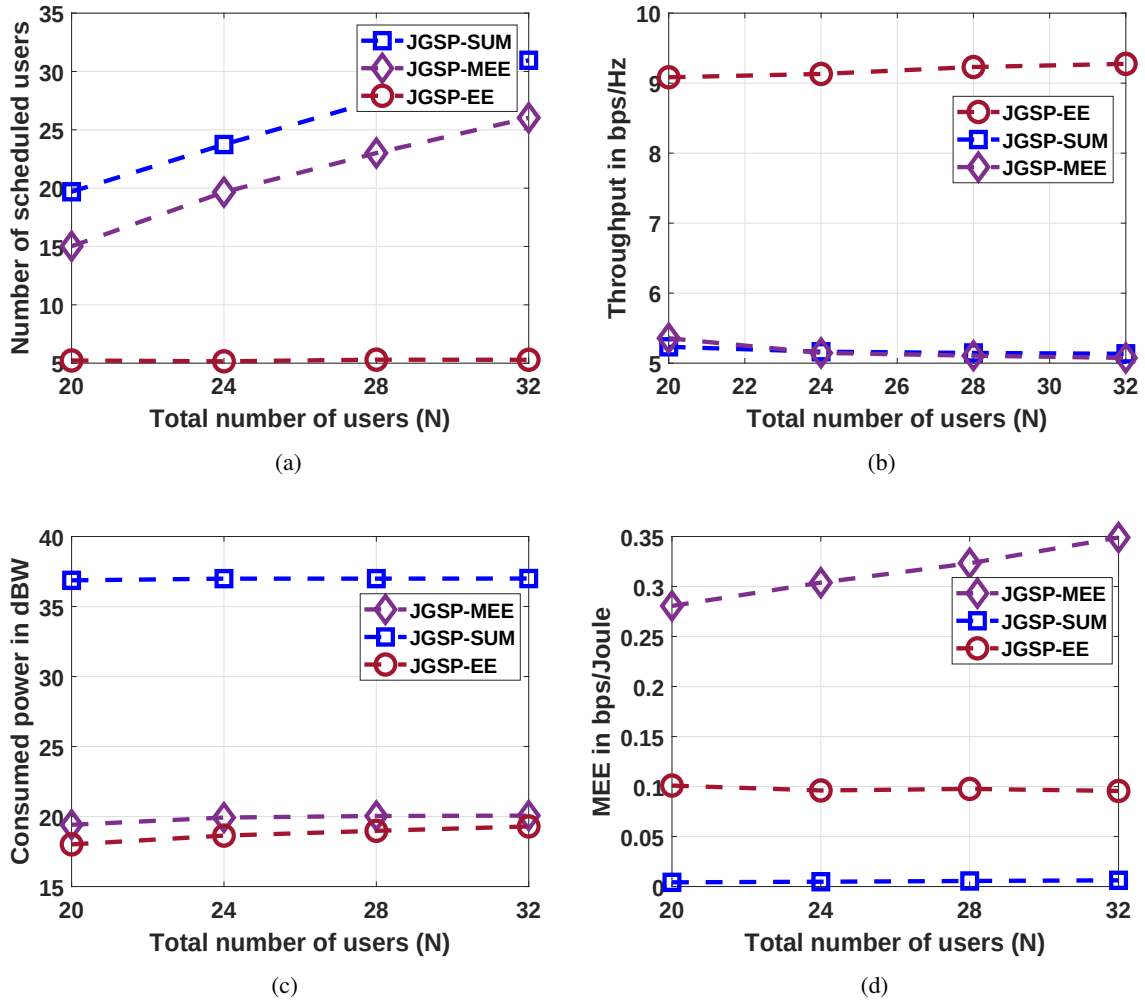

FIGURE 3.1: Comparison of proposed algorithms as a function of N varying from 20 to 32 for $M = 5, G = 8$, $\{\epsilon_i = 1\text{bps/Hz}\}_{j=1}^{N}$, and $P_T = 20\text{dBW}$ (a) number of scheduled users (b) throughput in bps (c) Consumed power in dBW (d) MEE in bits/Joule versus N

gains: EE swaps the existing user with the best available user in the pool as scheduling the second best user decreases the minimum rate of the group hence lower EE. 3) Orthogonal users with equal channel gains: This is an unlikely event; even if such users exist, as mentioned earlier, their scheduling is not guaranteed as the EE objective is unaffected.

Throughput versus N

In figure 3.1(b), the throughput in bps obtained by JGSP-MEE, JGSP-EE, and JGSP-SUM is illustrated as a function of N. The nature of JSP-MEE to schedule more users and consume fewer power results in lower throughput than JSP-SUM and JSP-EE. On the other hand, as the JSP-EE objective includes throughput in the objective, hence, it naturally achieves higher throughput than JSP-SUM. Moreover, as N increases the probability of finding M orthogonal users with good channels increases. This leads to a better throughput in JSP-EE with an increase of N. However, the gains in throughput for JGSP-EE diminishes as the gains in multiuser diversity diminish. On the contrary, an increase in multiuser diversity with N is utilized to schedule a higher number of users by JSP-MEE and JSP-SUM which can be observed in figure 3.1(a). Moreover, the degradation in throughput in JSP-MEE and JSP-SUM is due to the combination of two factors: 1) for relatively lower N i.e., 20, after scheduling the maximum number of users, resources could be used to improve minimum throughput of the groups. 2) for relatively higher N, as scheduling

higher users improve the objectives of JSP-SUM and JSP-EEE, the available power is used to schedule more users and this is also achieved by keeping their achieved minimum rate close to the required rates of the groups. Hence, the throughput by JSP-MEE and JSP-SUM decreases slightly with an increase of N.

Consumed power versus N

In figure 3.1(b), the consumed power in Watts by JSP-SUM, JSP-EE and JSP-MEE is illustrated as a function of N. As the JSP-SUM does not optimize power, in the process of scheduling the maximum number of users (as shown in figure 3.1(a)) it inefficiently utilizes the power by consuming all of the available power as depicted in figure 3.1(c). On the contrary, as the EE and MEE objectives are penalized inversely for excess usage of power, both JSP-EE and JSP-MEE utilize power efficiently as shown in figure 3.1(c). However, JSP-MEE slightly utilizes more power than JSP-EE as illustrated in figure 3.1(c) to schedule a higher number of users (as shown in figure 3.1(a)) as it improves over the MEE.

MEE versus N

Recall that MEE can be interpreted as the number of received bits for one joule of transmitted energy as explained in Section 3.2.2. It can be seen in figure 3.1(d), by directly optimizing MEE, JGSP-MEE obtains the highest MEE value compared to JGSP-EE and JGSP-SUM. The linear increase in MEE with respect to N can be observed in JSP-MEE and JSP-SUM as the number of scheduled users linearly with N in both the methods. However, as JSP-SUM utilizes the power inefficiently, it results in poorer MEE overall compared to JSP-MEE. Unlike JSP-MEE and JSP-SUM, the improvement in MEE obtained by JSP-EE is negligible as it does not gain in scheduled users and the increase in throughput is comparatively negligible.

Convergence of JSP-MEE versus iterations

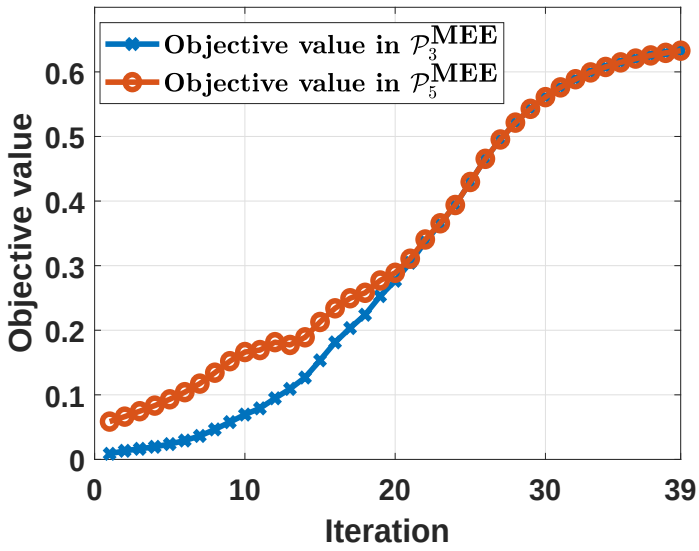

FIGURE 3.2: Convergence of JSP-MEE as a function of iterations for $M = 5, G = 8$, $\{\epsilon_i = 1\text{bps/Hz}\}_{j=1}^{N}$, $N = 40$ and $P_T = 30$ dBW

Figure 3.2 illustrates the convergence behavior of the proposed algorithm as function of iteration. The objective value in $\mathcal{P}_3^{\text{MEE}}$ is simply the MEE value i.e., $\sum_{i=1}^{N}\sum_{j=1}^{G} f\left(\eta_{ij}, \Theta_j, t\right)$

and the objective value in $\mathcal{P}_5^{\text{MEE}}$ contains the MEE value plus the penalty values added to ensure binary nature of $\boldsymbol{\eta}, \boldsymbol{\delta}$ and GSC constraint i.e., $\sum_{i=1}^{N}\sum_{j=1}^{G} f\left(\eta_{ij}, \Theta_j, t\right) + \lambda_2 \sum_{j=1}^{G} \mathbb{P}\left(\delta_j\right) + \sum_{j=1}^{G}\sum_{i=1}^{N} \lambda_1 \mathbb{P}\left(\eta_{ij}\right) - \Omega_1 \left\| \sum_{j=1}^{G} \delta_j - M \right\|^2$. In the initial iterations, $\boldsymbol{\eta}, \boldsymbol{\delta}$ and GSC constraints are not satisfied, hence, $\mathcal{P}_5^{\text{MEE}}$ has higher objective value than $\mathcal{P}_3^{\text{MEE}}$ which can be observed in Figure 3.2 until iteration 18. However, from iteration 19 the objective value of $\mathcal{P}_5^{\text{MEE}}$ and $\mathcal{P}_3^{\text{MEE}}$ almost same. This is because the additional penalty objective in $\mathcal{P}_5^{\text{MEE}}$ becomes zero i.e., $+\lambda_2 \sum_{j=1}^{G} \mathbb{P}\left(\delta_j\right) + \sum_{j=1}^{G}\sum_{i=1}^{N} \lambda_1 \mathbb{P}\left(\eta_{ij}\right) - \Omega_1 \left\| \sum_{j=1}^{G} \delta_j - M \right\|^2 = 0$ as the binary nature of $\boldsymbol{\eta}, \boldsymbol{\delta}$ and GSC constraints are satisfied by iteration 19. The proposed algorithm converges in 39 iterations for the system with $N = 40$, $M = 5$ and $G = 8$.

Number of scheduled users versus versus MEE

In figure 3.3, MEE obtained by JSP-MEE is plotted as function of the number of users scheduled by JSP-MEE. The linear increase in MEE of JSP-MEE with respect to the number of scheduled users is observed in figure 3.3. In other words, figure 3.3 confirms that major contributing factor to MEE maximization is the number of scheduled users.

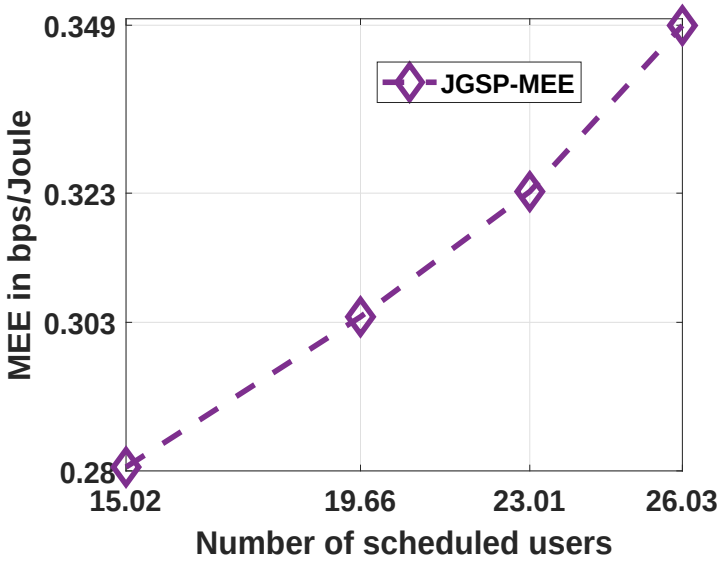

FIGURE 3.3: Performance of JSP-MEE as function of Number of scheduled users versus MEE for N varying from 20 to 32, $M = 5, G = 8$, $\{\epsilon_i = 1\text{bps/Hz}\}_{j=1}^{N}$, and $P_T = 30$ dBW

3.5.3 Performance as a function of total power P_T

In figure 3.4, the performance of the proposed algorithms i.e., JGSP-MEE, JGSP-EE, and JGSP-SUM is illustrated as a function of P_T varying from 6 to 12 in steps of 2 dBW for $M = 5$, $G = 8$, $N = 15$ and $\epsilon_j = 1$ bps/Hz, $\forall j$.

Number of scheduled users versus P_T

In figure 3.4(b), number of scheduled users is illustrated as function of P_T. By directly maximizing the number of scheduled users, JSP-SUM schedules the maximum number of users compared to JGSP-MEE and JGSP-EE. In the low-available power regime i.e., $P_T = 6$ dBW and 8 dBW, JSP-SUM schedules only few users. However, in the high-available power regime, due to the sufficient power, JSP-SUM schedules almost all the users i.e., 15 users by utilizing all of the power. Unlike

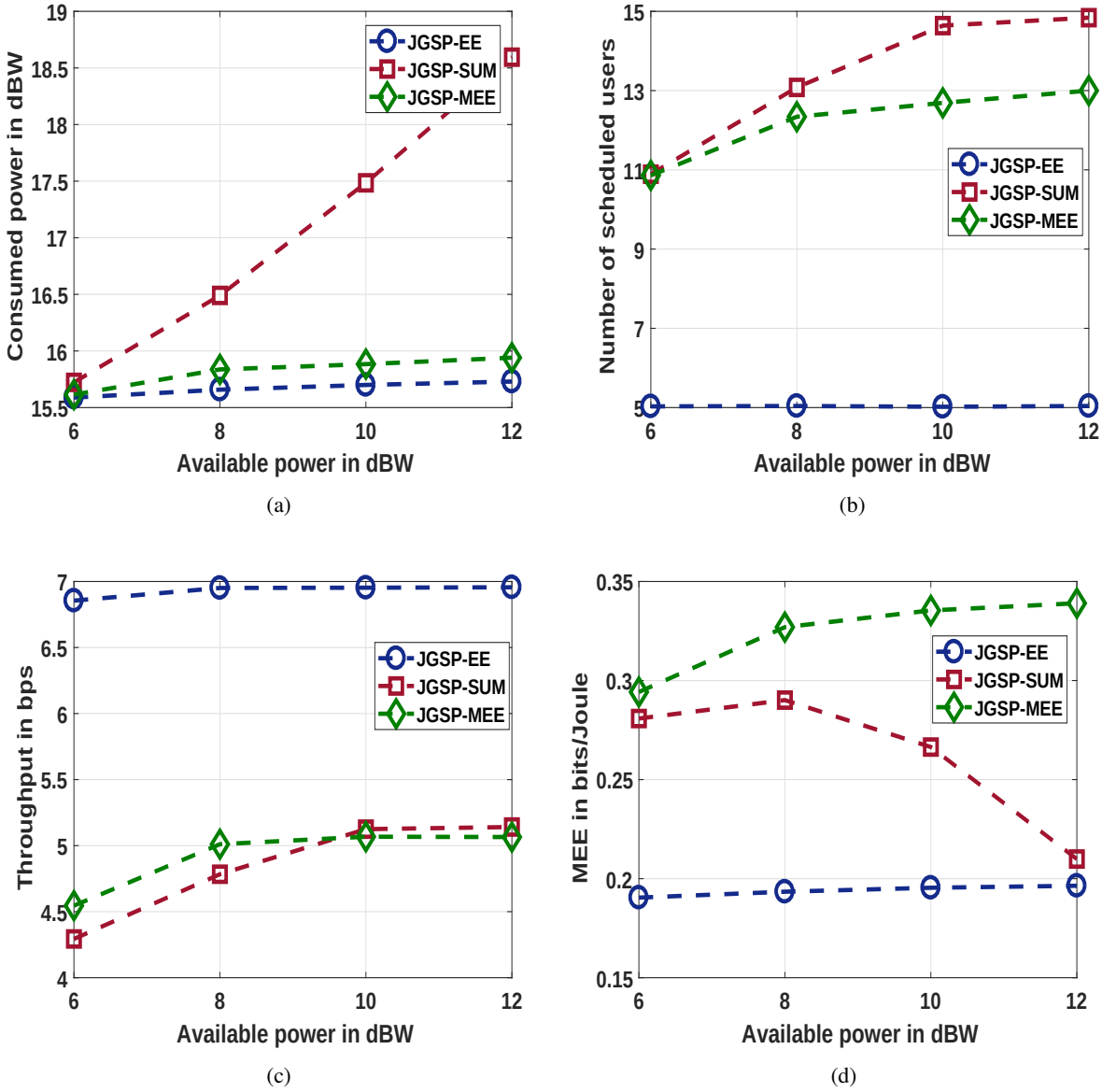

FIGURE 3.4: Comparison of proposed algorithms as a function of P_T varying from 6 to 12 for $M = 5, G = 8$, $\{\epsilon_i = 1\text{bps/Hz}\}_{j=1}^{N}$, and $N = 15$ (a) consumed power in dBW versus P_T (b) number of scheduled users versus P_T (c) throughput in bps versus P_T (d) MEE in bits/Joule versus P_T

JSP-SUM, despite the increased available power, the number of scheduled users in JSP-MEE is saturated to 13 users. This is because scheduling those extra users results in the consumption of huge power which decreases the overall MEE. Moreover, for the available for 8 dBW, JSP-SUM and JSP-MEE schedules almost equal number of users, however, JSP-MEE consumes almost 6.8 dBW less than JSP-SUM. On the contrary, for the reasons mentioned in section 3.5.2, JSP-EE schedules only M despite the availability of power.

Throughput versus P_T

In figure 3.4(c), the throughput in bps obtained by JGSP-MEE, JGSP-EE, and JGSP-SUM is illustrated as a function of P_T. Since JSP-MEE and JSP-SUM sacrifice in throughput to schedule more users for the available power, the lower throughput of JSP-MEE and JSP-SUM compared to JSP-EE can be observed in figure 3.4(c). Moreover, the throughput of JSP-EE saturates to 8 bps for available power of 8 dBW as improving throughput further results in the consumption of huge

power which results in overall lower EE. On the other hand, in the low-available power regime $P_T = 6$ and 8 dBW, the number of scheduled users (by JSP-SUM) are around 11 and 13 which less than total number of users $N = 15$. In other words, scheduling a higher number of users than 13 requires higher available power than 8 dBW. Therefore, the available-power in this regime is used to improve the minimum throughput of scheduled groups by JSP-MEE which can be observed in figure 3.4(d). In this high-available power regime i.e., $P_T \geq 10$ dBW, JSP-SUM uses all of the available power to schedule almost all the users as shown in figure 3.4(d). On the contrary, despite the availability of the power to schedule all users and/or to improve the throughput, JSP-MEE relatively maintains the same throughput as for the case of $P_T = 8$ dBW since the improvement in throughput leads to consumption of huge power.

Consumed power versus P_T

In figure 3.4(a), the consumed power in Watts by JSP-SUM, JSP-EE and JSP-MEE is illustrated as a function of N. As the JSP-SUM does not optimize power, the inefficient utilization of the available power of JSP-SUM can be observed in figure 3.4(a). On the contrary, as the EE and MEE objectives include the consumed power in the denominator, the objective values of EE and MEE are decreases inversely for a linear increase in consumed power. Hence, JSP-EE and JSP-MEE utilize power efficiently as shown in figure 3.4(a).

MEE versus P_T

In figure 3.4(d), the MEE in bits/Joule obtained by JGSP-MEE, JGSP-EE, and JGSP-SUM is illustrated as a function of P_T. By striking the trade-off among optimizing the number of scheduled users, throughput, and consumed power, JSP-MEE obtains higher MEE compared to JSP-EE and JSP-SUM as shown in figure 3.4(d). Although JSP-SUM schedules more users than JSP-MEE, it does so by consuming huge power and also by inefficiently utilizing the available power. This results in decreasing in MEE of JSP-SUM with the increase of available power. On the other hand, JSP-MEE schedules also increase the number of users while simultaneously optimizing power and throughput. This results in an overall better MEE of JSP-MEE. On the contrary, JSP-EE schedules only $M = 5$ users despite the opportunity to schedule more users. Hence, JSP-EE results in the lowest MEE. However, JSP-MEE schedules more users while efficiently utilizing power and throughput.

3.6 Conclusions

In this chapter, the joint design of user grouping, scheduling, and precoding problem was considered for the message-based multigroup multicast scenario in multiuser MISO downlink channels. In this context, to fully leverage the multicast potential, a novel metric called multicast energy efficiency is considered as a performance metric. Further, this joint design problem is formulated as a structured MINLP problem with the help of Boolean variables addressing the scheduling and grouping, and linear variables addressing the precoding aspect of the design. Noticing the structure in MINLP to be difference-convex/concave, this paper proposed efficient reformulations and relaxations to transform it into structured DC programming problems. Subsequently, the paper proposed CCP based algorithms for MEE and its variants i.e., EE and SUM problems (JSP-MEE, JSP-EE, and JSP-SUM) which are guaranteed to converge to a stationary point for the aforementioned DC problems. Finally, the paper proposed low-complexity procedures to obtain good feasible initial points, critical to the implementation of CCP based algorithms. Through simulations, the paper established the efficacy of the proposed joint techniques and studied the influence of the algorithms on the different parameters namely scheduled users, multicast throughput and consumed power.

4

Joint Scheduling and Precoding over Multiple Time Slots: A Structured Group Sparsity based Design

4.1 Introduction

Most of the existing works focus on the design of joint scheduling and precoding solely in the current time slot [27,37,81]. However, the users served in the current slot influence the scheduling in the future time slot. In the worst-case scenario, the design of scheduling and precoding in the current slot without considering its impact on the future time slots may lead to infeasibility (the inability of finding a scheduling and precoding solution meeting the QoS constraints) of the joint design in the future slots. This could happen due to the following reasons::

- Unmet capacity: In a typical network, user channels are independent resulting in some users may have good channel gains over multiple slots and some users may experience decay in channel gains over the slots. Failing to schedule the users with decaying channel gains in the early slots makes it impossible for the design to serve these users in the future slots with their required capacity.

- Unmet latency: Typically, each user's request is associated with a time constraint and the data needs to be delivered within this time constraint. This is referred to as a latency requirement. Scheduling users with relatively lower timer values may not always be a feasible choice. For example, users with co-linear channels (channels correlation equals to one) can not be scheduled (or served successfully) irrespective of the urgent latency requirement. Failing to consider the impact of scheduling in the current slot on the future slots may lead to the aforementioned co-linear channels, hence, the infeasibility of the joint design.

- Unmet capacity and latency: In a typical network, each user is associated with an independent capacity and latency requirements. This case subsumes both the aforementioned situations

It is clear from the above discussion that it is vital to consider the joint design of scheduling and precoding over all time slots. However, such a joint design entails the availability of channel state information (CSI) of all users over the time slots of interest. Since the wireless channels are time-varying and independent, it may seem unrealistic to assume the availability of CSI over all

time slots. However, in many cases like low-mobility scenario or satellite, channels usually admit a quasi-static behavior or can be predicted accurately up to a few slots [83]. Further, with the advancements of machine learning the channel prediction can be predicted quite accurately with reasonable complexity [84–86]. Furthermore, it would be of practical interest for an academic evaluation of the performance improvement with multiple slots to ascertain bounds on performance. Therefore, joint design can be applied over these few slots. The number of slots over which the CSI is the information of all users is available is referred to as *block*. Assuming the availability of CSI over the block, in this work, we focus on the joint design of scheduling and precoding over a block of time slots to minimize the service time (ST) required to serve all the users. This multislot joint design of scheduling and precoding is simply referred to as a joint multislot design (JMSP) in the rest of the paper.

ST minimization as a structured group sparsity problem Similar to [81], we address the scheduling aspects of the joint block design by controlling the power of precoding vectors through binary variables. In other words, user i in slot j is scheduled if the associated binary variable is 1 and is not scheduled otherwise. With the help of the binary variables, each of which is associated with a user in a time slot, the ST minimization problem for the JMSP can be modeled as a *structured group-sparsity (SGS)* problem. To see this, let $\boldsymbol{\eta}$ be a binary scheduling matrix with rows representing users and columns representing time slots. An all zero column represents no user being scheduled in that slot and a non-zero column represents at least one user being scheduled in that slot. Thus, the number of non-zero columns of $\boldsymbol{\eta}$ represents the number of slots in which at least one user is served. For the static channels, i.e., where CSI is the same over all the time slots in a block, ST can be defined as the minimization of the number of non-zero columns because of the possibility to permute the columns without loss of performance; this problem is widely addressed in the domain of sparse signal recovery under *group-sparsity (GS)* [87]. However, when the CSI is different over different slots (non-static CSI), the ST is defined as the highest index of the non-zero column. Therefore, the matrix with all the non-zero columns, in the beginning, has a lower ST; this leads to the imposition of structure in addition to group sparsity leading to SGS.

In this work, we focus on the joint design of scheduling and precoding over a block in multiuser multiple-input single-output (MISO) downlink channels for two transmission scenarios: unicast system (UC) and multigroup multicast system (MC). Further, to accommodate serving the users with a large payload, scheduling a user over multiple slots is considered. Further, service time minimization is considered as the objective subject to latency, rate, per slot power and total power. The joint design over the block is simply referred to as *joint block design* and the service time minimization problem as STM in the rest of the paper. To the best of our knowledge, this is the first work that considers the joint design of scheduling and precoding over a block.

Related work

The design of scheduling and precoding is considered in many works in the past decade [25, 37, 41, 81]. All of these can be categorized as follows:

- One-shot decoupled solution: In this approach, the design is considered as a decoupled design: usually scheduling followed by precoding [25, 34]

- Iterative decoupled solution: In this approach, scheduling and precoding are updated/refined iteratively wherein each iterate scheduling and precoding are solved separately [27, 37–39].

- Relaxed joint design of scheduling and precoding: In this approach, at the problem formulation the design of scheduling and precoding are considered jointly. However, due to the

difficulty in obtaining the joint update of scheduling and precoding, the design is either relaxed simply as a precoding problem [40] or an alternate update of scheduling and precoding is considered [41].

- Joint design of scheduling and precoding: In this approach, the joint design of scheduling and precoding is formulated as a mixed-integer non-linear problem (MINLP) that is amenable for the joint update of scheduling and precoding [81, 88]. Further, by transforming the MINLP problem as a difference-of-convex (DC) a convex-concave procedure (CCP) based iterative algorithm is proposed wherein each iterate scheduling and precoding are updated jointly.

Related work

The design of scheduling and precoding is considered in many works in the past decade [25, 37, 41, 81]. All of these can be categorized as follows:

- One-shot decoupled solution: In this approach, the design is considered as a decoupled design: usually scheduling followed by precoding [25, 34]

- Iterative decoupled solution: In this approach, scheduling and precoding are updated/refined iteratively wherein each iterate scheduling and precoding are solved separately [27, 37–39].

- Relaxed joint design of scheduling and precoding: In this approach, at the problem formulation the design of scheduling and precoding are considered jointly. However, due to the difficulty in obtaining the joint update of scheduling and precoding, the design is either relaxed simply as a precoding problem [40] or an alternate update of scheduling and precoding is considered [41].

- Joint design of scheduling and precoding: In this approach, the joint design of scheduling and precoding is formulated as a mixed-integer non-linear problem (MINLP) that is amenable for the joint update of scheduling and precoding [81, 88]. Further, by transforming the MINLP problem as a difference-of-convex (DC) a convex-concave procedure (CCP) based iterative algorithm is proposed wherein each iterate scheduling and precoding are updated jointly.

Long term admission control and precoding Although many works considered joint design admission control and precoding problems in a slot [27, 32, 37, 81] only a few works considered the long-term joint design of admission control and precoding [89, 90]. In [89], the authors proposed a sequential algorithm to provide the long-term fair admission control in a dynamic network based on channel statistics. Moreover, the authors in [89] consider the sequential approach of design one-time slot at a time without latency constraints. Instead objective of the optimization is average fairness and max-min fair in [89]. In [90], the authors addressed the stability of long-term admission control by minimizing the switching frequency of admissible users. The objective of optimization in [90] is weighted power and switching frequency minimization. Moreover, users' latency is not considered in [90]. Further, the extension of [90] minimize ST under latency data-fragmentation (or multislot per user) constraint is not clear.

Group sparsity GS based precoding or beamforming designs have been considered in the wireless networks [40, 48, 91–93]. GS is typically addressed through mixed $\ell_{p,q}$ norm [87] where ℓ_q norm typically quantifies each group and ℓ_p norm quantifies number of non-zero groups. While, $p = 0$ delivers the best performance, ℓ_0 norm is highly non-convex and non-smooth requiring a combinatorial search for obtaining the optimal solution. Therefore, several convex and non-convex approximations have been proposed in the literature [94, 95]. In convex approximation, ℓ_0 norm is

typically approximated by its tightest convex ℓ_1 norm [91,92,92,94]. To further enhance the sparsity, re-weighted $\ell_{1,q}$ norm-based methods are proposed in [96,97]. In non-convex approximation, ℓ_0 norm is typically approximated by a smooth functions [48,98]. However, all these methods are developed for promoting the sparsity or group sparsity. To the best of our knowledge, approximations to promote the resulting SGS are not readily available in the literature. Therefore, we take the opportunity of tailoring the existing approximations to promote the solutions with SGS.

Contributions

The aforementioned discussion reflects on the novelties of the paper-based both on problem formulation and its solution. The contributions of the paper include:

- The joint design of scheduling and precoding over a block of time slots is considered for two transmission scenarios: unicast and multicast. In this context, the task of minimizing the service time is considered as an objective for both unicast and multicast scenarios subject to user scheduling, latency, minimum rate constraints. To the best of our knowledge, true joint design of scheduling and precoding over multiple slots is not considered in literature.
- With the help of binary scheduling matrix, where rows represents users and columns represent slots and the variable represents the scheduling a user in that slot, the joint design problem is modelled as a structured mixed-integer non-linear programming problem (MINLP).
- Further, the service time minimization objective is rendered as a structured group sparsity (SGS) problem by formulating it as a minimization of highest column index of the non-zero column in the matrix. Noticing the lack of regularizations to promote the intended SGS, a regularization function is proposed. Noticing the special structure in STM problem, following transformation and penalization proposed in [81], the MINLP nature is transformed as difference-of-convex (DC) problem.
- Further, two convex-concave procedure (CCP) based iterative algorithm is proposed for UC and UC models respectively: JMSP-UC and JMSP-MC. Noticing the necessity of feasible initial point (FIP) for these algorithms to converge to a stationary point [54, 55], a simple procedure is proposed to obtain a FIP that yields quality stationary points.Subsequently, the per iteration complexity of JMSP-UC and JMSP-MC is discussed.
- Finally, the efficiency and necessity of the joint design of scheduling and precoding over multiple slots over sequential design is shown through average service time and probability of infeasibility respectively, through the Monte-Carlo simulations.

4.2 Unicast transmission

4.2.1 System Model

We consider the downlink transmission of a multiuser MISO system in a single cell with a total of N users served by a BS with M ($\leq N$) transmit antennas. Further, unicast transmission is employed at the BS i.e., each user is assumed to be requesting independent data. Since $M \leq N$, a BS can serve the utmost M users in any given time slot; this is simply referred to as scheduling constraint. Therefore, multiple time slots are required to serve all N users; this is simply referred to as multi-slot transmission. Typically, in real scenarios, some users have a larger payload which may not be delivered in one slot. Such users with large payloads are usually served by fragmentation and multi-slot scheduling. In the fragmentation step, the large payload is split into multiple payloads such that each portion can be delivered in a slot. In multi-slot scheduling, the same user is scheduled in multiple slots until all the fragments are delivered. Further, in practice, a scheduled user i must transmit with a minimum rate of $\theta_i^{\min}$ to ensure the successful decoding at the receiver;

this is simply referred to as minimum rate requirement. Furthermore, the total payload of user i must be delivered with a target rate $\theta_i > \theta_i^{\min}$ within T_i slots; the former rate requirement is referred to as target rate requirement and the latter time requirement referred to as latency requirement. Further, all time slots are assumed to be of equal length. Channels of users are constant during the transmission in any given time slot and CSI may vary across the slots. Further, CSI of all users across all time slots is assumed to be available at BS. Further, noise at all users is assumed to be an independent realization of a zero-mean additive white complex Gaussian with variance σ^2 in all time slots. The above-considered system model is simply referred to as *unicast system (UC)*.

Towards defining the signal model mathematically, let $\mathbf{h}_{ij} \in \mathbb{C}^{M\times 1}$, $\mathbf{w}_{ij} \in \mathbb{C}^{M\times 1}$ and n_{ij} denote the downlink channel, precoding vector and noise of user i at time slot j respectively. Letting x_{ij} to be the fragmented data of the user i in slot j with $\mathbb{E}\left\{|x_{ij}|^2\right\} = 1$, the received signal of user i at time slot j, say y_{ij}, is given by,

$$y_{ij} = \mathbf{h}_{ij}^H \mathbf{w}_{ij} x_{ij} + n_{ij},\ u \in \{1,\ldots,N\},\ t \in \{1,\ldots,T_i\} \tag{4.1}$$

Similarly, let $\gamma_{ij} = \dfrac{|\mathbf{h}_i^H \mathbf{w}_{ij}|^2}{\sum_{l\neq i} |\mathbf{h}_i^H \mathbf{w}_{lt}|^2 + \sigma^2}$ and $R_{ij} = \log(1+\gamma_{ij})$ be the signal-to-interference and noise ratio (SINR) and rate of user i in slot j respectively, and P_S is available transmit power per time slot.

In this work, we consider the joint design of scheduling and precoding to minimize the number of time slots to serve all the N users subject to the following constraints:

- Worst case per slot rate constraint: A scheduled user i in slot j must be served with at least $\theta_i^{\min}$ i.e., $R_{ij} \geq \theta_i^{\min}$.
- Worst case target rate and latency constraint: The overall rate of user i must be greater than θ_i i.e.,$\sum_{j=1}^{T_i} R_{ij} \geq \theta_i$. Notice that the target rate and latency constraints are intertwined.
- Maximum scheduled users per slot constraint: Number of scheduled users in any slot must not be greater than the number of transmit antennas i.e., M.
- Per slot power and total power constraint: The consumed power in any time slot must be lower than or equal to a maximum allowed power P_S, and the total consumed power across all the slots must not exceed total available power P_T

The above optimization problem is simply referred to as the service time minimization (STM) problem in the rest of the paper. Towards formulating the STM problem, scheduling of user i in slot j is simply addressed through the norm of the corresponding precoder as given below,

$$\|\mathbf{w}_{ij}\|_2 = \begin{cases} = 0;\ \text{user not scheduled,} \\ \neq 0;\ \text{user scheduled.} \end{cases} \tag{4.2}$$

4.2.2 Problem formulation: UC

Towards formulating STM, without loss of generality, let $T_i = T, \forall i$, $\mathbf{W}_i = [\mathbf{w}_{i1},\ldots,\mathbf{w}_{iT}]$ be the precoding matrix of user i, $\mathbf{W} = \left[\mathbf{W}_i^T,\ldots,\mathbf{W}_N^T\right]^T$, and $f(\mathbf{W})$ be the highest index of the non-zero column of $\mathbf{W}$. Each non-zero column of $\mathbf{W}$ represents an active slot with at least one user being scheduled. Each slot is associated with set of user channels which may be different from other slots. Therefore, the highest non-zero column (active slot) in $\mathbf{W}$ i.e., $f(\mathbf{W})$ represents the service time. With the help of defined notations, the STM problem is mathematically formulated as,

$$\mathcal{P}_\infty^{\text{UC}}:\ \min_{\mathbf{W}}\ \{(\mathbf{W}) \qquad \text{s.t. } C_1:\ \left\|\left[\|\mathbf{w}_{1j}\|_2,\ldots,\|\mathbf{w}_{Nj}\|_2\right]\right\|_0 \leq M,\ \forall j, \tag{4.3}$$

$$C_2: \sum_{i=1}^{N} \|\mathbf{w}_{ij}\|_2^2 \leq P_S,\ \forall j, \qquad C_3: R_{ij} \geq \left\lceil \frac{\|\mathbf{w}_{ij}\|_2}{P_S} \right\rceil \theta_i^{\min},\ \forall i,\ \forall j,$$

$$C_4: \sum_{j=1}^{T} R_{ij} \geq \theta_i,\ \forall\, i, \qquad C_5: \sum_{i=1}^{N}\sum_{j=1}^{T} \|\mathbf{w}_{ij}\|_2^2 \leq P_T,$$

where $\forall i$ refers to $i \in \{1, \ldots, N\}$ and $\forall j$ refers to $j \in \{1, \ldots, T\}$.

Remarks:

- *Maximum scheduled users per slot constraint*: From constraint C_1, utmost M precoders can be non-zero in a slot j. In other words, in time slot j, constraint C_1 precludes the design from scheduling more than the number of antennas i.e., M users.
- *Per time slot power constraint* C_2: Constraint C_2 thwarts the design from consuming more power than P_S in time slot j.
- *Per time slot minimum rate constraint* C_3: The ceil operator on the right hand side of constraint C_3 returns unity if $\|\mathbf{w}_{ij}\|_2^2 \neq 0$ and zero otherwise. Hence, constraint C_3 effectively becomes $R_{ij} \geq \theta_i$ if user i scheduled in slot j else $R_{ij} \geq 0$. The latter requirement is satisfied by the definition of R_{ij}.
- *target minimum rate and latency constraint* C_4: Due to constraint C_1, the power of the precoder, thereby the rate, of an unscheduled user i in slot j is zero. Therefore, $\sum_{j=1}^{T} R_{ij}$ provides the overall achievable sum rate of user i, and, hence, the C_4 imposes target minimum rate requirement and, also, inherently ensures the latency requirement.

The problem $\mathcal{P}_1^{UC}$ is combinatorial due to the ℓ_0 norm in constraint C_1, and non-convex due to the objective, constraints C_3 and C_4. Hence, obtaining an optimal solution requires exhaustive search-based solutions. Further, for each combination, a non-convex precoding problem needs to be solved. Hence, obtaining an optimal solution is not only challenging but also NP-hard [44]. So, we focus on obtaining a low-complexity sub-optimal solution to $\mathcal{P}_1^{UC}$. To the best of our knowledge, no framework exists that can be applied to solve the problem $\mathcal{P}_1^{UC}$ in its original form. Therefore, in the sequel, we focus on transforming $\mathcal{P}_1^{UC}$ as a structured non-convex problem with the structure being difference-of-convex programming (DC). Thereafter, the first-order stationary point of $\mathcal{P}_1^{UC}$ is obtained by employing the existing framework of the convex-concave procedure (CCP) [63].

4.2.3 DC programming transformation: UC

Towards obtaining the tractable formulation of $\mathcal{P}_1$, let $\eta_{ij} \in \{0, 1\}$ to be the binary scheduling variable (used for controlling the norm of precoding vector $\mathbf{w}_{ij}$) associated with user $i \in \{1, \ldots, N\}$ in slot $j \in \{1, \ldots, T\}$. In other words, $\eta_{ij} = 1$ indicates that user i in slot j is scheduled and is not scheduled otherwise. With the help of $\{\eta_{ij}\}_{\forall i, \forall j}$, the problem $\mathcal{P}_1^{\text{UC}}$ is reformulated as,

$$\mathcal{P}_{\in}^{\text{UC}}: \max_{\mathbf{W}, \boldsymbol{\eta}} f(\mathbf{W}) \qquad \text{s.t. } C_1: \eta_{ij} \in \{0, 1\},\ \forall i,\ \forall j, \tag{4.4}$$

$$C_2: \|\mathbf{w}_{ij}\|_2^2 \ \leq\ P_S \eta_{ij},\ \forall i,\ \forall j, \qquad C_3: \sum_{j=1}^{T} \eta_{ij} \leq M,\ \forall i,$$

$$C_4: \sum_{j=1}^{N} \|\mathbf{w}_{ij}\|_2^2 \leq P_S, \forall i, \qquad C_5: R_{ij} \geq \eta_{ij}\theta_i^{\min}, \forall i,\ , \forall j,$$

$$C_6: \sum_{j=1}^{T} R_{ij} \geq \theta_i, \forall i, \qquad C_7: \sum_{i=1}^{N}\sum_{j=1}^{T} \|\mathbf{w}_{ij}\|_2^2 \leq P_T,$$

where $\boldsymbol{\eta} = [\boldsymbol{\eta}_1, \ldots, \boldsymbol{\eta}_T]$ and $\boldsymbol{\eta}_j = [\eta_{1j}, \ldots, \eta_{Nj}]^T$.
Remarks:

- Constraint C_1 in $\mathcal{P}_{\in}^{\text{UC}}$ together with C_2 controls the scheduling of users. For $\eta_{ij} = 0$, C_2 implies $\|\mathbf{w}_{ij}\|_2^2 = 0$ and the user i in slot j is not scheduled. Similarly for scheduled user i.e., $\eta_{ij} = 1$, the constraint C_2 yields an upper bound on $\|\mathbf{w}_{ij}\|_2^2$ i.e., $\|\mathbf{w}_{ij}\|_2^2 \leq P_S$; this bound is trivial due to C_4.
- Constraint C_3 ensures the maximum number of scheduled users per slot constraint.
- The constraint C_5 ensures the per slot minimum rate requirement. For a scheduled user, C_5 implies $R_{ij} \geq \theta_i^{\min}$. Similarly, for an unscheduled user, C_5 becomes $R_{ij} \geq 0$ which is satisfied by definition. In fact, for $\eta_{ij} = 0$, C_5 is met with equality i.e., $R_{ij} = 0$ due to C_2.

Following [81], with the help of slack variable ζ_{ij} associated with user i in slot j, constraint C_5 in $\mathcal{P}_2^{\text{UC}}$ is reformulated as DC constraint as given below,

$$\begin{aligned}
&\mathcal{P}_{\ni}^{\text{UC}} : \min_{\mathbf{W},\boldsymbol{\zeta},\boldsymbol{\eta}} f(\mathbf{W}) && \text{s.t. } C_1, C_2, C_3, C_4 \text{ in (4.4)}, \\
&C_5 : \mathcal{I}_{ij}(\mathbf{W}) - \mathcal{G}_{ij}(\mathbf{W}, \zeta_{ij}) \leq 0, \forall i, \forall j, && C_6 : \ \log(\zeta_{ij}) \geq \eta_{ij}\theta_i^{\min}, \ \forall i, \ \forall j. \\
&C_7 : \sum_{j=1}^{T} \log \zeta_{ij} \geq \theta_i, \forall i, && C_8 : \sum_{i=1}^{N}\sum_{j=1}^{T} \|\mathbf{w}_{ij}\|_2^2 \leq P_T,
\end{aligned} \tag{4.5}$$

where $\boldsymbol{\zeta} = [\boldsymbol{\zeta}_1, \ldots, \boldsymbol{\zeta}_T]$, $\boldsymbol{\zeta}_j = [\zeta_{1j}, \ldots, \zeta_{Nj}]^T$, $\mathcal{I}_{ij}(\mathbf{W}) = \sigma^2 + \sum_{l \neq i} |\mathbf{h}_{ij}^H \mathbf{w}_{lj}|^2$ and $\mathcal{G}_{ij}(\mathbf{W}, \zeta_{ij}) = \dfrac{\sigma^2 + \sum_{l=1}^{N} |\mathbf{h}_{ij}^H \mathbf{w}_{lj}|^2}{\zeta_{ij}}$, and C_5 is simply the rearrangement of $1 + \gamma_{ij} \geq \zeta_{ij}$.

Notice that $\mathcal{I}_{ij}(\mathbf{W})$ is convex in $\mathbf{W}$, and for $\zeta_{ij} > 0$ (which is satisfied by the construction of lower bound in C_5 in $\mathcal{P}_3$), $\mathcal{G}_{ij}(\mathbf{W}, \zeta_i)$ is also jointly convex in $\mathbf{W}$ and ζ_{ij}. Hence, C_5 in $\mathcal{P}_3$ is a DC constraint. Further, by relaxing the binary constraint on $\{\eta_{ij}\}$s to a box constraint between 0 and 1 i.e., $C_1 : 0 \leq \eta_{ij} \leq 1, \forall i, \ \forall i$, the constraint set of $\mathcal{P}_4$ can be transformed as a DC set. However, the obtained solutions due to this relaxation may not be binary, hence, may not be feasible [81]. Therefore, to promote binary solutions, $\{\eta_{ij}\}$s are penalized with a penalty function $\mathbb{P}(\eta_{ij})$ as given below,

$$\begin{aligned}
&\mathcal{P}_{\triangle}^{\text{UC}} : \min_{\mathbf{W},\boldsymbol{\eta},\boldsymbol{\zeta}} \{ (\mathbf{W}) + \lambda_{\infty} \sum_{\rangle=\infty}^{\mathcal{N}} \sum_{|=\infty}^{\mathcal{T}} \mathbb{P}\left(\eta_{\rangle|}\right) \\
&\text{s.t. } C_1 : 0 \leq \eta_i \leq 1, \forall i, \forall j, && C_2, C_3, C_4, C_5, C_6, C_7, C_8 \text{ in (4.5)}.
\end{aligned} \tag{4.6}$$

where $\lambda_1 > 0$ is a penalty parameter. As explained in [81], the appropriate value of λ_1 together with a concave penalty function $\mathbb{P}(\eta_{ij})$ with the following two properties suffices to ensure the binary nature of η_{ij}: 1) $\mathbb{P}(\eta_{ij})$ should have minimum at $\eta_{ij} = 0$ and 1. 2) The value of $\mathbb{P}(\eta_{ij})$ should increase as η_{ij} drifts away from 0 and 1 with maximum being at $\eta_{ij} = 0.5$. The entropy based concave penalty function i.e., $\mathbb{P}(\eta_i) \triangleq -\eta_i \log \eta_i - (1 - \eta_i) \log(1 - \eta_i)$ is considered in this work [81].

4.2.4 Structured group sparsity

The problem $\mathcal{P}_4^{\text{UC}}$ involves the minimization of a non-convex objective subject to a DC constraint set. Moreover, a tractable formulation of $f(\mathbf{W})$ is not known. Therefore, we need to resort to surrogate functions that indirectly optimize the highest index of the non-zero column. As mentioned in the problem formulation, one such way is to focus on obtaining $f(\mathbf{W})$ matrix with as few initial non-zero columns. The structure of having all the non-zero columns at the beginning

of a matrix is simply referred to as *structured group sparsity (SGS)* in the rest of the paper. Notice that *group-sparsity (GS)* is a special case of SGS. GS methods typically focus on obtaining the matrix with few non-zero columns as possible without any emphasis on their position in the matrix [87, 99]. Contrary to GS, the position of non-zero columns is crucial for the STM problem as mentioned previously. Therefore, the existing GS based method can not be directly used as surrogate functions.

Notice that the highest non-zero column in $\mathbf{W}$ is also the highest non-zero column in $\boldsymbol{\eta}$ i.e., $f(\mathbf{W}) = f(\boldsymbol{\eta})$. Since it is easy to work with $\boldsymbol{\eta}$, service time is transformed as a function of $\boldsymbol{\eta}$. In this work, penalization of the columns of $\boldsymbol{\eta}$ in the order of the column index is considered for promoting SGS. This column penalization can also be applied to the existing GS regularizers for promoting SGS as shown below:

- *Modified reweighted ℓ_1 norm*: The modified reweighted ℓ_1 norm based function that promotes the SGS is,

$$\tilde{f}_1(\boldsymbol{\eta}) = \sum_{j=1}^{T} \Omega_j \left\| \boldsymbol{\eta}_j \right\|_p \tag{4.7}$$

  where Ω_j is a weight factor for column j and $p \geq 1$. Notice that the weights factors proposed in [100] or [101] depends only the number of non-zeros in the column not the column index and, hence, do not promotes SGS. Therefore, the weights proposed in [100] or [101] can not applied to this problem.

Weights for promoting SGS One way to promote the SGS is to penalize the columns in the order of their column index i.e., $\Omega_j \geq \Omega_{j-1}, \forall j$. Another way to promote the SGS is to ensure the product inside the summation in (4.7) increases in the order of column index j. For example, letting $\boldsymbol{\eta}^{k-1}$ to be solution from iteration $k-1$, in iteration k, the update given of Ω_j given in (4.8) ensures that $\Omega_j \geq \Omega_{j-1}$.

$$\Omega_j = \sum_{l=1}^{j-1} \Omega_l \left(1 + \left\| \boldsymbol{\eta}_j^{k-1} \right\|_p \right) \tag{4.8}$$

. Notice that for group sparsity Ω_j is solely a function of current column [100, 101]. However, for SGS Ω_j needs to be function of previous columns and weights.

With the replacement of $f(\mathbf{W})$ by $\tilde{f}_1(\boldsymbol{\eta})$, the problem $\mathcal{P}_{\triangle}^{\text{UC}}$ becomes a DC problem. Therefore, given the feasible initial point (FIP), the first order stationary point of $\mathcal{P}_{\triangle}^{\text{UC}}$ can be obtained by convex-concave procedure. However, the constraint C_7 in $\mathcal{P}_{\triangle}^{\text{UC}}$ limits the choices of FIP. To ease the process of finding an FIP, constraint C_7 is brought into objective with penalization method as given below,

$$\mathcal{P}_{\triangledown}^{\text{UC}} : \min_{\mathbf{W},\boldsymbol{\eta},\boldsymbol{\zeta}} \ \tilde{f}_1(\boldsymbol{\eta}) + \lambda_1 \sum_{i=1}^{N}\sum_{j=1}^{T} \mathbb{P}(\eta_{ij}) + \sum_{i=1}^{N} \alpha_i \max\left\{ \theta_i - \sum_{j=1}^{T} \log \zeta_{ij}, 0 \right\} \tag{4.9}$$

$$\text{s.t. } C_1 : 0 \leq \eta_{ij} \leq 1, \ \forall i, \ \forall j, \qquad C_2 : \ \|\mathbf{w}_{ij}\|_2^2 \ \leq \ P_S \eta_{ij}, \ \forall i, \ \forall j,$$

$$C_3 : \sum_{j=1}^{T} \eta_{ij} \leq M, \forall i, \qquad C_4 : \ \sum_{i=1}^{N} \|\mathbf{w}_{ij}\|_2^2 \leq P_S, \forall j,$$

$$C_5 : \mathcal{I}_{ij}(\mathbf{W}) - \mathcal{G}_{ij}(\mathbf{W}, \zeta_{ij}) \leq 0, \forall i, \ \forall j, \qquad C_6 : \ \log \zeta_{ij} \geq \eta_{ij} \theta_i^{\min}, \ \forall i, \ \forall j.$$

$$C_7 : \sum_{i=1}^{N}\sum_{j=1}^{T} \|\mathbf{w}_{ij}\|_2^2 \leq P_T,$$

where $\alpha_i > 0$ are the penalty parameters. Notice that point-wise maximum of convex function is convex, hence, problem $\mathcal{P}_{\bigtriangledown}^{\text{UC}}$ is also a DC problem. In the sequel, the CCP based iterative algorithm is proposed for solving $\mathcal{P}_{/}^{\text{UC}}$.

4.2.5 JMSP-UC: A CCP based algorithm

In this section, a CCP based iterative algorithm is proposed for the JMSP for the STM model which is simply referred to as *JMSP-UC*. The CCP is an iterative algorithm wherein each iterate the following two steps are executed until the convergence:

- Convexification: Let $(\mathbf{W}, \boldsymbol{\eta}, \boldsymbol{\zeta})^{k-1}$ be the estimates of $\mathbf{W}, \boldsymbol{\eta}, \boldsymbol{\zeta}$ in iteration $k-1$. Further, let $\tilde{\mathbb{P}}\left(\eta_{ij}; \eta_{ij}^{k-1}\right)$ and $\tilde{\mathcal{G}}_{ij}\left(\mathbf{W}, \zeta_{ij}; \mathbf{W}^{k-1}, \zeta_{ij}^{k-1}\right)$ be the first order Taylor approximations of $\mathbb{P}\left(\eta_{ij}\right)$ and $\mathcal{G}_{ij}\left(\mathbf{W}, \zeta_{ij}\right)$ around $(\mathbf{W}, \boldsymbol{\eta}, \boldsymbol{\zeta})^{k-1}$ respectively and their corresponding expressions can easily obtained as given in [81]. In convexification step, in iteration k, the concave part of the objective in $\mathcal{P}_{\bigtriangledown}^{\text{UC}}$ i.e., $\lambda_1 \sum_{i=1}^{N} \sum_{j=1}^{T} \mathbb{P}\left(\eta_{ij}\right)$ is replaced by $\lambda_1 \sum_{i=1}^{N} \sum_{j=1}^{T} \tilde{\mathbb{P}}\left(\eta_{ij}; \eta_{ij}^{k-1}\right)$ and the concave part of constraint C_5 i.e., $-\mathcal{G}_{ij}\left(\mathbf{W}, \zeta_{ij}\right)$ is replaced by $-\tilde{\mathcal{G}}_{ij}\left(\mathbf{W}, \zeta_{ij}; \mathbf{W}^{k-1}, \zeta_{ij}^{k-1}\right)$. This approximation renders the problem $\mathcal{P}_{\bigtriangledown}^{\text{UC}}$ into a convex problem. In other words, this step convexifies the problem at the current iterate, hence, the name convexification. Notice that this convex problem, obtained from the convexification step, provides a global upper bound for the original non-convex DC problem $\mathcal{P}_{/}^{\text{UC}}$. So, the CCP iteratively constructs a global upper bound at the current iterate which is solved in the optimization step.

- Optimization: The next update $(\mathbf{W}, \boldsymbol{\eta}, \boldsymbol{\zeta})^{k}$ is obtained by solving the following convex problem :

$$\begin{aligned}
\mathcal{P}_{\text{ı}}^{\text{UC}} : \min_{\mathbf{W}, \boldsymbol{\eta}, \boldsymbol{\zeta}} \; & f_1\left(\boldsymbol{\eta}\right) + \sum_{i=1}^{N} \alpha_i \max\left\{\theta_i - \sum_{j=1}^{T} \log \zeta_{ij}, 0\right\} + \lambda_1 \sum_{i=1}^{N} \sum_{j=1}^{T} \tilde{\mathbb{P}}\left(\eta_{ij}\right) \qquad (4.10) \\
\text{s.t. } & C_1, C_2, C_3, C_4, C_6, C_7 \text{ in (4.9)}, \\
& C_5 : \mathcal{I}_{ij}\left(\mathbf{W}\right) - \tilde{\mathcal{G}}_{ij}\left(\mathbf{W}^{k-1}, \zeta_{ij}^{k-1}\right) \leq 0, \forall i, \; \forall j.
\end{aligned}$$

Remarks:

- The proposed JMSP-UC algorithm is based on the CCP framework. Therefore, to ensure the convergence to a stationary point, JMSP-UC needs to be initialized with a feasible point [54, 55].

- An FIP and the appropriate choice of λ_1 and $\{\alpha_i\}$s ensure the convergence of JMSP-UC to a stationary point with binary $\boldsymbol{\eta}$. Hence, the obtained stationary point by JMSP-UC is also feasible to original problem $\mathcal{P}_1^{\text{UC}}$.

In the next section, a simple procedure is proposed to obtain a FIP for JMSP-UC.

4.2.6 Feasible Initial Point: UC

The performance of CCP based algorithms is dependent on the quality of FIPs. The JMSP-UC can simply be initialized with an all-zero trivial FIP i.e., $\boldsymbol{\eta} = 0$, $\boldsymbol{\zeta} = 0$ and $\mathbf{W} = 0$. However, the all-zero trivial FIP has the worst performance, hence, the algorithm is likely to converge to a stationary point in the region around the trivial FIP which typically performs poorly [81]. Hence, the simple iterative procedure, inspired by [81], is proposed to obtain a better choice of FIPs.

- Step 1: Initialize $\hat{\boldsymbol{\eta}}$ that satisfies constraints C_1 and C_3 in $\mathcal{P}_{/}^{\text{UC}}$, and $0 < \epsilon < 1$.
- Step 2: Solve the following optimization:

$$\begin{aligned}
&\mathcal{P}_{\text{FES}}^{\text{UC}} : \hat{\mathbf{W}} : \text{ find } \mathbf{W} \qquad (4.11)\\
&\text{s.t. } C_1 : \ \|\mathbf{w}_{ij}\|_2^2 \ \leq \ P_S \eta_{ij}, \ \forall i, \forall j, \quad C_2 : \mathbb{R}\{\mathbf{h}_{ij}^H \mathbf{w}_{ij}\} \geq 0, \forall i, \forall j,\\
&C_3 : \Im\{\mathbf{h}_{ij}^H \mathbf{w}_{ij}\} = 0, \forall i, \forall j, \qquad C_4 : \left\| \left[\sigma \ldots \{\mathbf{h}_{ij}^H \mathbf{w}_{lj}\}_{l \neq i} \ldots\right] \right\|_2 \leq \frac{\mathbf{h}_{ij}^H \mathbf{w}_{ij}}{\sqrt{\hat{\eta}_{ij} \theta_i^{\min}}}, \ \forall i, \forall j\\
&C_5 : \ \sum_{i=1}^{N} \|\mathbf{w}_{ij}\|_2^2 \leq P_S, \forall j. \qquad C_6 : \ \sum_{i=1}^{N} \sum_{j=1}^{T} \|\mathbf{w}_{ij}\|_2^2 \leq P_T.
\end{aligned}$$

- Step 3: If $\mathcal{P}_{\text{FES}}^{\text{UC}}$ is feasible go to step 4 else update $\hat{\boldsymbol{\eta}} = \epsilon \hat{\boldsymbol{\eta}}$ and go to step 2.
- Step 4: Set $\mathbf{W}^0 = \hat{\mathbf{W}}$ and $\boldsymbol{\eta}^0 = \hat{\boldsymbol{\eta}}$. Choose ζ_{ij}^0 such that $1 + \eta_{ij} \theta_i^{\min} \leq \zeta_{ij}^0 \leq 1 + \gamma_{ij}^0$ where γ_{ij}^0 is the SINR of the user i in slot j calculated using $\mathbf{W}^0$.

Remarks:

- the updates of $\hat{\boldsymbol{\eta}}$ chosen in step1 are always feasible. Different choices of initial $\hat{\boldsymbol{\eta}}$ and $\epsilon \in (0, 1)$ in step 1 may lead to different FIPs.
- For a fixed $\hat{\boldsymbol{\eta}}$, with the help of C_3 and C_4 in $\mathcal{P}_{\text{FES}}^{\text{UC}}$, the the QoS constraint, i.e. $\gamma_{ij} \geq \hat{\eta}_{ij} \theta_i^{\min}$ is reformulated as a second-order cone (SOC) constraint C_2 in $\mathcal{P}_{\text{FES}}^{\text{UC}}$ [9]. Problem $\mathcal{P}_{\text{FES}}^{\text{UC}}$ is convex and it can be solved efficiently using convex optimization solver like CVX to a large dimension [67].
- Notice that the proposed procedure always yields a feasible initial point. To see this, If the initial iterates fail to result an non trivial feasible point, the update in step 3 eventually lead to $\hat{\boldsymbol{\eta}} = \mathbf{0}$ and thus $\mathcal{P}_{\text{FES}}^{\text{UC}}$ in step 2 becomes feasible with $\hat{\mathbf{W}} = 0$. Hence, the proposed methods always result in FIP.
- The FIP obtained by this procedure may not be feasible for the original problem $\mathcal{P}_{\text{UC}}^{\infty}$ unless $\hat{\boldsymbol{\eta}}$ and $\hat{\mathbf{W}}$ satisfies the constraint set of $\mathcal{P}_{\infty}^{\text{UC}}$. However, the stationary point obtained by JMSP-UC with this FIP becomes a feasible to $\mathcal{P}_{\infty}^{\text{UC}}$ since it satisfies the scheduling and QoS constraints of $\mathcal{P}_{\infty}^{\text{UC}}$.

4.2.7 Complexity: UC

The JMSP-UC is an iterative algorithm and its overall complexity is the summation of complexity to obtain FIP by the procedure proposed in Section 4.2.6 and the complexity to obtain a stationary point by the procedure proposed in Section 4.2.5. The complexity of iterative procedure proposed in Section 4.2.6 depends on the per iteration complexity of the problem $\mathcal{P}^{\text{FES-UC}}$. $\mathcal{P}^{\text{FES-UC}}$ is a convex problem with MNT decision variables, $2NT+T$ convex constraints and $2NT$ linear constraints. Hence, the computational complexity of $\mathcal{P}_{\text{FES}}^{\text{UC}}$ is $\mathcal{O}\left((MNT)^3 (4NT + T)\right)$ [64]. Similarly, the complexity of obtaining a stationary point by the procedure in Section 4.2.5 depends on the per iteration complexity of the convex problem $\mathcal{P}_{7}^{\text{UC}}$. The problem $\mathcal{P}_{\text{'}}^{\text{UC}}$ has $(MNT + 2NT)$ decision variables and $(3NT + T)$ convex constraints and $2NT + N$ linear constraints. Hence, the computational complexity of $\mathcal{P}_{\text{'}}^{\text{UC}}$ is $\mathcal{O}\left((MNT + 2NT)^3 (5NT + T + N)\right)$ [64].

Letting $\mathcal{P}_{/}^{\text{UC}}(\|)$ to be the objective value of the problem $\mathcal{P}_{/}^{\text{UC}}$ at iteration k, the pseudo code of JMSP-UC is given in algorithm 6.

Algorithm 6 JMSP-UC

Input: $\{\mathbf{h}_{ij}\}_{i=1,j=1}^{N,T}, \kappa, P_S, \{\omega_j,\ \delta_j\}_{j=1}^{T}, \boldsymbol{\eta}^0, \boldsymbol{\zeta}^0, \mathbf{W}^0, \lambda_1 = 0, \{\alpha_i, \theta_i\}_{i=1}^{N}, k = 1;$
Output: $\mathbf{W}, \boldsymbol{\eta}$
while $|\mathcal{P}_{/}^{\mathrm{UC}}(\|) - \mathcal{P}_{/}^{\mathrm{UC}}(\| - \infty)| \geq \kappa$ **do**
  Convexification: Convexify the problem (4.9).
  Optimization: Update $(\mathbf{W}, \boldsymbol{\eta}, \boldsymbol{\zeta})^k$ by solving $\mathcal{P}_{\text{'}}^{\mathrm{UC}}$
  Update : $\mathcal{P}_{/}^{\mathrm{UC}}(\|), \lambda_\infty, \{\alpha_\rangle\}_{\rangle=\infty}^{\mathcal{N}}, \{\omega_|\}_{|=\infty}^{\mathcal{T}}, \|$
end while

4.3 Multigroup multicasting

In this section, we consider the joint design of user scheduling and precoding over for the multigroup multicast (MGMC) transmission scenario. Within the framework proposed in Section 4.2 together with [102], joint design for MGMC system with number of groups larger than transmit antennas (referred to as group scheduling in [102]) and multislot transmission per user (similar to Section 4.2) can be addressed. Therefore, to focus more on addressing MGMC characteristics associated with joint design, we consider the following system model. Let M be the number of groups and without of loss of generality, and for notional simplicity, $\bar{N}$ be the number of users in each group. Generally, groups with a large number of users with huge variations in the channel gains of users may not be served with required QoS in a slot completely. This is accommodated by serving each group over multiple slots. However, a user belonging to a group is allowed to be scheduled in exactly one slot. Furthermore, all the users in group k must be served with a latency requirement of $\bar{T}_k$ and with a target rate of $\bar{\theta}_k$.

Towards defining the signal model mathematically, let $\mathbf{h}_{ij,k} \in \mathbb{C}^{M\times 1}$, $\mathbf{w}_{j,k} \in \mathbb{C}^{M\times 1}$ and $n_{ij,k}$ denote the downlink channel, precoding vector and noise of user i in group k at time slot j respectively. Similarly, let $\gamma_{ij,k} = \dfrac{|(\mathbf{h}_{ij,k})^H \mathbf{w}_{j,k}|^2}{\sum_{l\neq i} |(\mathbf{h}_{ij,k})^H \mathbf{w}_{j,k}|^2 + \sigma^2}$ and $R_{ij,k} = \log(1+\gamma_{ij,k})$ be the SINR and rate of user i in group k in slot j respectively. Further, $\gamma_{j,k} = \min_{\forall i} \gamma_{ij,k}$ and $R_{j,k} = \min_{\forall i} R_{ij,k}$ be the SINR and rate of group k in slot j respectively. Finally, let $\eta_{ij,k} \in \{0,1\}$ be the binary scheduling variable associated with user i in group k in time slot j and $\delta_{j,k} \in \{0,1\}$ be the binary variable associated with group k in time slot j.

Similar to the UC model, service time minimization required to serve all the groups is considered as the objective of design subject to minimum rate and latency requirements of each group, and per slot and total transmission power limitations; this problem is simply referred to as STM-MC. Without of loss of generality and notional simplification, let $\bar{T}_k = T, \forall k$. With the help of defined notations, the STM-MC problem is formulated as,

$$\mathcal{P}_{\infty}^{\mathrm{MC}}: \min_{\mathbf{W},\boldsymbol{\eta},\boldsymbol{\delta}} f(\mathbf{W}) \qquad \text{s.t. } C_1:\ \eta_{ij,k} \in \{0,1\},\ \forall i,\ \forall j,\ \forall k, \tag{4.12}$$

$$C_2: \delta_{j,k} \in \{0,1\},\ \ \forall j,\ \forall k, \qquad C_3:\ \|\mathbf{w}_{j,k}\|_2^2 \leq P_S \delta_{j,k},\ \forall j,\ \forall k,$$

$$C_4: \sum_{j=1}^{T} \eta_{ij,k} = 1, \forall i, \forall g, \qquad C_5:\ \sum_{i=1}^{N} \eta_{ij,k} \geq \delta_{j,k},\ \forall j,\ \forall k,$$

$$C_6: \sum_{k=1}^{G} \|\mathbf{w}_{j,k}\|_2^2 \leq P_S, \forall j, \qquad C_7:\ R_{ij,k} \geq \eta_{ij,k}\bar{\theta}_k, \forall i,\ \forall j,\ \forall k,$$

$$C_8: \sum_{j=1}^{T}\sum_{k=1}^{G} \|\mathbf{w}_{j,k}\|_2^2 \leq P_T. \tag{4.13}$$

Remarks

- Constraint C_3 in $\mathcal{P}_{\infty}^{\mathrm{MC}}$ controls the scheduling of groups.

- Constraint C_4 in $\mathcal{P}_{\infty}^{\text{MC}}$ ensure that user i belong to group k is scheduled exactly in one of the time slots within the latency requirement T.
- Constraint C_5 ensures that in a scheduled group at least one user is scheduled
- C_6 is the per slot maximum allowed power constraint and C_8 is the total power constraint.
- Constraint C_7 ensures that scheduled users satisfy the corresponding QoS requirement.

Notice that the problem $\mathcal{P}_{\infty}^{\text{MC}}$ is combinatorial and non-convex. Similar to $\mathcal{P}_3^{\text{UC}}$, the constraints C_1 and C_2 can also be addressed by relaxation and binary penalization. The transformed DC formulation of $\mathcal{P}_{\infty}^{\text{MC}}$ using slack variables $\zeta_{ij,k}$s followed by binary relaxation of $\eta_{ij,k}, \delta_{j,k}$s and penalization is,

$$\mathcal{P}_{\in}^{\text{MC}}: \min_{\mathbf{W},\boldsymbol{\eta},\boldsymbol{\delta},\boldsymbol{\zeta}} \tilde{f}_1(\boldsymbol{\delta}) + \lambda_2 \sum_{i=1}^{N}\sum_{j=1}^{T}\sum_{k=1}^{G} \mathbb{P}(\eta_{ij,k}) + \lambda_3 \sum_{j=1}^{T}\sum_{k=1}^{G} \mathbb{P}(\delta_{j,k}) + \sum_{i=1}^{N}\sum_{k=1}^{G} \beta_{i,k} \left\| \sum_{j=1}^{T} \eta_{ij,k} - 1 \right\|_2 \tag{4.14}$$

$$\text{s.t. } C_1: \ 0 \le \eta_{ij,k} \le 1, \forall i, \ \forall j, \ \forall k, \qquad C_2: \ \|\mathbf{w}_{ij}\|_2^2 \ \le \ P_S \eta_{ij}, \forall i, \ \forall j, \ \forall k,$$

$$C_3: \ 0 \le \delta_{j,k} \le 1, \ \forall i, \ \forall j, \ \forall k, \qquad C_4: \ \sum_{i=1}^{N} \eta_{ij,k} \ge \delta_{j,k}, \ \forall j, \ \forall k,$$

$$C_5: \ \sum_{k=1}^{G} \delta_{j,k} \le M, \ \forall j, \qquad C_6: \ \mathcal{I}_{ij,k}(\mathbf{W}) - \mathcal{G}_{ij,k}(\mathbf{W}, \zeta_{ij,k}) \le 0, \forall i, \ \forall j, \ \forall k,$$

$$C_7: \ \log \zeta_{ij,k} \ge \eta_{ij,k} \bar{\theta}_k, \forall i, \ \forall j, \ \forall k, \qquad C_8: \sum_{j=1}^{T}\sum_{k=1}^{G} \|\mathbf{w}_{j,k}\|_2^2 \le P_T,$$

where $\boldsymbol{\delta}_k = [\boldsymbol{\delta}_{1,k}, \ldots, \boldsymbol{\delta}_{T,k}]$, $\boldsymbol{\delta} = \left[\boldsymbol{\delta}_1^T, \ldots, \boldsymbol{\delta}_k^T\right]^T$, $\lambda_2 > 0$ and $\lambda_3 > 0$ penalty parameters for promoting the binary nature of $\eta_{ij,k}$ and δ_j^k respectively, and $\mathcal{I}_{ij,k}(\mathbf{W}) = \sigma^2 + \sum_{l \ne k} |\mathbf{h}_{ij,k}^H \mathbf{w}_{j,l}|^2$ and $\mathcal{G}_{ij,k}(\mathbf{W}, \zeta_{ij,k}) = \dfrac{\sigma^2 + \sum_{l=1}^{N} |\mathbf{h}_{ij,k}^H \mathbf{w}_{j,l}|^2}{\zeta_{ij,k}}$. Notice that for the ease of finding the FIPs, the constraint C_3 in $\mathcal{P}_{\infty}^{\text{MC}}$ brought into objective of $\mathcal{P}_{\in}^{\text{MC}}$ with the help of penalty parameter $\beta_{i,k} > 0$.

The problem $\mathcal{P}_{\in}^{\text{MC}}$ is a DC problem and, hence, given a FIP its first-order stationary point can be obtained through CCP based algorithm JMSP-MC given in Appendix B

A FIP to $\mathcal{P}_{\in}^{\text{MC}}$ can be obtained by the following procedure:

- Step 1: Initialize $\hat{\boldsymbol{\eta}}$, $\hat{\boldsymbol{\delta}}$ that satisfy constraints C_1, C_3, C_4 and C_5 in $\mathcal{P}_{\in}^{\text{UC}}$, and $0 < \epsilon < 1$.
- Step 2: Solve the following optimization:

$$\mathcal{P}_{\text{FES}}^{\text{MC}}: \hat{\mathbf{W}}: \ \text{find } \mathbf{W} \tag{4.15}$$

$$\text{s.t. } C_1: \ \|\mathbf{w}_{j,k}\|_2^2 \ \le \ P_S \eta_{ij,k}, \ \forall i, \forall j, \qquad C_2: \mathbb{R}\left\{ (\mathbf{h}_{ij,k})^H \mathbf{w}_{j,k} \right\} \ge 0, \forall i, \forall j,$$

$$C_3: \Im\left\{ (\mathbf{h}_{ij,k})^H \mathbf{w}_{j,k} \right\} = 0, \forall i, \forall j,$$

$$C_4: \left\| \left[\sigma \ldots \left\{ (\mathbf{h}_{ij,k})^H \mathbf{w}_{j,l} \right\}_{l \ne k} \ldots \right] \right\|_2 \le \frac{(\mathbf{h}_{ij,k})^H \mathbf{w}_{j,k}}{\sqrt{\hat{\eta}_{ij,k} \bar{\theta}_k}}, \ \forall i, \forall j$$

$$C_5: \sum_{k=1}^{G} \|\mathbf{w}_{j,k}\|_2^2 \leq P_S, \forall j. \qquad C_6: \sum_{k=1}^{G}\sum_{j=1}^{T} \|\mathbf{w}_{j,k}\|_2^2 \leq P_T.$$

- Step 3: If $\mathcal{P}_{\text{FES}}^{\text{MC}}$ is feasible go to step 4 else update $\hat{\boldsymbol{\eta}} = \delta\hat{\boldsymbol{\eta}}$, $\hat{\boldsymbol{\delta}} = \epsilon\hat{\boldsymbol{\delta}}$ and go to step 2.
- Step 4: Set $\mathbf{W}^0 = \hat{\mathbf{W}}$, $\boldsymbol{\eta}^0 = \hat{\boldsymbol{\eta}}$ and $\boldsymbol{\delta}^0 = \hat{\boldsymbol{\delta}}$. Choose ζ_{ij}^0 such that $1 + \eta_{ij,k}\theta_i^{\min} \leq \zeta_{ij,k}^0 \leq 1 + \gamma_{ij}^0$ where $\gamma_{ij,k}^0$ is the SINR of the user i belong to group to group k in slot j calculated using $\mathbf{W}^0$.

The FIP obtained by this procedure may not be feasible for the original problem $\mathcal{P}_{\infty}^{\text{MC}}$ unless the solution of $\mathcal{P}_{\text{FES}}^{\text{UC}}$ i.e., $\hat{\boldsymbol{\eta}}, \hat{\mathbf{W}}$ satisfies the constraint set of $\mathcal{P}_{\infty}^{\text{MC}}$. However, the stationary point obtained by JMSP-MC with this FIP becomes a feasible to $\mathcal{P}_{\text{MC}}^{\infty}$ since it satisfies the scheduling and QoS constraints of $\mathcal{P}_{\infty}^{\text{MC}}$.

4.4 Simulation results

In this section, we evaluate the performance of the proposed algorithms i.e., JMSP-UC and JMSP-MC for UC and MC system models respectively.

4.4.1 Simulation setup and parameter initialization

The system and algorithmic parameters that are discussed in this paragraph are common to all the presented cases. Receiver noise variance is assumed to unity i.e., $\sigma^2 = 1$. The algorithms JMSP-UC and JMSP-MC are prioritized to ensure the relaxed constraints C_1 in $\mathcal{P}_1^{\text{UC}}$ and C_7 in $\mathcal{P}_3^{\text{UC}}$ over obtaining binary solutions. Therefore, $\{\alpha_i, \beta_i\}_{i=1}^T$ are initialized with relatively larger values than λ_1 and λ_2. The penalty parameters λ_1 and λ_2 are initialized each to 0.5 and incremented by a factor 1.1 until $\lambda_1, \lambda_2 \leq 100$ and $\{\alpha_i, \beta_i\}_{i=1}^T$ are initialized each with 50 and incremented until the constraints C_1 in $\mathcal{P}_1^{\text{UC}}$ and C_7 in $\mathcal{P}_3^{\text{MC}}$ are met. Correlated Rayleigh channel coefficients in time across multiple time slots is generated as in [103] independently for each combination of user and BS transmit antenna with the following parameters: sampling rate 1Hz and maximum Doppler shift is 0.1Hz. Simulation results in all the figures are averaged over 500 different channel realizations (CRs).

4.4.2 Sequential benchmark solution

Due to a lack of available benchmark solutions, the performance of the proposed JMSP algorithms is compared with a sequential benchmark solution (SBS). In SBS, each iteration fills the current time slot considering the previous results and current channel/ user requirement conditions. In the sequel, we propose SBS algorithms for both the UC and MC models, and are referred to as SBS-UC and SBS-MC respectively.

SBS-UC

In SBS-UC, in iteration (or time slot) j, a joint scheduling and precoding algorithm (proposed in [81]) is performed based on the channel states of the users whose QoS requirements are not yet fully served in the previous $j-1$ time slots. The proposed SBS-UC executes the following steps:

- Step 1: Initialize $\mathcal{N} = \{1, \ldots, N\}$, $j = 1$, $\hat{\theta}_i = \theta_i, \forall i$, $\hat{T}_i = T_i, \forall i$, $\hat{P}_T = P_T$, and $\hat{P}_S = P_S$
- Step 2: In iteration j, solve the following problem:

$$\mathcal{P}^{\text{SBS-UC}}: \max_{\mathbf{Z},\boldsymbol{b}} \sum_{i\in\mathcal{N}} \frac{\tilde{\theta}_i}{\hat{T}_i} b_i \qquad \text{s.t. } C_1: \; b_i \in \{0,1\}, \; \forall i \in \mathcal{N},$$

$$C_2: \|\mathbf{w}_i\|_2^2 \leq P_S b_i, \forall i \in \mathcal{N}, \qquad C_3: \sum_{i\in\mathcal{N}} b_i \leq M, \forall i \in \mathcal{N},$$
$$C_4: \sum_{i\in\mathcal{N}} \|\mathbf{w}_i\|_2^2 \leq \hat{P}_S, \qquad C_5: \tilde{R}_{ij} \geq b_i \theta_i^{\min}, \forall i \in \mathcal{N},$$

where $b_i \in \{0,1\}$, $\mathbf{z}_i \in \mathcal{C}^{M\times 1}$ be the binary scheduling variable and precoding vector associated with user i respectively, and $\tilde{R}_{ij} = \log\left(1 + \frac{|\mathbf{h}_{ij}^H \mathbf{z}_i|^2}{\sum_{l\neq i} |\mathbf{h}_{ij}^H \mathbf{z}_l|^2 + \sigma^2}\right)$, $\boldsymbol{b} = [\ldots, b_{i\in\mathcal{N}}, \ldots]$, and $\mathbf{Z} = [\ldots, \mathbf{z}_{i\in\mathcal{N}}, \ldots]$.

- Step 3: SBS-UC is infeasible if $\mathcal{P}^{\text{SBS-UC}}$ in step 2 is infeasible and exit the procedure. If $\mathcal{P}^{\text{SBS-UC}}$ in step 2 is feasible then then update $\tilde{P}_T = \tilde{P}_T - \sum_{i\in\mathcal{N}} \|\mathbf{z}_i\|_2^2$, $\tilde{P}_S = \min\left\{\tilde{P}_S, \tilde{P}_T\right\}$, $\mathcal{N} = \mathcal{N} \setminus \{i \text{ if } R_i >= \tilde{\theta}_i\}_{i\in\mathcal{N}}$, and $\tilde{T}_i = \tilde{T}_i - 1, \forall i \in \mathcal{N}$. For the updated $\mathcal{N}$ and $\tilde{T}_i$s three possibilities can occur:
  - If $|\mathcal{N}| \neq 0$ and $\max_i T_i <= 0$ then SBS-UC is infeasibe and exit the procedure; this is because at least one of the users' latency requirement is not met.
  - If $|\mathcal{N}| = 0$ then SBS-UC is feasible with j being the minimum number of required slots.
  - If $|\mathcal{N}| \neq 0$ and $\max_i T_i >= 0$ then update $\tilde{\theta}_i = \tilde{\theta}_i - R_i, i \in \mathcal{N}\}$ and go to step 2

The problem $\mathcal{P}^{\text{SBS-UC}}$ in step 2 maximizes the sum-rate for $\mu = 1$ and maximizes the scheduled users for $\mu = 0$. In SBS-UC, in iteration or slot j, to account for QoS and latency requirements, a weighted maximization of sum of scheduled users (or sum-rate depending on μ) is considered where weights are ratio of remaining rate to be met to the remaining latency requirements. Notice that the problem $\mathcal{P}^{\text{SBS-UC}}$ is combinatorial and non-convex hence it is difficult to obtain its optimal solution. However, the first-order stationary points of $\mathcal{P}^{\text{SBS-UC}}$ can be obtained by [81].

SBS-MC

Similar to SBS-UC, the sequential solution for MC model i.e. SBS-MC executes the following steps:

- Step 1: Initialize $\mathcal{N}_k = \{1, \ldots, \bar{N}\}$, $\forall k$, $j = 1$, $\tilde{T}_k = T_k, \forall k$, $\tilde{P}_T = P_T$, $\mathcal{K} = \{1, \ldots, M\}$ and $\tilde{P}_S = P_S$
- Step 2: In iteration j, solve the following problem:

$$\mathcal{P}^{\text{SBS-MC}}: \max_{\mathbf{Z}, \{\boldsymbol{b}_k\}_{\forall k}} \sum_{k\in\mathcal{K}} \sum_{i\in\mathcal{N}_k} \frac{\bar{\theta}_k}{\tilde{T}_k} b_{i,k} \qquad \text{s.t. } C_1: b_{i,k} \in \{0,1\}, \forall i \in \mathcal{N}_k, \forall k \in \mathcal{K},$$
$$C_2: a_k \in \{0,1\}, \forall k \in \mathcal{K}, \qquad C_3: \|\mathbf{w}_k\|_2^2 \leq \tilde{P}_S a_k, \forall \forall k \in \mathcal{K},$$
$$C_4: \sum_{\forall i\in\mathcal{N}_k} b_{k,i} \geq a_k, \forall k \in \mathcal{K}, \qquad C_5: \sum_{\forall k\in\mathcal{K}} a_k \leq M,$$
$$C_5: \tilde{R}_{ij,k} \geq b_{i,k}\bar{\theta}_k, \forall i, \qquad C_6: \sum_{k=1}^{G} \|\mathbf{z}_k\|_2^2 \leq \tilde{P}_S,$$

where $b_{i,k} \in \{0,1\}$ is the binary scheduling variable associated with user i in group k, a_k and $\mathbf{z}_k \in \mathcal{C}^{M\times 1}$ are the binary variable and precoding vector associated with group k respectively, and $\tilde{R}_{ij,k} = \log\left(1 + \frac{|\mathbf{h}_{ij,k}^H \mathbf{z}_k|^2}{\sum_{l\neq k} |\mathbf{h}_{ij,k}^H \mathbf{z}_l|^2 + \sigma^2}\right)$, $\boldsymbol{b}_k = [\ldots, b_{i\in\mathcal{N}_k,k}, \ldots]$, and $\mathbf{Z} = [\ldots, \mathbf{z}_{k\in\mathcal{K}}, \ldots]$.

- Step 3: SBS-MC is infeasible if $\mathcal{P}^{\text{SBS-MC}}$ in step 2 is infeasible and exit the procedure. If $\mathcal{P}^{\text{SBS-MC}}$ in step 2 is feasible then update $\tilde{P}_T = \tilde{P}_T - \sum_{k\in\mathcal{K}} \|\mathbf{z}_i\|_2^2$, $\tilde{P}_S = \min\left\{\tilde{P}_S, \tilde{P}_T\right\}$, $\mathcal{N}_k = \mathcal{N}_k \setminus \{i \text{ if } \tilde{R}_{ij,k} >= \tilde{\theta}_k\}_{i\in\mathcal{N}}$, $\mathcal{K} = \mathcal{K} \setminus \{k \text{ if } \mathcal{N}_k = \emptyset\}$ and $\tilde{T}_i = \tilde{T}_i - 1, \forall i \in \mathcal{N}$. For the updated $\mathcal{K}$, $\mathcal{N}_k$s and $\tilde{T}_i$s three possibilities can occur:
  - If $|\mathcal{K}| \neq 0$ and $\max_i T_i <= 0$ then SBS-UC is infeasible and exit the procedure; this is because at least one of the users' latency requirement is not met.
  - If $|\mathcal{K}| \neq 0$ and $\max_i T_i >= 0$ then go to step 2.
  - If $|\mathcal{K}| = 0$ then SBS-UC is feasible with j being the minimum number of required slots.

The problem $\mathcal{P}^{\text{SBS-MC}}$ in step 2 maximizes the scheduled users. To account for QoS and latency requirements of groups, a weighted maximization of the sum of scheduled users is considered where weights are the ratio of the remaining rate to be met to the remaining latency requirements. Similar to to the problem $\mathcal{P}^{\text{SBS-UC}}$, the problem $\mathcal{P}^{\text{SBS-MC}}$ is combinatorial and non-convex hence it is difficult to obtain its optimal solution. The problem $\mathcal{P}^{\text{SBS-MC}}$ is a special case of JMSP-MC or [88], and hence its first-order stationary points of $\mathcal{P}^{\text{SBS-UC}}$ can be obtained easily from by following the procedure similar to JMSP-MC or by [88].

Notice that the problem $\mathcal{P}^{\text{SBS-UC}}$ is combinatorial and non-convex hence it is difficult to obtain its optimal solution. However, the first-order stationary points of $\mathcal{P}^{\text{SBS-UC}}$ can be obtained the JMSP-WSR algorithm proposed in [81].

4.4.3 UC scenario

In this section, we evaluate the performance of the proposed framework for the unicast scenario. For comparison, we also consider the unstructured group sparsity based solution, where $\Omega_j, \forall j$ in JMSP-UC are updated according to [100] and it is termed as *GS based JMSP-UC*. Similarly, if the weights $\Omega_j, \forall j$ in JMSP-UC are updated according to (4.8) then it is termed as *proposed JMSP-UC*.

Performance comparison as a function of N

In figure 4.1, performance of the proposed JMSP-UC, GS based JMSP-UC and SBS-UC are compared as function of N. The simulation set up of figure 4.1 is as follows: $M = 3$, $P_S = 5$ Watts, $P_T = 30$ Watts, $\{\theta_i = [5, 7] \text{ dB}\}_{i=1}^N$, $\{\theta_i^{\min} = 0 \text{ dB}\}_{i=1}^N$, and $T_i = \lceil \frac{N}{M} \rceil + 3$ and N varying from 6 to 15 in steps of 3. Notice that the target SINR requirement for user $i \in [1, \ldots, N]$ is randomly drawn from $[5, 7]$ dB. In figure 4.1(a), Average service time (measured in time slots) in plotted as a function N. Notice that as GS based JMSP-UC does not promote the solutions with SGS, it requires the maximum service time. On the contrary, proposed JSBP-UC outperforms the GS based JMSP-UC as the weights proposed in (4.8) promote the SGS. Although SBS-UC manages to obtain feasible solution when the number of slots relatively larger with probability 0.4 (see in figure 4.1(b)) for $N = 6$, it fails completely for higher N e.g., $N = 12$. As SBS-UC can not foresee the consequences or advantages of scheduling or rejecting some users, it fails to obtain even a feasible solution in most of the cases. On the other hand, the joint design methods i.e., GS based JMSP-UC and proposed JMSP-UC obtain a feasible solution in most cases as they facilitate permuting users across the slots in order to obtain a feasible solution. Further, the joint design methods can foresee the split of SINR across the slots such that users' SINR requirement is met within the latency requirement.

In figure 4.1(b), the infeasibility of proposed JMSP-UC, GS based JMSP-UC and SBS-UC are depicted as a function of N. Due to the per slot maximum allowed power constraint P_S, scheduling at a conducive slot offers the only possibility to serve users whose SINR requirements

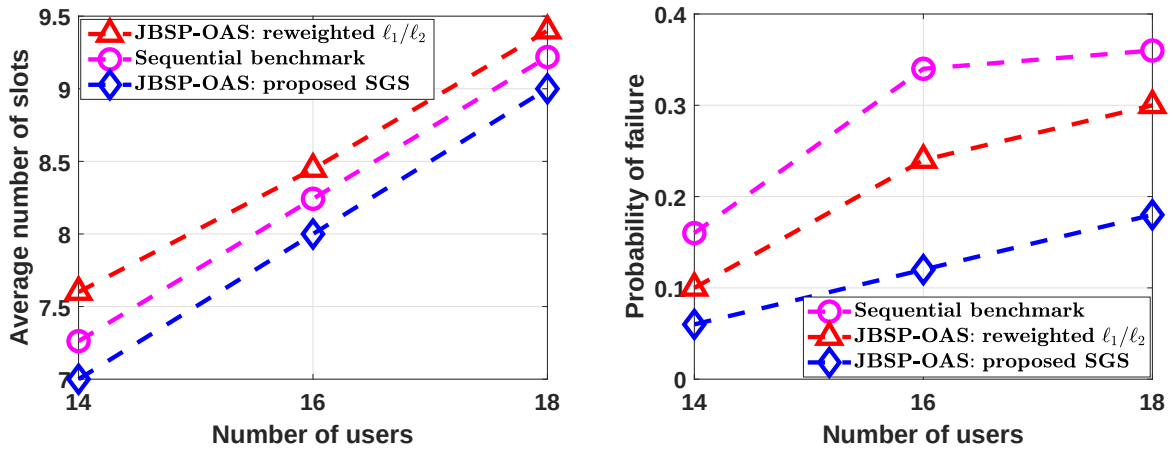

(a) (b)

FIGURE 4.1: Comparison of different optimization approaches for $M = 3$, $P_S = 5$ Watts, $P_T = 30$ Watts, $\{\theta_i = [5, 7]\text{dB}\}_{i=1}^{N}$, $\{\theta_i^{\min} = 0\text{ dB}\}_{i=1}^{N}$, and $T_i = \lceil \frac{N}{M} \rceil + 3$ and N varying from 6 to 15 in steps of 3 (a) average service time in slots (b) Probability of infeasibility

are not met currently.. This indicates that some users may require multiple slots which can be seen in figure 4.1(a) (e.g., for $N = 12$ case on an average the design requires 4.6 slots to serve all the users). In $\lceil \frac{N}{M} \rceil + L$, $\lceil \frac{N}{M} \rceil$ can be seen as the minimum number of slots to serve and L is the buffer to accommodate multiple slots per user and in figure 4.1(a), we use $L = 3$. For the given range of SINR requirement, when $\lceil \frac{N}{M} \rceil \leq 3$, the probability of infeasibility almost zero (as given in figure 4.1(b)) indicating that an excess of 3 slots is sufficient to serve all the users. The increase in N also typically increases the users requiring multiple slots and hence necessitating larger number slots to serve all users. Since SBS-UC does not consider the joint design across the slots it fails to obtain a feasible even for $N = 9$ with 0.9 probability. On the contrary, the joint design methods obtain a feasible for $N = 9$ almost with probability 1. This shows the efficacy of joint design methods over sequential methods.

As the superiority of the proposed JMSP-UC is established over SBS-UC and GS-based JMSP-UC, in the sequel we focus on evaluating JMSP-UC in different scenarios.

Performance comparison as a function of θ_i

In figure 4.2, performance of JMSP-UC illustrated as a function of target SINR requirement i.e., θ_i for $M = \{3, 4, 5\}$, $P_T = 40$ Watts, $N = 15$, $T_i = \lceil \frac{N}{M} \rceil + 3$ and θ_i varying from 4 to 10 dB in steps of 2 dB. For a fixed combination of N, M, P_S, P_T and $\theta_i^{\min}$, increment in the service time with respect to increase in the target SINR requirement can be observed in figure 4.2(a). This is because per slot maximum allowed power constraint limits the SINR at which a user can be served As a result, the users with relatively higher θ_i requirement need to be scheduled over a number of slots to meet the target SINR requirement of users. Further, the decrease in the service time with more antennas, i.e.,M, for the same θ_i requirements can be observed in figure 4.2(a). This is due to the multiplexing capability brought out by the antennas. As a result, the required service time decreases with an increase of M.

In figure 4.2(b), probability of infeasibility of problem $\mathcal{P}_1^{\text{UC}}$ is illustrated as a function of target SINR requirement. An increase in the probability of infeasibility can be observed as the target SINR requirement increases in figure 4.2(b). This could happen for two reasons: 1) Power outage: the total available power P_T is insufficient to serve all the users with required θ_i 2) Exceeding latency: Serving all the users with high θ_i within T_is is not possible. However, the improvement in the probability of infeasibility can be observed for a higher number of transmit antennas in figure 4.2(b).

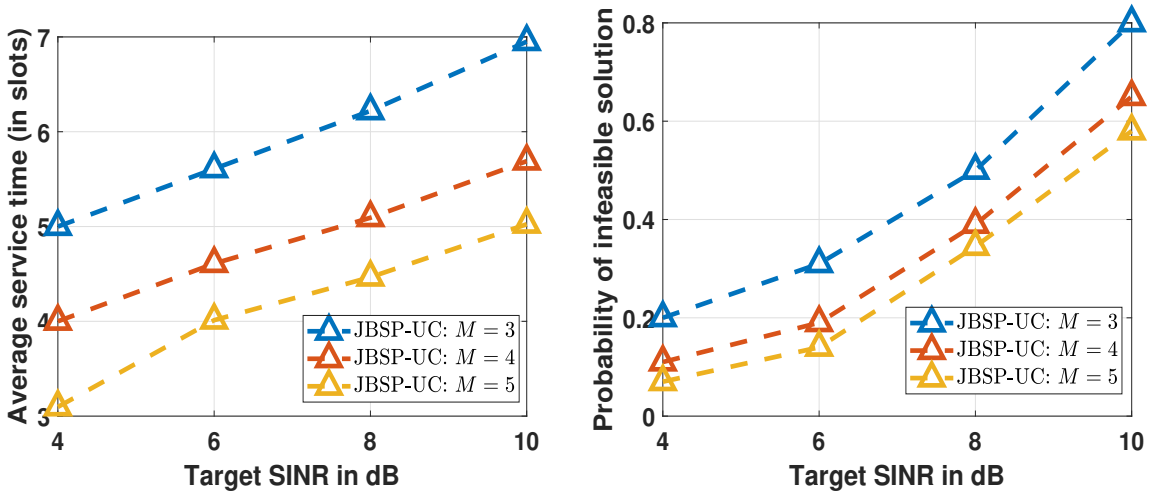

(a) (b)

FIGURE 4.2: Performance of JMSP-UC as a function of target SINR (i.e., θ_i) for $M = \{3, 4, 5\}$, $P_T = 40$ Watts, $\{\theta_i^{\min} = 0 \text{ dB}\}_{i=1}^{N}$, $N = 15$, $T_i = \lceil \frac{N}{M} \rceil + 3$, and $P_S = 5$ Watts and θ_i varying from 4 to 10 dB in steps of 2 dB (a) average service time in slots (b) Probability of infeasibility

Performance comparison as function of P_S

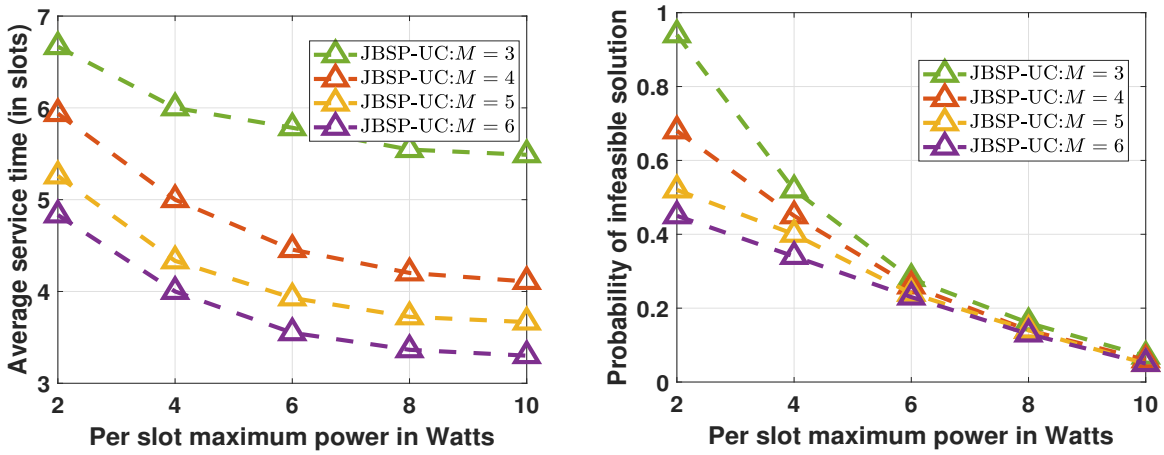

(a) (b)

FIGURE 4.3: Performance of JMSP-UC as a function per slot maximum allowed power (i.e., P_S) for $M = \{3, 4, 5, 6\}$, $P_T = 40$ Watts, $\{\theta_i = [7]\text{dB}\}_{i=1}^{N}$, $\{\theta_i^{\min} = 0 \text{ dB}\}_{i=1}^{N}$, $N = 15$, $T_i = \lceil \frac{N}{M} \rceil + 3$, and $P_S =$ varying from 2 to 10 Watts in steps of 2 Watts (a) average service time in slots (b) Probability of infeasibility

In figure 4.3, performance of JMSP-UC is illustrated as a function of per slot maximum allowed power i.e., P_S for $M = \{3, 4, 5\}$, $P_T = 40$ Watts, $\{\theta_i = 7 \text{ dB}\}_{i=1}^{N}$, $\{\theta_i^{\min} = 0 \text{ dB}\}_{i=1}^{N}$, $N = 15$ and P_S varying from 2 to 10 Watts in steps of 2 Watts. In figure 4.3(a), average service time (in slots) is plotted as a function of P_S. As the P_S limits the per slot achievable rates of users, for lower values P_S the design requires higher number of slots to fulfill the user QoS requirements. Similarly, relatively higher values P_S facilitate the users to obtain higher rates per slot; as a as result the total number of slots to serve all the users decreases in figure 4.3(a). The lower values of P_S in combination with tighter latency requirements can be lead to a higher probability of feasibility as shown in figure 4.3(b). On the other higher values of P_S facilitate the design to

meet the relatively tighter latency requirements as a result the lower probability of infeasibility can be observed in the right-hand side of figure 4.3(b).

4.4.4 MC scenario

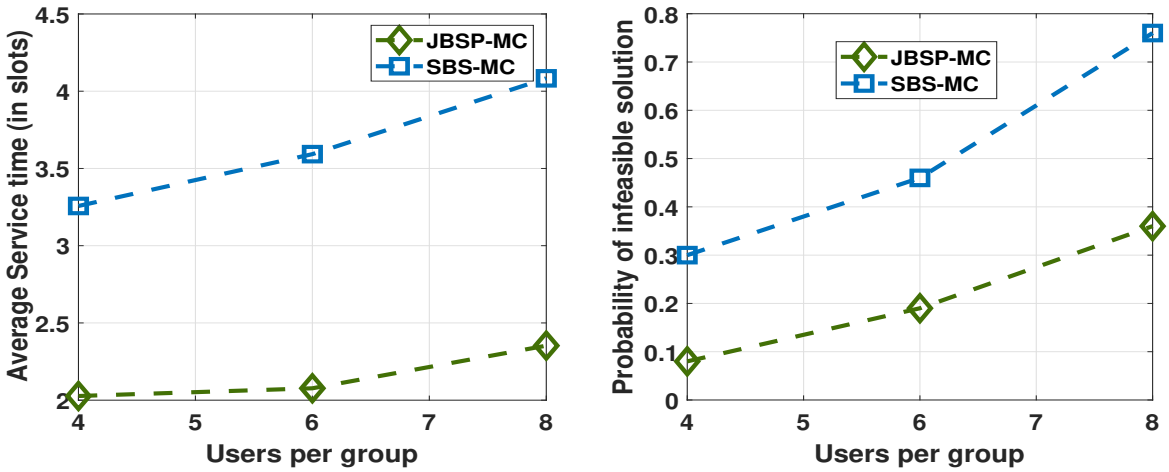

(a) (b)

FIGURE 4.4: Performance of JMSP-MC and SBS-MC as a function of users per group (i.e., $\bar{N}$) for $M = M = 3$, $P_T = 40$ Watts, $\{\bar{\theta}_k = 3\text{dB}\}_{i=1}^{N}$, and $P_S = 10$ dB (a) average service time in slots (b) Probability of infeasibility

In figure 4.4, performance of JMSP-MC against SBS-MC is illustrated as a function of user per group (i.e., $\bar{N}$) for $M = M = 3$, $P_T = 40$ Watts, $\{\bar{\theta}_k = [3]\text{dB}\}_{i=1}^{N}$, and $P_S = 10$ dB and $\bar{N}$ varying from 4 to 8 in steps of 2. In figure 4.4(a), average service time (in slots) required by JMSP-MC and SBS-MC is plotted. The superior performance of JMSP-MC over SBS-MC can be observed in figure 4.4(a) as it jointly design the scheduling and precoding over all the slots. SBS-MC iteratively maximizes the scheduled users in each slots, hence, it fails to foresee the consequence of scheduling particular users in this slot. One situation could be, it may schedule the users with orthogonal channels in the initial slots and leaves the correlated users to the later slots. As a result, it may schedule most of the users in the initial slots and may take more slots to schedule remaining fewer correlated users. On the other hand, JMSP-MC foresees these situations due to the joint and explore other combinations which result in relatively less service time.

In figure 4.4(b), the probability of failure to find the feasible solution is illustrated as a function of users per group. SBS-MC has a higher probability of finding a feasible solution compared to JMSP-MC as shown in figure 4.4(b). This could happen due to multiple reasons: 1) As SBS-MC tries to schedule relatively orthogonal users in different groups in the initial slots, it might be left with extremely correlated users whose SINR requirements can not be met [31]. 2) Power outage: as the power may not be optimized optimally, the joint scheduling and precoding problems in later iterations of SBS-MC could be infeasible due to insufficient power. On the other hand, JMSP-MC can foresee these scenarios might avoid putting users with extremely correlated channels from different groups in the same slot thus reducing the probability of infeasibility as shown in figure 4.4(b). Further, as the JMSP-MC considers the joint design across all the slots, it uses the power more efficiently in a way that improves the chances of the joint design becoming feasible compared to SBS-MC as shown in figure 4.4(b)

In figure 4.5, performance of JMSP-MC against SBS-MC is illustrated as a function of number of groups (i.e., M) for for $\bar{N}$,$P_T = 40$ Watts, $\{\bar{\theta}_k = 3\text{dB}\}_{i=1}^{N}$, and $P_S = 10$ dB and M varying from 2 to 6 in steps of 2. The superiority in performance of JMSP-MC compared to SBS-MC can

be observed in average service time in figure 4.5(a) and in the probability of finding a feasible solution in figure 4.5(b). Further, as the number of groups increases interference among the groups' increases and, hence, the achievable minimum SINR of the groups could be decreased. Therefore, all the users within a group may not be served in one slot. As a result, few users in a group can be served in a slot. Therefore, the average service time increases along with the increase in the number of groups which can be observed in figure 4.5(a). Moreover, the increase in the number of groups also leads to exhaustion of resources like power more quickly. As a result, the probability of problem becoming infeasible increases with an increase in the number of groups as shown in figure 4.5(b)

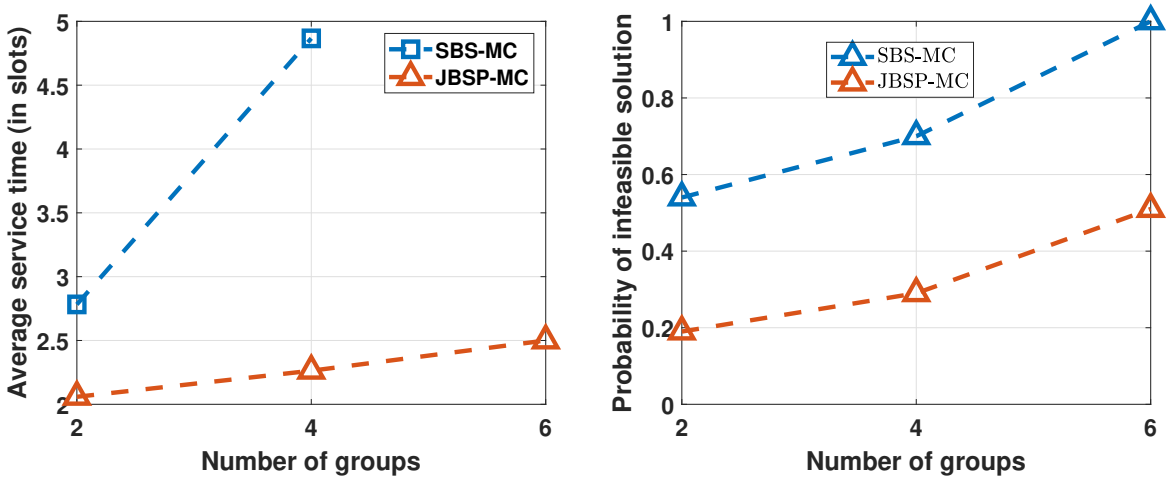

(a) (b)

FIGURE 4.5: Performance of JMSP-MC and SBS-MC as a function of groups (i.e., M) for $\bar{N}$,$P_T = 40$ Watts, $\{\bar{\theta}_k = 3\text{dB}\}_{i=1}^{N}$, and $P_S = 10$ dB (a) average service time in slots (b) Probability of infeasibility

4.5 Conclusions

In this paper, the joint design of user scheduling and precoding over multiple slots is addressed for two transmission scenarios: unicast and multicast. In this context, minimization of service time is considered as the objective of optimization adhering minimum rate, latency, per slot power and total power constraints. Further, this joint multislot design problem, with the help of Boolean variables addressing the scheduling and grouping, and linear variables addressing the precoding aspect of the design, is formulated as a structured MINLP problem. Furthermore, the service time minimization is transformed as a structured group sparsity problem with structure being having only few initial non-zero columns. These transformations render the problem as a DC programming problem. Subsequently, the paper proposed CCP based algorithms for both the models. Finally, the paper proposed low-complexity procedures to obtain good feasible initial points, critical to the implementation of CCP based algorithms. Through simulations, the paper establishes necessity of the joint multislot design over sequential solutions through probability of obtaining feasible solutions and also establishes superiority in service time.

5 Joint Sparse Scheduling and Precoding in Satellite Systems

5.1 Introduction

In the past few decades, satellite communication (SatCom) systems have exploited new techniques and technologies that were originally implemented in terrestrial communications. For instance, while in the mid-1980s advanced analog-to-digital and digital-to-analog converters (ADC and DAC, respectively) were used in delay-sensitive audio/voice applications, satellite systems adapted them into more complex digital signal processing techniques in delay-tolerant video broadcasting. Adaptation is critical due to the peculiarities of the SatCom system when compared to its terrestrial counterparts, including satellite channels, system constraints, and processing.

In the past few years, two important new trends have been observed in the satellite sector. The first one relies on the vast potential of the new generation of the so-called very high and high throughput satellite (V/HTS), as is explained in the next sub-section. Many operators are currently upgrading their constellations to deliver higher radio frequency (RF) power, enhanced functionality, and higher frequency reuse with V/HTS technology. The second one takes into account the fact that terrestrial wireless communications are going up in frequency and, due to that, the coexistence with the SatCom systems for using the same frequency bands will be needed. These new trends pose interesting challenges regarding new interference limited scenarios, and signal processing (SP) offers valuable tools to cope with them. Before going more into the details of these new challenges, let us comment about the actual and future context of SatCom services.

5.1.1 High Throughput Satellites: A New Interference-Limited Paradigm

In contrast to mono-beam satellites, high throughput satellites split the service area into multi-spot beam service areas, which allows higher aggregate throughput and more service flexibility to satisfy a heterogeneous demand. The system architecture is shown in figure 5.1 and comprises a Gateway (GW), a satellite, and multiple UTs. The gateway (GW) is connected to the core network and serves a set of users that are geographically far away using the satellite as relaying node. The link from the GW to the satellite, and from the satellite to the UT are known as the feeder link and the user link, respectively. In the usual star configuration that is observed in Fig. 1, the feeder link presents high directivity and gain. As this link presents a SNR that is considerably higher than the one in the user link, it is assumed in general to be noiseless and perfectly calibrated against channel power variations due to atmospheric events. Also, depending

on the direction of the communication, the link receives the name forward link when it goes from the GW to the UT and reverse link when it goes from the UT to the GW. Each of the four mentioned links usually works in a different frequency band. The frequency selection is driven by many considerations, among them coverage and beam size, atmospheric conditions in the served region, and availability of a robust ecosystem of ground equipment technologies. For instance, current-generation GEO HTSs typically use the Ka-band, which is less congested than the C/Ku-band. For fixed satellite services (FSS), this refers to the exclusive satellite band from 19.7 to 21.2 GHz for the forward link and from 29.5 to 31 GHz for the reverse link. In land mobile satellite services (MSS) generally use lower frequencies such as the L-band (i.e., from 1.5 to 2.5 GHz) because of its lower attenuation, which enables a less complex UT. Note, however, that recently the Ka-band is also being considered to provide in-flight and maritime connectivity.

The HTSs that are currently operative (e.g., Viasat-2, SES-12) provide aggregate data rates of more than 100 Gbps. These HTS systems use the Ku/Ka-band in both feeder and user link, and serve in the user link as much as 200 beams in the same frequency band. VHTS systems (e.g., Viasat-3) aim at achieving data rates in the range of Tbps and, due to that, they need higher frequencies in the Q-band (30 to 50 GHz), V-band (50 to 75 GHz), and W-band (75 to 110 GHz), in order to serve as much as 3000 beams in the user link. For these reasons, advanced SP is required in order to reduce the interference among so many multiple beams, facilitate adaptive coverage, dynamically optimize the traffic, and share the spectrum with terrestrial services, among other functions. Flexibility in the resource allocation per beam can significantly improve the quality of service and bring down the incurred cost of the V/HTS system per transmitted bit.

Today there are approximately 1300 fully operational communication satellites. Every type of orbit has an important role to play in the overall communications system. Geostationary earth orbit (GEO), at 35,000 km, present an end-to-end propagation delay of 250 ms; therefore, they are suitable for the transmission of delay-tolerant data. Medium earth orbit (MEO), at 10,000 km, introduce a typical delay of 90 ms; based on that, they can offer a compromise in latency and provide fiber-like data rates. Finally, low earth orbit (LEO) is at between 350 and 1,200 km, and introduce short delays that range from 20 to 25 ms. In all these cases, the satellite is a very particular wireless relaying node, whose specificities lead to a communication system that cannot be treated like a wireless terrestrial one. This is because the channel, communication protocols, and complexity constraints of the satellite system create unique set of features [104], notably:

- Due to the long distance to be covered from the on-ground station to the satellite, the satellite communication link may introduce both a high round-trip delay and a strong path-loss of hundreds of dB. To counteract the latter, satellites are equipped with high power amplifiers (HPA) that may operate close to saturation and create intermodulation and nonlinear impairments.

- Satellite communications traverse about 20 km of atmosphere and introduce high molecular absorption, which is even higher in the presence of rain and clouds, particularly for frequencies above 10 GHz. Therefore, satellite links are designed based on thermal noise limitations and on link budget analysis that considers large protection margins for additional losses (e.g., rain attenuation).

- In the non-geostationary orbits (i.e., MEO and LEO), there are high time-channel variations due to the relative movement of the satellites with respect to the ground station.

- Due to the long distance and carrier frequencies, the satellite antenna feeds are generally seen as a point in the far-field, thus making the use of spatial diversity schemes challenging. Also, due to the absence of scatters near the satellite (i.e., there are no objects in space that create multiple paths) and the strong path-loss (i.e., it is a long distance communication), the presence of a line-of-sight component, which focuses all the transmitted power and is not blocked or shadowed, is much more critical than in terrestrial cellular communications.

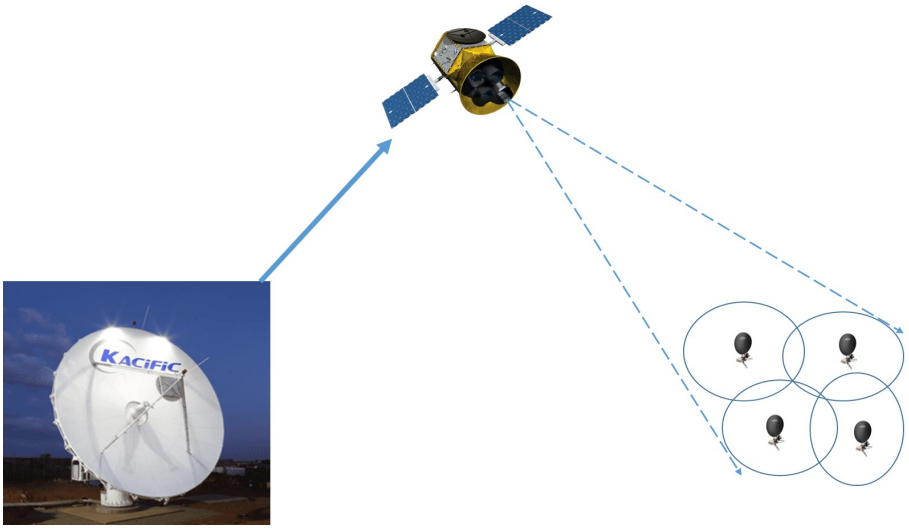

FIGURE 5.1: Caption

On the positive side, due to the lack of rich scatters, satellite communications experience higher cross-polarization isolation than terrestrial communication networks

- The processing complexity on-board the satellite is limited, as it is highly correlated with its power consumption, mass, and ultimately, with the final cost of the system.

- The received signal-to-noise Ratio (SNR) is very low and therefore the user terminal (UT) must have high sensitivity, good receiver antenna gains, and good tracking capabilities to steer the beam of the UT such that it continuously points to the satellite.

- The practical challenges of the satellite system require solutions that are different from the ones used in the terrestrial wireless communications. An important one is the specific satellite multi-user protocol framing that is defined in the current broadcast and broadband standards (i.e., DVB-S2X). In these protocols, in order to overcome the satellite channel noise, channel codes are long and, therefore, must take into account data from multiple users. This fact creates a multicast transmission, because the same information has to be decoded by a group of users. Multicast transmission creates specific precoding techniques, as section II explains.

- Finally, satellite solutions are generally characterized by a relatively long development phase before deployment. This is different from terrestrial solutions, where it is easier to test new technologies without incurring in excessive deployment costs.

Finally, it is important to note that V/HTS systems require the most advanced transmission standards. Currently, DVB S2/S2X are the standards of both forward broadcast and broadband satellite networks. Using high efficiency modulation and coding schemes (MODCODs) up-to 256APSK combined with advanced interference management techniques enable aggressive and flexible frequency reuse. DVB-S2X incorporates the novel super-framing structure that enables the use of SP techniques that have never been used before in the satellite context, such as precoding and multi-user detection at the user terminal. Among other things, it incorporates orthogonal Walsh-Hadamard (WH) sequences as reference/training sequences, allowing simultaneous estimation of the channel state information of multiple beams. The super-frame concept was designed to maximize the efficiency of the channel coding scheme by encapsulating the information intended to several UTs using the same MODCOD. Remarkably, the length of the super-frame remains unaffected by the various transmission parameters that are applied on the different beams (e.g. MODCODs).

5.2 Precoding in multibeam satellites

With the aim of increasing the offered data rates of a given satellite, both operators and manufacturers are investigating a variety of alternatives. One main approach is to consider satellite communication links at extremely high frequencies such as the W-band [105]. However, large investments are required for implementing the communication subsystems in these bands; in addition, new challenging channel impairments appear. As a result, spectrally efficient alternatives that exploit the current frequency bands are of great interest. This is the case of precoding techniques that allow a high frequency reuse factor among different beams. With the aid of precoding, a satellite UT can obtain a sufficiently large signal to interference and noise ratio (SINR) even though the carrier bandwidth is reused by adjacent beams. In order to maintain a certain SINR value, the precoder mitigates the interference that can affect the satellite UT. Resorting to the system architecture depicted schematically in Fig. 5.1, the precoding matrix is computed at the satellite GW. After that, the beam signals are precoded and transmitted through the feeder link using a Frequency Division Multiplexing (FDM) scheme. Then, the satellite payload performs a frequency shift and routes the resulting radio signal over an array-fed reflector antenna that transmits the precoded data over a larger geographical area that is served by the multiple beams in the user link.

Multibeam precoded satellite systems can be modeled as a multiple-input-multiple-output (MIMO) broadcast channel [106]. As it happens, in terrestrial systems, low complexity linear precoding techniques are of great interest. Indeed, the computational complexity that is required to implement multibeam satellite precoding techniques gains importance as the dimensions of multibeam satellite systems grow. For instance, the forthcoming Viasat-3 system is expected to utilize nearly 1000 beams to serve the coverage area that is presented in Fig. 4. As a result, the on-ground equipment should be prepared to update a precoding matrix of 1000 users on a per-frame basis.

Apart from the already mentioned interference limitation, another major issue of multibeam systems is to deal with the large spectral demands on the feeder link, i.e. the bidirectional link between satellite and the Gateway (GW), whose bandwidth requirements increase as it aggregates the traffic of all users. Keeping a full frequency reuse allocation ($N_c = 1$), the required feeder link resources can be calculated as

$$\mathrm{B}_{\text{feeder-link}} = N\mathrm{B}_{\text{beam}}, \tag{5.1}$$

where N is the number of on-board feed signals. The notations B_{beam} and $\mathrm{B}_{\text{feeder-link}}$ are the per-beam and the feeder link required bandwidths, respectively. From (5.1), it is evident that any beam available bandwidth enhancement forces the feeder link resources to be increased accordingly and, eventually the feeder link might become the communication bottleneck.
In the context of applying interference mitigation techniques and optimizing feeder link resources in multibeam networks, the following possible configurations can be conceived:

- Ground Processing (GP): single GW employs an interference mitigation technique to cope with increased level of inter-beam interference. Satellite payload works in the transparent mode. There is no certain feeder link optimization strategy such that a set of $\mathrm{B}_{\text{feeder-link}}$ in (5.1) is required [107].

- Multi Gateway Processing (MGP): this architecture exploits the multiplexing diversity by reusing all the available feeder link bandwidth across multiple GWs. The GWs employ interference mitigation techniques and the required feeder link bandwidth is optimized with the number of GWs. In this context, the required feeder link bandwidth becomes [108] $\mathrm{B}_{\text{feeder-link-MG}} = \frac{N}{F}\mathrm{B}_{\text{beam}}$, where F is the number of GWs, and $\mathrm{B}_{\text{feeder-link-MG}}$ denotes the feeder link bandwidth which is required at MGP architecture. Indeed, the MGP architecture reduces the required feeder link bandwidth to $\mathrm{B}_{\text{feeder-link-MG}} < \mathrm{B}_{\text{feeder-link-onboard}}$. Nevertheless, the deployment of several GWs increases the cost of the system.

This study investigates the forward link of a MGP scheme, where a OBP scheme is applied at the payload. The OBP is developed while:

(i) A low complex payload infrastructure is targeted.

(ii) Inter-beam interference shall be mitigated, leading to optimize achievable rate at each user terminal.

Furthermore, we develop a OBP scheme aiming to fulfill the requirements in (i) and (ii). Some additional benefits can be realized via applying OBP in MGP network. First, it is not necessary to establish a CSI feedback mechanism between satellite and the GWs. Second, CSI exchange mechanism is not needed among GWs, leading to a low complex transmitting segment infrastructure. Third, in case of failing one GW, the traffic can be easily rerouted to the satellite through other GWs without applying any extra signal processing schemes at the GWs.

5.3 Sparse precoding

The realization of on-board precoding entails low complexity beamformer design and low implementation cost. Many iterative and non-iterative low complexity beamformer designs exist in the literature. Design of classical zero-forcing (ZF) and minimize mean square error (MMSE) are two widely used non-iterative beamformers due to their low-complexity in the design. Several convex and non-convex iterative beamformer designs addressing various design aspects of precoding such as power minimization [9], weighted sum rate (WSR) maximization [109] etc are proposed in the literature. Iterative methods are generally have high complexity than non-iterative methods. However, to the best of our knowledge, design of beamformer with the objective of minimizing implementation cost is not addressed in the literature.

As the satellite operates on signal bandwidth, which is usually of the order of several GHzs, implementation of on-board precoding in the real-time and power consumed for implementation become pivotal. As mentioned previously, the implementation cost involves multiplication and additions of the beamformer coefficients with on-board frame symbols or sample and it is primarily dominated by multiplications. Although efficient implementation techniques, exist in the literature, aids in reducing multiplication cost, further contribution can be made by avoiding the multiplications to the extent possible. In this chapter, we address the low-implementation cost of the beamformer by sparsifying the beamformer matrix subject to design constraints.

Following are the contributions made through the first part of the chapter:

- We formulate the on-board precoding problem with objective of minimizing implementation subject to minimum rate constraints of users with the help of sparsity constraints. We refer this problem as sparse precoding problem
- Aforementioned sparse precoding problem contains the ℓ_0 norm of the beamformer as the objective, hence it is a NP-hard in general which requires non-polynomial time complexity algorithm for attaining a global solution. Hence, we relax ℓ_0 norm to ℓ_1 norm, which convexifies the problem.
- We show the efficacy of the proposed design, over the traditional designs with respect to implementation cost, through Monte-carlo simulations.

5.3.1 System Model and Scenario description

Consider the forward link of a MGP multibeam satellite system, where a single geosynchronous (GEO) satellite with multibeam coverage provides fixed broadband services to a large set of users with N feeds and K beams, with $N = K$.
By employing a Time Division Multiplexing (TDM) scheme, at each time instant, a total of K

single antenna users, i.e. exactly one user per beam, is simultaneously served by a set of F GWs. Without loss of generality, we assume each GW has access to an identical number of feeds[1]. In particular, we let f-th GW, with $f = 1, \ldots, F$, employs $N_f = \frac{N}{F}$ on-board feeds to transmits its signals. In addition, it is conceived that each GW transmits a subset of traffic streams to satellite. Again, without loss of generality, we consider an identical set of traffic streams at each GW. In this context, for available K number of beams, f-th GW calculates and transmits a subset of $K_f = \frac{K}{F}$ traffic streams, one stream per user such that f-th GW serves a subset of K_f out of K user terminals within the whole coverage area. To make sure that the user demands are met, we further assume an aggressive $N_c = 1$ frequency reuse where all the beams use the same user link spectrum leading to inter-beam interference among the beams. In consequence, inter-beam interference in user link become the bottleneck of the whole system motivating the use of the interference mitigation techniques.

Remark 1. Even with highly directive antennas the feeder link originating at different GWs are partially interfering. Nevertheless, in this chapter we assume that GWs are sufficiently separated on the Earth surface and space so that the inter-feeder link interference can be ignored. In this context, the received signal at the coverage area can be modeled as

$$\mathbf{y} = \sqrt{\kappa}\mathbf{H}\mathbf{W}\mathbf{x} + \mathbf{n}, \tag{5.2}$$

where $\mathbf{y}$ is a $K \times 1$ vector containing the symbols received by K users, one per beam, at a given time instant. The $K \times 1$ vector $\mathbf{x} = [\mathbf{x}_1, ..., \mathbf{x}_f, ..., \mathbf{x}_F]^T$ denotes the stacked transmitted signals at all the on-board feeds with $\mathrm{E}\{\mathbf{x}\mathbf{x}^H\} = \mathbf{I}_K$. The notation $\mathbf{x}_f$ of size $K_f \times 1$ is a vector denotes the signals transmitted by f-th GW to the satellite. The vector $\mathbf{n}$ of size $K \times 1$ contains the stacked zero mean unit variance Additive White Gaussian Noise (AWGN) at K users such that $\mathrm{E}\{\mathbf{n}\mathbf{n}^H\} = \mathbf{I}_K$. The OBP weights are included in matrix $\mathbf{W}$. The scalar κ is the power scaling factor and must adapt with

$$\mathrm{trace}(\mathbf{W}\mathbf{W}^H) \leq P, \tag{5.3}$$

where P is the transmit power of N feeds.

Note that the transmit power constraint in (5.3) is set considering $\mathbf{W}$. Throughout this paper it is conceived that the power allocation mechanism is located at the array fed reflector system with N embedded feeds.

In the sequel, $\mathbf{H}$ is the overall $K \times N$ user link channel matrix whose element $(\mathbf{H})_{ij}$ represents the gain of the link between the i-th user (in the i-th beam) and the j-th satellite feed. The matrix $\mathbf{H}$ includes the propagation losses and radiation pattern, and as such is decomposed as [108]

$$\mathbf{H} = \mathrm{diag}\left(\frac{1}{\sqrt{A}_1}, ..., \frac{1}{\sqrt{A}_K}\right)\mathbf{R}, \tag{5.4}$$

where A_k denotes the propagation losses from the satellite to the k-th user. $\mathbf{R}$ is a $K \times N$ matrix which models the feed radiation patterns, the path loss and the received antenna gain. The (k, n)-th entry of $\mathbf{R}$ is modeled as

$$(\mathbf{R})_{kn} = \frac{\sqrt{W_R}\, g_{kn}}{4\pi\frac{d_k}{\lambda}\sqrt{k_B T_R B_W}}, \tag{5.5}$$

where W_R denotes the user receive antenna's power gain. g_{kn} is referring to the amplitude gain from feed n toward the k-th user such that the respective feed transmit gain is $10\log_{10}(|(\mathbf{R})_{kn}|^2)$ if expressed in dBi. Finally, d_k is the distance between the k-th user and the satellite, λ the carrier wavelength, k_B the Boltzmann constant, T_R the receiver noise temperature, and B_W the carrier bandwidth.

[1]This implies the fact that an identical number of feeder link resources and on-board feeds is assumed so that the OBP directly converts one by one feeder link signals to on-board feed signals.

5.3.2 Design of On-Board precoding

On-board design of precoding entails two factors into the design: Low design complexity and low implementation cost. While the design complexity considers the complexity involved in calculation of precoding matrix, implementation cost considers the cost of implementing precoding feature with designed precoding matrix. The dominant factor in the implementation cost is incurred by multiplication of precoding coefficients with data symbols or samples. Hence, we assume that implementation cost which includes the power and time required to implement precoding feature on-board can be translated into the order of number of multiplications. Moreover, the number of multiplications can be translated to number of non-zeros in OBP matrix. While efficient implementation techniques help in reduction of complexity, sparsification of OBP (zeroing out precoding coefficients) helps further in reduction as it reduces number of multiplications. In this chapter, we address the implementation cost of OBP by sparsifying the precoding matrix to minimize implementation cost subject to total transmit power and minimum rate constraints.

Low implementation cost modeling

Let $\mathbf{h}_i$ be the i^{th} row of $\mathbf{H}$ and $\mathbf{W}_i$ be i^{th} column of $\mathbf{W}$. With the help of aforementioned definitions, the problem of minimizing the implementation cost subject to total power and minimum SINR constraints can mathematically be formulated as:

$$\begin{aligned} \mathcal{P}_1: \ & \min_{\mathbf{W}} \ \|\mathbf{W}\|_0 \\ \text{subject to } C_1: \ & \frac{|\mathbf{h}_i^H \mathbf{W}_i|^2}{\sigma^2 + \sum_{j \neq i}^{N} |\mathbf{h}_i^H \mathbf{W}_j|^2} \geq \epsilon_i, \ \forall i \\ C_2: \ & \|\mathbf{W}\|_2 \leq P_0, \ \forall i, \end{aligned} \tag{5.6}$$

where P_0 is the available total transmit power, $\|\mathbf{W}\|_0$ is the ℓ_0 norm of $\mathbf{W}$ and ϵ_i is the minimum SINR constraint of user i.

Remarks:

- The problem $\mathcal{P}_1$ is non-convex due to non-convex objective
- $\|\mathbf{W}\|_0$ counts number of non-zeros in $\mathbf{W}$. Hence the the objective is also combinatorial and known to be NP-hard for high dimensional matrices.
- The minimum rate constraint of user i, for $i = 1, \ldots, N$, in C_1 in $\mathcal{P}_1$ appears to be non-convex. However, constraint C_1 can be written as a second order cone constraint which is convex.

Obtaining a global solution to $\mathcal{P}_1$ entails the exhaustive search over the precoding space due to the combinatorial nature of the problem (i.e. $\|\mathbf{W}\|_0$). Exhaustive search based algorithms become non-polynomial time complex even for practically realizable dimensions of $\mathbf{W}$. Many non-combinatorial relaxations of $\mathbf{W}$ are proposed in literature. Relaxations are primarily classified into two categories: Convex and non-convex. In non-convex relaxations, $\|\mathbf{W}\|_0$ is relaxed to $\|\mathbf{W}\|_p$ for $0 < p < 1$. In convex relaxation, $\|\mathbf{W}\|_0$ is relaxed to $\|\mathbf{W}\|_1$. Under particular conditions, $\|\mathbf{W}\|_1$ based relaxation is shown to obtain the same solution as $\|\mathbf{W}\|_0$ [110].

In this chapter, we adopt the ℓ_1 relaxation as it results the convex objective. The problem $\mathcal{P}_1$ with convex relaxation of $\|\mathbf{W}\|_0$ can be mathematically formulated as

$$\begin{aligned} \mathcal{P}_2: \ & \min_{\mathbf{W}} \ \|\mathbf{W}\|_1 \\ \text{subject to } C_1: \ & \frac{|\mathbf{h}_i^H \mathbf{W}_i|^2}{\sigma^2 + \sum_{j \neq i}^{N} |\mathbf{h}_i^H \mathbf{W}_j|^2} \geq \epsilon_i, \ \forall i \end{aligned} \tag{5.7}$$

$$C_2: \ \|\mathbf{W}\|_2 \leq P_0, \ \forall i,$$

Although, the objective in P_2 is convex, the problem P_2 can not be solved efficiently with existing tools, that can solve convex problems efficiently, due to constraint C_1. The constraint C_1 can rearranged as

$$\left(1+\frac{1}{\epsilon_i}\right)|\mathbf{h}_i^H\mathbf{W}_i|^2 \geq \left\| \begin{matrix} \sigma \\ \mathbf{h}_i^H\mathbf{W}_1 \\ \vdots \\ \mathbf{h}_i^H\mathbf{W}_N \end{matrix} \right\|_2^2, \ \forall i \tag{5.8}$$

Suppose $\mathbf{W}$ is an optimal precoding matrix for P_2, then $\mathbf{W}\ \mathrm{diag}\{\mathrm{e}^{j\phi_i}\}$, where ϕ_i for $i = 1,\ldots,N$ are arbitrary phases, is also optimal. This can be easily verified as the phase does not alter the objective nor the constraints. Hence, we restrict ourselves to the design of the beamformers with $\mathbb{R}\mathrm{e}\{\mathbf{h}_i^H\mathbf{W}_i\} \geq 0, \ \mathbb{I}\mathrm{m}\{\mathbf{h}_i^H\mathbf{W}_i\} = 0, \ i = 1,\ldots,N$ as it helps to reformulate the constraint as a convex constraint. With this newly imposed restriction on real and imaginary parts of $\mathbf{h}_i^H\mathbf{W}_i$, for $i = 1,\ldots,N$, the constraint C_1 in P_2 is reformulated as

$$\left(\sqrt{1+\frac{1}{\epsilon_i}}\right)\Re\{\mathbf{h}_i^H\mathbf{W}_i\} \geq \left\| \begin{matrix} \sigma \\ \mathbf{h}_i^H\mathbf{W}_1 \\ \vdots \\ \mathbf{h}_i^H\mathbf{W}_N \end{matrix} \right\|, \ \forall i \tag{5.9}$$

The problem P_2 with the convex reformulation of constraint C_1 is

$$\begin{aligned} \mathcal{P}_3: \ & \min_{\mathbf{W}} \ \|\mathbf{W}\|_1 \\ \text{subject to } C_1: \ & \left(\sqrt{1+\frac{1}{\epsilon_i}}\right)\mathbf{h}_i^H\mathbf{W}_i \geq \left\| \begin{matrix} \sigma \\ \mathbf{h}_i^H\mathbf{W}_1 \\ \vdots \\ \mathbf{h}_i^H\mathbf{W}_N \end{matrix} \right\|, \ \forall i \\ & C_2: \ \|\mathbf{W}\|_2 \leq P_0, \ \forall i, \end{aligned} \tag{5.10}$$

The problem P_3 is convex problem since the objective and the constraint are convex. Hence, the problem P_3 can be solved globally and efficiently. Existing tools like CVX can be used to solve the problem P_3 efficiently. In the next section we present the performance of P_3 through Monte-Carlo simulations.

5.3.3 Numerical Results

System setup

To compare the performance of the proposed scenarios in this study, Monte Carlo simulations have been carried out. The simulation setup is based on an array fed reflector antenna/feed provided by European Space Agency (ESA) in the context of NGW project with $N = K = 12$ feeds/beams, at each time instant, which serve a single user per beam and spread over the whole Europe [111]. Results have been averaged for a total of 500 channel realizations. For each beam different user positions is considered at consecutive channel realizations. The detail of simulation parameters are collected in precoding 5.1. Note that the channel fading statistics corresponds to the city of Rome. We compare the achieved implementation cost for different transmit powers by the problem $P3$, referred as ℓ_1-minimization (ℓ_1-min), with classical power minimization problem [9], referred as ℓ_2-minimization (ℓ_2-min). The classical power minimization problem given in [9] can be obtained replacing $\|\mathbf{W}\|_1$ in (5.6) with $\|\mathbf{W}\|_2$ and ignoring constraint C_2.

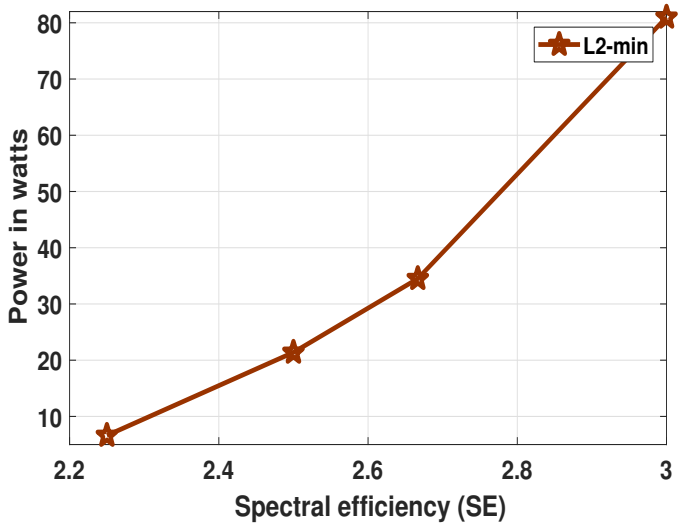

FIGURE 5.2: Power consumed by ℓ_2-minimization versus spectral efficiency for 12 beam HTS system with one user per beam

TABLE 5.1: User link simulation parameters

Parameter	**Value**
Satellite height	35786 km (GEO)
Satellite longitude, latitude	$10°East, 0°$
Frequency	20×10^9
Earth radius	6378.137 Km
Feed radiation pattern	Provided by ESA [111]
Number of feeds N	12
Number of beams	12
Carrier frequency	20 GHz (Ka band)
Total bandwidth	500 MHz
Atmospheric fading	Rain attenuation [111]
Roll-off factor	0.25
User antenna gain	41.7 dBi
clear sky gain	17.68 dB/K

Results

In figure 5.2, The total transmit required in watts for 4 different spectal efficiencies (SE) (2.20, 2.5, 2.666, 3 bps) is plotted. In figure 5.3(a), we compare the implementation cost of ℓ_2-min with ℓ_1-min for the previously mentioned SEs. The reduction in the implementation cost of ℓ_1-min can be observed that in figure 5.3(a), when it is supplied with small percentage of extra power (EP) than ℓ_2-min. For example in figure 5.3(a) for SE=2.25 bps/Hz, the number of non-zeros in precoding matrix of ℓ_2-minimization is 144 for the transmit power of 6dB but with total transmit power of 6.07 dB (see figure 5.4(a) for extra power needed), ℓ_1-minimization can achieve the same SE with beamformer matrix which has less than 60 non-zero coefficients. Similarly, it can be observed in figure 5.3(a), the implementation cost that can be achieved with ℓ_1-min for different SEs and transmit powers.

In figure 5.4(a), we plot the amount extra power needed for different SEs in achieving the implementation costs provided in figure 5.3(a). From figure 5.5, we can observe that ℓ_1-min can achieve only a small gain in the implementation cost if P_0 is same as optimal power, say P_{opt},

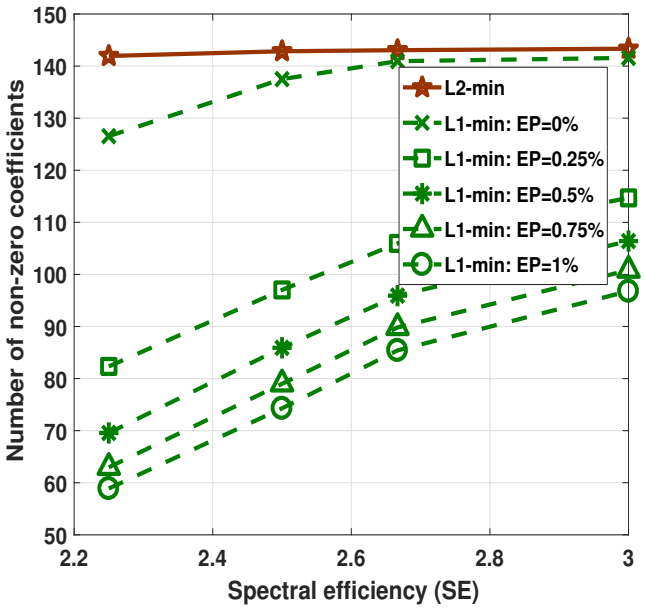

(a)

FIGURE 5.3: Number non-zero precoder coefficients for ℓ_2-min and ℓ_1-min for different transmission powers versus spectral efficiency

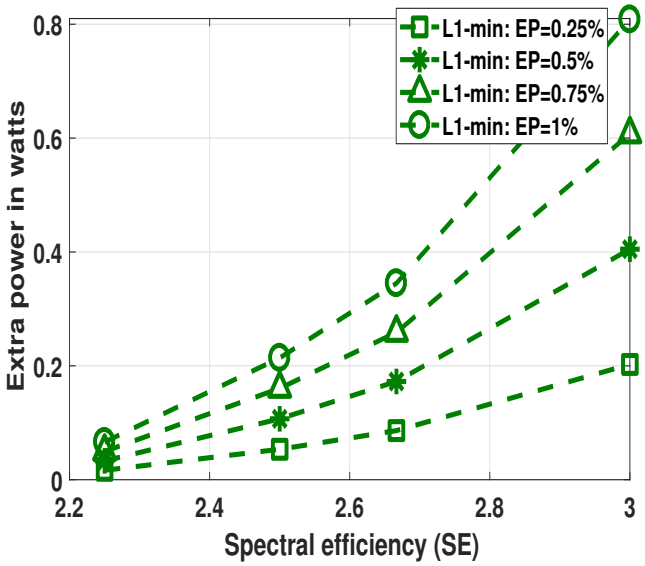

(a)

FIGURE 5.4: Extra power consumed by ℓ_1-minimization versus spectral efficiency

FIGURE 5.5: Performance comparison of ℓ_2-min with ℓ_1-min for different transmission powers for 12 beam HTS system with one user per beam.

achieved by ℓ_2-min. However, we can see larger gain in implementation cost of ℓ_1-min for P_0 which is slightly greater than P_{opt}. We also observe that the gain in implementation cost are larger for lower SEs, this because lower SEs can afford to have some interference. As a result, ℓ_1-min makes the most of the precoding coefficients zeros allowing the interference that can be affordable at this low SEs. However, we see the gain in the implementation cost diminishes with increase in SE, this is due to the fact that higher SEs demand the lowest interference also to be canceled hence the ℓ_1-min can not make many of the coefficients as it allows the interference that can not be affordable at this high SEs.

5.3.4 Conclusion

In this section, design of on-board precoding is considered with the objective of minimizing implementation cost subject to minimum SINR requirement of users and total transmission power constraints. The major contribution of the implementation cost is by the multiplications involved in applying the precoder coefficients to the data symbols. Hence, we modeled the objective of minimizing the implementation cost as the objective of minimizing the number of non-zero precoder coefficients as a zero precoder coefficient avoids the need of multiplication. Hence, the minimizing the implementation cost is modelled with the help ℓ_0 norm constraint on precoding matrix. However, the ℓ_0 norm objective problem is NP-hard so we relax objective to ℓ_1 norm which makes the problem convex. Finally, we show the reduction in the implementation cost compared to the classical power minimization problem through Monte-Carlo simulations.

5.4 Joint Scheduling and Precoding for Frame-Based Multigroup Multicasting in Satellite Communications

In this section, we address the frame-based MGMC precoding for forward link of a multibeam system where each beam equipped with a single transmit antenna covers a large number of users equipped with single antenna receivers. Due to practical constraints such as limited power and frame length, only a few users can be accommodated into a frame transmitted over a beam. Naturally, this leads to the scheduling of users that maximizes the objective of interest. In this chapter, the summation over all the beams of per beam minimum user rate, termed as sum rate (SR) is considered as the objective. Clearly, the rate and hence the user scheduling in a beam is a function of signal-to-interference plus noise ratio (SINR). Moreover, the interference to users in a beam depends on the precoding, which in turn, depends on the scheduled users (SU) in other beams. Thus, the maximization of the objective requires the joint design of scheduling and precoding across the users in all the beams. In this context, the joint design of scheduling and precoding simply refer to as joint design.

Related works

The sum-rate maximization (SRM) for MGMC was initially addressed in [79] under the sum power constraint. Therein, a heuristic algorithm based on decoupling of precoding and power allocation is proposed. The authors in [112] proposed a heuristic user scheduling and extended the precoding framework in [79] to SRM under PBPC for frame-based MGMC. Noticing the complexity of the algorithms in [79] and [112], the authors in [113] propose a heuristic two-stage low-complexity solution where the precoder design for inter-beam is followed by the precoder design for intra-beam interference. User scheduling is not addressed [79], [113] and the proposed user scheduling in [112] is heuristic. Further, the precoding solutions proposed in [79, 112, 113] for SRM problem are heuristic without any guarantees on performance. Moreover, as mentioned previously, the SRM problem entails a joint design of scheduling and precoding. Hence, the

decoupled approach adopted in [112] provides only a feasible solution and results in loss of performance compared to the joint design methods. To the best of our knowledge, joint design for MGMC systems is not addressed in the literature.

To this end, the contributions of this chapter are as follows:

- To capture the coupled nature of scheduling and precoding, a novel formulation of the SRM problem is proposed that embodies scheduling aspects of the design with the help of binary variables besides precoding. Unlike the formulations in [79, 112], the proposed formulation results a continuous precoding problem for given SUs.

- With the help of novel reformulations, the non-convex nature of the problem arising from SINR terms is transformed as a difference-of-convex/concave (DC) functions. The binary constraint is handled with appropriate relaxation and penalization. Thus by rendering the joint design as a DC problem, a fact hitherto not considered.

- Within the framework of the convex-concave procedure (CCP), an iterative algorithm is proposed to solve the resulting DC problem wherein, each iterate, a convex problem is solved. Convergence to a stationary point is inherently guaranteed and performance is enhanced.

5.4.1 MGMC Scenario and Problem Formulation

MGMC Scenario

We consider the forward link of a geostationary satellite having multibeam capabilities and offering broadband services. Considering the evolving trends in satellite systems, full frequency reuse is considered for the multiple beams; this results in multi-user interference, whose mitigation is the key aspect of the paper. The system is assumed to support the DVB-S2x Physical layer based on superframing [114] to support the synchronized frames of the same length and the required CSI pilots as necessitated by precoding [112]. Further, the users are assumed to possess a single antenna with processing power to demodulate one data stream. Furthermore, the feeder link is assumed ideal and the satellite is operated in the linear mode. Finally, the service needed for a much larger number of users compared to the number of beams is provided by scheduling different users in frames transmitted over time.

We consider an MGMC transmission in the aforementioned multibeam scenario comprising N beams formed by N transmit antennas. The beam i serves U_i users and the total number of users in all beams is assumed greater than number of beams (also antennas) i.e., $\sum_{i=1}^{N} U_i > N$. In a given time slot, exactly say, $K_i \leq U_i$, users are served by multiplexing the users' data in a codeword designed for the transmission to users in beam i; this is referred to as frame-based multicasting [112]. The generic case of $K_i \geq 1$ arises from the need to use spectrally efficient long codewords while avoiding transmission inefficiency due to concatenating a user's data with sizable dummy bits in the codeword [112]. Further, due to the use of full frequency reuse, a multicast group of K_i users in beam i is interfered by $K_j, j \neq i$, users from other co-channel beams leading to the MGMC scenario. Since $K_i \leq U_i$, this naturally leads to the selection of K_i of users out of U_i which is referred to as user scheduling in this paper (which is also referred to equivalently as user selection or admission control in the literature).

Performance metric and problem formulation

In this chapter, we consider the sum of minimum rates achieved by each of the different multicast groups as the performance metric. This metric considers the minimum rate of SUs in each beam and summation is across the beams; this will be simply referred to as a sum-rate henceforth (also in the literature in the context of MGMC [112]). In the sequel, we focus on maximization of this sum-rate subject to constraints on the number of SUs per beam, minimum SINR (MSINR) or

equivalently minimum rate of SUs per beam and the consumed power per beam; this problem is compactly referred to *SR* in the rest of paper.

Towards formulating the SR, let $\mathbf{w}_i \in \mathbb{C}^{N\times 1}$, $P_i > 0$ and $\epsilon_i > 0$ be the precoding vector, maximum allowed per beam transmit power and MSINR (i.e., QoS) requirement of beam i respectively. Noise at each user is characterized to be as additive white Gaussian with zero mean and variance σ^2. Let $\mathbf{h}_{ij} \in \mathbb{C}^{N\times 1}$, and $\gamma_{ij} = \dfrac{|\mathbf{h}_{ij}^H \mathbf{w}_i|^2}{\sum_{l\neq i} |\mathbf{h}_{ij}^H \mathbf{w}_l|^2 + \sigma^2}$ be the downlink channel and SINR of user j belonging to beam i respectively. Let $\mathcal{S}_i$ be any subset of $\{1,\ldots,U_i\}$ with cardinality equal to K_i and $\mathcal{T}_i$ be the dictionary of all sets of type $\mathcal{S}_i$. Clearly, the number of sets in $\mathcal{T}_i$ is $\binom{U_i}{K_i}$ for $i \in \{1,\ldots,N\}$. With the notations defined, the SR is formulated as,

$$
\begin{aligned}
\mathcal{P}_1 : \max_{\{\mathbf{w}_i, \mathcal{S}_i \in \mathcal{T}_i\}_{i=1}^N} \; & \sum_{i=1}^{N} \log\left(1+\Omega_i\right) \\
\text{s.t. } C_1 : \Omega_i &= \min_{j\in\mathcal{S}_i} \gamma_{ij}, i \in \{1,\ldots,N\}, \\
C_2 : \gamma_{ij} &\geq \epsilon_i, i \in \{1,\ldots,N\}, j \in \mathcal{S}_i, \\
C_3 : \sum_{j=1}^{N} |\mathbf{w}_{ij}|^2 &\leq P_i, i \in \{1,\ldots,N\}.
\end{aligned}
\tag{5.11}
$$

Remarks:

- $\mathcal{S}_i$ contains the set of SUs in beam i, hence the constraint C_1 in $\mathcal{P}_1$ represents the MSINR of the SUs.
- Constraint C_2 in $\mathcal{P}_1$ enforces the SUs in each beam to satisfy the corresponding MSINR requirement associated with the beam. This enables the flexibility to support different rates on different beams.
- Constraint C_3 is the PBPC. This follows from the use of a separate transponder for each beam due to co-channel assumption [115].
- The objective in $\mathcal{P}_1$ denotes the sum-rate.

Notice that the problem $\mathcal{P}_1$ is coupled in two levels:

- Design of scheduler and precoder in a beam entails their joint design as the scheduling of a user depends on the precoder and the precoder design depends on the user.
- Design of scheduling and precoding in a beam requires joint design across all the beams as the precoder of a beam (which in turn depends on scheduled user) contributes to the interference to other beams.

Hence, the optimal solution to problem $\mathcal{P}_1$ entails the joint design of scheduling and precoding where the scheduling is performed across all the users in all beams (multicast groups) and precoding is performed across all beams.

The problem $\mathcal{P}_1$ is combinatorial due to the selection of sets of users and also non-convex due to constraint C_1 and C_2. Hence, obtaining the optimal solution to $\mathcal{P}_1$ requires the exhaustive search algorithms whose complexity grows exponentially with the increase in problem dimension (e.g., dictionary for each beam has dimensions $\binom{U_i}{K_i}$ and their joint design is entailed). Therefore, in the next section, we focus on transforming the problem $\mathcal{P}_1$ into a continuous problem and exploiting the hidden DC structure in the non-convexity.

5.4.2 DC formulation: A tractable approach

Towards formulating the problem $\mathcal{P}_1$ without the set notions, let $\eta_{ij} \in \{0,1\}$ be the binary variable associated with user j in beam i, where $\eta_{ij} = 1$ when the corresponding user is scheduled and zero otherwise. With the help η_{ij}s, the problem $\mathcal{P}_1$ is reformulated as,

$$\begin{aligned}
\mathcal{P}_2 : \max_{\mathbf{W},\boldsymbol{\eta},\boldsymbol{\Omega}} \; & \sum_{i=1}^{N} \log\left(1+\Omega_i\right) \\
\text{s.t. } C_1 &: \eta_{ij} \in \{0,1\}, \forall i, \forall j, \\
C_2 &: \gamma_{ij} \geq \eta_{ij}\Omega_i, \forall i, \forall j, \\
C_3 &: \Omega_i \geq \epsilon_i, \forall i, \\
C_4 &: \sum_{j=1}^{U_i} \eta_{ij} = K_i, \forall i, \\
C_5 &: \sum_{j=1}^{N} |\mathbf{w}_{ij}|^2 \leq P_i, \forall i,
\end{aligned} \tag{5.12}$$

where $\forall i$ refers to $i \in \{1,\ldots,N\}$, $\forall j$ refers to $j \in \{1,\ldots,U_i\}$, $\mathbf{W} = [\mathbf{w}_1,\ldots,\mathbf{w}_N]$, $\boldsymbol{\eta}_i = [\eta_{i1},\ldots,\eta_{iU_i}]^T$, for $i \in \{1,\ldots,N\}$, $\boldsymbol{\eta} = [\boldsymbol{\eta}_1,\ldots,\boldsymbol{\eta}_N]$ and $\boldsymbol{\Omega} = [\Omega_1,\ldots,\Omega_N]$. *Remarks*:

- When $\eta_{ij} = 0$, the constraint C_2 imposes a trivial lower bound on SINR of the unscheduled user j in beam i i.e., $\gamma_{ij} \geq 0$. When $\eta_{ij} = 1$, constraint C_2 leads to $\gamma_{ij} \geq \Omega_i$.
- Letting U_i^S to be the set of SUs in beam i, the constraint C_2 ensures $\Omega_i \geq min_{j \in U_i^S}\, \gamma_{ij}$. Hence, maximization of the objective in the problem $\mathcal{P}_2$ equivalently maximizes the sum-rate in $\mathcal{P}_1$.
- Constraint C_3 is the MSINR requirement of users.
- Constraint C_4 imposes a limit on the number of SUs in each beam; this ensures each user gets sufficient share of the physical layer frame.

Novelty of $\mathcal{P}_2$ The proposed reformulation transforms non-smooth non-tractable joint design problem $\mathcal{P}_1$ into a tractable problem given in $\mathcal{P}_2$. Moreover, this reformulation is crucial for the reformulations that are proposed in sequel to transform $\mathcal{P}_1$ to a smooth DC problem. The novelty mainly lies in the reformulation of C_1 in $\mathcal{P}_1$ to C_2 in $\mathcal{P}_2$. To the best of our knowledge, the formulation given in $\mathcal{P}_2$ is the first of its kind that captures both scheduling and precoding.

The problem $\mathcal{P}_2$ is non-smooth and combinatorial due to constraint C_1; further the constraint C_2 is non-convex. Towards uncovering structure in the non-convexity, let β_{ij} be the slack variable for lower bounding the SINR of user j and beam i. A reformulation of $\mathcal{P}_2$ with the help of $\beta_{ij}s$ is,

$$\begin{aligned}
\mathcal{P}_3 : \max_{\mathbf{W},\boldsymbol{\eta},\boldsymbol{\Omega},\boldsymbol{\beta}} \; & \sum_{i=1}^{N} \log\left(1+\Omega_i\right) \\
\text{s.t. } & C_1, C_3, C_4, C_5 \text{ in (5.12)} \\
C_2 &: \gamma_{ij} \geq \beta_{ij}, \forall i, \forall j, \\
C_6 &: \beta_{ij} \geq \eta_{ij}\Omega_i, \forall i,
\end{aligned} \tag{5.13}$$

where $\boldsymbol{\beta} = [\boldsymbol{\beta}_i,\ldots,\boldsymbol{\beta}_N]$ and $\boldsymbol{\beta}_i = [\beta_{i1},\ldots,\beta_{iU_i}]^T$. Following [81], a DC reformulation of constraint C_2 in $\mathcal{P}_2$ is,

$$C_2 \Rightarrow 1+\gamma_{ij} \geq 1+\beta_{ij} \Rightarrow \mathcal{I}_{ij}\left(\mathbf{W}\right) - \mathcal{J}_{ij}\left(\mathbf{W},\beta_{ij}\right) \leq 0, \tag{5.14}$$

where $\mathcal{I}_{ij}(\mathbf{W}) = \sigma^2 + \sum_{l\neq i}^{N} |\mathbf{h}_{ij}^H \mathbf{w}_l|^2$ and $\mathcal{J}_{ij}(\mathbf{W}, \beta_{ij}) = \dfrac{\sigma^2 + \sum_{l=1}^{N} |\mathbf{h}_{ij}^H \mathbf{w}_l|^2}{1+\beta_{ij}}$. Notice that $\mathcal{I}_{ij}(\mathbf{W})$ is convex and $\mathcal{J}_{ij}(\mathbf{W}, \beta_{ij})$ is also jointly convex in $\mathbf{W}$ and β_{ij}. Hence, by the equivalent reformulation given in (5.14), the constraint C_2 in $\mathcal{P}_3$ is a DC constraint. Further, a DC form of C_6 is,

$$C_6 : 4\beta_{ij} + (\eta_{ij} - \Omega_i)^2 \geq (\eta_{ij} + \Omega_i)^2 . \tag{5.15}$$

With the reformulations given in (5.14) and (5.15), and ignoring the combinatorial constraint C_1 for the moment, the problem $\mathcal{P}_3$ leads to the maximization of concave objective subject to difference-of-convex, convex and linear constraints; this is a DC problem [63] and can be solved efficiently by CCP [63].

As the final step, the combinatorial constraint C_1 is addressed by relaxing η_{ij}s to a box constraint between 0 and 1 i.e., $0 \leq \eta_{ij} \leq 1$. This relaxation along with the aforementioned reformulations renders $\mathcal{P}_3$ as a DC programming problem. However, the resulting η_{ij}s obtained with this relaxation might be non-binary. Hence, to ensure their binary nature, η_{ij} is penalized with $\mathbb{P}(\eta_{ij})$. Letting λ to be the penalty parameter, the resulting penalized reformulation is,

$$\begin{aligned}
\mathcal{P}_4 : \max_{\mathbf{W},\boldsymbol{\eta},\boldsymbol{\Omega},\boldsymbol{\beta}} & \sum_{i=1}^{N} \left(\log(1+\Omega_i) + \lambda \sum_{j=1}^{U_i} \mathbb{P}(\eta_{ij}) \right) \\
\text{s.t. } & C_1 : 0 \leq \eta_{ij} \leq 1, \ \forall i, \forall j, \\
& C_2 : \ \mathcal{I}_{ij}(\mathbf{W}) - \mathcal{J}_{ij}(\mathbf{W}, \beta_{ij}) \leq 0, \forall i, \forall j \\
& C_3, C_4, C_5 \text{ in (5.13)} \\
& C_6 : 4\beta_{ij} + (\eta_{ij} - \Omega_i)^2 \geq (\eta_{ij} + \Omega_i)^2 , \forall i, \forall j
\end{aligned} \tag{5.16}$$

It is easy to see that any choice of convex function $\mathbb{P}(\eta_{ij})$ that promotes the binary solutions suffice to transform $\mathcal{P}_4$ as a DC problem of our interest. For example, the penalty functions proposed in [81] and [99] can be chosen as $\mathbb{P}(\eta_{ij})$. The log-entropy based penalty function proposed in [81] i.e., $\mathbb{P}(\eta_i) \triangleq \eta_i \log \eta_i + (1-\eta_i)\log(1-\eta_i)$ is considered for this chapter. With this choice of $\mathbb{P}(\eta_i)$, the problem $\mathcal{P}_4$ becomes a DC problem. In order to apply the CCP framework to the problem $\mathcal{P}_4$, a feasible initial point (FIP) needs to supplied. However, the constraint C_4 in $\mathcal{P}_4$ limits the choices of FIPs. For ease of finding the FIPs, the constraint C_2 is brought into the objective with another penalty parameter $\gamma > 0$ as,

$$\mathcal{P}_5 : \max_{\mathbf{W},\boldsymbol{\eta},\boldsymbol{\Omega},\boldsymbol{\beta}} \mathcal{F}(\boldsymbol{\Omega}, \boldsymbol{\eta}) \ \text{ s.t. } C_1, C_2, C_3, C_5, C_6 \text{ in (5.16).} \tag{5.17}$$

where $\mathcal{F}(\boldsymbol{\Omega}, \boldsymbol{\eta}) = \sum_{i=1}^{N} \left(\log(1+\Omega_i) + \lambda \sum_{j=1}^{U_i} \mathbb{P}(\eta_{ij}) \right)$
$- \sum_{i=1}^{N} \gamma \left(\sum_{j=1}^{U_i} \eta_{ij} - K_i \right)^2$. Given a non-empty solution set, a solution of the problem $\mathcal{P}_4$ is always obtained by solving $\mathcal{P}_5$ with right choice of γ (usually larger value).

5.4.3 CCP based Joint Design Algorithm

In this section, a CCP [63] based algorithm is proposed to solve the DC problem in (5.16). CCP is an efficient tool to find a stationary point of DC programming problems [55]. It is an iterative framework wherein the two steps of Convexification and Optimization are executed in each iteration. In the convexification step, the DC problem is approximated as a convex problem by linearizing the convex part of the objective and the concave part of the DC constraints by their first-order Taylor approximations. The convex problem obtained from convexification step provides a global lower bound for the original problem where the lower bound is tight at the previous iteration. The optimization step involves the maximization of the lower bound obtained from Convexification step.

Joint Scheduling and Precoding (JSP) Algorithm

The convexifcation and optimization steps of CCP framework, applied to the DC problem $\mathcal{P}_5$, are as follows,

- Convexification: Let $(\mathbf{W}, \boldsymbol{\eta}, \boldsymbol{\beta}, \boldsymbol{\Omega})^{k-1}$ be the estimates of $(\mathbf{W}, \boldsymbol{\eta}, \boldsymbol{\beta}, \boldsymbol{\Omega})$ in iteration $k-1$ respectively. In iteration k, the convex part of the objective, $\left(\sum_{i=1}^{N} \lambda \mathbb{P}\left(\eta_i\right)\right)$ is replaced by $\tilde{\mathbb{P}}\left(\eta_i\right) \triangleq \lambda\left(\mathbb{P}\left(\eta_i^{k-1}\right)+\left(\eta_i-\eta_i^{k-1}\right) \nabla \mathbb{P}\left(\eta_i^{k-1}\right)\right)$. So, the objective of $\mathcal{P}_5$ after convexification, say $\tilde{\mathcal{F}}\left(\boldsymbol{\Omega}, \boldsymbol{\eta}\right)$, is $\tilde{\mathcal{F}}\left(\boldsymbol{\Omega}, \boldsymbol{\eta}\right)=\sum_{i=1}^{N}\left(\log\left(1+\Omega_i\right)+\lambda \sum_{j=1}^{U_i} \tilde{\mathbb{P}}\left(\eta_i\right)\right)$ $-\sum_{i=1}^{N} \gamma\left(\sum_{j=1}^{U_i} \eta_{ij}-K_i\right)^2$. Similarly, the concave part of C_2 i.e., $\mathcal{J}_{ij}\left(\mathbf{W}, \beta_{ij}\right)$ is replaced by

$$\tilde{\mathcal{J}}_{ij}(\mathbf{W}, \beta_{ij})^{k-1} \triangleq -\mathcal{J}_{ij}(\mathbf{W}, \beta_{ij}) - \Re\left\{\nabla^H \mathcal{J}_i(\mathbf{W}, \beta_{ij})^{k-1}\begin{bmatrix}\{\mathbf{w}_l-\mathbf{w}_l^{k-1}\}_{l=1}^{N} \\ \beta ij-\beta_{ij}^{k-1}\end{bmatrix}\right\},$$

and concave part of C_6 i.e., $\left(\eta_{ij}-\Omega_i\right)^2$ is replaced by

$$\mathcal{G}_{ij}(\eta_{ij}, \Omega_i) \triangleq \left(\eta_{ij}^{k-1}-\Omega_i^{k-1}\right)^2 + \begin{bmatrix}2\left(\eta_{ij}^{k-1}-\Omega_i^{k-1}\right) \\ -2\left(\eta_{ij}^{k-1}-\Omega_i^{k-1}\right)\end{bmatrix}^T \begin{bmatrix}\left(\eta_{ij}^{k-1}-\eta_{ij}\right) \\ \left(\Omega_i^{k-1}-\Omega_i\right)\end{bmatrix}.$$

- Optimization: Updated $\left(\mathbf{W}^{k+1}, \boldsymbol{\Omega}^{k+1}, \boldsymbol{\eta}^{k+1}, \boldsymbol{\beta}^{k+1}\right)$ is obtained by solving the following convex problem,

$$\begin{aligned}\mathcal{P}_6: \max_{\mathbf{W}, \boldsymbol{\eta}, \boldsymbol{\Omega}, \boldsymbol{\beta}} & \tilde{\mathcal{F}}\left(\boldsymbol{\Omega}, \boldsymbol{\eta}\right) \\ C_1: & 0 \leq \eta_{ij} \leq 1, \ \forall i, \forall j, \\ C_2: & \mathcal{I}_{ij}\left(\mathbf{W}\right)-\tilde{\mathcal{J}}_{ij}(\mathbf{W}, \beta_{ij})^{k-1} \leq 0, \forall i, \forall j \\ C_3: & \Omega_i \geq \epsilon_i, \forall i, \\ C_4: & \sum_{j=1}^{N}\left|\mathbf{w}_{ij}\right|^2 \leq P_i, \forall i, \\ C_5: & 4\beta_{ij}+\mathcal{G}_{ij}(\eta_{ij}, \Omega_i) \geq \left(\eta_{ij}+\Omega_i\right)^2, \forall i, \forall j\end{aligned} \tag{5.18}$$

The problem in $\mathcal{P}_6$ optimizes the sum-rate over scheduling and precoding variables jointly. This joint scheduling and precoding (JSP) algorithm is based on CCP framework. It is well known that a FIP is sufficient for the CCP procedure to converge to a stationary point (kindly refer [54, 55]). The QOS problem for fixed $\boldsymbol{\eta}$ can be solved using [8]. Let $\hat{\mathbf{W}}$ be the solution for fixed $\boldsymbol{\eta}=\delta$ where $0 \leq \delta \leq 1$ is constant. For $\delta \approx 0$, the corresponding QOS problem always becomes feasible (kindly refer to [8]). So, a FIP of the problem $\mathcal{P}_5$ can be $\left(\hat{\mathbf{W}}, \hat{\boldsymbol{\eta}}, \hat{\boldsymbol{\beta}}, \hat{\boldsymbol{\Omega}}\right)$ where $\hat{\boldsymbol{\beta}}$ is the SINRs obtained with $\hat{\mathbf{W}}$, $\hat{\boldsymbol{\eta}}=\delta$ and $\hat{\Omega}_i=\epsilon_i$ for $i=1, \ldots, N$.

5.4.4 Complexity of JSP and its reduction

Since JSP is a CCP based iterative algorithm, its complexity depends on complexity of the convex sub-problem $\mathcal{P}_5$. The convex problem $\mathcal{P}_5$ has $\left(N^2+2\sum_{i=1}^{N} U_i+N\right)$ decision variables and

$\left(2\sum_{i=1}^{N} U_i + N\right)$ convex constraints and $\left(2\sum_{i=1}^{N} U_i + 2N\right)$ linear constraints. Hence, the computational complexity of $\mathcal{P}_{\triangledown}$ is $\mathcal{O}\left(\left(N^2 + 2\sum_{i=1}^{N} U_i + N\right)^3 \left(4\sum_{i=1}^{N} U_i + 3N\right)\right)$ [64]. Commercial software such as CVX can solve the convex problem of type $\mathcal{P}_5$ efficiently. Besides the complexity per iteration, the overall complexity also depends on the convergence speed of the algorithm. Through simulations, we observe that the JSP converges typically in 20-30 iterations.

Pre-selection of Users for Large System Dimensions

The proposed JSP algorithm is computationally efficient for small to medium system dimensions. However, the complexity per iteration of $\mathcal{P}_5$ grows in the order of power seven to number of users as the system dimension increases. Such a situation is inherent in satellite systems with increasing user base per beam. A case in point is the satellite system (for which we present numerical results in the next section) with $N = 9$ and $\{U_i = 100, K_i = 2\}_{i=1}^{N}$; the number of users is much larger than what could be accommodated in a beam. Such scenarios inhibit the applicability of JSP or the obtained solution may become obsolete due to lengthier processing times. However, for special cases of large dimension systems with $\{U_i \gg K_i\}_{i=1}^{N}$, the proposed joint design algorithm can be still applied by adopting the following two step process:

- Pre-selection: In this step, a small subset of users, say ζ_i, in beam i, for $i = 1, \ldots, N$ is selected based on some scheduling scheme. This is step is referred to as pre-selection. Typically ζ_i is chosen as $K_i \leq \zeta_i \leq U_i$.
- Joint design for the pre-selected users: In this step, the proposed JSP algorithm is employed for the beams with pre-selected users to jointly schedule K_i users out of ζ_i and design corresponding precoders.

The proposed pre-selection based JSP with two step process is simply referred to PS-JSP. The values of $\{\zeta_i\}_{i=1}^{U}$ are chosen such that the complexity of proposed JSP algorithm is affordable. The proposed two step process typically results in loss of performance in comparison with JSP algorithm employed for original system dimension. This performance loss is typically a function of the scheduling scheme employed in pre-selection step and also on $\{\zeta_i - K_i\}_{i=1}^{N}$.

5.4.5 Simulation results

In this section, the performance of JSP and PS-JSP are evaluated based on the system setup described in Section 5.4.1 and simulation model defined in [111]. We consider the Shannon rate for JSP and PS-JSP for its analytical appeal. However, in satellite systems, the throughput is defined by the modulation and coding (MODCOD) schemes used. In this context, while the optimization problem is solved for the Shannon rate, the resulting SINRs are used to compute the following metric,

$$R_{\text{avg}} = \frac{2B_u}{1+\alpha}\frac{1}{N}\sum_{i=1}^{N} f_{\text{DVB-S2X}}\left(\min_{i\in\hat{\mathcal{S}}_i}\{\text{SINR}_i\}\right). \tag{5.19}$$

This metric, in [Gbps/beam], represents average user throughput when using DVB-S2x framing; the relevant parameters are defined in Table 5.2. The function $f_{\text{DVB-S2X}}$ in (5.19) maps the received MSINR of a beam to the highest MODCOD scheme (defined in [114]) that can be supported. In this chapter, a MSINR threshold ϵ_i of -2.85 dB corresponding to minimum transmission and σ^2 is assumed to be 0dB at all user terminals. Number of beams N is fixed to be 9 for all results. Further, the results are averaged over 100 different channel realizations.

The solution proposed in [112] is considered as a benchmark (BM) for all the performance comparisons. As discussed previously, the joint design entails the design of scheduling and precoding across all the users in all the beams jointly. The BM algorithm proposed in [112] is based

TABLE 5.2: Simulation Parameters

Frequency Band	Ka (20 GHz)
User terminal clear sky temp, T_{cs}	235.3K
User Link Bandwidth, B_u	500 MHz
Output Back Off, OBO	5 dB
On board Power, P_{tot} hline Atmospheric fading	50 dBW Rain attenuation [111]
Roll-off factor, α	0.20
User terminal antenna gain, G_R	41.7 dBi
Multibeam Antenna Gain, G_{ij}	Ref: [111]

on the decoupled design of scheduling followed by precoding. Moreover, the scheduling and precoding algorithms proposed in [112] are heuristic methods without any guarantees on the nature of the solutions. On the contrary, the proposed JSP algorithm jointly designs the scheduling and precoding over all the users in all beams and PS-JSP jointly design the scheduling and precoding for the given subset of users in all the beams; further, the optimization algorithm is based on a CCP which inherently provides qualifications on the solution. Hence, the gains obtained by JSP or PS-JSP is attributed to two factors: (i) improved precoder design *per-se* even for a given user set, (ii) jointly optimizing scheduling and precoding. Through the following numerical results, the gains in different scenarios are quantified. These scenarios are reflective of the typical operational aspects encountered in satellite communications.

R_{avg} as a function of total users per beam

It is quite essential in satellite communications to achieve higher spectral efficiencies with limited power. In figure 5.6, R_{avg} is illustrated as a function of total users per beam for a limited power of 100 Watts. The number of users per beam $\{U_i = \Delta\}_{i=1}^{N}$ is varied from 10 to 50 in steps of 10, and users per frame $\{K_i\}_{i=1}^{N}$ is fixed to be 2. Recalling the PS-JSP, the joint design is carried out on a pre-selected user pool containing ζ_i users in the ith beam; here it is further assumed that $\zeta = \zeta_i, \forall i$. Figure 5.6 further illustrates the impact of choosing different ζ. The scheduling algorithm proposed in [112] is employed to pre-select ζ users from U_i in the pre-selection step of PS-JSP. Following are the gains obtained by JSP and PS-JSP over BM for this scenario:

- Precoding gain: For $\{\zeta_i = K_i = 2\}_{i=1}^{N}$, the scheduling algorithms employed in PS-JSP and BM are the same leading to same set of SUs. In other words, the second step of PS-JSP (i.e., JSP) essentially designs only the precoder as $\{\zeta = K_i\}_{i=1}^{N}$. So, the gains obtained by PS-JSP over BM for $\zeta_i = K_i$, which amounts to approximately 12%, is solely attributed to efficiency in the precoding of JSP which is introduced before as precoding gains.

- Joint optimization gain: For $\{\zeta_i > K_i\}_{i=1}^{N}$, the gains of PS-JSP over BM is due to both scheduling and precoding. In other words, the JSP step of PS-JSP schedules the users that contribute less interference to other beams and also users that consume less power to meet the MSINR requirements. The gains obtained by PS-JSP for $\{\frac{\zeta_i}{K_i} = 4\}_{i=1}^{N}$ amounts to approximately 50% for $\{U_i\}_{i=1}^{N} = 10$ (and 20% for $\{U_i\}_{i=1}^{N} = 50$) is referred to as joint optimization gains.

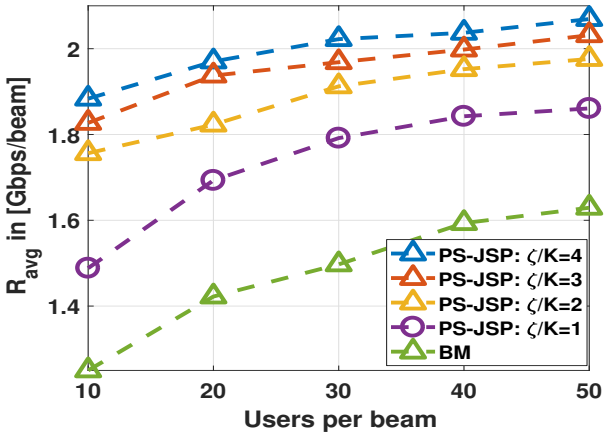

FIGURE 5.6: Performance comparison of R_{avg} (in Gbps/beam) versus U_i for $N = 9$, $\{K_i = 2, P_i = 11.11 \text{ Watts}\}_{i=1}^{N}$.

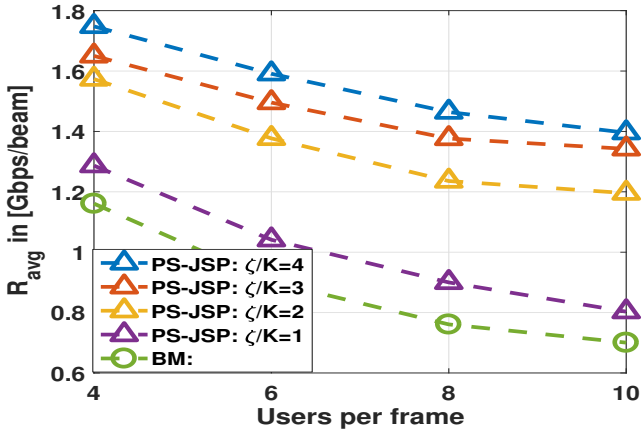

FIGURE 5.7: Performance comparison of R_{avg} in Gbps/beam versus U_i for $N = 9$, $\{U_i = 100, P_i = 11.11 \text{ Watts}\}_{i=1}^{N}$.

Multiuser Diversity Due to increased diversity in selecting users, (MUD: multiuser user diversity), the performance of PS-JSP improves as $\{\zeta_i\}_{i=1}^{N}$ increases. For example, when $\{U_i = 10\}_{i=1}^{N}$, the gain for $\{\zeta_i = 4K_i\}_{i=1}^{N}$ is larger than that for $\{\zeta_i < 4K_i\}_{i=1}^{N}$ as the former case benefits from higher MUD. In other words, as $\{\zeta_i\}_{i=1}^{N}$ increases, the probability of finding the orthogonal users with good channel gains across beams increases. Moreover, probability of finding parallel users within the beam with good channel gains also increases with $\{\zeta_i\}_{i=1}^{N}$. This is shown in figure 5.6. However, the gains diminish as ζ increases further; additional users included due to increase in ζ tend to be less orthogonal with users in other beams and possess low correlation with users of the same beam. Similarly, as the number of users per beam increases, the aforementioned probability increases. Hence, the performance of BM and PS-JSP improves as the number of users per beam increases initially, but these gains *per-se* diminish with further increase in users per beam.

R_{avg} as a function of users per frame

The throughput of PS-JSP against BM is illustrated in figure 5.7 as a function of number of users per frame i.e., $\{K_i\}_{i=1}^{N}$. It is easy to see that due to systematic joint design, PS-JSP outperforms the BM. Similar to figure 5.6, for $\{\zeta_i = K_i\}_{i=1}^{N}$ the gains obtained by PS-JSP is solely attributed to the precoding gains and the gains for $\{\zeta_i > K_i\}_{i=1}^{N}$ are attributed to the gains from joint scheduling and precoding. The performance in a beam (or frame) is dependent on the MSINR of the frame.

Notice, scheduling in BM and pre-selection in PS-JSP are based on orthogonality of users across beams and co-channel nature of users within the beam. Since the channel dimensions are finite, the correlation between the newly added SUs with those already selected tends to increase (less orthogonal). Hence, newly added SUs increase interference. Further, due to the nature of adopted scheduling, newly SUs have less channel gains. Hence, the increased interference with more SUs and reduced channel gains of the newly SUs lead to lower MSINR of a frame. As a result, R_{avg} decreases as $\{K_i\}_{i=1}^{N}$ increases which is shown in figure 5.7.

5.4.6 Conclusions

In this section, the joint scheduling and precoding problem was considered for an MGMC scenario in frame-based satellite systems from a physical layer perspective. Unlike the existing works, the joint design problem is formulated that facilitates the update of scheduling and precoding jointly. Noticing the problem to be MINLP, an efficient framework is developed that transform it as a DC problem. Finally, an efficient low-complexity CCP based iterative algorithm is proposed. Through Monte-Carlo simulations, the superiority in performance of the proposed algorithm over the state-of-the-art methods is illustrated.

6
Future works

This thesis focuses on the joint design of various scheduling and precoding aspects that occur in unicast and multicast downlink transmission in cellular and satellite systems. Noticing the prevalence of challenges that preclude the joint update prevail across all the designs, this thesis provides the methodology, that could be applicable to many designs, to the joint design problems in the rudimentary single cell multiuser MISO downlink channels. In this chapter, the issues for future work are identified and discussed.

This thesis adopted somewhat ideal system assumptions e.g., the availability of perfect channel informations. This means that the results can be regarded as upper bounds for the achievable performance in practice. The next step would be to take these non-idealities into account to bridge the gap between theory and reality. For example, an interesting future research project would be to study robust joint design considering the imperfect channel state information. Further, the complexity of solutions increases in the cubic order with number of variables of optimizations. This could limit the applicability of the framework to large dimensional systems. This could be addressed by parallelizing the solutions.

The frameworks proposed in this thesis can easily be extended to multi cell scenarios. However, the existing joint design framework for multicell network requires centralized processing. Generally, the centralized processing increases communication overhead and processing power, imperfect. Thus, some form of decentralized joint designs are necessary. Further, robust centralized joint design, to account for the imperfectness of the channel information, is also interesting.

Another important research direction would be to consider cloud-RAN systems with cache-aware scheduling and precoding. Caches enable base stations to store a certain amount of content for future use, without the need to download the content to be transmitted every time from the center. In terms of network energy efficiency, the cache size, caching time, and the decisions as to whether to store some content or not play important roles.

This dissertation has only covered a few exemplary problems regarding discrete resource allocation in modern cellular networks. There are many practical discrete resource allocation problems in wireless networks that can be addressed using the MINLP framework presented in this thesis, e.g., wireless link activation [116], delay-constrained routing in multihop networks [117], and resource block scheduling in 3GPP LTE systems [118], to name but a few. As more advanced discrete and mixed-integer optimization techniques and algorithms are emerging, more and more practical discrete resource allocation problems in wireless communications and signal processing can be addressed within the developed MINLP framework.

A

Chapter3 appendix

Appendix I

$$\tilde{\mathbb{P}}^k(\eta_{ij}) \triangleq \eta_{ij}\nabla\mathbb{P}\left(\eta_{ij}^{k-1}\right);\ \tilde{\mathbb{P}}^k(\delta_j) \triangleq \delta_j\nabla\mathbb{P}\left(\delta_j^{k-1}\right),$$
$$f^k(\eta_{ij},\Theta_j,t) \triangleq B\left(2\frac{\left(\eta_{ij}^{k-1}+\Theta_j^{k-1}\right)(\eta_{ij}+\Theta_j)}{t^{k-1}} - \left(\frac{\eta_{ij}^{k-1}+\Theta_j^{k-1}}{t^{k-1}}\right)^2 t - \frac{\eta_{ij}^2}{t} - \frac{\Theta_j^2}{t}\right).$$

Similarly, linearization of the concave part of C_6, C_7 and C_9 in $\mathcal{P}_5^{\text{MEE}}$ is given by

$$\tilde{\mathcal{G}}_{ij}^k(\eta_{ij},\Theta_j) \triangleq -\left[\eta_{ij}^{k-1}\right]^2 - \left[\Theta_j^{k-1}\right]^2 + 2\eta_{ij}^{k-1}\eta_{ij} + 2\Theta_j^{k-1}\Theta_j,$$
$$\tilde{\mathcal{K}}_{ij}^k(\delta_j,\Theta_j) \triangleq \left(\delta_j^{k-1}+\Theta_j^{k-1}\right)^2 - 2\begin{bmatrix}\delta_j^{k-1}+\Theta_j^{k-1}\\ \delta_j^{k-1}+\Theta_j^{k-1}\end{bmatrix}^H\begin{bmatrix}\left(\delta_j-\delta_j^{k-1}\right)\\ \Theta_j-\Theta_j^{k-1}\end{bmatrix}$$
$$\tilde{\mathcal{J}}_{ij}^k(\mathbf{W},\alpha_{ij}) \triangleq -\mathcal{J}_{ij}(\mathbf{W}^{k-1},\alpha_{ij}^{k-1}) - \Re\left\{\nabla^H\mathcal{J}_{ij}(\mathbf{W}^{k-1},\alpha_{ij}^{k-1})\begin{bmatrix}\{\mathbf{w}_l-\mathbf{w}_l^{k-1}\}_{l=1}^G\\ \alpha_{ij}-\alpha_{ij}^{k-1}\end{bmatrix}\right\},$$

where

$$\nabla\mathcal{J}_{ij}(\mathbf{W}^{k-1},\alpha_{ij}^{k-1}) = \begin{bmatrix}\{\frac{2\mathbf{h}_i\mathbf{h}_i^H\mathbf{w}_l^{k-1}}{\alpha_{ij}^{k-1}}\}_{l=1}^G\\ -\frac{\sigma^2+\sum_{l=1}^G|\mathbf{h}_i^H\mathbf{w}_l^{k-1}|^2}{{\alpha_{ij}^{k-1}}^2}\end{bmatrix}. \tag{A.1}$$

Appendix II

DC formulation and CCP based algorithm: SUM

Applying reformulations and relaxations proposed in Section 3.3, the problem $\mathcal{P}_1^{\text{SUM}}$ is reformulated into DC problem as,

$$\mathcal{P}_2^{\text{SUM}}: \max_{\mathbf{W},\boldsymbol{\Theta},\boldsymbol{\eta},\boldsymbol{\delta}} \sum_{i=1}^N\sum_{j=1}^G\eta_{ij} - \Omega_3\left\|\sum_{j=1}^G\delta_j - M\right\|^2 + \lambda_4\sum_{j=1}^G\sum_{i=1}^N\mathbb{P}(\eta_{ij}) + \sum_{j=1}^G\lambda_5\mathbb{P}(\delta_j) \tag{A.2}$$

$$\text{s.t. } C_1:\ 0 \leq \eta_{ij} \leq 1,\ \forall i,\ \forall j, \qquad C_4:\ 0 \leq \delta_j \leq 1, \forall j,$$

$$C_7:\ \sum_{l \neq i} |\mathbf{h}_i^H \mathbf{w}_l|^2 + \sigma^2 \leq \frac{\sum_{l=1}^{G} |\mathbf{h}_i^H \mathbf{w}_l|^2 + \sigma^2}{1 + \eta_{ij}\epsilon_j},\ \forall i,\ \forall j, \quad C_2, C_3, C_5 \text{ and } C_6 \text{ in (3.14)},$$

where λ_5, λ_6 and Ω_3 are the penalty parameters.

The convexified problem to be solved as part of JGSP-SUM (CCP based algorithm applied to the DC problem $\mathcal{P}_2^{\text{SUM}}$) algorithm at iteration k is:

$$\mathcal{P}_3^{\text{SUM}}:\ \max_{\mathbf{W},\boldsymbol{\Theta},\boldsymbol{\eta},\boldsymbol{\delta}}\ \sum_{i=1}^{N}\sum_{j=1}^{G} \eta_{ij} - \Omega_3 \left\| \sum_{j=1}^{G} \delta_j - M \right\|^2 + \lambda_4 \sum_{j=1}^{G}\sum_{i=1}^{N} \tilde{\mathbb{P}}^k(\eta_{ij}) + \sum_{j=1}^{G} \lambda_5 \tilde{\mathbb{P}}^k(\delta_j) \tag{A.3}$$

$$\text{s.t. } C_1, C_2, C_3, C_5 \text{ to } C_6 \text{ in (A.2)}, \quad C_7: \sum_{l \neq i} |\mathbf{h}_i^H \mathbf{w}_l|^2 + \sigma^2 \leq \mathcal{I}^k(\mathbf{W}, \eta_{ij}),\ \forall i,\ \forall j,$$

where $\mathcal{I}^k(\mathbf{W}, \eta_{ij}) = \dfrac{\sum_{l=1}^{G} |\mathbf{h}_i^H \mathbf{w}_l^{k-1}|^2 + \sigma^2}{1 + \eta_{ij}^{k-1}\epsilon_j} +$

$$\Re\left\{ \left[\{ \frac{2\mathbf{h}_i \mathbf{h}_i^H \mathbf{w}_l^{k-1}}{1 + \eta_{ij}^{k-1}\epsilon_j} \}_{l=1}^{G} - \epsilon_j \frac{\sigma^2 + \sum_{l=1}^{G} |\mathbf{h}_i^H \mathbf{w}_l^{k-1}|^2}{\left(1 + \eta_{ij}^{k-1}\epsilon_j\right)^2} \right]^H \begin{bmatrix} \{\mathbf{w}_l - \mathbf{w}_l^{k-1}\}_{l=1}^{G} \\ \eta_{ij} - \eta_{ij}^{k-1} \end{bmatrix} \right\}.$$

Letting $\mathcal{P}_3^{\text{SUM}}(k) +$ be the objective value of the problem $\mathcal{P}_3^{\text{SUM}}$ at iteration k, the pseudo code of JGSP-EE-SR for the joint design problem is given in algorithm 7.

Algorithm 7 JGSP-SUM

Input: $\mathbf{H}, [\epsilon_1, \ldots, \epsilon_N], P_T, \Delta, \mathbf{W}^0, \boldsymbol{\delta}^0, \boldsymbol{\Theta}^0, \boldsymbol{\eta}^0, \lambda_4 = 0, \lambda_5 = 0, \Omega_3 = 0, k = 1$;
Output: $\mathbf{W}, \boldsymbol{\eta}$
while $|\mathcal{P}_3^{\text{SUM}}(k) - \mathcal{P}_3^{\text{SUM}}(k-1)| \geq \Delta$ **do**
  Convexification: Convexify the problem (A.3)
  Optimization: Update $(\mathbf{W}, \boldsymbol{\eta}, \boldsymbol{\delta}, \boldsymbol{\Theta})^k$ by solving $\mathcal{P}_3^{\text{SUM}}$
  Update : $\mathcal{P}_3^{\text{SUM}}(k), \lambda_4, \lambda_5, \Omega_3, k$
end while

B

Chapter 4 appendix

Appendix I

$$\tilde{h}\left(\eta_{ij}^{k-1}\right) \triangleq h\left(\eta_{ij}^{k-1}\right) + \left(\eta_{ij} - \eta_{ij}^{k-1}\right)\nabla h\left(\eta_{ij}^{k-1}\right),$$
$$\tilde{\mathbb{P}}\left(\eta_{ij}^{k-1}\right) \triangleq \mathbb{P}\left(\eta_{ij}^{k-1}\right) + \left(\eta_{ij} - \eta_{ij}^{k-1}\right)\nabla \mathbb{P}\left(\eta_{ij}^{k-1}\right),$$
$$\tilde{\mathcal{G}}_i(\mathbf{W},\zeta_i)^{k-1} \triangleq -\mathcal{G}_i(\mathbf{W},\zeta_i) - \mathbb{R}\left\{\nabla^H \mathcal{G}_i(\mathbf{W},\zeta_i)^{k-1}\begin{bmatrix}\{\mathbf{w}_l - \mathbf{w}_l^{k-1}\}_{l=1}^N \\ \zeta i - \zeta_i^{k-1}\end{bmatrix}\right\},$$

where

$$\nabla \mathcal{G}_i(\mathbf{W},\zeta_i)^{k-1} = \left[\frac{2\mathbf{h}_i\mathbf{h}_i^H\mathbf{w}_1^{k-1}}{\zeta_i^{k-1}}, \ldots, \frac{2\mathbf{h}_i\mathbf{h}_i^H\mathbf{w}_N^{k-1}}{\zeta_i^{k-1}}, -\frac{\sigma^2 + \sum_{j=1}^N |\mathbf{h}_i^H\mathbf{w}_j^{k-1}|^2}{{\zeta_i^{k-1}}^2}\right]^T. \quad \text{(B.1)}$$

Appendix II

JBSP-MC: A CCP based algorithm for MC scenario

The proposed JBSP-MC is a CCP based algorithm that executes the following steps iteratively to solves the DC problem $\mathcal{P}_2^{\text{MC}}$:

- Convexification: Let $(\mathbf{W}, \boldsymbol{\eta}, \boldsymbol{\zeta}, \boldsymbol{\delta})^{l-1}$, be the estimates of $\mathbf{W}, \boldsymbol{\eta}, \boldsymbol{\zeta}$ in iteration $l-1$. Further, let $\tilde{\mathbb{P}}\left(\eta_{ij}^{l-1}\right)$ and $\tilde{\mathcal{G}}_{ij,k}\left(\mathbf{W}^{l-1}, \zeta_{ij}^{l-1}\right)$ be the first order Taylor approximations of $\mathbb{P}(\eta_{ij,k})$, $\mathbb{P}(\delta_{j,k})$ and $\mathcal{G}_{ij,k}(\mathbf{W}, \zeta_{ij,k})$ around $(\mathbf{W}, \boldsymbol{\eta}, \boldsymbol{\delta}, \boldsymbol{\zeta})^{k-1}$ respectively and their corresponding expressions can be easily obtained similar to Appendix B.
- Optimization: The next update $(\mathbf{W}, \boldsymbol{\eta}, \boldsymbol{\delta}, \boldsymbol{\zeta})^{k+1}$ is obtained by solving the following convex problem :

$$\mathcal{P}_\ni^{\text{MC}} : \min_{\mathbf{W},\boldsymbol{\eta},\boldsymbol{\delta},\boldsymbol{\zeta}} \tilde{f}_1(\boldsymbol{\delta}) + \lambda_2 \sum_{i=1}^N \sum_{j=1}^T \sum_{k=1}^G \tilde{\mathbb{P}}(\eta_{ij,k}) + \lambda_3 \sum_{j=1}^T \sum_{k=1}^G \tilde{\mathbb{P}}(\delta_{j,k}) + \sum_{i=1}^N \sum_{k=1}^G \beta_{i,k} \left\| \sum_{j=1}^T \eta_{ij,k} - 1 \right\|_2 \quad \text{(B.2)}$$

$$\text{s.t. } C_1: \ 0 \leq \eta_{ij,k} \leq 1, \forall i, \ \forall j, \ \forall k, \quad C_2: \ \|\mathbf{w}_{ij}\|_2^2 \ \leq \ P_S \eta_{ij}, \forall i, \ \forall j, \ \forall k,$$

$$C_3: \ 0 \leq \delta_{j,k} \leq 1\}, \ \forall i, \ \forall j, \ \forall k, \quad C_4: \ \sum_{i=1}^{N} \eta_{ij,k} \geq \delta_{j,k}, \ \forall j, \ \forall k,$$

$$C_5: \ \sum_{k=1}^{G} \delta_{j,k} \leq M, \ \forall j, \qquad C_6: \ \mathcal{I}_{ij,k}\left(\mathbf{W}\right) - \tilde{\mathcal{G}}_{ij,k}\left(\mathbf{W}, \zeta_{ij,k}\right) \leq 0, \forall i, \ \forall j, \ \forall k,$$

$$C_7: \ \log \zeta_{ij,k} \geq \eta_{ij,k} \bar{\theta}_k, \forall i, \ \forall j, \ \forall k, \quad C_8: \sum_{j=1}^{T} \sum_{k=1}^{G} \|\mathbf{w}_{j,k}\|_2^2 \leq P_T,$$

7 Publications

Publications that are part of thesis

Accepted

Journals

J1: **A. Bandi**, B. Shankar M. R, S. Chatzinotas and B. Ottersten, "A Joint Solution for Scheduling and Precoding in Multiuser MISO Downlink Channels," in IEEE Transactions on Wireless Communications, vol. 19, no. 1, pp. 475-490, Jan. 2020, doi: 10.1109/TWC.2019.2946161.

J2: **A. Bandi**, R. Bhavani Shankar Mysore, S. Chatzinotas and B. Ottersten, "Joint User Grouping, Scheduling, and Precoding for Multicast Energy Efficiency in Multigroup Multicast Systems," in IEEE Transactions on Wireless Communications, doi: 10.1109/TWC.2020.3020081.

Conferences

C1: **A. Bandi**, B. S. Mysore R, S. Maleki, S. Chatzinotas and B. Ottersten, "A Novel Approach to Joint User Selection and Precoding for Multiuser MISO Downlink Channels," 2018 IEEE Global Conference on Signal and Information Processing (GlobalSIP), Anaheim, CA, USA, 2018, pp. 206-210, doi: 10.1109/GlobalSIP.2018.8646373.

C2: **A. Bandi**, B. S. Mysore R., S. Chatzinotas and B. Ottersten, "Joint Scheduling and Precoding for Frame-Based Multigroup Multicasting in Satellite Communications," 2019 IEEE Global Communications Conference (GLOBECOM), Waikoloa, HI, USA, 2019, pp. 1-6, doi: 10.1109/GLOBECOM38437.2019.9014235.

C3: **A. Bandi**, B. S. Mysore R., S. Chatzinotas and B. Ottersten, "Joint User Scheduling, and Precoding for Multicast Spectral Efficiency in Multigroup Multicast Systems," 2020 IEEE International Conference on Signal Processing and Communications (SPCOM), Bangalore, India, 2020.

C4: **A. Bandi**, V. Joroughi, B. S. Mysore R., J. Grotz and B. Ottersten, "Sparsity-Aided Low-Implementation cost based On-Board beamforming Design for High Throughput Satellite Systems," 2018 9th Advanced Satellite Multimedia Systems Conference and the 15th Signal Processing for Space Communications Workshop (ASMS/SPSC), Berlin, 2018, pp. 1-6, doi: 10.1109/ASMS-SPSC.2018.8510731.

Under review

Journals

J3: **A. Bandi**, B. Shankar M. R, S. Chatzinotas and B. Ottersten, "A Joint Solution for Multi-slot Scheduling and Precoding for Unicast and Multicast Scenario in Multiuser MISO Downlink Channels," submitted to IEEE Transactions on Communications.

J4: **A. Bandi**, B. Shankar M. R, B. Ottersten, and J Grotz "Joint Beam selection, User scheduling and Frame-based Multigroup Multicast Precoding in High Throughput Satellite Systems, submitted to International Journal of Satellite Communications and Networking (IJSCN).

Publications that are not part of thesis

Accepted

Journals

J5: S Gautam, E Lagunas, **A Bandi**, S Chatzinotas ; Shree Krishna Sharma ; Thang X. Vu et al., "Multigroup Multicast Precoding for Energy Optimization in SWIPT Systems With Heterogeneous Users," in IEEE Open Journal of the Communications Society, vol. 1, pp. 92-108, 2020, doi: 10.1109/OJCOMS.2019.2962077.

J6: P. Korrai, E. Lagunas, S. K. Sharma, **A. Bandi**, S. Chatzinotas, and B. Ottersten, "A RAN Resource Slicing Mechanism for Multiplexing of eMBB and URLLC Services in OFDMA Based 5G Wireless Networks," in IEEE Access, vol. 8, pp. 45674-45688, 2020, doi: 10.1109/ACCESS.2020.2977773.

J7: P. Korrai, E. Lagunas, **A. Bandi**, S. K. Sharma, and S. Chatzinotas, "Joint Power and Resource Block Allocation for Mixed-Numerology-Based 5G Downlink Under Imperfect CSI" accepted in IEEE Open Journal of the Communications Society

Bibliography

[1] ITU-R, "IMT vision – framework and overall objectives of the future development of IMT for 2020 and beyond," *Tech. Rep.*, 2015.

[2] S. Stańczak, M. Wiczanowski, and H. Boche, "Fundamentals of resource allocation in wireless networks - theory and algorithms (2. ed.)," in *Foundations in Signal Processing, Communications and Networking*, 2008.

[3] D. Gesbert, S. Hanly, H. Huang, S. S. Shitz, O. Simeone, and W. Yu, "Multi-cell mimo cooperative networks: A new look at interference," *IEEE J. Sel. Areas Commun.*, vol. 28, no. 9, pp. 1380–1408, December 2010.

[4] H. Weingarten, Y. Steinberg, and S. S. Shamai, "The Capacity Region of the Gaussian Multiple-Input Multiple-Output Broadcast Channel," *IEEE Trans. Inf. Theory*, vol. 52, no. 9, pp. 3936–3964, Sept 2006.

[5] H. Viswanathan, S. Venkatesan, and H. Huang, "Downlink capacity evaluation of cellular networks with known-interference cancellation," *IEEE J. Sel. Areas Commun.*, vol. 21, no. 5, pp. 802–811, June 2003.

[6] P. Zetterberg and B. Ottersten, "The spectrum efficiency of a base station antenna array system for spatially selective transmission," *IEEE Trans. Veh. Technol.*, vol. 44, no. 3, pp. 651–660, Aug 1995.

[7] S. Anderson, M. Millnert, M. Viberg, and B. Wahlberg, "An adaptive array for mobile communication systems," *IEEE Trans. Veh. Technol.*, vol. 40, no. 1, pp. 230–236, Feb 1991.

[8] M. Bengtsson and B. Ottersten, "Optimal and suboptimal transmit beamforming," in *Handbook of Antennas in Wireless Communications*. CRC Press, 2001, pp. 18–1–18–33, qC 20111107.

[9] A. Wiesel, Y. C. Eldar, and S. Shamai, "Linear precoding via conic optimization for fixed MIMO receivers," *IEEE Trans. Signal Process.*, vol. 54, no. 1, pp. 161–176, Jan 2006.

[10] G. Dimic and N. D. Sidiropoulos, "On downlink beamforming with greedy user selection: performance analysis and a simple new algorithm," *IEEE Trans. Signal Process.*, vol. 53, no. 10, pp. 3857–3868, Oct 2005.

[11] J. Wang, D. J. Love, and M. D. Zoltowski, "User selection with zero-forcing beamforming achieves the asymptotically optimal sum rate," *IEEE Transactions on Signal Processing*, vol. 56, no. 8, pp. 3713–3726, 2008.

[12] C. Farsakh and J. A. Nossek, "Spatial covariance based downlink beamforming in an sdma mobile radio system," *IEEE Transactions on Communications*, vol. 46, no. 11, pp. 1497–1506, 1998.

[13] D. Tse and P. Viswanath, *Fundamentals of Wireless Communication*. USA: Cambridge University Press, 2005.

[14] B. Ottersten, "Spatial division multiple access (sdma) in wireless communications," in *Proceedings of Nordic Radio Symposium*, 1995.

[15] S. Sesia, I. Toufik, and M. Baker, *LTE, The UMTS Long Term Evolution: From Theory to Practice*. Wiley Publishing, 2009.

[16] E. Dahlman, S. Parkvall, and J. Skold, *4G: LTE/LTE-Advanced for Mobile Broadband*, 1st ed. USA: Academic Press, Inc., 2011.

[17] D. Astely, E. Dahlman, G. Fodor, S. Parkvall, and J. Sachs, "LTE release 12 and beyond [Accepted From Open Call]," *IEEE Communications Magazine*, vol. 51, no. 7, pp. 154–160, 2013.

[18] ——, "E-utra: Physical channels and modulation (release 11). 3gpp ts 36.211," *IEEE Communications Magazine*.

[19] F. Rashid-Farrokhi, K. J. R. Liu, and L. Tassiulas, "Transmit beamforming and power control for cellular wireless systems," *IEEE Journal on Selected Areas in Communications*, vol. 16, no. 8, pp. 1437–1450, 1998.

[20] M. Schubert and H. Boche, "Solution of the multiuser downlink beamforming problem with individual sinr constraints," *IEEE Transactions on Vehicular Technology*, vol. 53, no. 1, pp. 18–28, 2004.

[21] W. Yu and T. Lan, "Transmitter optimization for the multi-antenna downlink with per-antenna power constraints," *IEEE Transactions on Signal Processing*, vol. 55, no. 6, pp. 2646–2660, 2007.

[22] D. W. K. Ng, E. S. Lo, and R. Schober, "Energy-efficient resource allocation in ofdma systems with large numbers of base station antennas," *IEEE Transactions on Wireless Communications*, vol. 11, no. 9, pp. 3292–3304, 2012.

[23] E. Karipidis, N. D. Sidiropoulos, and Z. Luo, "Far-field multicast beamforming for uniform linear antenna arrays," *IEEE Transactions on Signal Processing*, vol. 55, no. 10, pp. 4916–4927, 2007.

[24] E. Karipidis, N. D. Sidiropoulos, and Z. Q. Luo, "Quality of service and max-min fair transmit beamforming to multiple cochannel multicast groups," *IEEE Trans. Signal Process.*, vol. 56, no. 3, pp. 1268–1279, March 2008.

[25] T. Yoo and A. Goldsmith, "On the optimality of multiantenna broadcast scheduling using zero-forcing beamforming," *IEEE J. Sel. Areas Commun.*, vol. 24, no. 3, pp. 528–541, March 2006.

[26] B. Song, Y. Lin, and R. L. Cruz, "Weighted max-min fair beamforming, power control, and scheduling for a MISO downlink," *IEEE Trans. Wireless Commun.*, vol. 7, no. 2, pp. 464–469, February 2008.

[27] E. Matskani, N. D. Sidiropoulos, Z. q. Luo, and L. Tassiulas, "Convex approximation techniques for joint multiuser downlink beamforming and admission control," *IEEE Trans. Wireless Commun.*, vol. 7, no. 7, pp. 2682–2693, July 2008.

[28] F. Meshkati, H. V. Poor, and S. C. Schwartz, "Energy-efficient resource allocation in wireless networks," *IEEE Signal Processing Magazine*, vol. 24, no. 3, pp. 58–68, 2007.

[29] E. Karipidis, N. D. Sidiropoulos, and Z. Luo, "Quality of service and max-min fair transmit beamforming to multiple cochannel multicast groups," *IEEE Trans. Signal Process.*, vol. 56, no. 3, pp. 1268–1279, March 2008.

[30] M. Alodeh, D. Spano, A. Kalantari, C. G. Tsinos, D. Christopoulos, S. Chatzinotas, and B. Ottersten, "Symbol-level and multicast precoding for multiuser multiantenna downlink: A state-of-the-art, classification, and challenges," *IEEE Commun. Surveys Tuts.*, vol. 20, no. 3, pp. 1733–1757, thirdquarter 2018.

[31] Z. Xiang, M. Tao, and X. Wang, "Coordinated multicast beamforming in multicell networks," *IEEE Trans. Wireless Commun.*, vol. 12, no. 1, pp. 12–21, January 2013.

[32] E. Matskani, N. D. Sidiropoulos, Z. Luo, and L. Tassiulas, "Efficient batch and adaptive approximation algorithms for joint multicast beamforming and admission control," *IEEE Trans. Signal Process.*, vol. 57, no. 12, pp. 4882–4894, Dec 2009.

[33] B. Hu, C. Hua, C. Chen, and X. Guan, "User grouping and admission control for multi-group multicast beamforming in MIMO systems," https://doi.org/10.1007/s11276-017-1510-5, pp. 2851–2866, Nov 2018.

[34] D. Christopoulos, S. Chatzinotas, and B. Ottersten, "Multicast multigroup precoding and user scheduling for frame-based satellite communications," *IEEE Trans. Wireless Commun.*, vol. 14, no. 9, pp. 4695–4707, Sept 2015.

[35] T. Yoo, N. Jindal, and A. Goldsmith, "Multi-Antenna Downlink Channels with Limited Feedback and User Selection," *IEEE J. Sel. Areas Commun.*, vol. 25, no. 7, pp. 1478–1491, September 2007.

[36] G. Lee and Y. Sung, "A New Approach to User Scheduling in Massive Multi-User MIMO Broadcast Channels," *IEEE Trans. Commun.*, vol. 66, no. 4, pp. 1481–1495, April 2018.

[37] W. Yu, T. Kwon, and C. Shin, "Multicell Coordination via Joint Scheduling, Beamforming, and Power Spectrum Adaptation," *IEEE Trans. Wireless Commun.*, vol. 12, no. 7, pp. 1–14, July 2013.

[38] M. Li, I. B. Collings, S. V. Hanly, C. Liu, and P. Whiting, "Multicell Coordinated Scheduling With Multiuser Zero-Forcing Beamforming," *IEEE Trans. Wireless Commun.*, vol. 15, no. 2, pp. 827–842, Feb 2016.

[39] M. Kountouris, D. Gesbert, and T. Sälzer, "Enhanced multiuser random beamforming: dealing with the not so large number of users case," *IEEE J. Sel. Areas Commun.*, vol. 26, no. 8, pp. 1536–1545, October 2008.

[40] M. L. Ku, L. C. Wang, and Y. L. Liu, "Joint Antenna Beamforming, Multiuser Scheduling, and Power Allocation for Hierarchical Cellular Systems," *IEEE J. Sel. Areas Commun.*, vol. 33, no. 5, pp. 896–909, May 2015.

[41] L. Yu, E. Karipidis, and E. G. Larsson, "Coordinated scheduling and beamforming for multicell spectrum sharing networks using branch and bound," in *Proc. EUSIPCO*, Aug 2012, pp. 819–823.

[42] A. Douik, H. Dahrouj, T. Y. Al-Naffouri, and M. S. Alouini, "Coordinated Scheduling and Power Control in Cloud-Radio Access Networks," *IEEE Trans. Wireless Commun.*, vol. 15, no. 4, pp. 2523–2536, April 2016.

[43] E. Castañeda, A. Silva, A. Gameiro, and M. Kountouris, "An Overview on Resource Allocation Techniques for Multi-User MIMO Systems," *IEEE Commun. Surveys Tuts.*, vol. 19, no. 1, pp. 239–284, Firstquarter 2017.

[44] O. Goussevskaia, R. Wattenhofer, M. M. Halldorsson, and E. Welzl, "Capacity of arbitrary wireless networks," in *IEEE INFOCOM 2009*, April 2009, pp. 1872–1880.

[45] E. Amaldi, A. Capone, F. Malucelli, and C. Mannino, "Optimization problems and models for planning cellular networks," in *Handbook of Optimization in Telecommunications*, M. G. C. Resende and P. M. Pardalos, Eds. Springer, 2006, pp. 917–939. [Online]. Available: https://doi.org/10.1007/978-0-387-30165-5_32

[46] F. F. Mazzini and G. R. Mateus, "A mixed-integer programming model for the cellular telecommunication network design," in *Proceedings of the 5th International Workshop on Discrete Algorithms and Methods for Mobile Computing and Communications*, ser. DIALM '01. New York, NY, USA: Association for Computing Machinery, 2001, p. 68–76. [Online]. Available: https://doi.org/10.1145/381448.381458

[47] B. Dai and W. Yu, "Sparse Beamforming and User-Centric Clustering for Downlink Cloud Radio Access Network," *IEEE Access*, vol. 2, pp. 1326–1339, 2014.

[48] M. Tao, E. Chen, H. Zhou, and W. Yu, "Content-Centric Sparse Multicast Beamforming for Cache-Enabled Cloud RAN," *IEEE Trans. Wireless Commun.*, vol. 15, no. 9, pp. 6118–6131, Sept 2016.

[49] R. Stridh, M. Bengtsson, and B. Ottersten, "System evaluation of optimal downlink beamforming with congestion control in wireless communication," *IEEE Transactions on Wireless Communications*, vol. 5, no. 4, pp. 743–751, 2006.

[50] M. Razaviyayn, M. Baligh, A. Callard, and Z. Luo, "Joint user grouping and transceiver design in a mimo interfering broadcast channel," *IEEE Transactions on Signal Processing*, vol. 62, no. 1, pp. 85–94, 2014.

[51] S. He, J. Wang, Y. Huang, B. Ottersten, and W. Hong, "Codebook-Based Hybrid Precoding for Millimeter Wave Multiuser Systems," *IEEE Trans. Signal Process.*, vol. 65, no. 20, pp. 5289–5304, Oct 2017.

[52] A. H. Phan, H. D. Tuan, H. H. Kha, and H. H. Nguyen, "Beamforming Optimization in Multi-User Amplify-and-Forward Wireless Relay Networks," *IEEE Trans. Wireless Commun.*, vol. 11, no. 4, pp. 1510–1520, April 2012.

[53] U. Rashid, H. D. Tuan, and H. H. Nguyen, "Relay Beamforming Designs in Multi-User Wireless Relay Networks Based on Throughput Maximin Optimization," *IEEE Trans. Commun.*, vol. 61, no. 5, pp. 1739–1749, May 2013.

[54] G. R. Lanckriet and B. K. Sriperumbudur, "On the Convergence of the Concave-Convex Procedure," in *Advances in Neural Information Processing Systems 22*, 2009, pp. 1759–1767.

[55] T. Lipp and S. Boyd, "Variations and extension of the convex-concave procedure," http://stanford.edu/~boyd/papers/cvx_ccv.html, 2016.

[56] H. Shi, R. V. Prasad, E. Onur, and I. G. M. M. Niemegeers, "Fairness in wireless networks:issues, measures and challenges," *IEEE Commun. Surveys Tuts.*, vol. 16, no. 1, pp. 5–24, First 2014.

[57] D. Christopoulos, S. Chatzinotas, and B. Ottersten, "Multicast multigroup precoding and user scheduling for frame-based satellite communications," *IEEE Trans. Wireless Commun.*, vol. 14, no. 9, pp. 4695–4707, Sept 2015.

[58] I. Mitliagkas, N. D. Sidiropoulos, and A. Swami, "Joint Power and Admission Control for Ad-Hoc and Cognitive Underlay Networks: Convex Approximation and Distributed Implementation," *IEEE Trans. Wireless Commun.*, vol. 10, no. 12, pp. 4110–4121, December 2011.

[59] Y. Cheng and M. Pesavento, "Joint Discrete Rate Adaptation and Downlink Beamforming Using Mixed Integer Conic Programming," *IEEE Trans. Signal Process.*, vol. 63, no. 7, pp. 1750–1764, April 2015.

[60] J. Rubio, A. Pascual-Iserte, D. P. Palomar, and A. Goldsmith, "Joint Optimization of Power and Data Transfer in Multiuser MIMO Systems," *IEEE Trans. Signal Process.*, vol. 65, no. 1, pp. 212–227, Jan 2017.

[61] C. T. K. Ng and H. Huang, "Linear Precoding in Cooperative MIMO Cellular Networks with Limited Coordination Clusters," *IEEE J. Sel. Areas Commun.*, vol. 28, no. 9, pp. 1446–1454, December 2010.

[62] S. You, L. Chen, and Y. E. Liu, "Convex-concave procedure for weighted sum-rate maximization in a MIMO interference network," in *Proc. Globecom*, Dec 2014, pp. 4060–4065.

[63] A. L. Yuille and A. Rangarajan, "The concave-convex procedure (CCCP)," in *NIPS*, 2001.

[64] P. Gahinet, A. Nemirovski, A. J. Laub, and M. Chilali, *LMI Control Toolbox User's Guide*. USA: MathWorks, 1995.

[65] D. W. H. Cai, T. Q. S. Quek, and C. W. Tan, "A Unified Analysis of Max-Min Weighted SINR for MIMO Downlink System," *IEEE Trans. Signal Process.*, vol. 59, no. 8, pp. 3850–3862, Aug 2011.

[66] L. Zheng, Y. . P. Hong, C. W. Tan, C. Hsieh, and C. Lee, "Wireless Max–Min Utility Fairness With General Monotonic Constraints by Perron–Frobenius Theory," *IEEE Trans. Inf. Theory*, vol. 62, no. 12, pp. 7283–7298, Dec 2016.

[67] CVX Research Inc., "CVX: Matlab software for disciplined convex programming, version 2.0," http://cvxr.com/cvx, Aug. 2012.

[68] Y. Chen, S. Zhang, S. Xu, and G. Y. Li, "Fundamental trade-offs on green wireless networks," *IEEE Commun. Mag.*, vol. 49, no. 6, pp. 30–37, June 2011.

[69] O. Tervo, L. Tran, H. Pennanen, S. Chatzinotas, B. Ottersten, and M. Juntti, "Energy-efficient multicell multigroup multicasting with joint beamforming and antenna selection," *IEEE Trans. Signal Process.*, vol. 66, no. 18, pp. 4904–4919, Sep. 2018.

[70] D. Lecompte and F. Gabin, "Evolved multimedia broadcast/multicast service (eMBMS) in LTE-advanced: overview and Rel-11 enhancements," *IEEE Commun. Mag.*, vol. 50, no. 11, pp. 68–74, November 2012.

[71] H. Zhou and M. Tao, "Joint multicast beamforming and user grouping in massive MIMO systems," in *2015 IEEE International Conference on Communications (ICC)*, June 2015, pp. 1770–1775.

[72] S. He, Y. Huang, S. Jin, and L. Yang, "Energy efficient coordinated beamforming design in multi-cell multicast networks," *IEEE Commun. Lett.*, vol. 19, no. 6, pp. 985–988, June 2015.

[73] J. Denis, S. Smirani, B. Diomande, T. Ghariani, and B. Jouaber, "Energy-efficient coordinated beamforming for multi-cell multicast networks under statistical CSI," in *2017 IEEE 18th International Workshop SPAWC*, July 2017, pp. 1–5.

[74] Y. Li, M. Xia, and Y. Wu, "Energy-efficient precoding for non-orthogonal multicast and unicast transmission via first-order algorithm," *IEEE Trans. Wireless Commun.*, vol. 18, no. 9, pp. 4590–4604, Sep. 2019.

[75] O. Tervo, A. Tölli, M. Juntti, and L. Tran, "Energy-efficient beam coordination strategies with rate-dependent processing power," *IEEE Trans. Signal Process.*, vol. 65, no. 22, pp. 6097–6112, Nov 2017.

[76] Y. Yang, M. Pesavento, S. Chatzinotas, and B. Ottersten, "Energy efficiency optimization in mimo interference channels: A successive pseudoconvex approximation approach," *IEEE Trans. Signal Process.*, vol. 67, no. 15, pp. 4107–4121, 2019.

[77] Y. Zhang, J. An, K. Yang, X. Gao, and J. Wu, "Energy-efficient user scheduling and power control for multi-cell ofdma networks based on channel distribution information," *IEEE Trans. Signal Process.*, vol. 66, no. 22, pp. 5848–5861, 2018.

[78] A. Zappone, L. Sanguinetti, G. Bacci, E. Jorswieck, and M. Debbah, "Energy-efficient power control: A look at 5g wireless technologies," *IEEE Trans. Signal Process.*, vol. 64, no. 7, pp. 1668–1683, 2016.

[79] M. Kaliszan, E. Pollakis, and S. Stańczak, "Multigroup multicast with application-layer coding: Beamforming for maximum weighted sum rate," in *2012 IEEE WCNC conference*, April 2012, pp. 2270–2275.

[80] T. X. Tran and G. Yue, "Grab: Joint adaptive grouping and beamforming for multi-group multicast with massive mimo," in *2019 IEEE Global Communications Conference (GLOBECOM)*, 2019, pp. 1–6.

[81] A. Bandi, B. S. M. R, S. Chatzinotas, and B. Ottersten, "A joint solution for scheduling and precoding in multiuser MISO downlink channels," *IEEE Trans. Wireless Commun.*, pp. 1–1, 2019.

[82] B. R. Marks and G. P. Wright, "Technical note-a general inner approximation algorithm for nonconvex mathematical programs," *Oper. Res.*, vol. 26, no. 4, p. 681–683, Aug. 1978. [Online]. Available: https://doi.org/10.1287/opre.26.4.681

[83] A. Duel-Hallen, "Fading channel prediction for mobile radio adaptive transmission systems," *Proceedings of the IEEE*, vol. 95, no. 12, pp. 2299–2313, 2007.

[84] W. Jiang and H. D. Schotten, "Neural network-based fading channel prediction: A comprehensive overview," *IEEE Access*, vol. 7, pp. 118 112–118 124, 2019.

[85] J. Huang, C. Wang, L. Bai, J. Sun, Y. Yang, J. Li, O. Tirkkonen, and M. Zhou, "A big data enabled channel model for 5g wireless communication systems," *IEEE Transactions on Big Data*, vol. 6, no. 2, pp. 211–222, 2020.

[86] L. Bai, C. Wang, Q. Xu, S. Ventouras, and G. Goussetis, "Prediction of channel excess attenuation for satellite communication systems at q-band using artificial neural network," *IEEE Antennas and Wireless Propagation Letters*, vol. 18, no. 11, pp. 2235–2239, 2019.

[87] N. Simon, J. Friedman, T. Hastie, and R. Tibshirani, "A sparse-group lasso," *Journal of Computational and Graphical Statistics*, 2013.

[88] A. Bandi, M. R. Bhavani Shankar, S. Chatzinotas, and B. Ottersten, "Joint scheduling and precoding for frame-based multigroup multicasting in satellite communications," in *IEEE Global Communications Conference*, December 2019.

[89] K. B. Shashika Manosha, S. K. Joshi, M. Codreanu, N. Rajatheva, and M. Latva-aho, "Admission control algorithms for qos-constrained multicell miso downlink systems," *IEEE Transactions on Wireless Communications*, vol. 17, no. 3, pp. 1982–1999, 2018.

[90] J. Lin, M. Ma, Q. Li, and J. Yang, "Joint long-term admission control and beamforming in green downlink networks: Offline and online approaches," *IEEE Transactions on Vehicular Technology*, vol. 69, no. 8, pp. 8710–8724, 2020.

[91] M. Hong, R. Sun, H. Baligh, and Z. Luo, "Joint base station clustering and beamformer design for partial coordinated transmission in heterogeneous networks," *IEEE Journal on Selected Areas in Communications*, vol. 31, no. 2, pp. 226–240, 2013.

[92] J. Zhao, T. Q. S. Quek, and Z. Lei, "Coordinated multipoint transmission with limited backhaul data transfer," *IEEE Transactions on Wireless Communications*, vol. 12, no. 6, pp. 2762–2775, 2013.

[93] O. Mehanna, N. D. Sidiropoulos, and G. B. Giannakis, "Joint multicast beamforming and antenna selection," *IEEE Transactions on Signal Processing*, vol. 61, no. 10, pp. 2660–2674, 2013.

[94] R. Tibshirani, "Regression shrinkage and selection via the lasso," *Journal of the Royal Statistical Society, Series B*, vol. 58, pp. 267–288, 1994.

[95] F. Zhuang and V. K. N. Lau, "Backhaul limited asymmetric cooperation for mimo cellular networks via semidefinite relaxation," *IEEE Transactions on Signal Processing*, vol. 62, no. 3, pp. 684–693, 2014.

[96] Y. Shi, J. Zhang, and K. B. Letaief, "Group sparse beamforming for green cloud-ran," *IEEE Transactions on Wireless Communications*, vol. 13, no. 5, pp. 2809–2823, 2014.

[97] ——, "Robust group sparse beamforming for multicast green cloud-ran with imperfect csi," *IEEE Transactions on Signal Processing*, vol. 63, no. 17, pp. 4647–4659, 2015.

[98] Y. Shi, J. Cheng, J. Zhang, B. Bai, W. Chen, and K. B. Letaief, "Smoothed l_p-minimization for green cloud-ran with user admission control," *IEEE Journal on Selected Areas in Communications*, vol. 34, no. 4, pp. 1022–1036, 2016.

[99] A. Bandi and C. R. Murthy, "Structured sparse recovery algorithms for data decoding in media based modulation," in *2017 IEEE International Conference on Communications (ICC)*, May 2017, pp. 1–6.

[100] E. Candès, M. Wakin, and S. Boyd, "Enhancing sparsity by reweighted ℓ_1 minimization," *Journal of Fourier Analysis and Applications*, vol. 14, no. 8, pp. 877–905, 2008.

[101] D. Wipf and S. Nagarajan, "Iterative reweighted ℓ_1 and ℓ_2 methods for finding sparse solutions," *IEEE Journal of Selected Topics in Signal Processing*, vol. 4, no. 2, pp. 317–329, 2010.

[102] A. Bandi, R. Bhavani Shankar Mysore, S. Chatzinotas, and B. Ottersten, "Joint user grouping, scheduling, and precoding for multicast energy efficiency in multigroup multicast systems," *IEEE Transactions on Wireless Communications*, pp. 1–1, 2020.

[103] K. E. Baddour and N. C. Beaulieu, "Autoregressive modeling for fading channel simulation," *IEEE Transactions on Wireless Communications*, vol. 4, no. 4, pp. 1650–1662, 2005.

[104] V. Agrawal and A. Maini, *Satellite Communications*. Wiley, 2010.

[105] C. Riva, C. Capsoni, L. Luini, M. Luccini, R. Nebuloni, and A. Martellucci, "The challenge of using the w band in satellite communication," *International Journal of Satellite Communications and Networking*, vol. 32, 05 2014.

[106] M. Costa, "Writing on dirty paper (corresp.)," *IEEE Trans. Inf. Theory*, vol. 29, no. 3, pp. 439–441, May 1983.

[107] D. Christopoulos, S. Chatzinotas, G. Zheng, J. Grotz, and B. Ottersten, "Linear and non-linear techniques for multibeam joint processing in satellite communications," *EURASIP Journal on Wireless Communications and Networking*, vol. 2012, 12 2012.

[108] V. Joroughi, A. Vazquez, and A. Perez-Neira, "Precoding in multigateway multibeam satellite systems," *IEEE Transactions on Wireless Communications*, vol. 15, 07 2015.

[109] P. C. Weeraddana, M. Codreanu, M. Latva-aho, A. Ephremides, and C. Fischione, *Weighted Sum-Rate Maximization in Wireless Networks:A Review*. Now Foundations and Trends, 2012. [Online]. Available: http://ieeexplore.ieee.org.proxy.bnl.lu/xpl/articleDetails.jsp?arnumber=8186919

[110] S. Foucart, "A note on guaranteed sparse recovery via ℓ_1-minimization," *Applied and Computational Harmonic Analysis*, vol. 29, no. 1, pp. 97–103, 2010.

[111] *Call of Order 2-Task 1: Fair comparison and combination of advanced interference mitigation techniques*.

[112] D. Christopoulos, S. Chatzinotas, and B. Ottersten, "Multicast Multigroup Precoding and User Scheduling for Frame-Based Satellite Communications," *IEEE Trans. Wireless Commun.*, vol. 14, no. 9, pp. 4695–4707, Sept 2015.

[113] V. Joroughi, M. A. Vazquez, and A. I. Perez-Neira, "Generalized multicast multibeam precoding for satellite communications," *IEEE Transactions on Wireless Communications*, vol. 16, no. 2, pp. 952–966, 2017.

[114] *Digital Video Broadcasting (DVB); Second Generation Framing Structure, Channel Coding and Modulation Systems for Broadcasting, Interactive Services, News Gathering and Other Broad-Band Satellite Applications. Part 2: DVB-S2 Extensions (DVB-S2X), European Broadcasting Union (EBU), .*

[115] D. Christopoulos, S. Chatzinotas, and B. Ottersten, "Frame based precoding in satellite communications: A multicast approach," in *2014 7th ASMS Conference/ 13th SPSC workshop*, Sep. 2014, pp. 293–299.

[116] D. Yuan, V. Angelakis, L. Chen, E. Karipidis, and E. G. Larsson, "On optimal link activation with interference cancelation in wireless networking," *IEEE Transactions on Vehicular Technology*, vol. 62, no. 2, pp. 939–945, 2013.

[117] H. Hijazi, P. Bonami, and A. Ouorou, "Robust delay-constrained routing in telecommunications," *Annals of Operations Research*, vol. 206, 07 2013.

[118] T. Q. S. Quek, G. de la Roche, I. Gven, and M. Kountouris, *Small Cell Networks: Deployment, PHY Techniques, and Resource Management*. USA: Cambridge University Press, 2013.